Mathematical Problems in Engineering

# Modelling for Sustainable Cities 2021

Lead Guest Editor: Haoran Zhang
Guest Editors: Xuan Song and Jinyu Chen

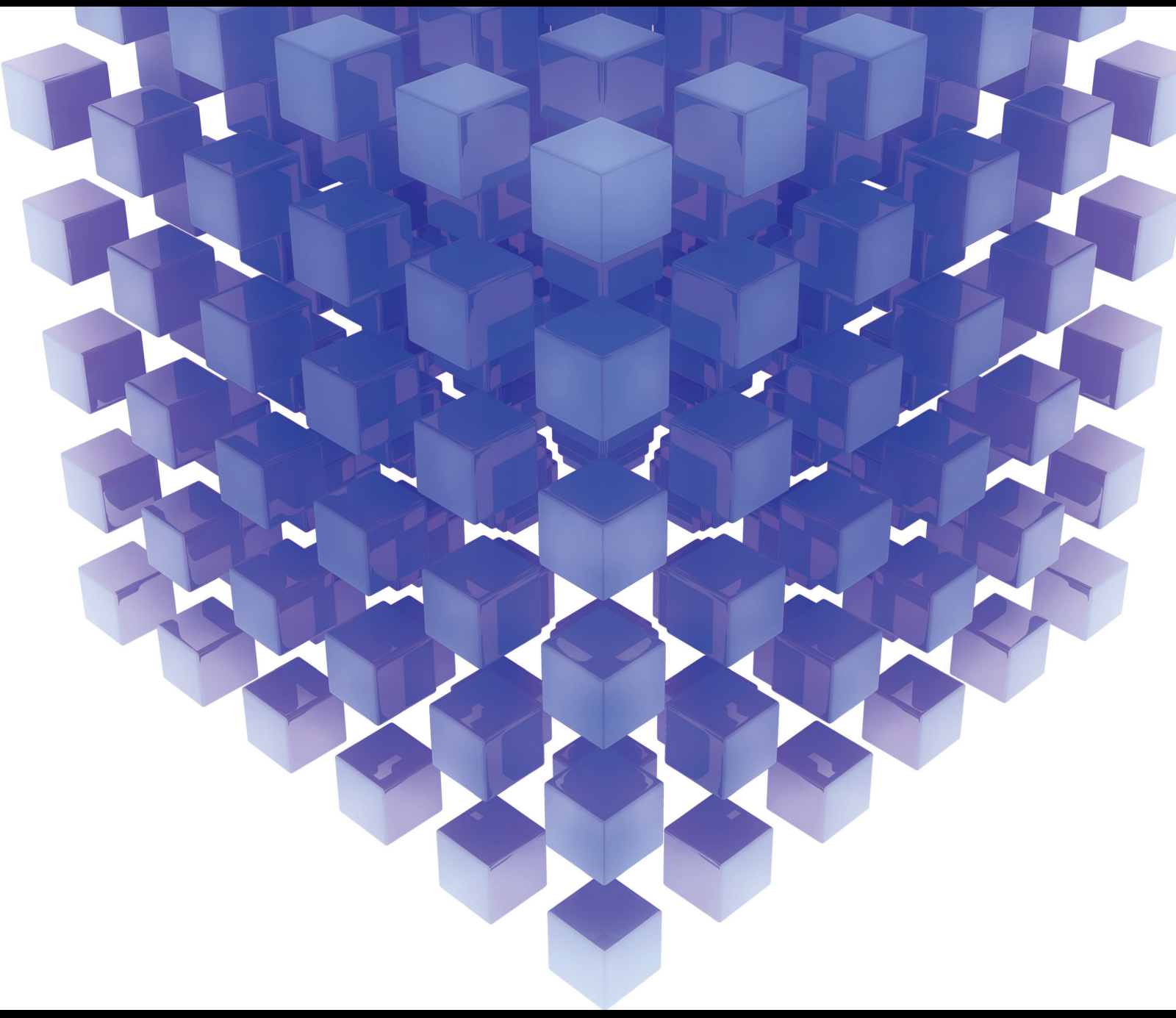

# Modelling for Sustainable Cities 2021

Mathematical Problems in Engineering

# Modelling for Sustainable Cities 2021

Lead Guest Editor: Haoran Zhang
Guest Editors: Xuan Song and Jinyu Chen

# Chief Editor



## Academic Editors

# Contents

Hindawi
Mathematical Problems in Engineering
Volume 2021, Article ID 4358661, 13 pages
https://doi.org/10.1155/2021/4358661

*Research Article*

# Impacts of Emission Reduction Technological Changes on China's City-Level PM2.5 Concentration Based on Sustainable Development

**Jiandong Chen, Yu Wei, Ming Gao, and Shuo Huang**

*School of Public Administration, Southwestern University of Finance and Economics, Chengdu 611130, China*

Correspondence should be addressed to Ming Gao; minggao1994@163.com

Received 5 October 2021; Accepted 11 November 2021; Published 24 November 2021

Academic Editor: Xuan Song



As an important field for human activities, cities play a critical role in PM2.5 reductions. Among the determinants for PM2.5 concentration, technological progress is considered to exhibit significant inhibitory effects. Although most extant research has focused on energy technologies or total factor productivity, due to limitations in data and methods, few scholars have focused on emission reduction technological changes at a city-level scale. Therefore, based on the combination of *k*-means clustering and the log-mean Divisia index method, this study estimates and explores the impact of PM2.5 emission reduction technology (PME) on the temporal changes and spatial differences of 262 Chinese cities' PM2.5 concentration during 2003–2017. The findings show the following: (1) although the results based on econometric methods indicate that emission reduction technological changes decreased China's city-level PM2.5 concentration, there were turning points in the yearly impacts, indicating that the improvements to emission reduction efficiency were not stable; (2) compared with PME, energy intensity played a more stable role in PM2.5 emissions reductions, implying that the improvement of energy efficiency was still very important in controlling PM2.5 concentrations; (3) based on the classified groups after clustering, most cities' PME contributed to negative differences, but the PME of a small number of cities was very weak to largely lower the average level of their group; and (4) distributions of the spatial decomposition of the three classified groups were stable in the period of 2003–2017, implying that the catch-up and transcendence effects of PME within the group were limited. Thus, policymakers should focus on the impact of different policies on PME differences between cities.

## 1. Introduction

In recent years, PM2.5 pollution has seriously concerned countries around the world due to the threats it represents to human survival and to the sustainable development of society [1–3]. In light of previous studies, PM2.5 emissions can not only lead to high haze reduction costs but also indirectly cause health costs through medical expenses and work-time loss. In particular, the emissions control cost in Shanghai would be about 1.01%–2.26% of the corresponding gross domestic product (DDP) values in 2030 [4]. And the direct external cost of residential health issues caused by PM2.5 pollution in Beijing and Changsha was as high as 0.3%–2.69% of the GDP during 2012–2017 [5, 6].

As one of the world's largest developing countries, China is undergoing a process of accelerating urbanization and industrialization, facing increasingly severe PM2.5 pollution [7, 8]. Thus, the government has focused on formulating a series of policy regulations, such as the Air Pollution Prevention and Control Law, switching from coal consumption to natural gas consumption, and setting emission reduction targets for PM2.5 concentration in the 12th Five-Year Plan (2011–2015) [9, 10]. At the same time, many actions have also been taken to monitor PM2.5. For example, China has established thousands of PM2.5 monitoring observatories, which have been reporting hourly and daily air quality since 2012. Additionally, China's grassroots government has intensified supervision of straw burning in rural areas to curb haze pollution.

Concurrently, an increasing number of scholars have begun to pay attention to the field of PM2.5 pollution and have provided some corresponding policy implications with respect to curbing it. Given that PM2.5 concentration has mainly been driven by human activities, such as vehicle emissions, power generation, and industrial production, many studies have paid specific attention to the impacts of socioeconomic drivers on PM2.5 pollution [11–14]. For example, Ma et al. [15] analyzed the relationships among GDP per capita, the price of refined oil, vehicle population, energy intensity, and PM2.5 concentration in 152 Chinese cities based on spatial linkage and found that the impacts of economic, social, and energy efficiency on different cities varied significantly. Similarly, Zhang et al. [16] used the log-mean Divisia index (LMDI) method to break down changes in the PM2.5 concentration in these 152 cities. Their results showed that the decline of PM2.5 concentration was mainly driven by energy intensity and emission intensity, while GDP per capita and population were responsible for the increasing PM2.5 concentration. Among the driving factors of PM2.5 concentration, many socioeconomic factors have been found to contribute to the increase in PM2.5 emissions and concentration. These factors, such as increasing urbanization, economic growth, and population growth, are difficult to reduce in order to decrease PM2.5 pollution. Therefore, several studies have focused on factors that directly contribute to reducing PM2.5 pollution.

Among many economic factors, technological progress has been considered to play an important inhibitory role [17, 18]. In particular, Chen et al. [18] studied the effects of foreign direction investment, export learning effects, research and development, and import technology on the reduction of PM2.5 concentrations in 48 Chinese cities during 2000–2015. Likewise, Li et al. [19] used spatial econometric models to study the potential relationship between environmental total factor productivity and 283 Chinese cities during 2000–2013. Similarly, Xu et al. [20] analyzed the impacts of total factor productivity on 281 prefecture-level cities in China from 2007 to 2017 based on a spatial dynamic panel model, concluding that technological progress has significant positive effects on alleviating PM2.5 concentration. In total, these studies have only considered energy technologies or total factor productivity, ignoring the effects of PM2.5 emission reduction technology (PME). There is no doubt that improvements to energy efficiency can reduce energy input and decrease PM2.5 emissions; however, there is a need to pay more attention to PME changes, since these determine the PM2.5 pollution produced under the same unit of energy consumption and economic output and directly influence the level of cities' sustainable development.

In the light of existing literature, although scholars have studied the impacts of drivers on PM2.5 pollution in China's prefecture-level cities from a socioeconomic perspective, the current literature on PM2.5 concentrations has several shortcomings. (1) Some scholars have analyzed the impacts of technological progress on PM2.5 pollution, but few studies have examined the impacts of PME changes on China's city-level PM2.5 pollution; (2) many studies have concluded that there is significant spatial and temporal heterogeneity in the determinants of PM2.5 pollution based on spatial econometrics, but have not outlined detailed temporal changes; and (3) although some scholars have used the LMDI method to analyze determinants of temporal PM2.5 pollution changes, they have not considered spatial differences, especially within classified groups.

Hence, this study explores the impacts of PME changes on PM2.5 concentrations of 262 Chinese cities during 2003–2017. First, we applied three spatial econometric models (SDM, SAR, and SEM) to identify the spatial autocorrelation and potential relationship between PME changes and PM2.5 concentrations. Next, we decomposed the temporal and spatial changes in the PM2.5 concentrations of the 262 cities based on the combination of LMDI and $k$-means clustering methods. Our study makes the following contributions and findings: (1) we estimate the PM2.5 PME of 262 cities and analyze its impacts on China's city-level PM2.5 concentration; (2) the results show that there have been turning points in the yearly impacts, indicating that improvements to the emission reduction efficiency have been limited and unstable; and (3) based on the combination of $k$-means clustering and spatial LMDI methods, we find that the gaps among the spatial decomposition in our classified three groups were stable in the period 2003–2017, implying that the ranking of the emission reduction technology development level of each prefecture-level city in each group was relatively stable.

## 2. Materials and Methods

*2.1. Spatial Impacts of PME on PM2.5 Concentrations.* In light of the modified production-theoretical decomposition analysis method proposed by Wang et al. [21], we first estimated the PME during 2001–2017. We selected three input factors, one desirable output, and one undesirable output: fixed capital stocks, employed population, energy consumption, real GDP, and PM2.5 concentrations. The calculation of PME was based on the Shephard distance functions:

$$
\begin{aligned}
&\mathrm{D}^{s}_{pm}\left(K^{t}_{i}, \mathrm{L}^{t}_{i}, E^{t}_{i}, PM^{t}_{i}\right) = \min \theta \\
&\text{s.t.} \quad \sum_{n=1}^{N} z_n E^{s}_{n} \le E^{t}_{n} + \tau_n, \\
&\sum_{n=1}^{N} z_n K^{s}_{n} \le K^{t}_{n} + \tau_n, \\
&\sum_{n=1}^{N} z_n L^{s}_{n} \le L^{t}_{n} + \tau_n, \\
&\sum_{n=1}^{N} z_n Y^{s}_{n} \ge Y^{t}_{n}, \\
&\sum_{n=1}^{N} z_n PM^{s}_{n} = \theta PM^{t}_{n}, \\
&z_n \ge 0, \quad n = 1, \ldots, N, \\
&\tau_n \ge 0, \quad n = 1, \ldots, N, \\
&s, t \in \{0, T\}, \\
&s \ne t,
\end{aligned}
\tag{1}
$$

where $K$ represents fixed capital stocks, $L$ represents labor force, $E$ represents energy consumption, $PM$ represents PM2.5 concentration, $Y$ represents gross domestic output, and $\theta$ represents PM2.5 reduction efficiency.

Thus, the PME can be estimated using the following equation:

$$PME = \left( \frac{D_{pm}^{t}\left(K_i^t, L_i^t, E_i^t, PM_i^t\right) \times D_{pm}^{t+1}\left(K_i^t, L_i^t, E_i^t, PM_i^t\right)}{D_{pm}^{t+1}\left(K_i^{t+1}, L_i^{t+1}, E_i^{t+1}, PM_i^{t+1}\right) \times D_{pm}^{t}\left(K_i^{t+1}, L_i^{t+1}, E_i^{t+1}, PM_i^{t+1}\right)} \right)^{(1/2)}, \tag{2}$$

where $PME$ denotes emission reduction technological changes.

Based on previous studies [22], we further used spatial econometric methods to explore the potential spatial impacts of PME on PM2.5 concentration. The spatial models of Durbin (SDM), autoregression (SAR), and error (SEM) were selected. The normal form of spatial econometric model is given as

$$PM = \lambda WPM + X\beta + \theta WX + \varepsilon, \tag{3}$$

where $PM$ represents PM2.5 concentration, $X$ represents explanatory variables, $W$ is the spatial distance weight matrix, and $\varepsilon$ is the error term. We used the reciprocal of the geographical distance of the city center to construct the spatial econometric weight.

*2.2. The Temporal and Spatial LMDI Methods.* Although spatial regression methods have the ability to reveal potential relationship between the expected values of PME and PM2.5 concentrations, they ignore temporal and spatial changes. Thus, we used the index decomposition analysis (IDA) method to analyze the yearly and spatial impacts of PME on PM2.5 concentration. In light of previous studies (e.g., [11, 16]), the IDA identity of PM2.5 concentrations can be described as follows:

$$PM_i^t = \frac{PM_i^t}{E_i^t} \times \frac{E_i^t}{Y_i^t} \times \frac{Y_i^t}{P_i^t} \times P_i^t, \tag{4}$$

where $PM_i^t$ denotes the $i$th city's PM2.5 concentration in period $t$, $E_i^t$ represents the $i$th city's energy consumption in period $t$, $Y_i^t$ is the $i$th city's real gross domestic productivity in period $t$, and $P_i^t$ denotes the $i$th city's population in period $t$.

Based on a proposition by Zhou and Ang [23], we can obtain the following equation:

$$\begin{aligned} PM_i^t = {} & \frac{PM_i^t / \left(D_{PM}\left(E_i^t, K_i^t, L_i^t, PM_i^t; t\right) \times D_{PM}\left(E_i^t, K_i^t, L_i^t, PM_i^t; 0\right)\right)^{0.5}}{E_i^t} \cdot \\ & \times \frac{E_i^t}{Y_i^t} \times \frac{Y_i^t}{P_i^t} \times P_i^t \times \left(D_{PM}\left(E_i^t, K_i^t, L_i^t, PM_i^t; t\right) \times D_{PM}\left(E_i^t, K_i^t, L_i^t, PM_i^t; 0\right)\right)^{0.5}. \end{aligned} \tag{5}$$

To simplify equation (5), it can be written as follows:

$$PM_i^t = PPME_i^t \times EI_i^t \times PI_i^t \times P_i^t \times PME_i^t, \tag{6}$$

where $PPME_i^t$ denotes the $i$th city's potential emission intensity of PM2.5 concentration without technological change's impacts in period $t$; $EI_i^t$ represents the $i$th city's energy intensity in period $t$, which reflects energy efficiency; $PI_i^t$ represents the $i$th city's GDP per capita in period $t$; and $\mathrm{PME}_i^t$ represents the $i$th city's PM2.5 emissions efficiency in period $t$, whose changes reflect the changes in PME.

Next, considering that there may be strong spatial heterogeneity in the effects of PME, we adopted a spatial clustering decomposition analysis method in this study. As described by Cheng et al. [24], this method entails a combination of spatial index decomposition analysis and clustering methods. In particular, we adopted the LMDI method to study the impacts of the five driving forces on PM2.5 concentrations because it is robust, easily understood, and has clear economic meaning. Appendix A presents the formula of the temporal and spatial LMDI method, which can indicate the temporal and spatial impacts of the five driving forces on PM2.5 concentration.

*2.3. The Cluster Method.* Regarding traditional spatial LMDI method, it is necessary to select a reference for the spatial index decomposition analysis. Normally, the average of total samples' may be used as a reference. However, it will ignore heterogeneity between and within groups. Thus, the clustering method was adopted in this study to combine with the traditional spatial LMDI method, better capturing differences between and within groups.

With regard to the clustering method, hierarchical and nonhierarchical cluster methods are the two main approaches used. The algorithms of hierarchical cluster analysis are related to the construction of the tree structure of clusters, while that of nonhierarchical cluster analysis aims to classify objects into a

predetermined number of disjointed clusters. Thus, we use a nonhierarchical cluster to make classifications among the observed cities. In particular, we selected *k*-means clustering because the algorithm has exhibited high efficiency and empirical success [25, 26] and has been widely adopted in many fields of study, such as environmental analysis, image classification, and so on [24, 27]. However, the operations of *k*-means clustering analysis need to assume the number of center points in advance, leading to some uncertainty. To overcome this disadvantage, we first used hierarchical cluster analysis based on the shortest Euclidean distance to identify the dendrogram and classifications [28] so as to provide a more intuitive and reasonable reference for the number of center points selected for *k*-means methods.

Additionally, with regard to the cluster indicators, the cities' PM2.5 concentrations and GDP in 2017 were considered. Given that the PM2.5 emission intensity (i.e., ratio of PM2.5 concentration to GDP), like carbon intensity, has often been used to represent the level of PME [16], PM2.5 concentrations and GDP would perform well in revealing the clustering and classifications of PME. Thus, we selected cities' PM2.5 concentrations and GDP in 2017 for this purpose.

The resulting dendrogram based on hierarchical cluster analysis is presented in Figure 1. From the dendrogram, we can clearly observe the clustering process of each sample. In total, 262 cities can be divided into 28 categories based on the shortest Euclidean distance. From the right to left, the 18th category can be regarded as a single big category, and the 17th category can also be regarded as a separate category. In addition, the 23rd category and the remaining categories can be combined into one big category. Therefore, we speculated that the cities may be classified into three categories. Thus, we preset the number of center points as three. Next, based on the main idea of the *k*-means clustering algorithm, we continuously optimize the selection of the center points according to the Euclidean distance between each point and the center point, until the center points are stable.

*2.4. Data.* Using the equations above, city-level data were derived for PM2.5 concentrations, energy consumption, fixed capital stock, population, and real GDP. Given the availability of PM2.5 concentration and fixed capital stock data, this paper focused on 262 cities, and the research period spanned from 2003 to 2017.

The data for PM2.5 concentrations were obtained from the real-time monitoring of the Ministry of Ecology and Environment monitoring site (https://106.37.208.233:20035). We estimated the data for city-level energy consumption based on city-level $CO_2$ emissions, as proposed by Chen et al. [29], due to the significant relationship between energy use and $CO_2$ emissions. The economic output was taken from the China Statistical Yearbook (2003–2017). To avoid the influence of price, we used the price in 2001 as the constant price and obtained the real GDP, which is consistent with the approach used by Chen et al. [30]. Additionally, we calculated the fixed capital stock based on the perpetual inventory method, which is consistent with Chen et al. [31].

## 3. Results and Discussion

*3.1. The Results of Spatial Regressions.* Based on the spatial econometric method outlined in Section 2.1, we used fixed effects, spatial Durbin (SDM), autoregression (SAR), and error (SEM) models to analyze the relationship between PM2.5 concentrations and PME. In line with Hao et al. [32], we selected GDP and population as the control variables. Table 1 shows the results. Among them, *P* denotes population and *Y* denotes GDP.

Column (1) shows that there was a significant negative relationship between PM2.5 concentrations and PME, indicating that PME helpfully reduced PM2.5 concentrations. Columns (2)–(4) imply that there should be spatial heterogeneity. At the same time, the SDM and SAR models individually report the direct, indirect, and total effects of PME progress, indicating that the impacts of PME on different regions' PM2.5 concentrations may vary by regions. In total, the regressions results indicate that China's PME has generally reduced the cities' PM2.5 concentration.

*3.2. Drivers of the Temporal Changes in PM2.5 Concentrations.* Based on the temporal LMDI method outlined in Section 2.2, we categorized the city-level changes in PM2.5 concentrations into five main driving forces that pertain to the influences of energy use. Given that there are no official data about city-level energy use, some scholars have used electronic power consumption to replace total energy use. However, such replacement may cause significant errors, since fluctuations in electronic power use are inconsistent with total energy combustion. Therefore, we calculated the energy use of the 262 cities during 2003–2017 based on data on city-level $CO_2$ emissions, as proposed by Chen et al. [29].

Considering that the calculation of city-level $CO_2$ emissions followed a top-down approach (i.e., provinces and cities), the corresponding city-level energy use can be estimated according to city-level $CO_2$ emissions and the relationship between provincial $CO_2$ emissions and energy consumption. To capture the provincial differences in the ratio of $CO_2$ emission to energy use, we used the varied coefficient model to conduct a regression between provincial $CO_2$ emissions and energy consumption during 1997–2017. At the same time, to avoid the negative values of city-level energy use, we used a no-constant model. Table 2 in Appendix A presents the results.

Evidently, the coefficient of determination was 0.986, implying that the estimated city-level energy consumption was highly accurate. Based on the city-level energy use, we can obtain the impacts of driving forces on the PM2.5 concentrations of the 262 cities.

To capture more temporal fluctuations of PME impacts, we divided the period of 2003–2016 into four parts: 2003–2006, 2006–2009, 2009–2012, and 2012–2017. These results are presented in Figure 2. They show that not all cities' PME continuously decreased the PM2.5 concentrations during 2003–2017, and detailed information thereon cannot be found based on regressions. At the same time,

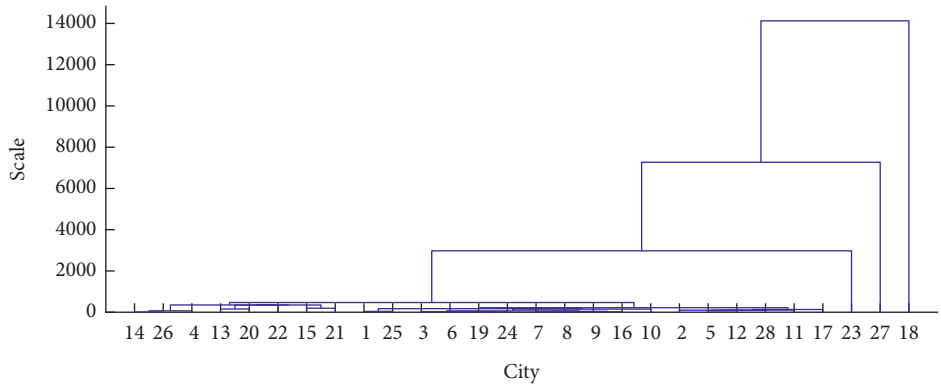


Figure 1: Hierarchical cluster results.

Table 1: Spatial econometric results of the four models.

| | Fe (1) | SDM (2) | SAR (3) | SEM (4) |
|---|---|---|---|---|
| *P* | 0.000000519***(1.26*E* − 07) | 1.40*E* − 07 (0.000000102) | −0.000000161*(9.63*E* − 08) | −1.54*E* − 07 (1.01*E* − 07) |
| PME | −0.24***(0.06) | −0.19***(0.05) | −0.211***(0.04) | −0.20***(0.05) |
| *Y* | 0.0003103***(0.0000927) | 0.0000706(0.0000447) | 0.0000781**(0.0000371) | 0.0000741*(0.0000447) |
| *Wx* | | | | |
| *P* | | −3.31*E* − 07 (6.25*E* − 07) | | |
| PME | | −0.17 (0.16) | | |
| *Y* | | 0.0000593 (0.0001256) | | |
| Rho | | 1.04***(0.0070891) | | |
| Lambda | | | 1.04***(0.0071271) | |
| *LR_direct* | | | | |
| *P* | | −0.000000204*(1.22*E* − 07) | −1.78*E* − 07 (1.13*E* − 07) | |
| PME | | 0.24***(0.0536886) | −0.24***(0.05) | |
| *Y* | | 0.000094**(0.0000446) | 0.0000929**( 0.0000409) | |
| LR_indirect | | | | |
| *P* | | −0.0000173 (0.0000222) | −5.40*E* − 06 (3.77*E* − 06) | |
| PME | | −12.38*(6.97) | −7.23***(2.42) | |
| *Y* | | 0.0047381 (0.0042833) | 0.0028055*(0.0015252) | |
| *LR_total* | | | | |
| p | | −0.0000175 (0.0000223) | −5.57*E* − 06 (3.87*E* − 06) | |
| PME | | −12.62*(6.99) | −7.47***(2.46) | |
| y | | 0.0048321 (0.0042962) | 0.0028983*(0.001561) | |
| *N* | 262 | 262 | 262 | 262 |

*Note*. *, **, and *** denote statistical significance levels at 10%, 5%, and 1%, respectively.

there were many turning points in the impacts of PME changes on PM2.5 concentrations, which again cannot be captured by regressions.

Given that serious PM2.5 emissions always occurred in large cities, we selected PME impacts in Beijing, Shanghai, Guangzhou, and Shenzhen for analysis. In particular, Beijing's PME impacts changed by about −0.59, −14.84, and −4.50 ug/m$^3$ in the periods of 2003–2006, 2006–2009, and 2013–2017, respectively; however, it increased by about 4.49 ug/m$^3$ during 2009–2013. PME changes reduced Shanghai's PM2.5 concentrations from 2003 to 2006 (−0.43 ug/m$^3$), while they increased by about 0.30, 9.30, and 8.18 ug/m$^3$ during 2006–2009, 2009–2013, and 2013–2017, respectively. Guangzhou's PME changes had a negative impact during 2009–2013 (−6.29 ug/m$^3$), while it stimulated PM2.5 concentrations in the other periods (+4.34, +0.56, and +7.81 ug/m$^3$). Shenzhen decreased its PM2.5 concentrations in 2003–2006 and 2009–2013 (−0.82 and −5.66 ug/m$^3$), but increased them in the periods 2006–2009 and 2013–2017 (+2.68 and + 2.91 ug/m$^3$, resp.). Evidently, Beijing fared better than the other three cities in developing PME, especially after 2013; this is consistent with Yang et al. [14] and Zíková et al.'s [33] findings. The reasons for this may derive from the issuance and implementation of more stringent policies related to smog control in the Beijing–Tianjin–Hebei region in 2012, such as "Beijing–Tianjin–Hebei regional environmental protection takes the lead in breaking through the cooperation framework agreement," switching from coal consumption to natural gas consumption, and implementation of the Atmospheric Pollution Prevention and Control Action Plan [11, 34].

Table 2: Regression between provincial $CO_2$ emissions and energy consumption based on the variable coefficient model.

| | Coefficient | Standard error | *P*-value |
|---|---|---|---|
| $CO_2$ emissions | 49.07 | 1.83 | ≤0.001 |
| id#c.$CO_2$ emissions | | | |
| Yunan | −23.22 | 2.16 | ≤0.001 |
| Inner Mongolia | 89.95 | 3.96 | ≤0.001 |
| Beijing | 17.42 | 4.23 | ≤0.001 |
| Jilin | −30.34 | 2.05 | ≤0.001 |
| Sichuan | 82.65 | 3.50 | ≤0.001 |
| Tianjin | −21.72 | 2.46 | ≤0.001 |
| Ningxia | 57.76 | 10.25 | ≤0.001 |
| Anhui | −12.96 | 2.30 | ≤0.001 |
| Shandong | 31.09 | 2.07 | ≤0.001 |
| Shanxi | 39.99 | 2.74 | ≤0.001 |
| Guangdong | 103.77 | 2.95 | ≤0.001 |
| Guangxi | −10.29 | 2.66 | ≤0.001 |
| Xinjiang | 11.02 | 2.89 | ≤0.001 |
| Jiangsu | −5.69 | 1.95 | 0.004 |
| Jiangxi | −7.98 | 3.03 | 0.009 |
| Hebei | 8.32 | 2.02 | ≤0.001 |
| Henan | 19.66 | 2.26 | ≤0.001 |
| Zhejiang | 71.60 | 3.38 | ≤0.001 |
| Hainan | −46.77 | 1.93 | ≤0.001 |
| Hubei | 9.60 | 2.42 | ≤0.001 |
| Hunan | 19.80 | 2.71 | ≤0.001 |
| Gansu | −35.43 | 2.02 | ≤0.001 |
| Gujian | 26.39 | 3.54 | ≤0.001 |
| Guizhou | 220.59 | 12.52 | ≤0.001 |
| Liaoning | −8.40 | 2.01 | ≤0.001 |
| Chongqing | −10.25 | 2.73 | ≤0.001 |
| Shaanxi | −16.14 | 2.31 | ≤0.001 |
| Qinghai | −44.93 | 1.91 | ≤0.001 |
| Heilongjiang | −0.97 | 2.48 | 0.690 |
| *N* | | 630 | |
| *R* | | 0.9861 | |
| *F*(30, 600) | | 1420.9*** | |

*Note*. *, **, and *** denote statistical significance levels at 10%, 5%, and 1%, respectively.

Figure 3 presents the impacts of the other four driving forces on PM2.5 concentrations. Potential emission intensity in 210 cities curbed PM2.5 concentrations, reflecting the optimization of the energy consumption structure. In particular, Jinchang (−42.93 ug/$m^3$), Hengshui (−40.87 ug/$m^3$), Anshan (−38.13 ug/$m^3$), Daqing (−37.39 ug/$m^3$), and Baoding (−33.40 ug/$m^3$) were the top five cities whose potential emission intensity decreased PM2.5 concentrations during 2003–2017. Energy intensity had reduction effects on PM2.5 concentrations in all observed cities during 2003–2017, which is consistent with Chen et al. [11], Zhang et al. [16], and Li et al. [35]. The results indicate that the improvement in energy efficiency may be responsible for energy conservation, leading to the decline in PM2.5 concentrations. GDP per capita and population in almost all cities contributed to increasing PM2.5 concentrations during 2003–2017. Among them, Zhengzhou's GDP per capita and Shengzhen's population individually contributed to the highest increases, of 139.21 and 29.85 ug/$m^3$, respectively.

*3.3. PME for the Spatial Changes in PM2.5 Concentrations among Cluster Cities.* Based on the above-described clustering methods, we divided the 262 cities into three groups. The first group was concentrated on the cities with the largest emissions intensity (0.026 ug/$m^{3*}$million yuan, averagely); the second group had the middle emissions intensity (0.006 ug/$m^{3*}$million yuan, averagely); and the third group's average emissions intensity were the lowest (0.002 ug/$m^{3*}$million yuan). The detailed classification is presented in Appendix A, Table 3.

Then, we studied the impacts of PME changes on within-group differences of PM2.5 concentrations. Figure 4 reports the impacts of PME on PM2.5 concentrations between each city and the classified group's average in 2003 and 2017.

Regarding the cities in the first group, 141 cities' PME contributed to negative differences within the first group's PM2.5 concentrations and reduced the within-group differences when the average PM2.5 concentrations in the first group in 2003 were set as the reference, indicating that these cities' PME did better than their average level. And there were 75 cities' PME stimulated within-group differences, implying that they failed to reach their groups' average level. Taking six cities in 2003 as examples, Daqing (−176.31 ug/$m^3$), Taizhou (−161.50 ug/$m^3$), and Xiamen (−147.90 ug/$m^3$)

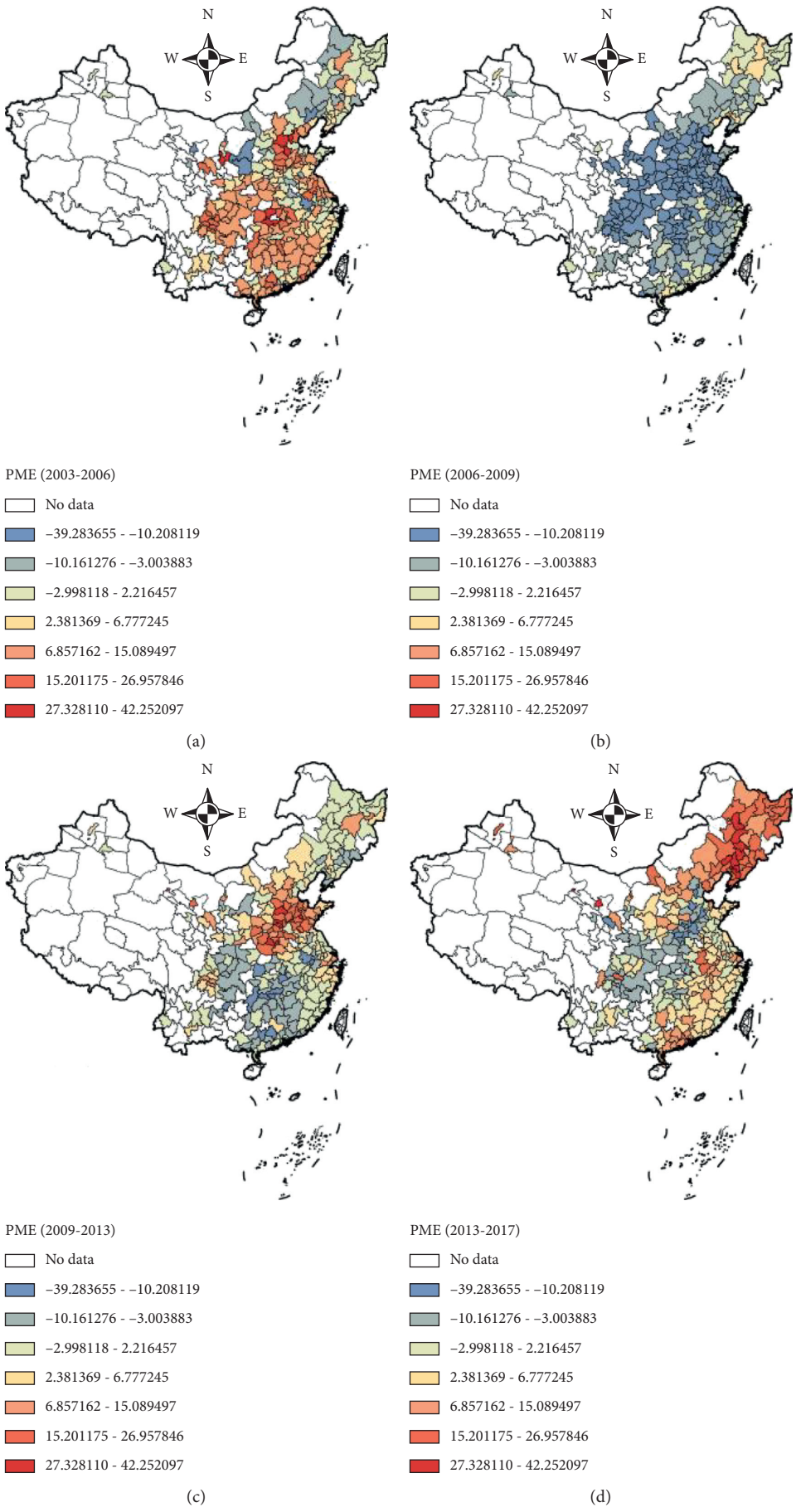


Figure 2: The effects of PME on PM2.5 concentrations during the periods of 2003–2006, 2006–2009, 2009–2013, and 2013–2017.

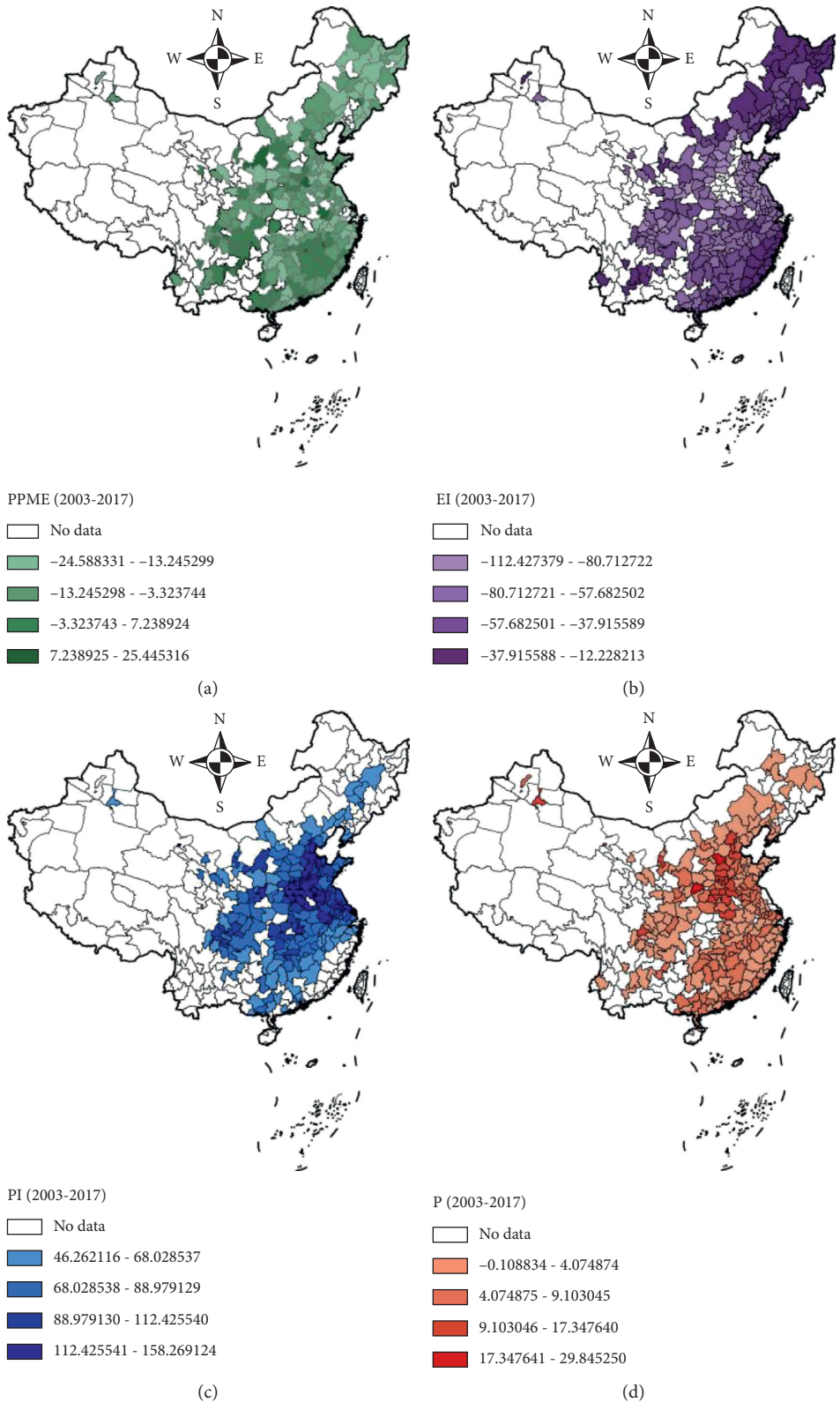


Figure 3: The effects of potential emission intensity, energy intensity, GDP per capita, and population on PM2.5 concentrations during 2003–2017.

Table 3: List of city clusters.

| Cluster | City name | Number of cities |
|---|---|---|
| First group | Ankang, Anqing, Anshun, Anyang, Anshan, Bazhong, Baicheng, Baishan, Baiyin, Bengbu, Baotou, Baoji, Baoding, Baoshan, Beihai, Benxi, Binzhou, Cangzhou, Changde, Chaoyang, Chaozhou, Chenzhou, Chengde, Chizhou, Chifeng, Chuzhou, Dazhou, Daqing, Datong, Dandong, Deyang, Dezhou, Dongying, Fangchenggang, Fushun, Fuzhou, Fuxin, Fuyang, Ganzhou, Guang'an, Guangyuan, Guigang, Guiyang, Guilin, Haikou, Handan, Hanzhong, Heyuan, Heze, Hebi, Hegang, Heihe, Hengshui, Hengyang, Hohhot, Huludao Huaihua, Huai'an, Huaibei, Huainan, Huanggang, Huangshan, Huangshi, Jixi, Ji'an, Jilin, Jiamusi, Jiaxing, Jiayuguan, Jiangmen, Jiaozuo, Jieyang, Jinchang, Jinhua, Jinzhou, Jincheng, Jinzhong, Jingmen, Jingdezhen, Jiujiang, Kaifeng, Karamay, Laiwu, Lanzhou, Langfang, Leshan, Lishui, Lianyungang, Liaoyang, Liaoyuan, Liaocheng, Linfen, Linyi, Liuzhou, Liuan, Liupanshui, Longyan, Loudi, Luzhou, Luoyang, Luohe, Ma'anshan, Maoming, Meishan, Meizhou, Mianyang, Mudanjiang, Nanchong, Nanning, Nanping, Neijiang, Ningde, Panzhihua, Panjin, Pingdingshan, Pingxiang, Putian, Puyang, Qitaihe, Qiqihar, Qinzhou, Qinhuangdao, Qingyuan, Quzhou, Qujing, Rizhao, Sanmenxia, Sanming, Sanya, Xiamen, Shantou, Shanwei, Shangqiu, Shangrao, Shaoguan, Shaoyang, Shiyan, Shizuishan, Shuangyashan, Shuozhou, Siping, Songyuan, Suihua, Suizhou, Suining, Taizhou, Taiyuan, Tai'an, Tianshui, Tieling, Tonghua, Tongliao, Tongchuan, Tongling, Weihai, Weinan, Wuhai, Urumqi, Wuhu, Wuzhong, Wuzhou, Xining, Xianning, Xianyang, Xiangtan, Xiaogan, Xinzhou, Xinxiang, Xinyu, Xinyang, Xingtai, Suqian, Suzhou, Xuchang, Xuancheng, Ya'an, Yan'an, Yangjiang, Yangquan, Yichun, Yibin, Yichang, Yichun, Yiyang, Yinchuan, Yingtan, Yingkou, Yongzhou, Yulin, Yuxi, Yueyang, Yunfu, Yuncheng, Zaozhuang, Zhanjiang, Zhangjiajie, Zhangjiakou, Zhangzhou, Changzhi, Zhaoqing, Zhenjiang, Zhongshan, Zhoushan, Zhoukou, Zhuhai, Zhuzhou, Zhumadian, Ziyang, Zigong, Zunyi | 216 |
| Second group | Changzhou, Chengdu, Dalian, Dongguan, Foshan, Fuzhou, Harbin, Hangzhou, Hefei, Jinan, Jining, Kunming, Nanchang, Nanjing, Nantong, Ningbo, Qingdao, Quanzhou, Shaoxing, Shenyang, Shijiazhuang, Taizhou, Tangshan, Weifang, Wenzhou, Wuxi, Wuhan, Xi'an, Xuzhou, Yantai, Yancheng, Yangzhou, Changchun, Changsha, Zhengzhou, Zibo | 36 |
| Third group | Beijing, Guangzhou, Shanghai, Shenzhen, Suzhou, Tianjin, Chongqing | 7 |

*, **, and *** denote statistical significance levels at 10%, 5%, and 1%, respectively.

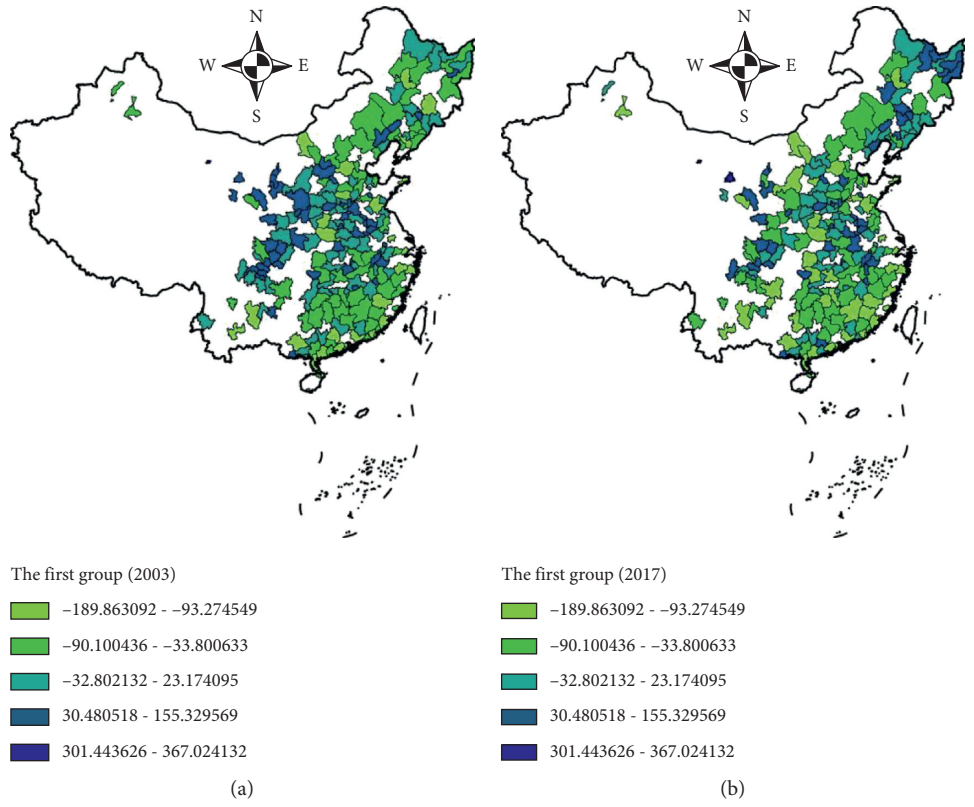


Figure 4: Continued.

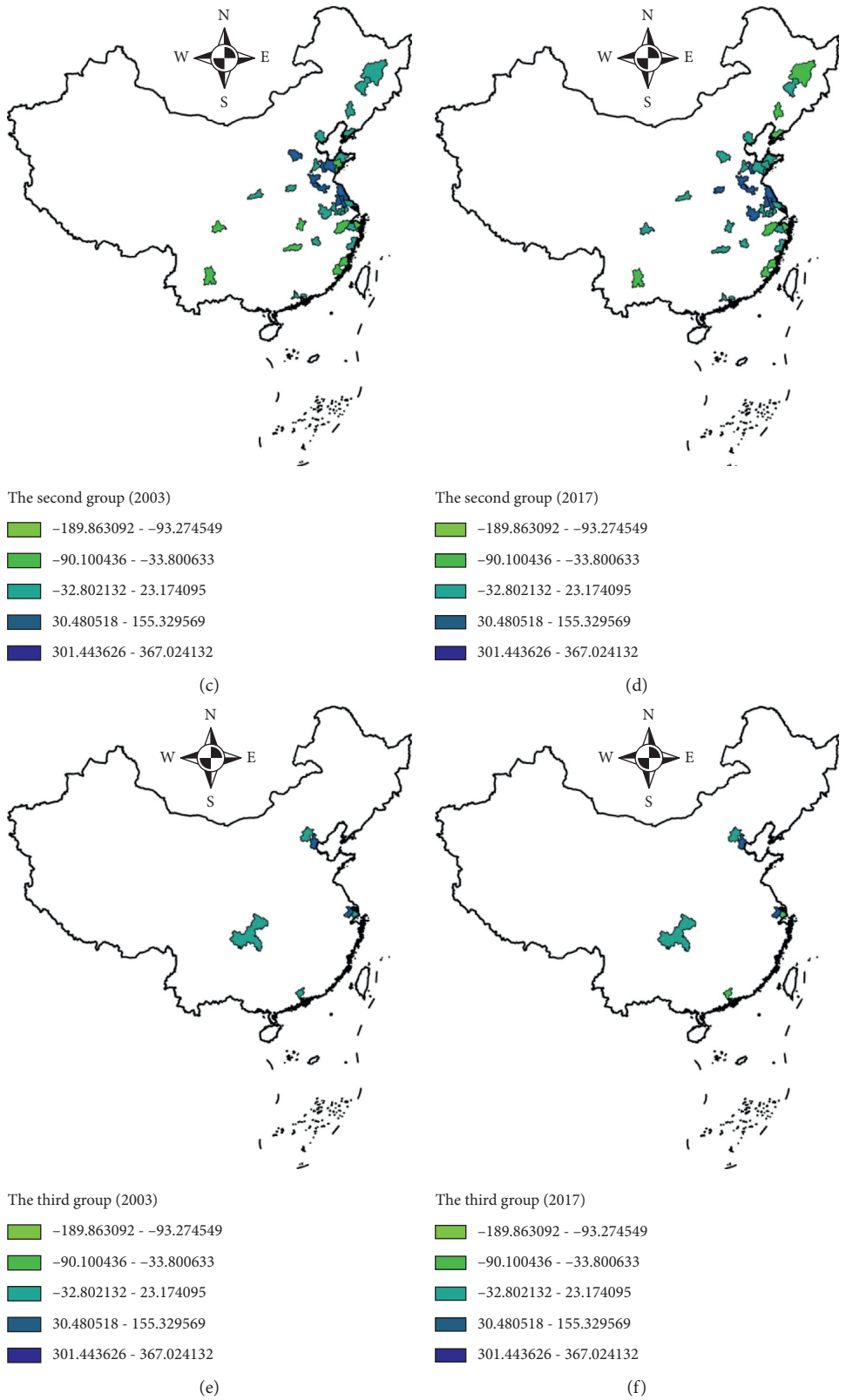


Figure 4: The impacts of emission reduction technological changes on PM2.5 concentrations between each city and the classified group's average.

were the top three cities with negative differences. Meanwhile, Jiayuguan (+270.48 ug/m$^3$), Jinchang (+152.6 ug/m$^3$), and Tongchuan (+151.10 ug/m$^3$) were the top three cities that contributed to positive within-group differences. Compared with 2003, there were several changes in the spatial decomposition results in 2017: 147 cities' PME lowered the between-emissions differences within the first group's PM2.5 concentrations, but PME changes in 69 cities caused a positive within-group gap. For example, Ankang city's PME reduced the within-group gap in 2013 (−54.28 ug/m$^3$) but failed in 2017 (+9.82 ug/m$^3$).

In the second group, the PME in 20 cities led to reductions in the within-group differences in 2003, and 16 cities' emission reductions caused positive within-group differences. Particularly, PME in the cities of Quanzhou (−51.10 ug/m$^3$), Hangzhou (−50.30 ug/m$^3$), and Fuzhou (−47.35 ug/m$^3$) contributed to a decline in the within-group difference, while Hefei (+54.07 ug/m$^3$), Taizhou (+52.57 ug/m$^3$), and Jining (+51.09 ug/m$^3$) saw an increase of the within-group gap. Moreover, there were 18 cities in which PME helped to reduce the within-group differences in 2017, implying that the spatial differences did not change much in these cities.

With regard to the third group, PME in the first-tier cities (Shanghai, −53.98 ug/m$^3$; Guangzhou, −35.47 ug/m$^3$; Shenzhen, −30.03 ug/m$^3$; and Beijing, −14.17 ug/m$^3$) contributed to reductions in the within-group differences in 2003. However, the PME of Tianjin, Suzhou, and Chongqing increased to 55.82, 24.16, and 19.30 ug/m$^3$ of the within-group differences, respectively. In 2017, the four first-tier cities' and Chongqing city's PME changes were responsible for the negative within-group differences (Shanghai, −18.89 ug/m$^3$; Guangzhou, −16.15 ug/m$^3$; Shenzhen, −27.79 ug/m$^3$; Beijing, −24.41 ug/m$^3$; and Chongqing, −10.41 ug/m$^3$), and the remaining cities still contributed to positive within-group gaps (Tianjin, +18.89 ug/m$^3$; Suzhou, +35.19 ug/m$^3$).

In summary, since most cities' PME contributed to negative impacts on the within-group differences, indicating that most cities' PME was better than their group's average level. However, it also should be noted that the PME of a small number of cities, such as Jiayuguan city and Tongchuan city, were lower than their groups' average level and had a very weak impact on curbing PM2.5 concentrations, which is consistent with the results proposed by Zhang et al. [16]. At the same time, the distributions of the spatial decomposition of the three groups were stable in the period of 2002–2017, implying that the catch-up effect within the group was not obvious. Thus, the governments should focus more on regional heterogeneity when encouraging the promotion of PM2.5 emission reduction technologies.

## 4. Conclusions

This study explored the impacts of PME changes on the PM2.5 concentrations of 262 Chinese cities during 2002–2017. First, we applied three spatial econometric models (SDM, SAR, and SEM), identifying the spatial autocorrelation and potential relationship between PME changes and PM2.5 concentrations. Furthermore, we decomposed the temporal and spatial changes in the 262 cities' PM2.5 concentrations based on a combination of LMDI and *k*-means clustering methods. In terms of the temporal changes, we found that most cities' PME impacts fluctuated during 2002–2017, and there were many turning points, indicating that the reduction effects in many cities were not stable. However, energy intensity continuously played a significant role in decreasing PM2.5 concentrations due to energy conservation caused by the improvement in energy efficiency. With regard to the spatial decomposition based on clusters, we found that most cities' PME contributed to negative differences, implying that the PME in a small number of cities, such as Jiayuguan City and Jinchang City, was not strong and lowered the average level of their group. At the same time, the distributions of the spatial decomposition of the three groups were stable in the period 2002–2017, implying that a catch-up effect within the group was not obvious.

Based on the analysis, we provide several policy implications for curbing PM2.5 concentrations from a socioeconomic perspective. First, although the results, based on econometric methods, show that PME progress had significant curbing impacts on China's city-level PM2.5 concentrations, the temporal and regional heterogeneity cannot be ignored. Given that the PME failed to continuously decrease China's city-level PM2.5 concentration, China's cities should pay more attention to increased fiscal expenditures in technological innovations, such as composite carbon slurry clean combustion technology, supercritical flue gas desulfurization (FGD) systems, and ultra-supercritical FGD systems [21, 35].

Second, in addition to increasing PME, it is important to promote the application of energy-saving technologies and the optimization of energy use structures. In light of the effects of energy intensity on PM2.5 concentrations, the promotion of energy efficiency will reduce the energy input, thus reducing PM2.5 emissions and concentrations under the same conditions of PME. In addition, since PM2.5 pollution is mainly driven by fossil fuel combustion [36], speeding up the use of clean energy would also significantly reduce PM2.5 concentration.

Third, considering that the spatial impacts of PME were relatively stable over time, regional advanced emission reduction technological innovations should be promoted around and selected as demonstrations so that the catching-up effects within group will be highlighted.

## Appendix

The temporal impacts of drivers on PM2.5 concentration can be estimated based on equations (A2.1)–(A2.5):

$$\Delta PM_{i,PPME}^{b,t} = \frac{\left(PM_i^t - PM_i^b\right)}{\ln\left(PM_i^t/PM_i^b\right)} \times \ln\left(\frac{PPME_i^t}{PPME_i^b}\right), \quad \text{(A.1)}$$

$$\Delta PM_{i,EI}^{b,t} = \frac{\left(PM_i^t - PM_i^b\right)}{\ln\left(PM_i^t/PM_i^b\right)} \times \ln\left(\frac{EI_i^t}{EI_i^b}\right), \quad \text{(A.2)}$$

$$\Delta PM_{i,PI}^{b,t} = \frac{\left(PM_i^t - PM_i^b\right)}{\ln\left(PM_i^t/PM_i^b\right)} \times \ln\left(\frac{PI_i^t}{PI_i^b}\right), \quad (A.3)$$

$$\Delta PM_{i,P}^{b,t} = \frac{\left(PM_i^t - PM_i^b\right)}{\ln\left(PM_i^t/PM_i^b\right)} \times \ln\left(\frac{P_i^t}{P_i^b}\right), \quad (A.4)$$

$$\Delta PM_{i,PME}^{b,t} = \frac{\left(PM_i^t - PM_i^b\right)}{\ln\left(PM_i^t/PM_i^b\right)} \times \ln\left(\frac{PME_i^t}{PME_i^b}\right), \quad (A.5)$$

where $\Delta PM_{i,PPME}^{b,t}$ denotes the impacts of potential emission intensity on the $i$th city's PM2.5 concentration from period $b$ to $t$; $\Delta PM_{i,EI}^{b,t}$ denotes the impacts of energy intensity on the $i$th city's PM2.5 concentration from period $b$ to $t$; $\Delta PM_{i,PI}^{b,t}$ denotes the impacts of GDP per capita on the $i$th city's PM2.5 concentration from period $b$ to $t$; $\Delta PM_{i,P}^{b,t}$ denotes the impacts of population on the $i$th city's PM2.5 concentration from period $b$ to $t$; and $\Delta PM_{i,PME}^{b,t}$ denotes the impacts of PM2.5 emission efficiency on the $i$th city's PM2.5 concentration from period $b$ to $t$.

Similarly, based on the definite reference, the spatial LMDI method can also be used for spatial decomposition; the corresponding formulas are presented as follows:

$$\Delta PM_{i,PPME}^{r} = \frac{\left(PM_i^t - PM_r^t\right)}{\ln\left(PM_i^t/PM_r^t\right)} \times \ln\left(\frac{PPME_i^t}{PPME_r^t}\right), \quad (A.6)$$

$$\Delta PM_{i,EI}^{r} = \frac{\left(PM_i^t - PM_r^t\right)}{\ln\left(PM_i^t/PM_r^t\right)} \times \ln\left(\frac{EI_i^t}{EI_r^t}\right), \quad (A.7)$$

$$\Delta PM_{i,PI}^{r} = \frac{\left(PM_i^t - PM_r^t\right)}{\ln\left(PM_i^t/PM_r^t\right)} \times \ln\left(\frac{PI_i^t}{PI_r^t}\right), \quad (A.8)$$

$$\Delta PM_{i,P}^{r} = \frac{\left(PM_i^t - PM_r^t\right)}{\ln\left(PM_i^t/PM_r^t\right)} \times \ln\left(\frac{P_i^t}{P_r^t}\right), \quad (A.9)$$

$$\Delta \mathrm{PM}_{i,PME}^{r} = \frac{\left(PM_i^t - PM_r^t\right)}{\ln\left(PM_i^t/PM_r^t\right)} \times \ln\left(\frac{PME_i^t}{PME_r^t}\right), \quad (A.10)$$

where $\Delta PM_{i,PPME}^{r}$ denotes the gap between the impacts of potential emission intensity on the $i$th city's PM2.5 concentration and the reference; $\Delta PM_{i,EI}^{r}$ denotes the gap between the impacts of energy intensity on the $i$th city's PM2.5 concentration and the reference; $\Delta PM_{i,PI}^{r}$ denotes the difference between effects of GDP per capita on the $i$th city's PM2.5 concentration and the reference; $\Delta PM_{i,P}^{r}$ denotes the gap between the effects of population on the $i$th city's PM2.5 concentration; and the reference $\Delta PM_{i,PME}^{r}$ denotes the gap between the impacts of PM2.5 emission efficiency on the $i$th city's PM2.5 concentration and the reference.

## Data Availability

The data can be obtained upon request from the corresponding author.

## Additional Points

PM2.5 emission reduction technology (PME) was estimated for 262 cities. The 262 cities were classified into three groups based on the $k$-means cluster method. The curbing impacts of PME on PM2.5 were fluctuated and unstable. Energy intensity played a more stable role in PM2.5 emissions reductions. The catch-up and transcendence effects of PME within the group were limited.

## Conflicts of Interest

The authors declare that there are no conflicts of interest regarding the publication of this paper.

## Acknowledgments

This work was supported by the National Key Natural Science Foundation of China (Grant no. 71934001), the National Natural Science Foundation of China (Grant nos. 71471001, 41771568, 71533004, and 71503001), the National Key Research and Development Program of China (Grant no. 2016YFA0602500), Sichuan Province Social Science High-Level Research Team Building Program, and the Program for Major Projects in Philosophy and Social Science Research under China's Ministry of Education (Grant no. 14JZD031).

## References

[1] R. T. Burnett, C. A. Pope III, M. Ezzati et al., "An integrated risk function for estimating the global burden of disease attributable to ambient fine particulate matter exposure," *Environmental Health Perspectives*, vol. 122, no. 4, pp. 397–403, 2014.

[2] X. Ji, Y. Yao, and X. Long, "What causes PM2.5 pollution? Cross-economy empirical analysis from socioeconomic perspective," *Energy Policy*, vol. 119, pp. 458–472, 2018.

[3] K. Park, T. Yoon, C. Shim, E. Kang, Y. Hong, and Y. Lee, "Beyond strict regulations to achieve environmental and economic health—an optimal PM2.5 mitigation policy for Korea," *International Journal of Environmental Research and Public Health*, vol. 17, no. 16, p. 5725, 2020.

[4] R. Wu, H. Dai, Y. Geng et al., "Economic impacts from PM2.5 pollution-related health effects: a case study in Shanghai," *Environmental Science and Technology*, vol. 51, no. 9, pp. 5035–5042, 2017.

[5] H. Yin, M. Pizzol, and L. Xu, "External costs of PM2.5 pollution in Beijing, China: uncertainty analysis of multiple health impacts and costs," *Environmental Pollution*, vol. 226, pp. 356–369, 2017.

[6] G. Yu, F. Wang, J. Hu, Y. Liao, and X. Liu, "Value assessment of health losses caused by PM2.5 in Changsha City, China," *International Journal of Environmental Research and Public Health*, vol. 16, no. 11, p. 2063, 2019.

[7] F. Dong, B. Yu, and Y. Pan, "Examining the synergistic effect of CO2 emissions on PM2.5 emissions reduction: evidence from China," *Journal of Cleaner Production*, vol. 223, pp. 759–771, 2019.

[8] W. Fan, S. Wang, X. Gu, Z. Q. Zhou, Y. Zhao, and W. D. Huo, "Evolutionary game analysis on industrial pollution control of

local government in China," *Journal of Environmental Management*, vol. 298, p. 113499, 2021.

[9] J. Liu, Y. Han, X. Tang, J. Zhu, and T. Zhu, "Estimating adult mortality attributable to PM2.5 exposure in China with assimilated PM2.5 concentrations based on a ground monitoring network," *The Science of the Total Environment*, vol. 568, pp. 1253–1262, 2016.

[10] Q. Xiao, G. Geng, F. Liang et al., "Changes in spatial patterns of PM2.5 pollution in China 2000–2018: impact of clean air policies," *Environment International*, vol. 141, Article ID 105776, 2020.

[11] J. Chen, M. Gao, D. Li, L. Li, M. Song, and Q. Xie, "Changes in PM2.5 emissions in China: an extended chain and nested refined laspeyres index decomposition analysis," *Journal of Cleaner Production*, vol. 294, Article ID 126248, 2021.

[12] W. Lyu, Y. Li, D. Guan, H. Zhao, Q. Zhang, and Z. Liu, "Driving forces of Chinese primary air pollution emissions: an index decomposition analysis," *Journal of Cleaner Production*, vol. 133, pp. 136–144, 2016.

[13] G. Xu, X. Ren, K. Xiong, L. Li, X. Bi, and Q. Wu, "Analysis of the driving factors of PM2.5 concentration in the air: a case study of the Yangtze River Delta, China," *Ecological Indicators*, vol. 110, Article ID 105889, 2020.

[14] J. Yang, D. Song, D. Fang, and F. Wu, "Drivers of consumption-based PM2.5 emission of Beijing: a structural decomposition analysis," *Journal of Cleaner Production*, vol. 219, pp. 734–742, 2019.

[15] Y. R. Ma, Q. Ji, and Y. Fan, "Spatial linkage analysis of the impact of regional economic activities on PM2.5 pollution in China," *Journal of Cleaner Production*, vol. 139, pp. 1157–1167, 2016.

[16] Y. Zhang, C. Shuai, J. Bian, X. Chen, Y. Wu, and L. Shen, "Socioeconomic factors of PM2.5 concentrations in 152 Chinese cities: decomposition analysis using LMDI," *Journal of Cleaner Production*, vol. 218, pp. 96–107, 2019.

[17] J. Chen, M. Gao, M. Shahbaz, S. Cheng, and M. Song, "An improved decomposition approach toward energy rebound effects in China: review since 1992," *Renewable and Sustainable Energy Reviews*, vol. 145, Article ID 111141, 2021.

[18] J. Chen, S. Wang, C. Zhou, and M. Li, "Does the path of technological progress matter in mitigating China's PM2.5 concentrations? Evidence from three urban agglomerations in China," *Environmental Pollution*, vol. 254, Article ID 113012, 2019.

[19] D. Li, M. Gao, W. Hou, M. Song, and J. Chen, "A modified and improved method to measure economy-wide carbon rebound effects based on the PDA-MMI approach," *Energy Policy*, vol. 147, Article ID 111862, 2020.

[20] N. Xu, F. Zhang, and X. Xuan, "Impacts of industrial restructuring and technological progress on PM2.5 Pollution: evidence from prefecture-level cities in China," *International Journal of Environmental Research and Public Health*, vol. 18, no. 10, p. 5283, 2021.

[21] Q. Wang, Y. H. Chiu, and C. R. Chiu, "Driving factors behind carbon dioxide emissions in China: a modified production-theoretical decomposition analysis," *Energy Economics*, vol. 51, pp. 252–260, 2015.

[22] J. Chen, M. Gao, K. Ma, and M. Song, "Different effects of technological progress on China's carbon emissions based on sustainable development," *Business Strategy and the Environment*, vol. 29, no. 2, pp. 481–492, 2020.

[23] P. Zhou and B. W. Ang, "Decomposition of aggregate $CO_2$ emissions: a production-theoretical approach," *Energy Economics*, vol. 30, no. 3, pp. 1054–1067, 2008.

[24] S. Cheng, Y. Chen, F. Meng, J. Chen, G. Liu, and M. Song, "Impacts of local public expenditure on CO2 emissions in Chinese cities: a spatial cluster decomposition analysis," *Resources, Conservation and Recycling*, vol. 164, Article ID 105217, 2021.

[25] A. Likas, N. Vlassis, and J. J. Verbeek, "The global k-means clustering algorithm," *Pattern Recognition*, vol. 36, no. 2, pp. 451–461, 2003.

[26] H. Ralambondrainy, "A conceptual version of the k-means algorithm," *Pattern Recognition Letters*, vol. 16, no. 11, pp. 1147–1157, 1995.

[27] L. H. Juang and M. N. Wu, "Psoriasis image identification using k-means clustering with morphological processing," *Measurement*, vol. 44, no. 5, pp. 895–905, 2011.

[28] P. Trebuňa and J. Halčinová, "Experimental modelling of the cluster analysis processes," *Procedia Engineering*, vol. 48, pp. 673–678, 2012.

[29] J. Chen, M. Gao, S. Cheng et al., "China's city-level carbon emissions during 1992–2017 based on the inter-calibration of nighttime light data," *Scientific Reports*, vol. 11, no. 1, pp. 1–13, 2021.

[30] J. Chen, S. Cheng, M. Song, and J. Wang, "Interregional differences of coal carbon dioxide emissions in China," *Energy Policy*, vol. 96, pp. 1–13, 2016.

[31] X. Chen, F. Li, J. Zhang, W. Zhou, X. Wang, and H. Fu, "Spatiotemporal mapping and multiple driving forces identifying of PM2.5 variation and its joint management strategies across China," *Journal of Cleaner Production*, vol. 250, Article ID 119534, 2020b.

[32] Y. Hao and Y. M. Liu, "The influential factors of urban PM2.5 concentrations in China: a spatial econometric analysis," *Journal of Cleaner Production*, vol. 112, pp. 1443–1453, 2016.

[33] N. Zíková, Y. Wang, F. Yang, X. Li, M. Tian, and P. K. Hopke, "On the source contribution to Beijing PM2.5 concentrations," *Atmospheric Environment*, vol. 134, pp. 84–95, 2016.

[34] M. Tan, E. Ayhan, and M. Baydas, "Sustainability and cleaner production: case of textile and clothing sectors in Bingöl," *The Journal of MacroTrends in Energy and Sustainability*, vol. 4, no. 1, pp. 22–33, 2016.

[35] G. Li, C. Fang, and S. He, "The influence of environmental efficiency on PM2.5 pollution: evidence from 283 Chinese prefecture-level cities," *The Science of the Total Environment*, vol. 748, Article ID 141549, 2020b.

[36] L. Li, Y. Lei, S. Wu et al., "Evaluation of future energy consumption on PM2.5 emissions and public health economic loss in Beijing," *Journal of Cleaner Production*, vol. 187, pp. 1115–1128, 2018.

Hindawi
Mathematical Problems in Engineering
Volume 2021, Article ID 9176501, 10 pages
https://doi.org/10.1155/2021/9176501

*Research Article*

# Using Smart Card Data of Metro Passengers to Unveil the Urban Spatial Structure: A Case Study of Xi'an, China

**Guohong Cheng**,[1] **Shichao Sun**,[2] **Linlin Zhou**,[2] **and Guanzhong Wu**[3]

[1]*Hangzhou Communications Planning and Design Institute Co., Ltd, Hangzhou, China*
[2]*College of Transportation Engineering, Dalian Maritime University, Dalian, China*
[3]*Shanghai Tongzhun Information Technology Co., Ltd, Shanghai, China*

Correspondence should be addressed to Shichao Sun; sunshichao1988@hotmail.com

Received 3 October 2021; Accepted 19 October 2021; Published 3 November 2021

Academic Editor: Jinyu Chen



This study adopted smart card data collected from metro systems to identify city centers and illustrate how city centers interacted with other regions. A case study of Xi'an, China, was given. Specifically, inflow and outflow patterns of metro passengers were characterized to measure the degree of population agglomeration of an area, i.e., the centricity of an area. On this basis, in order to overcome the problem of determining the boundaries of the city centers, Moran's I was adopted to examine the spatial correlation between the inflow and outflow of ridership of adjacent areas. Three residential centers and two employee centers were identified, which demonstrated the polycentricity of urban structure of Xi'an. With the identified polycenters, the dominant spatial connections with each city center were investigated through a multiple linkage analysis method. The results indicated that there were significant connections between residential centers and employee centers. Moreover, metro passengers (commuters mostly) flowing into the identified employee centers during morning peak-hours mainly came from the northern and western area of Xi'an. This was consistent with the interpretation of current urban planning, which validated the effectiveness of the proposed methods. Policy implications were provided for the transport sector and public transport operators.

## 1. Introduction

Uncovering city structure and urban spatial connections can benefit from appropriate allocation of certain kinds of resources, e.g., land use, medical facilities, educational resources, and transport infrastructures. Specifically, the underlying urban structure is commonly interpreted beyond its physical form, because cities run as dynamic systems [1]. Therefore, the urban spatial connections beneath the complex system are not only related to the distribution of physical environments and economic resources, but also heavily involved with intracity movements [2,3]. Flows of people or cargo function as ties that integrate static physical resources into a dynamic system and generate spatial interactions [4–7]. In this context, a large number of studies have unveiled the city structure via passenger flow systems [8–10]. Specifically, the centers within city structure are found highly related to the spatial agglomeration of population [8], while the flow patterns of passengers are commonly utilized to denote how the identified city centers interact with other regions [11]. Given these practical enlightenments, policy implications and targeted strategies are always developed to guide the urban planning and hinder uncontrolled urban sprawl [12].

It has drawn much attention of researchers to investigate the urban spatial structure by using trajectory-based data [13], such as taxi GPS data [1,5], smart card data [8,12], and social network check-in data [9]. In this respect, Liu et al. [1] studied passengers' travel patterns and detected the polycentric city structure of Shanghai, China, by using taxi trajectory data. Tanahashi et al. [14] applied graph-partitioning methods to analyze the flow patterns of people between partitioned subregions by the use of mobile phone data and then revealed the urban spatial structure associated with travel activities. Yu et al. [15] proposed a methodology framework involving the community detection method and

mobile phone data, through which the urban structure was described by decomposing commuting demands. However, taxi trajectory data are plagued by the population coverage, and mobile phone data involve privacy and security issues.

In addition to taxi trajectory data and mobile phone data, smart card data are also recognized as a promising data source to provide insights on the identification of urban spatial structure [16,17]. It is because smart card data can provide rich and high-quality check-in records of public transport passengers [18–22], and mostly important, these passengers' riderships constitute a crucial part of urban spatial movements [21, 23, 24]. Compared with other data sources, smart card data are accessible with less cost, and the data are refined in spatial and temporal granularity [25]. In addition, the coverage of smart card data is relatively wide both in space and in population [23]. Tang et al. [26] proposed a clustering refinement approach to investigate the agglomeration pattern of passenger flows by using smart card data and then elaborated five clusters of metro stations to represent the underlying structure. Long and Shen [27] combined smart card data and POIs (points of interest) and proposed a clustering approach to identify different functional zones of the city and understand their spatial distribution characteristics. Nevertheless, the two studies did not conduct an in-depth analysis of urban spatial connections. Gong, Lin and Duan [4] used principle component analysis method to decompose the passenger flows obtained from the Automatic fare collection (AFC) data and investigated the spatiotemporal structure of urban form. Zhong et al. [28] used the smart card data collected from different time periods in Singapore and then investigated the overall spatial structure by monitoring urban movements from daily transportation. However, compared with the studies of [26, 27], they paid more attention to the spatial connections of discrete regions, but little was discussed on the identification of the city centers within the urban structure.

With respect to the methods used to reveal urban spatial connections, a number of previous studies adopted community detection technology to find the substructures of a complex spatial network [29]. However, the communities detected in the urban spatial network only denote the regions where their internal spatial connections are obviously stronger than those interacting with other areas [1]. Thus, it is weak to employ the community detection method to investigate the spatial connections between city centers and other discrete regions. Graph-partitioning method and spatial clustering approach are another two conventional methods commonly used to identify city centers and then reveal urban spatial interactions. Compared with community detection technology, these two methods can better illustrate the polycenters and regional connections, which constitute the main city structure [4, 8, 14]. Nevertheless, it is still not a straightforward task to determine the boundaries of city centers, which are regarded as key nodes in the spatial connections. For instance, Roth et al. [8] employed smart card data collected from London Underground to identify the urban spatial structure through a spatial clustering approach. However, the data adopted in their study were collected at station-based level, so that the basic O-D matrix obtained to illustrate the spatial connections and could only be described at station-to-station granularity. Thus, this led to the problem that it was difficult to determine which adjacent stations should be merged and then employed to represent the regions of city centers. In this context, the urban spatial structure could not be further interpreted in a more specific, refined and microperspective way.

Therefore, this study tried to use the smart card data collected from a metro system to reveal the urban spatial structure, through a spatial analysis approach. Compared with previous studies, the contributions of this paper could be summarized as follows:

(i) In order to identify the city centers and precisely determine their boundaries, the spatial autocorrelation analysis method was employed to merge the adjacent regions where the characteristics of trip generation were highly correlated.

(ii) Based on the O-D matrix obtained from smart card data, the multiple linkage analysis method was proposed to illustrate how the identified city centers dynamically interacted with other discrete regions, resulting in the dominated structure of regional connections.

The remainder of this paper is organized as follows. Section 2 gives a description of the study area and datasets involved in this paper. Section 3 introduces the methods employed in this study. The results and corresponding discussions are elaborated in Section 4. Conclusions and future works are drawn in Section 5.

## 2. Study Area and Datasets

*2.1. Study Area.* Xi'an city is the capital of Shaanxi province in north-central China. According to the census in 2019, the city is administering 11 districts and 2 counties with nearly 10-million population. Xi'an Metro refers to the rail transit system serving the urban area of the city. It was first open for operation in September, 2011, and up to 2021, it has eight metro lines (153 stations) with a total length of 244 kilometers. However, the smart card data used for this study were harvested in 2018. Therefore, this study mainly focused on the approach proposed to reveal the urban spatial structure but took the relatively outdated urban form of Xi'an as a demonstration. In this respect, regardless of the dynamic changes of urban form, the proposed approach can retain its resilience, which can be justified through the following empirical study. Besides, only three metro lines had been put into operation in 2018. Nevertheless, as the capital of ancient China, the urban form of Xi'an has always been an axial development. Therefore, the first three metro lines basically covered the main functional areas of the city. That is, the smart card data collected from the metro system in 2018 could be used to demonstrate the dominated urban spatial structure at that time. In addition, from the perspective of ridership, the daily average passenger ridership of Xi'an Metro had exceeded 2 million, which accounted for 30.3% of the total [30]. Thus, its coverage of passenger flows was wide enough and even better than taxi trajectory data used in previous studies, to unveil the overall spatial interactions.

*2.2. Datasets.* Up to 2018, over 85% of transactions in Xi'an public transit system were completed through smart cards. This proportion would reach nearly 100% in the metro (fare evasion behavior was not considered). Thus, it implied that smart card data collected from Xi'an Metro would record all the transaction information. The smart card data used in this study were collected from the AFC systems of Xi'an Metro. The data were not linked with passengers' bus trips. Thus, only the trips generated in the metro network were included. The dataset covered nearly 10 million transaction records, which were generated during the period from 17 April, 2018, to 21 April, 2018. The raw data were preprocessed by service providers, and invalid data were filtered out, which contained incomplete travel information. With each record of the data, we could obtain the card number (unique for each cardholder), the transaction time, the inbound information, the outbound information, and the transaction amount, as shown in Table 1.

## 3. Methods

*3.1. The Conceptual Framework.* The high agglomeration of population has been considered as good proxies for evaluating the centricity of an area [8]. However, the population distribution in a city is dynamically changing, which results from people's daily intracity movements. In this context, the centricity degree of an area shall be assessed accordingly by its inflow as well as outflow of public transport ridership. In addition, passenger flows within a day are commonly back and forth; e.g., a typical commuting can be characterized as going to work in the morning and returning home after work. Thus, it may lead to the fact that a potential city center, which attracts a large inflow of ridership, may also have almost equal outflow of ridership within a day. In this respect, we categorized the city centers into residential centers and employee centers. A residential center commonly refers to an area where the living density is very high, and a large outflow of passengers are generated in the morning due to the commuting demand, while an employee center can be defined as an area where commercial and industrial activities are frequent, and a large inflow of passengers are attracted. In order to distinguish between residential centers and employee centers, we assumed that the outflow of passengers of residential centers during morning peak-hours should be obviously larger than other areas. In contrast, the characteristic of passenger flows of an employee center would be exactly the opposite. That is, the inflow of passengers of employee centers should dominate in the morning.

Specifically, the outflow of passengers of an area could be measured by the inbound ridership of corresponding metro stations. Similarly, the outbound ridership of metro stations could be used to denote the inflow of passengers of the area where these stations served. However, a city center may cover a larger area served by multiple metro stations. Thus, in order to identify the city centers and their boundaries, it is necessary to investigate not only the inflow and outflow of passengers of metro stations, but also the spatial correlation between them. With respect to this, we tried to use global and local Moran's I to achieve the spatial correlation analysis between inflow or outflow of ridership of adjacent metro stations. Then, the identified hotspot areas and a part of outliers could be regarded as the city centers. On this basis, we attempted to examine the interactions between city centers and other regions, so as to illustrate the urban spatial structure of Xi'an. In particular, we provided insights on the forms in which passenger flows were distributed based on the O-D matrix extracted from the smart card data. The multiple linkage analysis method was employed to determine the significant connections of each city center.

*3.2. Global Moran's I.* Spatial autocorrelation analysis has been widely used in GIS to better understand the spatial dependency between one object with other nearby objects. In other words, it was commonly used to measure the degree to which one spatial area is similar to other vicinities. Spatial autocorrelation is multidimensional, thus being more complex than conventional one-dimensional autocorrelation. In 1950s, Moran [31] firstly developed Moran's I (Index) to measure spatial autocorrelation based on both feature locations and feature values simultaneously. Global Moran's I is defined as follows:

$$I = \frac{N}{S_0} \frac{\sum_i \sum_j w_{ij} \left(X_i - \overline{X}\right)\left(X_j - \overline{X}\right)}{\sum_i \left(X_i - \overline{X}\right)^2}, \tag{1}$$

where spatial objects are indexed by $i$ and $j$, and the number of which is denoted as $N$; $X_i$ represents the vector of feature values of object $i$; $\overline{X}$ is the mean of $X_i$; $w_{ij}$ is the matrix of spatial weights between objects $i$ and $j$, and the diagonal of the matrix is with zeros; $S_0$ is the sum of all $w_{ij}$. In addition, $w_{ij}$ is found to exert a strong influence on the value of Moran's I, and the distance decay function is commonly used to assign the spatial weights.

Based on the value of Moran's I (range from -1 to 1), we can classify the spatial dependency between the objects in space as positive, negative, and no correlation. Among them, positive spatial dependency (the value of Moran's I exceeds 0) implies that feature values of the objects are similar and clustered together in space. On the contrary, negative spatial dependency (the value of Moran's I is less than 0) is obtained when similar feature values of objects are dispersed in space. Regarding no spatial correlation, it indicates that the spatial distribution of objects' features is random. Thus, spatial autocorrelation analysis can be used to indicate whether there is clustering or dispersion in space, e.g., city centers where populations are spatially agglomerated. In addition, the statistical significance of Moran's I Index is commonly assessed by Z-score as well as $P$-value. Specifically, Z-score is suggested to be greater than 1.96 or smaller than -1.96, which can demonstrate positive or negative spatial dependency at the 5% significance level.

*3.3. Anselin Local Moran's I.* Even, given Moran's I, it still cannot help us directly identify statistically significant hotspot areas (i.e., city centers to be determined in this paper), cold spot areas, and spatial outliers in space. As an

extension of global Moran's I, Anselin local Moran's I was developed by Anselin [32], and it was defined as follows:

$$I_i = \frac{X_i - \overline{X}}{S_i^2} \sum_{j=1, j\neq i}^{N} w_{ij}\left(X_j - \overline{X}\right),$$
$$S_i^2 = \frac{\sum_{j=1, j\neq i}^{N}\left(X_j - \overline{X}\right)^2}{N-1}, \tag{2}$$

where $N$ denotes the number of spatial objects, which are indexed by $i$ and $j$; $X_i$ represents the vector of feature values of object $i$; $\overline{X}$ is the mean of $X_i$; $w_{ij}$ is the spatial weight between objects $i$ and $j$.

Other than Z-score and $P$-value, which are used to assess the statistical significance of local Moran's I, clustering or outlier types will be attached to each study object. Specifically, the values of Z-score and Lisa are simultaneously positive or negative when the study object is surrounded by other objects with similar values in space. Thus, it demonstrates a typical partial clustering in space, and the type L-L or H–H can be attached to the clustering. Clustering type H–H indicates a high-feature-value clustering, while clustering type L-L implies the clustering consisting of objects with low feature value. We can distinguish the clustering type H–H from the clustering type L-L by evaluating the value of Lisa (clustering type H–H can be determined when the value of Lisa is positive; otherwise, clustering type L-L will be attached). On the other side, a study object can be regarded as an outlier in space when the value of Z-score and the value of Lisa have different signs. It demonstrates that the study object is surrounded by other objects with dissimilar values. Specifically, the outlier will be attached with clustering type H-L when it owns high feature values but surrounded by others with low feature values. Conversely, the outlier with clustering type L-H is characterized by low feature values but surrounded by others with high feature values. Thus, as defined with the clustering type H–H and the outlier type H-L, the city centers where large populations are agglomerated in partial spatial areas can be identified by adopting local Moran' I, because it can be used to reflect the characteristics of spatial clustering of ridership.

*3.4. Multiple Linkage Analysis Based on O-D Matrix.* It has been long recognized as a straightforward task to obtain the O-D matrix by using smart card data collected from metro systems [18, 19, 33]. Specifically, the inbound information can provide the passengers' origin stations, while the outbound information can be used to infer the destination stations. In this context, the O-D matrix derived from the smart card data can be utilized to reflect passenger flows and underlying travel patterns in both spatial and temporal dimensions. Thus, smart card data own the natural property to illustrate the dynamic urban spatial interactions related to the movements of people.

Nevertheless, it is still necessary to find dominant passenger flows that construct the main city structure, because most of the elements involved in the O-D matrix are not significant to reflect the primary spatial connections of a city. Therefore, in order to distinguish between significant flows and insignificant flows, this paper employed multiple linkage analysis method to investigate dominant passenger flows based on the O-D matrix [12]. Regarding multiple linkage analysis, it assumes that there are a total of $k+1$ centers within the spatial structure. All flows from or to each spatial center are sorted from the largest ($W_1$) to the smallest ($W_k$) by their passenger ridership. These ordered flows constitute a set of observed flows $\{W_k\}$. Moreover, a set of expected flows $\{W_k{}'\}$ is generated for the same spatial center by different cycles, and the definition is as follows:

$$\begin{aligned}
&1^{st}cycle:\ W_1' = \sum_{i=1}^{K} W_i, \quad W_2' = W_3' = W_4' \cdots = W_k' = 0,\\
&2^{n\,d}cycle:\ W_1' = W_2' = \frac{1}{2}\sum_{i=1}^{K} W_i, \quad W_3' = W_4' \cdots = W_k' = 0,\\
&j^{th}cycle\,(j<k):\ W_1' = W_2' = \cdots = W_j' = \frac{1}{j}\sum_{i=1}^{K} W_i, \quad W_{j+1}{}' = W_{j+2}{}' \cdots = W_k' = 0,\\
&k^{th}cycle:\ W_1' = W_2' = \cdots = W_k' = \frac{1}{k}\sum_{i=1}^{K} W_i.
\end{aligned} \tag{3}$$

The goodness-of-fit between the set of observed flows and each cycle of expected flows is measured by R-square [12]. Then, the number of dominated flows from or to each center can be determined by finding the $j^{th}$ cycle where the highest R-square value places. In short, the mechanism of multiple linkage analysis is to minimize the difference between the real configurations and ideal configurations where the flows are distributed over each link in shares of equal magnitude.

Table 1: Smart card datasets.

| Card # | Date | Time | In-station | In-line | Out-station | Out-line | Amount |
|---|---|---|---|---|---|---|---|
| 51050*** | 20180420 | 06 : 12 : 51 | Beiyuan | 2 | Beikezhan | 2 | 2 RMB |
| 68800*** | 20180420 | 06 : 13 : 21 | Banpo | 1 | Fangzhicheng | 1 | 2 RMB |
| 50096*** | 20180420 | 06 : 16 : 42 | Zaohe | 1 | Houweizhai | 1 | 2 RMB |

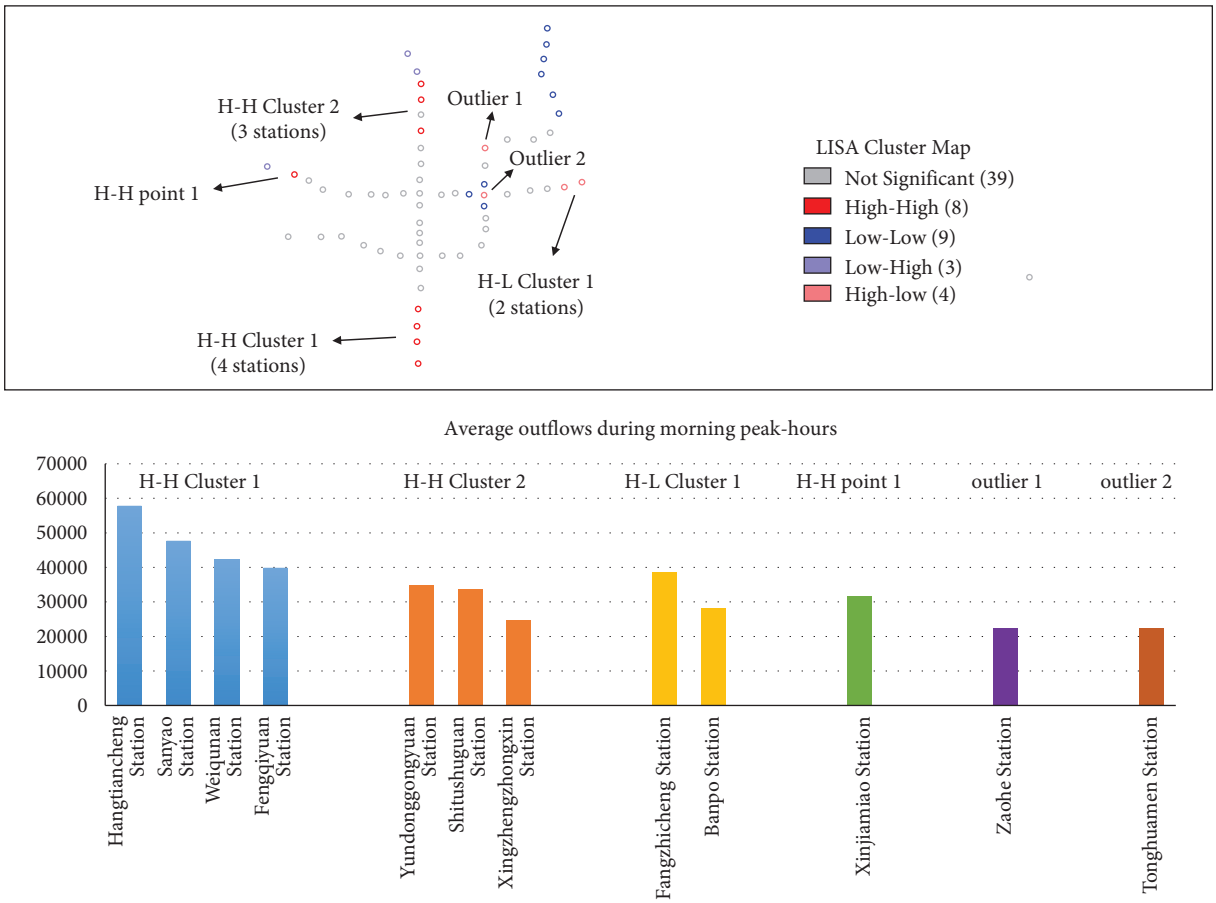


Figure 1: Spatial autocorrelation analysis on the outflow of ridership of metro stations.

## 4. Results and Discussions

*4.1. Determination of the Polycenters of Urban Structure.* In this study, global Moran's I was used to measure whether there was a spatial correlation of ridership (including inflow and outflow) between adjacent metro stations. Then, local Moran's I was further adopted to identify where the cluster or outlier was. Specifically, the morning peak-hours of Xi'an on weekdays was set as 06 : 00 am to 09 : 00 am. The average inflow and outflow of ridership of each metro station during morning peak-hours were obtained from the smart card data. The software GeoDa (version 1.12) was used to analyze the spatial dependency in the map, where an embedded default distance decay function was employed to build the spatial weights matrix. The results were shown as follows.

First, the global Moran's I regarding the outflow of ridership was 0.2881 with a Z-score of 5.1169, greater than the cut-off value (1.96) at 0.05 significance level. Thus, it demonstrated a positive spatial autocorrelation, namely, spatial clustering of passenger outflows in the map. On this basis, given the Lisa cluster map shown in Figure 1, it indicated that two clusters were identified with type H–H, namely, H–H Cluster 1 (consisted of 4 stations) and H–H Cluster 2 (consisted of 3 stations). Moreover, a spatial agglomeration of H-L outliers was identified, called H-L Cluster 1 (consisted of 2 stations). The results indicated that the outflow of ridership of the above identified three clusters was dominant, which averagely accounted for more than 35% of the daily total during morning peak hours on weekdays. Thus, combined with further validation through the current status data of land use, these three clusters could be recognized as residential centers. Other than spatial clusters, a H–H point (namely, Xinjiamiao Station) and two H-L points (namely, Zaohe Station and Tonghuamen Station) were identified. Nevertheless, they were all relatively isolated in space with no significant passenger outflows. In summary, three residential centers were finally determined, and we, respectively, named H–H Cluster 1 as

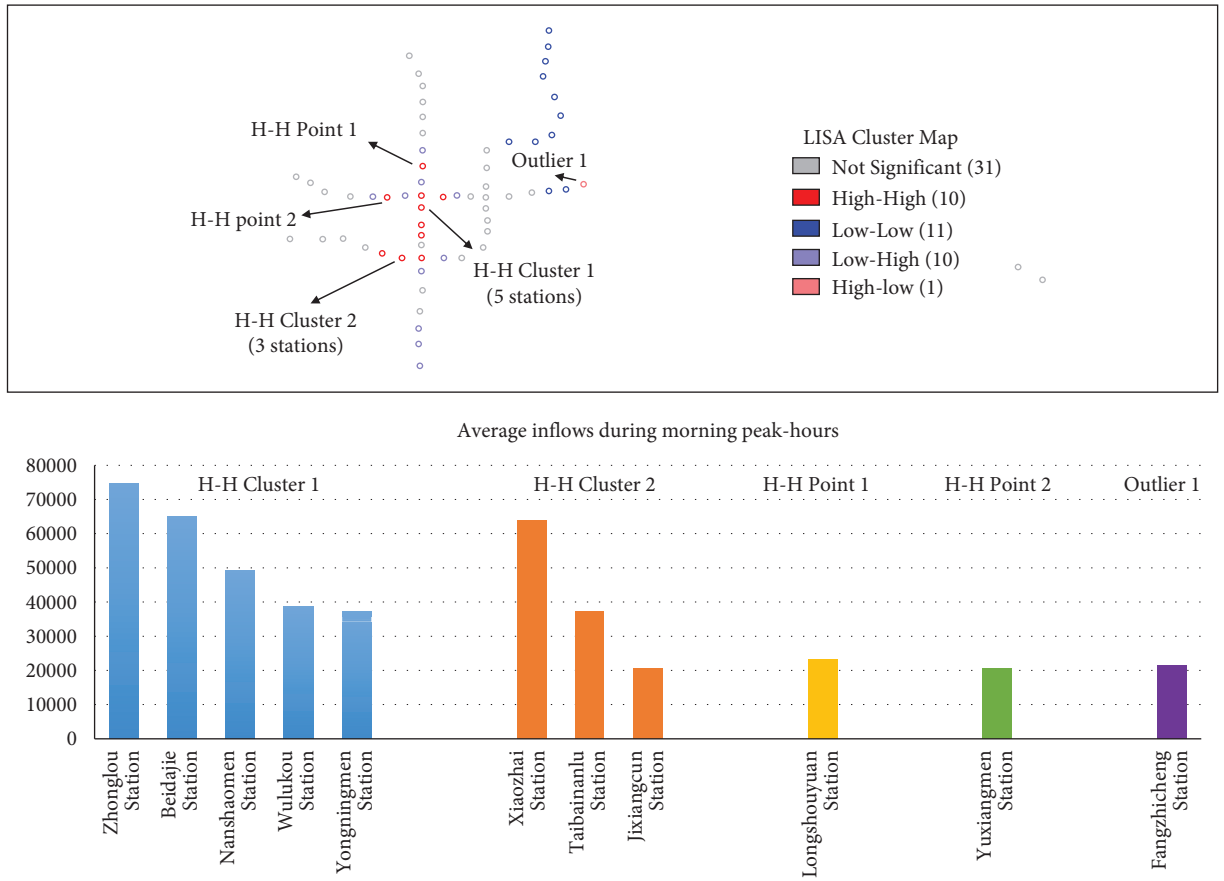


Figure 2: Spatial autocorrelation analysis on the inflow of ridership of metro stations.

Hangtiancheng Center, H–H Cluster 2 as Yundonggongyuan Center, and H-L Center as Fangzhicheng Center.

On the other side, the results of spatial autocorrelation analysis on the inflow of ridership are given in Figure 2. They indicated that the value of global Moran's I was 0.3472 with Z-score (5.5868) greater than the cut-off value (1.96) at the 0.05 significance level. Thus, it implied that the inflow of ridership was also spatially clustered in the map. On the basis of Lisa cluster map shown in Figure 2, two H–H clusters of were identified, which were, respectively, defined as H–H Cluster 1 (consisted of 5 stations) and H–H Cluster 2 (consisted of 3 stations). The inflows of these two clusters accounted for more than 40% of the daily total during morning peak hours on weekdays. In addition to the clusters, two H–H points and one H-L point were identified, but regarded as isolated outliers with no significant inflow of ridership. Therefore, two employee centers were finally determined, and we, respectively, named H–H Cluster 1 as Zhonglou Center and H–H Cluster 2 as Xiaozhai Center.

In summary, based on the results of above spatial autocorrelation analysis, we identified three residential centers and two employee centers. The residential centers included Hangtiancheng Center (4 stations), Yundonggongyuan Center (3 stations), and Fangzhicheng Center (2 stations), while the employee centers consisted of Zhonglou Center (5 stations) and Xiaozhai Center (3 stations). Therefore, the results demonstrated the polycentricity of urban structure of Xi'an.

*4.2. Determination of the Significant Flows of Polycenters.* With the identified polycenters, the significant flows connecting with each city center were investigated. Specifically, MLA was applied to the O-D matrix between identified clusters and other metro stations, which was obtained from the smart card data. The number of significant flows of each city center is listed in Table 2. The results indicated that the number of significant connections of employee centers was obviously larger than that of residential centers. Therefore, it implied that the inflows of passengers of employee centers were more evenly distributed on the dominant linkages. On the contrary, the significant outflows of passengers of residential centers were relatively concentrated on less linkages.

*4.3. Determination of the Urban Spatial Structure of Xi'an.* In order to intuitively illustrate how the identified polycenters interacted with other regions, the urban spatial structure of Xi'an was revealed by demonstrating the significant linkages of each city center through the software NodeXL, as shown in Figure 3.

Specifically, the results indicated that there existed strong connections between residential centers and employee centers. For instance, all the residential centers have significant connections with Zhonglou Center, which was identified as one of the employee centers in Xi'an. In addition, Yundonggongyuan Center and Hangtiancheng

Table 2: The number of significant flows of each city center

| Center type | Center | The number of significant flows |
|---|---|---|
| Residential center | Hangtiancheng center | 12 |
| | Yundonggongyuan center | 6 |
| | Fangzhicheng center | 5 |
| Employee center | Zhonglou center | 20 |
| | Xiaozhai center | 14 |

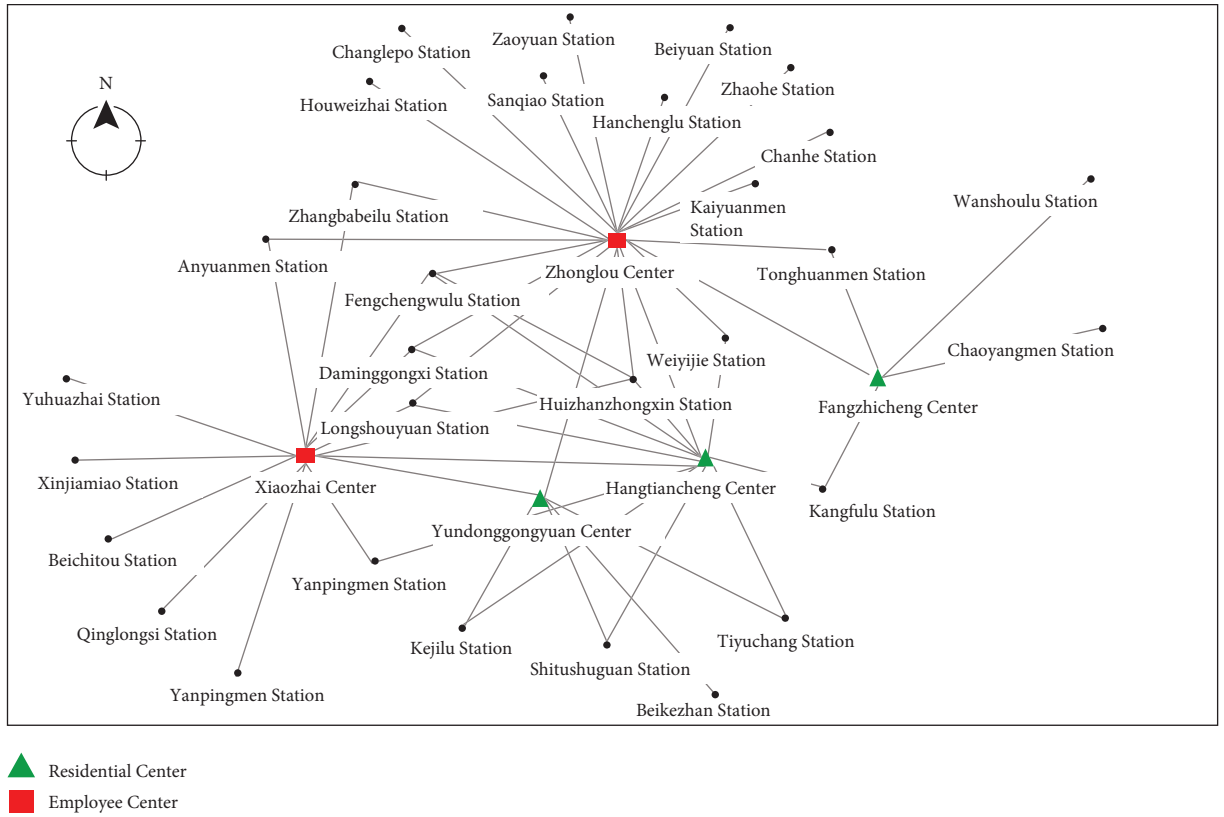


Figure 3: The urban spatial structure of Xi'an.

Center, two of the identified residential centers, were found to have strong connections with Xiaozhai Center, the other employee center. It also showed that the ridership from the identified residential centers to the employee centers accounted for nearly 40% of the total significant flows. On the other side, the spatial interactions reflected by passenger flows between the residential centers or the employee centers were not significant. Thus, the urban spatial structure could be further divided into two hierarchies, i.e., a fundamental spatial structure and a comprehensive spatial structure. The comprehensive spatial structure is shown in Figure 3, while the spatial connectivity between the identified residential and employee centers could be regarded as a fundamental spatial structure beyond the comprehensive one.

*4.4. Discussions.* Other than the urban spatial structure, commuting demand by metro could be reflected by the identified dominated flows of passengers during morning peak-hours. Specifically, as shown in Figure 4, it illustrated the dominant inflows of ridership of Zhonglou Center; the layout had been adjusted according to the actual geography.

The results indicated that metro passengers (commuters mostly) flowing into Zhonglou Center in morning peak-hours mainly came from the northern and western area of Xi'an, which accounted for more than 70% of the total inflows of the center. It was consistent with the current urban planning and land use situation of Xi'an. Specifically, Zhonglou Center refers to the area around the Xi'an Bell Tower, which is located in the geographical center of the city; at the same time, the earliest development of commerce of Xi'an also began in the Bell Tower area. Thus, it was not a surprise to see the Bell Tower area to be identified as an employee center. In addition, the northern and western regions of Xi'an were developed earlier, and according to the overall urban planning of Xi'an, these regions were planned to be developed in the form of small but scattered areas. Thus, this was why most of the dominated inflows were concentrated in these two regions but scattered on multiple linkages. Separately, the identified three residential centers

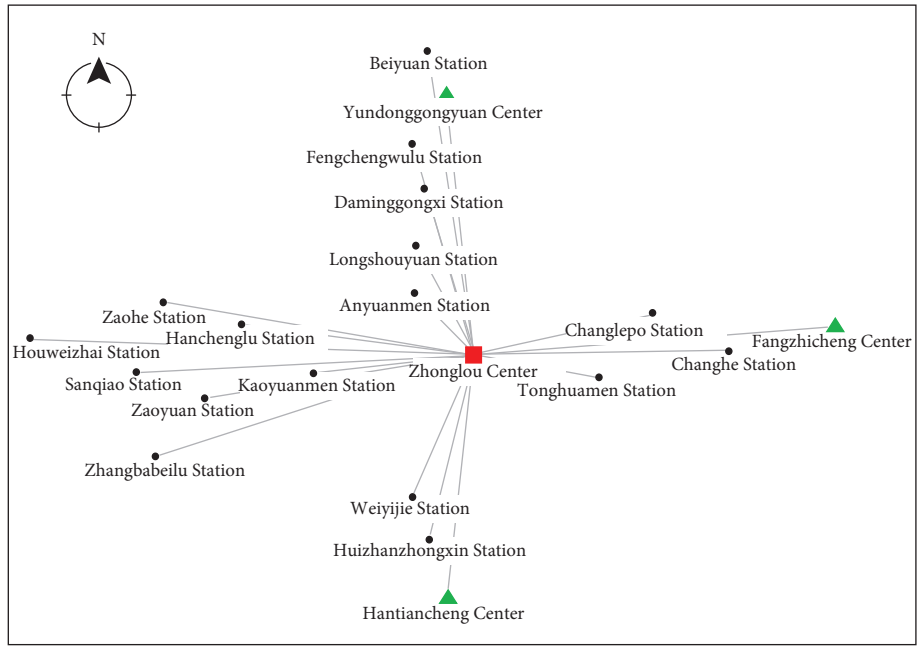


Figure 4: Dominant inflows of passengers of Zhonglou Center.

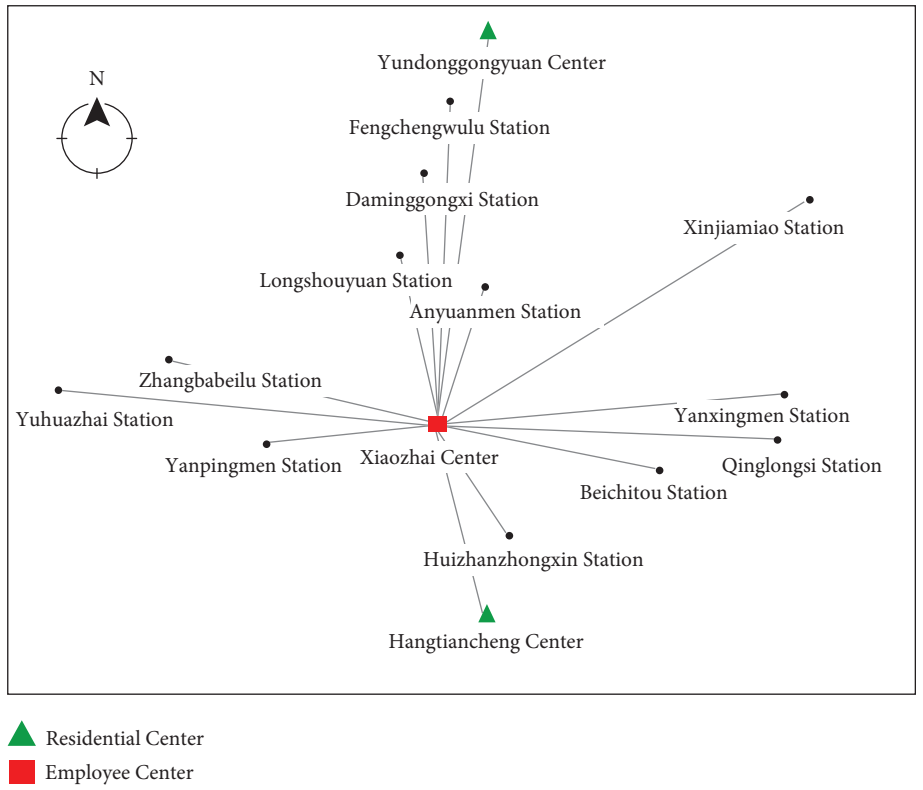


Figure 5: Dominant inflows of passengers of Xiaozhai Center.

covered several large residential communities of Xi'an, which led to their high outflows of ridership during morning peak-hours; they all had strong commuting demand with Zhonglou Center.

With regard to Xiaozhai Center, the dominant inflows of passengers are illustrated in Figure 5. The results indicated that, compared with Zhonglou Center, the distribution of dominant inflows of Xiaozhai Center was relatively

dispersed but mainly came from the north area of Xi'an. Thus, it was a surprise to find that although Xiaozhai Center was located in the south of the city, there was still a lot of commuting demand from the north. Actually, according to the development of urban planning of Xi'an, Xiaozhai Center could be regarded an emerging urban commercial center. Nevertheless, since the northern regions of the city were developed earlier with very completed functions, most populations preferred to live in the north of the city. Therefore, it led to the large long-distance commutes from the north to the south.

Overall, the urban spatial structure of Xi'an unveiled in this study was reasonable, including the city centers identified by spatial correlation analysis and dominant spatial connections obtained by MLA. Thus, to some extent, this recognized the effectiveness of the methods presented in this study. As for policy implications, the interpretation of the structure of passenger flows would benefit the transport sector and public transport operators to determine the development direction. For example, nonstop service, express service, and all-stop service can be mixed and organized for Xi'an Metro. Specifically, nonstop service can be implemented to smooth the connectivity between residential centers and employee centers. Express service can be adopted for the direction of dominant spatial connections during morning peak-hours.

## 5. Conclusions

As probably one of the most complex spatial systems, the city structure is highly correlated with urban movements of people or cargo. Thus, the urban spatial structure is not static but should be interpreted from the perspective of dynamic flows. The understanding of the underlying urban structure can contribute to targeted strategies that can better guide the overall urban planning and hinder uncontrolled sprawl in urban areas. This paper used the characteristics of metro passenger flows, which were obtained from the smart card data, to reveal the urban spatial structure. A case study of Xi'an, China, was given, and conclusions were drawn as follows:

(i) Spatial correlations of inflows and outflows of ridership of metro stations during weekday morning peak-hours were examined through global and local Moran's I. The clustering of spatially adjacent metro stations, which had a high agglomeration of passengers, was identified as city centers. The identified city centers were subdivided into residential centers and employee centers based on the flow direction of passengers. As a consequence, three residential centers and two employee centers were determined, which demonstrated the polycentricity of urban structure of Xi'an.

(ii) In order to investigate the dominant flows of the identified city centers, the method of MLA was proposed to unveil the most significant spatial connections that constituted the city structure. A two-hierarchical structure was revealed, including a fundamental spatial structure, which consisted of the strong spatial interactions between the residential centers and the employee centers, and a comprehensive spatial structure, which consisted of all the dominant connections with the identified city centers.

(iii) Dominant inflows of ridership of employee centers during morning peak-hours were illustrated, and they were interpreted based on the overall urban planning of Xi'an. The results indicated that the identified urban spatial structure was reasonable, which recognized the effectiveness of the methods proposed in this study. In addition, policy implications were provided for the transport sector and public transport operators. For example, nonstop service, express service, and all-stop service can be mixed and organized for Xi'an Metro.

However, this study also has its limitations that should be improved in future researches. First, compared with the metro network of Shanghai, Beijing, and Guangzhou, the network scale of Xi'an Metro is relatively small. It leads to huge differences between them in terms of passenger flow and rail transit coverage. Thus, the adaptability of the methods proposed in this study still needs further verification by using the data collected from other large-scale metro systems. Second, due to the emergence of bike-sharing or MASS systems, there are more and more transport modes that can be used to connect the metro system. In this context, other than the O-D matrix obtained from the metro AFC system, the actual trip distribution of metro passengers should also be brought into future studies.

## Data Availability

Access to data is restricted because of third-party rights and personal privacy.

## Conflicts of Interest

The authors declare that they have no conflicts of interest.

## Acknowledgments

This research was supported by the Open Funding Project of Key Laboratory of Road and Traffic Engineering of the Ministry of Education (Tongji University) and the Fundamental Research Funds for the Central Universities (3132019163).

## References

[1] X. Liu, L. Gong, Y. Gong, and Y. Liu, "Revealing travel patterns and city structure with taxi trip data," *Journal of Transport Geography*, vol. 43, pp. 78–90, 2015.

[2] Y. Yue, H.-d. Wang, B. Hu, Q.-Q. Li, Y.-G. Li, and A. G. O. Yeh, "Exploratory calibration of a spatial interaction model using taxi GPS trajectories," *Computers, Environment and Urban Systems*, vol. 36, no. 2, pp. 140–153, 2012.

[3] Y. Song, L. Merlin, and D. Rodriguez, "Comparing measures of urban land use mix," *Computers, Environment and Urban Systems*, vol. 42, pp. 1–13, 2013.

[4] Y. Gong, Y. Lin, and Z. Duan, "Exploring the spatiotemporal structure of dynamic urban space using metro smart card records," *Computers, Environment and Urban Systems*, vol. 64, pp. 169–183, 2017.

[5] Y. Liu, F. Wang, Y. Xiao, and S. Gao, "Urban land uses and traffic 'source-sink areas': evidence from GPS-enabled taxi data in Shanghai," *Landscape and Urban Planning*, vol. 106, no. 1, pp. 73–87, 2012.

[6] L. Hu, J. Yang, T. Yang, Y. Tu, and J. Zhu, "Urban spatial structure and travel in China," *Journal of Planning Literature*, vol. 35, no. 1, pp. 6–24, 2020.

[7] Y. Long and J.-C. Thill, "Combining smart card data and household travel survey to analyze jobs-housing relationships in Beijing," *Computers, Environment and Urban Systems*, vol. 53, pp. 19–35, 2015.

[8] C. Roth, S. M. Kang, M. Batty, and M. Barthelemy, "Structure of urban movements: polycentric activity and entangled hierarchical flows," *PLoS One*, vol. 6, 2011.

[9] Y. Liu, Z. Sui, C. Kang, and Y. Gao, "Uncovering patterns of inter-urban trip and spatial interaction from social media check-in data," *Plos One*, vol. 9, Article ID e86026, 2014.

[10] N. Green, "Functional polycentricity: a formal definition in terms of social network analysis," *Urban Studies*, vol. 44, no. 11, pp. 2077–2103, 2007.

[11] C. Kang, X. Ma, D. Tong, and Y. Liu, "Intra-urban human mobility patterns: an urban morphology perspective," *Physica A: Statistical Mechanics and Its Applications*, vol. 391, no. 4, pp. 1702–1717, 2012.

[12] S. Sun, Z. Duan, D. Yang, and W. Li, *Polycentricity of the Urban Structure: Spatial Movements Analysis in Shanghai with Smart Card Data*, World Congress Conference, Detroit, Michigan, 2014.

[13] Y. Yue, T. Lan, A. G. O. Yeh, and Q.-Q. Li, "Zooming into individuals to understand the collective: a review of trajectory-based travel behaviour studies," *Travel Behaviour And Society*, vol. 1, no. 2, pp. 69–78, 2014.

[14] Y. Tanahashi, J. R. Rowland, S. North, and K. L. Ma, "Inferring human mobility patterns from anonymized mobile communication usage," in *Proceedings of the 10th International Conference on Advances in Mobile Computing and Multimedia*, pp. 151–160, New York, NY, USA, July 2012.

[15] Q. Yu, W. F. Li, D. Y. Yang, and H. R. Zhang, "Mobile phone data in urban commuting: a network community detection-based framework to unveil the spatial structure of commuting demand," *Journal of Advanced Transportation*, vol. 2020, p. 15, 2020.

[16] M.-P. Pelletier, M. Trépanier, and C. Morency, "Smart card data use in public transit: a literature review," *Transportation Research Part C: Emerging Technologies*, vol. 19, no. 4, pp. 557–568, 2011.

[17] Y. Sun, J. Shi, and P. M. Schonfeld, "Identifying passenger flow characteristics and evaluating travel time reliability by visualizing AFC data: a case study of Shanghai Metro," *Public Transport*, vol. 8, no. 3, pp. 341–363, 2016.

[18] X. Ma, C. Liu, H. Wen, Y. Wang, and Y.-J. Wu, "Understanding commuting patterns using transit smart card data," *Journal of Transport Geography*, vol. 58, pp. 135–145, 2017.

[19] X. Ma, Y.-J. Wu, Y. Wang, F. Chen, and J. Liu, "Mining smart card data for transit riders' travel patterns," *Transportation Research Part C: Emerging Technologies*, vol. 36, pp. 1–12, 2013.

[20] J. Y. Park, D.-J. Kim, and Y. Lim, "Use of smart card data to define public transit use in seoul, South Korea," *Transportation Research Record: Journal of the Transportation Research Board*, vol. 2063, no. 1, pp. 3–9, 2008.

[21] S. Sun and Z. Duan, "Modeling passengers' loyalty to public transit in a two-dimensional framework: a case study in Xiamen, China," *Transportation Research Part A: Policy and Practice*, vol. 124, pp. 295–309, 2019.

[22] S. Sun, L. Xu, Y. Yao, and Z. Duan, "Investigating the determinants to retain spurious-loyalty passengers: a data-fusion based approach," *Transportation Research Part A: Policy and Practice*, vol. 152, pp. 70–83, 2021.

[23] S. C. Sun and D. Y. Yang, "Identifying public transit commuters based on both the smartcard data and survey data: a case study in xiamen, China," *Journal of Advanced Transportation*, vol. 2018, Article ID 9693272, 2018.

[24] S. C. Sun, "Public transit loyalty modeling considering the effect of passengers' emotional value: a case study in xiamen, China," *Journal of Advanced Transportation*, vol. 2018, Article ID 4682591, 2018.

[25] S. Tao, D. Rohde, and J. Corcoran, "Examining the spatial-temporal dynamics of bus passenger travel behaviour using smart card data and the flow-comap," *Journal of Transport Geography*, vol. 41, pp. 21–36, 2014.

[26] L. Tang, Y. Zhao, K. L. Tsui, Y. He, and L. Pan, "A clustering refinement approach for revealing urban spatial structure from smart card data," *Applied Sciences*, vol. 10, no. 16, p. 5606, 2020.

[27] Y. Long and Z. Shen, "Discovering functional zones using bus smart card data and points of interest in Beijing," in *Geospatial Analysis to Support Urban Planning in Beijing*, pp. 193–217, Springer, Berlin/Heidelberg, Germany, 2015.

[28] C. Zhong, S. M. Arisona, X. Huang, M. Batty, and G. Schmitt, "Detecting the dynamics of urban structure through spatial network analysis," *International Journal of Geographical Information Science*, vol. 28, no. 11, pp. 2178–2199, 2014.

[29] Y. Long and Z. Shen, *Geospatial Analysis to Support Urban Planning in Beijing*, Springer International Publishing, Berlin/Heidelberg, Germany, 2015.

[30] Xi'an Natural Resources and Planning Bureau, *Xi'an Transportation Development Annual Report in 2018*, Xi'an Natural Resources and Planning Bureau, Xi'an, China, 2019.

[31] P. A. P. Moran, "Notes on continuous stochastic phenomena," *Biometrika*, vol. 37, no. 1-2, pp. 17–23, 1950.

[32] L. Anselin, "Local indicators of spatial association – LISA," *Geographical Analysis*, vol. 27, pp. 93–115, 1995.

[33] X.-l. Ma, Y.-h. Wang, F. Chen, and J.-f. Liu, "Transit smart card data mining for passenger origin information extraction," *Journal of Zhejiang University - Science C*, vol. 13, no. 10, pp. 750–760, 2012.

Hindawi
Mathematical Problems in Engineering
Volume 2021, Article ID 3871148, 15 pages
https://doi.org/10.1155/2021/3871148

*Research Article*

# Financial Agglomeration, Energy Efficiency, and Sustainable Development of China's Regional Economy: Evidence from Provincial Panel Data

**Haiman Liu, Jiancheng Long, and Zunhuan Shen**

*School of Economics and Management, Xidian University, Xi'an 710100, China*

Correspondence should be addressed to Haiman Liu; 19061110543@stu.xidian.edu.cn

Received 12 July 2021; Accepted 12 October 2021; Published 1 November 2021

Academic Editor: Jinyu Chen



Ecological deterioration, air pollution, and resource depletion have shrouded the vast regions of China, raising widespread concerns about the sustainable development of the domestic economy. Although financial agglomeration has become a pivotal approach for China to realize green transformation, there is a lack of evidence against the causal correlation between financial agglomeration and sustainable development of the regional economy. To fill this gap, using the data of 29 provincial capital cities in China spanning from 2009 to 2019 and adopting individual time bidirectional fixed effect model, IV-GMM approach, and alternative modeling techniques, this paper investigates the impact of financial agglomeration on sustainable development of the regional economy for the first time. The results indicate that there is a significant positive correlation between financial agglomeration and the sustainable development of the regional economy. Financial agglomeration facilitates the improvement of regional energy efficiency, and the latter further mediates the relationship between financial agglomeration and sustainable development of the regional economy. In addition, the empirical results also demonstrate that the higher the economic policy uncertainty, the weaker the positive relationship between financial agglomeration and energy efficiency. The present study is of great significance for China to implement energy-saving and emission-reduction tasks and achieve sustainable urban construction.

## 1. Introduction

With increasing appeals to overcome energy shortage and environmental degradation, it is imperative for local government to continuously seek effective approaches to improve energy using efficiency, strengthen the green industry, and facilitate sustainable growth, especially for China. In China, the steady growth of GDP is accompanied by a series of enormous challenges such as global environmental turbulence, resource depletion, and ecosystem degradation. For example, in 2019, China's foreign dependence on petroleum and crude oil exceeded 70%. A total of 1152 days of severe pollution occurred in 337 cities in 2020, and the days with PM2.5, PM10, and O3 as the primary pollutants accounted for 77.7%, 22.0%, and 1.5% of the days with severe pollution and above, respectively. In this context, local government realizes that restoring nature is vital to the survival of the Earth and mankind and proposes to actively establish a green, low-carbon, and circular economic system. According to this proposal, the Chinese government pledges to strive to achieve a carbon peak by 2030 and achieve carbon neutrality by 2060 during the UN General Debate and encourages all regions to keep the economic operation within a reasonable range following the strategic deployment of the State Council while doing a good job of normalizing epidemic prevention and control. However, regional economic development is still unbalanced in China due to its vast territory and differentiated resource endowments. Therefore, considering the heterogeneity of economic development, how to enhance the sustainable development level of

China's regional economy (RESD) has become one of the hot issues under the background of high-quality economic development.

Forming a new pattern of modern financial development in which the real economy and the financial industry promote each other and making further efforts to build a modern financial agglomeration area that meets the requirements of all-round revitalization play a fundamental role in sustainable economic development. Under China's unique institutional background, financial agglomeration is a considerable catalyst towards the low-carbon cities' sustainable development because it improves the spatial and geographic allocation efficiency of financial resources, cuts down transaction costs, and facilitates economic growth [1]. For instance, in 2017, the "Jiang Bei Zui" financial center on the upper reaches of the Yangtze River achieved a financial added value of 13.68 billion yuan, up 26.6 percent year on year. Local governments vigorously have deployed various preferential policies for financial companies such as settlement subsidies and investment subsidies. Such phenomenon is deeply rooted in the fact that, in production and consumption activities, financial agglomeration offers a "double dividend" through resource accumulation and appropriate allocation of capital in a suboptimal case [2, 3]. Proponents of this view contend that financial agglomeration not only accelerates regional economic growth through diffusion and agglomeration effects [4] but also dramatically stimulates the upgrading of green industries and strengthens regional environmental protection via technical and ecological effects [5, 6], consequently posing opportunity and inexhaustible impetus to the sustainable development of regional economy [7].

Most studies believe that moderate financial agglomeration has greatly broadened financing channels, abated the information cost of financing, and thus stimulated technological innovation and energy conservation of enterprises at an alarming power [6, 8]. Against the backdrop of China's advocacy of green development, financial institutions in agglomeration areas provide financial support to the upstream and downstream of the green and low-carbon industry chain, allowing the capital to lean from cumbersome and low-productivity industries to higher-productivity industries [9]. This undoubtedly eliminates backward production capacity and triggers the optimization of industrial structure, thereby indirectly heightening energy efficiency [10]. Moreover, subsidies for petroleum products are eliminated while more investment is introduced into technological innovation in an attempt to ameliorate energy efficiency as a partial approach for boosting sustainable development [11]. Research demonstrates that, in the face of increasing pressure replete with resource overexploitation and climate deterioration, improving energy efficiency injects hope for China to achieve the win-win goal of environmental protection and effective economic growth [12, 13]. Therefore, a financial agglomeration-energy efficiency-regional economic sustainable development nexus may exist during China's economic transformation.

In addition, extensive research related to financial agglomeration relies on a stable economic policy environment. However, China's Economic Policy Uncertainty (EPU) index did not look promising and soared from 96.9 in 2009 to 687.6 at the end of 2019, which reflects that Chinese companies wallow in the quagmire of drastic external risks. The uncertainty of economic policy constitutes a pivotal exogenous factor for China's industrial environment uncertainty because high EPU leads to higher business risks and stronger strategic defense capabilities [14]. Multiple shreds of evidence propound that high EPU has exacerbated the agency problem of companies [15], led to tactical judgment errors [16], increased the risk of technological innovation [17], and brought more carbon emissions [18]. Therefore, the uncertainty of economic policy may affect firms' energy-related innovation decisions and R&D investment, thereby narrowing or amplifying the influence of financial agglomeration on energy efficiency.

However, the impact of financial agglomeration on the regional economy's sustainable development has been seriously neglected in existing studies. Only Cheng et al. [19] discussed the relationship between the penetration of information technology and the sustainable development of the regional economy. Empirical evidence related to financial agglomeration only concerned green development, urbanization, and marine eco-efficiency [5, 6]. Qu et al. [10] affirmed that there was a link between financial agglomeration and energy efficiency, but scant quantitative studies have specifically investigated the relationship between energy efficiency and sustainable economic development. Hence, it is intriguing to adopt a comprehensive theoretical framework to authenticate the impact of financial agglomeration on the sustainable development of the regional economy. At the same time, what role does energy efficiency play in the relationship between financial agglomeration and the sustainable development of regional economy? How does financial agglomeration affect the regional energy practices in a high EPU environment? The resolution of these issues has important theoretical significance for China's sustainable production practice.

In order to solve the above three main problems, we first manually collect the total number of financial institutions, financial talent data, and the list of financial assets to calculate the financial agglomeration level of 29 provincial capital cities in China with an objective to reveal the relationship between financial agglomeration and the sustainable development of the regional economy. Scant research has provided insight into the catalyzing factors of regional economy's sustainable development. Upon our knowledge, our paper first addresses this gap. Secondly, unlike the existing literature which widely adopts stochastic frontier method and data envelopment analysis to assess energy efficiency, this article prefers to apply an inclusive approach, the superefficiency SBM model, to estimate energy efficiency and treats energy efficiency as a mediating variable. This not only helps to expand the research on the antecedent variables of regional economy's sustainable development but also enriches the study on the economic consequences of energy efficiency in the existing body of knowledge. Finally, scholars have pointed that considering financial agglomeration alone ignores the fundamental role of the economic

policy environment on energy efficiency [20]. Hence, we propose a novel model leveraging economic policy uncertainty as a moderating variable to reveal the policy scenarios of financial agglomeration's influence on energy efficiency, which is a beneficial extension of the research on economic policy uncertainty.

## 2. Theoretical Analysis and Research Hypothesis

*2.1. Financial Agglomeration and the Sustainable Development of Regional Economy.* It is necessary to clarify the theoretical logic that financial agglomeration affects the sustainable development of a regional economy. In literature, Ye et al. [1] accentuated that financial agglomeration relies on the accumulation and allocation effects of financial capital to reinforce the city's infrastructure allocation. Financial agglomeration's active impact on green development is attributed to financial agglomeration's scale effect, technical effect, structural effect, and network effect [6]. Unfortunately, the ecological or environmental benefits induced by financial agglomeration have been largely ignored in past studies. Hence, this article attempts to reclassify the functional effects of financial agglomeration and postulates that the direction to which financial agglomeration affects the regional economy's sustainable development is primarily contingent on its economic, technical, and ecological effects.

The economic effect refers to that enterprises in a specific financial agglomeration area could increase the output ratio by obtaining scale economy effect and diffusion effect, thus driving the economic growth. From the perspective of economies of scale, financial institutions and related enterprises in financial clusters are more proactive in executing the highly relevant division of labor and collaboration to enable the quick flow of production factors such as information, capital, technology, and labor in clusters [21]. This has an inductive effect on economic growth because the agglomeration center has integrated various resources, reduced time cost, and transaction cost [1]. Concomitantly, the benefits of economies of scale can only be shared when there exists close proximity of banking, securities, and insurance industries [4]. Besides, the development of financial agglomeration drives the spillover effect of industries other than the financial industry in technological innovation, knowledge, economy, and other fields, thereby driving the coordinated development of the financial industry and other fields. Under such a premise, the flow of expertise and specialized resources raises the service level of diverse institutions and mitigates the instability of the economic environment [22].

Technological effect means that financial agglomeration becomes more relevant to boost sustainable development by stimulating technological innovation. In China, the technological effect always occurs in the financial agglomeration center [6]. The financial cluster is characterized as having a strong technological willingness and could provoke novel sophisticated products in the fields of energy science, material science, and ecological ethics [21]. Currently, China's ecological civilization construction requires scientific and technological innovation to be unified with the goal of sustainable development, while the formation of financial agglomeration centers could just ease the credit constraints faced by enterprises and supply basic capital guarantees for potential technological innovation initiatives, such as the development of new materials and utilization of new energy [23]. Furthermore, the spatial accumulation of financial industries not only broadens the market capacity of a specific region but also intensifies the sharing of positive externalities of information overflow [24], thereby indirectly serving the production innovation.

Stimulated by financial agglomeration, firms have become more and more environmentally friendly through green development. China's financial industries inevitably shoulder the dual missions of economic development and environmental preservation, which compels financial institutions to increase the proportion of green products and ameliorate the ecological environment by adjusting the direction of resource flow [7]. For instance, in the context of the conversion of new and old kinetic energy, financial institutions dominate the flow of capital underpinning the green high-end industries, smart manufacturing industries, and clean industries, thereby releasing green dividends [25]. This has promoted the green transformation of regional industrial structures [26]. In short, the agglomeration of financial elements would change the pattern, efficiency, and benefits of traditional industries and promote the expansion of green industries, thus not only achieving the goal of pollution control but also transforming ecological advantages into economic advantages. Then, the following hypothesis is proposed.

*2.1.1. Hypothesis 1.* Financial agglomeration has a positive effect on the sustainable development of the regional economy.

*2.2. Financial Agglomeration and Energy Efficiency.* Technical and management indicators were advocated by scholars as the most direct and powerful drivers affecting energy efficiency [27, 28]. For example, J. M. Simkoff et al. [28] demonstrated that the precise control of enterprise control systems achieved novel instantaneous operations such as conversion smoothing or demand response, thereby raising energy efficiency. From the perspective of metafrontier inefficiency and its decomposition, Cheng et al. [29] concluded that, less than 40% of energy inefficiency stemmed from technological gap inefficiency, and more than 60% came from management inefficiency. Therefore, the theoretical derivation of the impact of financial agglomeration on regional energy efficiency is inseparable from the perspectives of technology and management.

Firstly, financial agglomeration is a probable catalyst for the upgrading of energy-saving technologies. Financial agglomeration better responds to the financial market's demand for capital investment and depositors' liquidity preferences on their assets, realizing an effective docking between investment and financing. Financial institutions

strictly ensure the credit scale of enterprises with serious environmental pollution, and low resource utilization is subject to certain restrictions [30]. Conversely, financial agglomeration not only furnishes sufficient financial support and long-term incentive for innovative entities aiming at developing energy technologies [31] but also provides these entities with feasible channels for risk diversification, which undoubtedly bolsters the development and diffusion of energy technology. Secondly, the agglomeration mode builds basic trust and integrity between enterprises through information sharing and business cooperation, aimed at promoting mutual exchanges among firms. Especially for energy-intensive enterprises, the potential trust constraints between organizations not only reduce the possibility of transaction defaults but also exert stringent supervision and governance over production activities of firms, which help to increase the proportion of good output [32]. Interestingly, the network synergy of financial agglomeration acts as a significant channel for enterprises to establish a platform of mutual trust. This would curb opportunistic tendencies in business management, improve governance, and raise energy efficiency. Therefore, we put forward the following assumption:

*2.2.1. Hypothesis 2.* Financial agglomeration has a positive effect on energy efficiency.

*2.3. The Mediating Role of Energy Efficiency.* Improving energy efficiency is an extremely cost-effective and readily scalable option to maintain a city's sustainable development because it could simultaneously address economic, environmental protection, and resource issues [33]. In terms of the environment, multiple benefits are obtained by improving energy efficiency. For instance, Ozbugday and Erbas [34] accentuated that, under the same scenario, a 1% increase in energy efficiency reduced carbon dioxide emissions by 0.55% in the future. Notably, the improvement of energy efficiency not only mitigates primary energy consumption, $CO_2$ emissions, and environmental pollution but also increases energy security and expands competitiveness [35]. Hence, while encouraging sustainable economic growth, energy conversion efficiency must be enhanced to produce more work with less carbon-based energy. In addition, although energy accounts for a small share of total production costs, it is a prerequisite for social activity and economic growth. For example, the U.S. government acknowledges that energy efficiency plays as an advantageous element toward trade competition strategy. Bataille and Melton [36] concluded that improvements in energy efficiency contributed to a 2.0% increase in Canada's GDP and a 0.19% increase in macroeconomic performance between 2002 and 2012. In terms of resource utilization, high energy efficiency reduces water usage and fuel input for power plants [37], and numerous studies advocate that high energy efficiency has a positive impact on ecological optimization and resource utilization and is the primary strategy towards sustainable economic development [3, 12, 38]. Therefore, based on the logic of financial development-energy efficiency-economic performance, this paper further conjectures that energy efficiency plays an intermediary role in the correlation between financial agglomeration and the sustainable development of a regional economy. To sum up, we have the hypothesis as follows:

*2.3.1. Hypothesis 3.* Financial agglomeration positively influences the sustainable development of the regional economy by improving the level of energy efficiency.

*2.4. The Moderating Role of Economic Policy Uncertainty.* The normal exertion of financial agglomeration's favorable effects would be subjected to the economic policy environment. Under the background of high EPU, firms tend to exhibit retreat, evasiveness, and conservativeness when implementing the technology innovation plan. Research has indicated that, due to the nondispersibility of political risk, policy uncertainty requires equity risk premiums [39], which may affect enterprises' cost of capital [40]. The increase in the cost of capital turns a project with a positive net present value into a negative one. As a result, economic policy uncertainty leads to an increase in the cost of capital, which reduces the motivation for companies to raise funds. Raza et al. [41] elucidated that high EPU suppressed corporate investment by triggering higher energy and resource prices. Therefore, although financial agglomeration offers financial incentives for innovation subjects, high EPU inhibits corporate innovation investment and aggravates the risk of innovation projects. In addition, high EPU causes fluctuations in business expectations and managerial judgments [16]. Although financial agglomeration has weakened the opportunism of corporate management, high EPU seriously affects the firms' information environment [42], exacerbates managerial complexity [15], and even induces a decline in the proportion of R&D devoted to environmental expenditure [43]. In an uncertain environment, industrial firms often make up for the low turnover rate by switching to cheap energy production, which in turn undermines corporate performance and brings more carbon emissions [20]. In a nutshell, economic policy uncertainty may inhibit the smooth development and utilization of energy-saving technologies, and in turn, moderate the relationship between financial agglomeration and energy efficiency. Thus, we develop the following hypothesis.

*2.4.1. Hypothesis 4.* EPU negatively regulates the positive correlation between financial agglomeration and energy efficiency.

Based on the above analysis, the present paper constructs a conceptual model as follows (see Figure 1):

## 3. Methodology

*3.1. Sample and Data.* Since complete data on Taiwan, Xinjiang, Macao, Tibet, and Hong Kong are not available, only 29 provinces in China were comprised in the sample. In order to mitigate the special lash of the global financial crisis

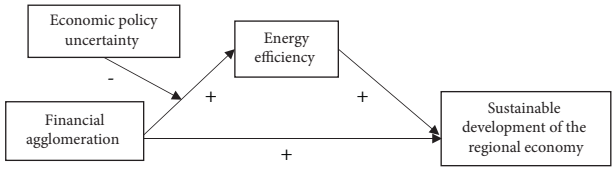


Figure 1: The conceptual model diagram.

on China's economy in 2008 and to maintain the validity and integrity of data, the sample observation time began in 2009. Therefore, this article attempted to test the impact of financial agglomeration on the regional economy's sustainable development based on the 29 provinces' panel data in mainland China over the period 2009 to 2019. The data were primarily derived from "China Energy Statistical Yearbook," "China City Statistical Yearbook," "China Environmental Statistical Yearbook," "China Information Industry Yearbook," "China Statistical Yearbook," and "Wind Financial Information Terminal." Concerning data processing, the missing data were supplemented by an interpolation method with the mean value of adjacent years, and data with different statistical units were converted during the sample sorting process. Lastly, a total of 319 observations were obtained, and the empirical analysis was carried out using STATA15.1 statistical software.

*3.2. Variable Definitions.* Sustainable development of the regional economy (RESD) is the dependent variable. Congruent with Cheng et al.'s [19] recommendation to address RESD, this article adopts a distinctive indicator of the sustainable development of China's regional economy which highlights three crucial subsystems of resources, environment, and economy. Combining the 22 evaluation indicators of the three subsystems with the measurement algorithm for each indicator's weight advocated by Cheng et al. [19], it is easy to engender the relatively objective and accurate RESD values for each province. Table 1 details the evaluation indicators of RESD.

Similarly, referring to the research of Cheng et al. [19], the calculation process of RESD is as follows:.

(1) Build the original matrix

$$Y = \left(y_{i,j}\right)_{\beta}. \tag{1}$$

(2) Standardization:

$$\begin{aligned} \text{positive index } \left(U_{i,j}\right)_{\beta} &= \frac{y_{i,j} - \min\left(y_{i,j}\right)}{\max\left(y_{i,j}\right) - \min\left(y_{i,j}\right)}, \\ \text{negative index } \left(U_{i,j}\right)_{\beta} &= \frac{\max\left(y_{i,j}\right) - y_{i,j}}{\max\left(y_{i,j}\right) - \min\left(y_{i,j}\right)}. \end{aligned} \tag{2}$$

(3) Index normalization processing:

$$\left(p_{i,j}\right)_{\beta} = \frac{\left(U_{i,j}\right)_{\beta}}{\sum_{\beta=1}^{m}\sum_{i=1}^{f}\left(U_{i,j}\right)_{\beta}}. \tag{3}$$

(4) Calculate the entropy of indicators:

$$\begin{aligned} E_{\beta} &= -f_1 \sum_{\beta=1}^{m}\sum_{i=1}^{f}\left(p_{i,j}\right)_{\beta}\ln\left(p_{i,j}\right)_{\beta}, \\ f_1 &= \frac{1}{\ln(m \times f)}, \quad m = 11, f = 29. \end{aligned} \tag{4}$$

(5) Calculate each indicator's weight:

$$w_{\beta} = \frac{1 - E_{\beta}}{\sum_{j=1}^{n}\left(1 - E_{\beta}\right)}. \tag{5}$$

(6) Calculate RESD:

$$\text{RESD}_{i,j} = \left(U_{i,j}\right)_{\beta} \times w_{\beta}. \tag{6}$$

$Y$ refers to the original matrix composed of a total of $\beta$ indicators in province $i$ and year $j$, and $(U_{i,j})\ \beta$ denotes the standardized matrix. $(p_{i,j})\ \beta$ refers to the normalization of the standardized matrix $(U_{i,j})\ \beta$. $E_{\beta}$ represents the information entropy of the calculated $\beta$ index, while $w_{\beta}$ is the weight of each indicator. Finally, $\text{RESD}_{i,j}$ signifies the sustainable development of the regional economy of $i$ province in $j$ year. Figure 2 visually plots the average index of RESD for 29 provinces from 2009 to 2019. From the perspective of comprehensive RSD value, Beijing is the province with the highest level of regional economic sustainable development, while Inner Mongolia and Qinghai have lower RSD values. On the whole, the average RESD values of many provinces are within the range of 0.3 and 0.4, reflecting that the sustainable development situation of China's regional economy is not optimistic.

In combination with characteristics of the financial industry and industrial agglomeration, financial agglomeration (FA) is simply defined as the optimization and restructuring process of the financial industry and relevant industries, resulting in the agglomeration of information, capital, and other resources in a certain region [1, 5, 10]. Previous studies generally assess the degree of financial agglomeration from four aspects of the financial environment, financial depth, financial breadth, and financial scale [5, 6]. Through the above theoretical discussion and literature review, this article argues that the measurement of financial agglomeration should treat the financial industry as a whole, which encompasses the expansion of financial assets, the concentration of financial institutions and entities, and the collection of financial talents. Therefore, based on the principles of accessibility and maneuverability, the present study constructs the evaluation indicators of financial agglomeration from 11 subindicators of 3 items, as shown in Table 2. In order to make the measurement of financial agglomeration reflect the actual

Table 1: Evaluation index of RESD.

| Subsystems | Measurement index |
|---|---|
| Resource subsystem | Internet penetration rate, $Y_1$<br>Mobile phone penetration rate, $Y_2$<br>Proportion of e-commerce sales, $Y_3$<br>Percentage of service industry websites, $Y_4$<br>The proportion of R&D investment, $Y_5$<br>The proportion of highly educated technical personnel, $Y_6$<br>The proportion of regional market contract transactions, $Y_7$<br>The development level of high-tech industry, $Y_8$<br>Number of companies conducting business via the internet, $Y_9$ |
| Economic subsystem | The proportion of software technology industry, $Y_{10}$<br>The proportion of information industry employment, $Y_{11}$<br>Number of legal persons in the service industry, $Y_{12}$<br>Network strength, $Y_{13}$<br>R&D and sales ratio of new products, $Y_{14}$<br>The degree of capital absorption of industrial enterprises, $Y_{15}$<br>The proportion of technological transformation of high-tech industry, $Y_{16}$<br>R&D expenditure ratio of industrial enterprises to universities, $Y_{17}$<br>Percentage of foreign investment, $Y_{18}$<br>The ratio of service industry value added to GDP, $Y_{19}$ |
| Environmental subsystem | Energy consumption, $Y_{20}$<br>The ratio of environmental pollution investment to GDP, $Y_{21}$<br>Electricity consumption, $Y_{22}$ |

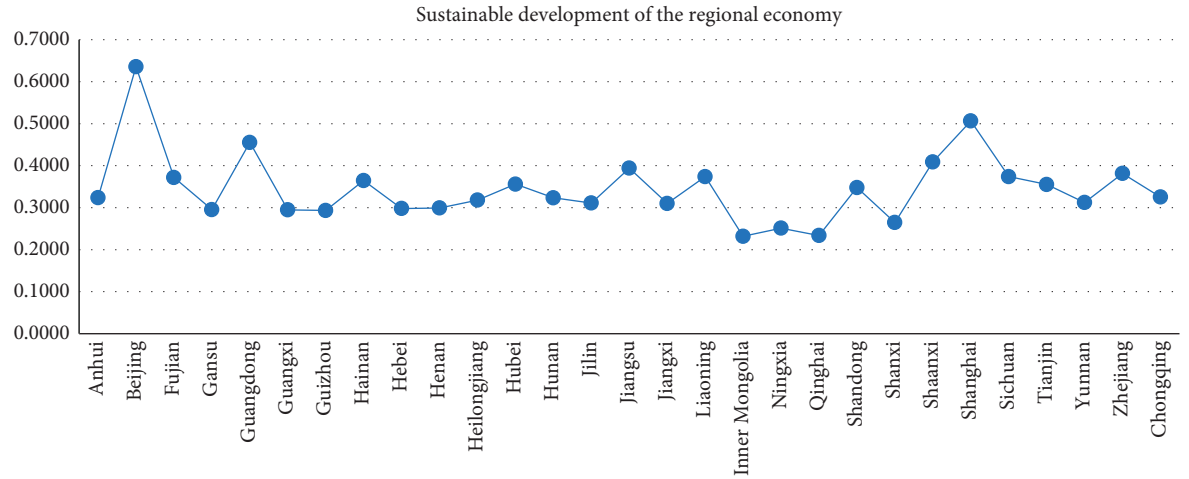


Figure 2: The line chart of the average value of RESD for 29 provinces.

Table 2: Evaluation index of financial agglomeration.

| First-level indicators | Secondary indicators | Polarity |
|---|---|---|
| Financial assets | Deposit balance of financial institution, $X_1$ | + |
| | Loan balance of financial institution, $X_2$ | + |
| | Total financing for shares and bonds, $X_3$ | + |
| | Original insurance premium income, $X_4$ | + |
| | Actual utilization of foreign direct investment amount, $X_5$ | + |
| | Added value of the financial industry, $X_6$ | + |
| Financial institutions | Number of financial institution outlets per unit area, $X_7$ | + |
| | Total number of securities, funds, and future companies headquartered in the jurisdiction, $X_8$ | + |
| | Total number of insurance companies headquartered in the jurisdiction, $X_9$ | + |
| | Total number of domestic listed companies at the end of the year, $X_{10}$ | + |
| Financial talents | Number of employees in the financial industry, $X_{11}$ | + |
| | Financial employment rate, $X_{12}$ | + |

agglomeration level of each province as much as possible, the relevant measurement of financial institutions, financial assets, and financial talents includes all information within each province. For example, when measuring the deposits of financial institutions, the financial institutions here include the number of network points of all financial institutions in the provincial capital and other cities.

Although the proliferation of practice adopting energy intensity to estimate energy efficiency in different cultural contexts [44], this measurement does not apply to China due to its vast territory and immense diversity in economic development between diverse provinces. Hence, the authors employ the location entropy index introduced by Qu et al. [10] that could precisely mirror the spatial distribution of China's financial agglomeration. The specific process is as follows.

(7) Build the original matrix:

$$X = \left(x_{i,j}\right). \tag{7}$$

(8) Standardization:

Dimensionless processing of data by year to obtain standardized data year by year.

$$x_{i,j}^{*} = \begin{cases} \dfrac{x_{i,j} - \min\left(x_{i,j}\right)}{\max\left(x_{i,j}\right) - \min\left(x_{i,j}\right)} & \text{the polarity of } x_{i,j} \text{ is positive,} \\ \dfrac{\min\left(x_{i,j}\right) - x_{i,j}}{\max\left(x_{i,j}\right) - \min\left(x_{i,j}\right)} & \text{the polarity of } x_{i,j} \text{ is negative.} \end{cases} \tag{8}$$

(9) Contribution of indicators:

$$p_{i,j} = \frac{x_{i,j}}{\sum_{i=1}^{29} x_{i,j}}. \tag{9}$$

(10) Calculate the information entropy of indicators:

$$e_j = -\frac{1}{\ln(n)} \sum_{i=1}^{29} p_{i,j} \ln\left(p_{i,j}\right), \text{and } n = 29. \tag{10}$$

(11) Calculate each indicator's weight:

$$w_j = \frac{1 - e_j}{\sum_{j=1}^{n}\left(1 - e_j\right)}. \tag{11}$$

(12) Calculate the financial agglomeration level:

$$\mathrm{FA}_i = \sum_{j=1}^{n} x_{i,j} \times w_j, \quad i = 1, 2, 3, \ldots, 29. \tag{12}$$

$X$ refers to the original matrix composed of indicators in province $i$ and year $j$. $x_{i,j}^{*}$ denotes the standardized matrix gained by standardizing the original matrix. $p_{i,j}$ acts as the contribution of province $i$ to the index $j$, while $e_j$ means the information entropy of the indicators. $w_j$ implies the weight of each indicator, and $\mathrm{FA}_i$ signifies the financial agglomeration level of $i$ province in $j$ year.

Total-factor energy efficiency is particularly suitable for measuring energy efficiency (EFF) since it has laid great emphasis on the substitution effect of other inputs on energy and is more in line with the Pareto efficiency theory in econometrics [45, 46]. Parametric frontier analysis and nonparametric frontier analysis are two mainstream approaches for estimating total-factor energy efficiency [47]. The nonradial data envelopment analysis (DEA) approach solves the problems of undesirable output and slack variables well and has been widely touted in research [48]. However, the efficiency value calculated by the traditional nonradial DEA model ranges between 0 and 1, and when the efficiency values of multiple decision-making units (DMUs) are efficient (that is, the efficiency value is 1), the difference between these DMUs cannot be further distinguished. Therefore, we follow the superefficiency SBM model advocated by Du et al. [49] and Zhang et al. [50] to make up for the defect of incomparability between multiple effective DMUs. Suppose there are $n$ decision-making units, and each DMU contains $m$ inputs, $D_1$ desirable outputs, and $D_2$ undesirable outputs. The specific vector is designed as $z \in R^m, w^a \in R^{D_1}$, and $w^b \in R^{D_2}$. $Z$, $W^a$, and $W^b$ are input matrix, desirable output matrix, and undesirable output matrix, respectively, where $Z = [z_1, z_2, \ldots, z_n] \in R^{m \times n}$, $W^a = [w_1^a, w_2^a, \ldots, w_n^a] \in R^{D_1 \times n}$, and $W^b = [w_1^b, w_2^b, \ldots, w_n^b] \varepsilon R^{D_2 \times n}$. The energy efficiency value of DMU can be expressed as follows:

$$\mathrm{EFF}^{*} = \frac{1/m \sum_{i=1}^{m} \overline{z_i}/z_{ie}}{1/D_1 + D_2\left(\sum_{r=1}^{D_1} w_{D_1}/w_{D_1 e} + \sum_{k=1}^{D_2} w_{D_2}/w_{D_2 e}\right)}, \tag{13}$$

subject to

$$\begin{aligned} \overline{z} &\geq \sum_{j=1, \neq e}^{n} z_j \beta_j \ (i = 1, 2, \ldots, m), \\ \overline{w^a} &\leq \sum_{j=1, \neq e}^{n} w_j^a \beta_j \left(r = 1, 2, \ldots, D_1\right), \\ \overline{w^b} &\geq \sum_{j=1, \neq e}^{n} w_j^b \beta_j \left(k = 1, 2, \ldots, D_2\right), \\ \beta_j &\geq 0, \ \sum_{j=1, \neq e}^{n} \beta_j = 1, \\ \overline{z} &\geq z_e \left(i = 1, 2, \ldots, m\right), \\ \overline{w^a} &\geq w_e^a \left(r = 1, 2, \ldots, D_1\right), \\ \overline{w^b} &\geq w_e^b \left(k = 1, 2, \ldots, D_2\right), \end{aligned} \tag{14}$$

where $\beta$ is a weight vector and $\beta_j$ is the weight of DMU $j$. The above nonlinear model can be transformed into a linear model by conversion of Charnes–Cooper method. $\mathrm{EFF}^{*}$ is the energy efficiency value of DMU, and a larger value of $\mathrm{EFF}^{*}$ means higher energy efficiency. Labor, capital stock, and energy consumption are the major input factors. Since

the employees' number does not truly reflect the labor quality's difference, we use the product of the number of employees and average years of education to measure labor input. The perpetual inventory method is applied to estimate capital stock. It is feasible to use the product of GDP and energy intensity as a proxy variable for energy consumption. The ideal output is expressed in terms of the gross domestic product of each region, and carbon dioxide emissions are selected to measure undesired output.

The aggregate index advocated by Baker et al. [51] is used to compute China's EPU. The establishment of this aggregate index relies mainly on the frequency of articles in the South China Morning Post on economic policy uncertainty. The annual EPU is preliminarily estimated using the natural logarithm of the monthly mean EPU.

Moreover, this paper contains some plausible controlling variables which have been proved to be significant factors affecting regional sustainable development [10, 19]. The main control variables include R&D input (RD), market demand (MD), and government intervention (GI), and the specific measurement methods are expounded in Table 3.

*3.3. Empirical Model.* In the objective to address the influence of FA on RESD and the mediation effect of energy efficiency between the two, the paper adopts the casual step means recommended by Baron and Kenny [52]. Relevant models are designed as follows:

$$\mathrm{RESD}_{i,t} = \alpha + \beta \mathrm{FA}_{i,t} + \gamma \mathrm{Control}_{i,t} + \mu_t + \varepsilon_{i,t}, \tag{15}$$

$$\mathrm{EFF}_{i,t} = \alpha + \beta \mathrm{FA}_{i,t} + \gamma \mathrm{Control}_{i,t} + \mu_t + \varepsilon_{i,t}, \tag{16}$$

$$\mathrm{RESD}_{i,t} = \alpha + \beta \mathrm{FA}_{i,t} + \delta \mathrm{EFF}_{i,t} + \gamma \mathrm{Control}_{i,t} + \mu_t + \varepsilon_{i,t}, \tag{17}$$

where $i$ represents province and $t$ is time. $\mathrm{RESD}_{i,t}$ means the sustainable development of regional economy in $t$ year of region $i$. $\mathrm{FA}_{i,t}$ indicates financial agglomeration level, and $\mathrm{EFF}_{i,t}$ is the regional energy efficiency in year $t$. $\mathrm{Control}_{i,t}$ consists of several control variables, including R&D input, market demand, and government intervention. $\mu_t$ stands for the unobservable and nonnegligible intercept term generated by individual heterogeneity, and $\varepsilon_{i,t}$ reflects the disturbance of time effect to the model.

Next, this paper verifies the moderating effect of economic policy uncertainty on the correlation between FA and EFF by constructing a moderation effect model. In equation (19), the interaction term between financial agglomeration and economic policy uncertainty is added.

$$\mathrm{EFF}_{i,t} = \alpha + \beta_1 \mathrm{FA}_{i,t} + \beta_2 \mathrm{EPU}_t + \gamma \mathrm{Control}_{i,t} + \mu_t + \varepsilon_{i,t}, \tag{18}$$

$$\mathrm{EFF}_{i,t} = \alpha + \beta_1 \mathrm{FA}_{i,t} + \beta_2 \mathrm{EPU}_t + \beta_3 \mathrm{EPU}_t \times FA_{i,t} + \gamma \mathrm{Control}_{i,t} + \mu_t + \varepsilon_{i,t}, \tag{19}$$

where coefficient $\beta_3$ is the main object of observation. If $\beta_3$ is significant statistically, it means that the moderating effect exists.

## 4. Empirical Results

*4.1. Descriptive Statistical Analysis.* Table 4 displays the descriptive statistical results of all variables. It is observed that the sustainable development level of China's regional economy is relatively low because the average value of RESD is very small, that is, 0.359. The maximum value of financial agglomeration is 0.793, with a minimum value of 0.015 and an average value of 0.196. This reflects that there exist remarkable differences in the degree of financial agglomeration among various provinces, and the level of financial agglomeration in China is comparatively low in general. The average value of energy efficiency is 0.657, with a standard deviation of 0.336, which demonstrates that the energy efficiency levels of different regions are quite different. In addition, the standard deviation of EPU is 0.523, meaning that China's EPU index fluctuates greatly from 2009 to 2019.

*4.2. Correlation Analysis and Multicollinearity Test.* Table 5 presents the results of correlation and multicollinearity analysis. There is a significant correlation between FA and RESD, suggesting that financial agglomeration plays a considerable role in the process of sustainable economic development. Financial agglomeration indeed imposes a positive impact on energy efficiency, which furnishes preliminary evidence for hypothesis 2. The correlation analysis results are basically consistent with the prior theoretical expectations. Furthermore, the variance inflation factors (VIFs) are less than 10, further stating that there is no multicollinearity between variables.

*4.3. Regression Analysis.* For the sake of being unaffected by spurious regression and maintaining the reliability of regression results, we first conduct a unit root test before regression. Unit root testing methods contain Im, Pesaran and Shin (IPS), Phillips–Perron test (PP), and augmented Dickey–Fuller test (ADF), etc. This study adopts these unit root testing methods and finds that all variables are stationary at the significance level of 5%, and thus the original hypothesis of the unit root of these variables could be rejected. The results of the Hausman test indicate that a fixed-effect model should be selected to control the influence of time differences on regression analysis. Meanwhile, in order to control the influence of individual (provincial) differences on regression, the individual-time bidirectional fixed effect model is ultimately employed for panel regression. Additionally, the present study employs bootstrap methods in virtue of the PROCESS program to verify the mediation effect, and variable substitution techniques and GMM regression are executed to test the robustness of the results and to deal with endogenous issues.

The corresponding regression results of equations (15)–(19) are summarized in Table 6. When other confounding factors are controlled, the impact of financial agglomeration on RESD is remarkably positive at the 1% level, representing that financial agglomeration significantly speeds up the sustainable development of China's regional economy. Therefore, hypothesis 1 is confirmed. Then, a

Table 3: Measurement of control variables.

| Variables | Measuring methods |
|---|---|
| R&D input (RD) | The ratio of the total number of employees in scientific research, technical services, and geological exploration to the total number of employees in the province |
| Market demand (MD) | The natural logarithm of the annual total consumption expenditure of each province's urban residents |
| Government intervention (GI) | Fiscal revenue divided by GDP |

Table 4: Descriptive statistics.

| Variables | $N$ | Max | Min | P50 | Mean | Std. dev.(SD) |
|---|---|---|---|---|---|---|
| RESD | 310 | 0.729 | 0.203 | 0.354 | 0.359 | 0.092 |
| FA | 310 | 0.793 | 0.015 | 0.129 | 0.196 | 0.189 |
| EFF | 310 | 1.698 | 0.201 | 0.601 | 0.657 | 0.336 |
| EPU | 310 | 6.132 | 4.594 | 5.170 | 5.276 | 0.523 |
| RD | 310 | 0.368 | 0.116 | 0.229 | 0.232 | 0.045 |
| MD | 310 | 10.736 | 9.081 | 9.652 | 9.770 | 0.331 |
| GI | 310 | 0.227 | 0.058 | 0.113 | 0.107 | 0.031 |

Table 5: Correlation between variables and multicollinearity test.

| Variables | RESD | FA | EFF | EPU | RD | MD | GI | VIF |
|---|---|---|---|---|---|---|---|---|
| RESD | 1 | | | | | | | |
| FA | 0.409** | 1 | | | | | | 5.952 |
| EFF | 0.453** | 0.324** | 1 | | | | | 6.105 |
| EPU | 0.246** | 0.088 | 0.160** | 1 | | | | 2.207 |
| RD | 0.359** | 0.291** | 0.328** | 0.014 | 1 | | | 2.035 |
| MD | 0.305** | 0.321** | 0.204** | 0.274** | 0.139** | 1 | | 5.110 |
| GI | 0.284** | 0.237* | 0.245** | 0.111 | 0.178** | 0.248** | 1 | 4.891 |

Note: $^{*}p < 0.05$ and $^{**}p < 0.01$.

Table 6: Regression results.

| Variables | (1) EFF | (2) RESD | (3) RESD | (4) EFF | (5) EFF |
|---|---|---|---|---|---|
| RD | 0.010 | 0.033* | 0.031* | 0.024 | 0.033 |
| | (0.276) | (1.652) | (1.649) | (0.414) | (0.257) |
| MD | 0.170*** | 0.359*** | 0.328*** | 0.360*** | 0.372*** |
| | (3.800) | (14.221) | (13.335) | (7.390) | (7.843) |
| GI | 0.026 | −0.116** | −0.120** | −0.116* | −0.132* |
| | (0.711) | (−2.960) | (−3.252) | (−1.735) | (−2.027) |
| FA | 0.315*** | 0.303*** | | 0.176** | 0.135* |
| | (4.619) | (7.063) | | (2.729) | (2.051) |
| EFF | | | 0.184*** | | |
| | | | (5.514) | | |
| EPU | | | | −0.050* | −0.056* |
| | | | | (−1.985) | (−1.830) |
| FA × EPU | | | | | −0.078*** |
| | | | | | (−2.952) |
| Constant | −0.226*** | −0.602*** | −0.618*** | 0.624*** | 0.658*** |
| | (−3.898) | (−10.145) | (−10.972) | (5.875) | (6.344) |
| Individual | Yes | Yes | Yes | Yes | Yes |
| Year | Yes | Yes | Yes | No | No |
| Observations | 310 | 310 | 310 | 310 | 310 |
| Adjusted $R^2$ | 0.846 | 0.951 | 0.956 | 0.886 | 0.892 |

Note: *, **, and *** indicate the significance level is 10%, 5%, and 1%, respectively.

stepwise regression method is used to determine the mediating effect of energy efficiency. Model 1 reveals that financial agglomeration exhibits a statistically positive influence on energy efficiency at the 1% level, illustrating that financial agglomeration acts as the determinant for the improvement of energy efficiency. Hypothesis 2 is thus supported. It can be seen from model 3 that, at 1% level, energy efficiency is significantly positively correlated with RESD, but the coefficient of financial agglomeration has reduced but is still significant. This supports hypothesis 3 and suggests that financial agglomeration provides opportunities for the sustainable development of the regional economy by improving energy efficiency. In order to improve the reliability, we further bootstrapped with 5000 in the study to produce bias-corrected confidence intervals of yield 95% to verify the mediation effect. The result demonstrated that the mediating effect of energy efficiency was significant with a 95% confidence interval excluding zero (index = 0.0289 and CI = (0.0117, 0.0528)). Consequently, the mediating effect of energy efficiency is statistically significant.

Model 6 of Table 6 introduces the interaction term between economic policy uncertainty and financial agglomeration to test hypothesis 4. Since controlling annual fixed effects has alleviated the impact of national macroeconomic fluctuations, and the coexistence of annual fixed effects and EPU would lead to multicollinearity. Model 4 and model 5 cancel the control of the annual fixed effects. It is worth noting that the required variables are standardized to further avoid multicollinearity. The coefficient of FA × EPU is −0.078, which is significant at 1% level, stating that economic policy uncertainty negatively moderates the relationship between financial agglomeration and energy efficiency. Hypothesis 4 is thus supported. The reason for this discovery may be that, in the face of high EPU, rational agents would delay the company's green technology investment due to political tensions, thereby inhibiting the improvement of energy efficiency. Furthermore, high EPU complicates the business environment and management of a company. In a weak regulatory environment, a company's energy efficiency policies would be compromised.

*4.4. Robustness Test and Endogenous Issues.* To ensure that the conclusions are robust, replacing the independent variable and the mediator is warranted. Congruent with Yuan et al.'s [6] work, this paper adopts the location entropy index to remeasure financial agglomeration. The specific reference formula is as follows:

$$\mathrm{FA}_2 = \frac{E_{i,t}/C_{i,t}}{M_t/N_t}, \tag{20}$$

where $\mathrm{FA}_2$ mirrors location entropy index, $i$ represents province, and $t$ is the year. $E_{i,t}$ reflects the number of financial industry employees of $i$ province in $t$ year. $C_{i,t}$ is the number of employees of all industries in $t$ year of province $i$. $M_t$ refers to the number of employees in the national financial industry during $t$, and $N_t$ means the number of all industries' employees across the country in $t$ year .

The methodology of NDDF is recommended to regauge energy efficiency by following the study of Ye et al. [1]. Firstly, suppose there exist $n = 1, 2, 3, \ldots, N$ decision-making units, and each unit is composed of three inputs, namely, labor input ($X$), energy input ($Y$), and capital input ($Z$), and two outputs: desirable output ($O$) and undesirable output ($T$). Meanwhile, the directional vector $f = (-Z, -X, -Y, O, -T)^T$ and weight vector $W = (1/9, 1/9, 1/9, 1/3, 1/3)^T$ are developed, respectively. Then, the linear programming is expressed as

$$\begin{aligned}
\overrightarrow{D} = (Z, X, Y, O, T; f) = \max &\left(W_Z B_Z + W_X B_X + W_Y B_Y + W_O B_O + W_T B_T\right) \\
\text{s.t.} &\sum_{n=1}^{N} v_n Z_n \le Z - B_Z f_Z \\
&\sum_{n=1}^{N} v_n X_n \le X - B_X f_X \\
&\sum_{n=1}^{N} v_n Y_n \le Y - B_Y f_Y \\
&\sum_{n=1}^{N} v_n O_n \ge O + B_O f_O \\
&\sum_{n=1}^{N} v_n T_n = T - B_T f_T \\
&v_n \ge 0, n = 1, 2, \ldots, N \text{ and } B_Z, B_X, B_Y, B_O, B_T \ge 0.
\end{aligned} \tag{21}$$

Table 7: Robustness test.

| Variables | (1) EFF2 | (2) RESD | (3) RESD | (4) EFF2 | (5) EFF2 |
|---|---|---|---|---|---|
| RD | 0.001 | 0.027 | 0.026* | 0.037 | 0.051* |
| | (0.028) | (0.198) | (2.125) | (0.228) | (1.732) |
| MD | 0.173*** | 0.373*** | 0.334*** | 0.353*** | 0.363*** |
| | (3.797) | (13.679) | (12.706) | (7.114) | (7.616) |
| GI | 0.013 | −0.126** | −0.129** | −0.061 | −0.089* |
| | (0.850) | (−3.101) | (−3.394) | (−0.967) | (−1.403) |
| $FA_2$ | 0.202** | 0.220*** | 0.168*** | 0.110** | 0.087 |
| | (2.660) | (4.847) | (3.898) | (1.557) | (1.030) |
| $EFF_2$ | | | 0.211*** | | |
| | | | (6.269) | | |
| EPU | | | | −0.049 | −0.058* |
| | | | | (−1.533) | (−1.886) |
| $FA_2 \times EPU$ | | | | | −0.094*** |
| | | | | | (−2.828) |
| Constant | −0.133*** | −0.563*** | −0.588*** | 0.636*** | 0.650*** |
| | (−2.971) | (−7.892) | (−8.827) | (5.774) | (6.152) |
| Individual | Yes | Yes | Yes | Yes | Yes |
| Year | Yes | Yes | Yes | No | No |
| Observations | 310 | 310 | 310 | 310 | 310 |
| Adjusted $R^2$ | 0.850 | 0.947 | 0.954 | 0.883 | 0.893 |

Note: *, **, and *** indicate the significance level is 10%, 5%, and 1%, respectively.

Assume that the optimal solution of equation (14) is $B_n^* = (B_{nZ}^*, B_{nX}^*, B_{nY}^*, B_{nO}^*, B_{nT}^*)^T$. Then, the energy efficiency index can be computed according to equation (15):

$$\begin{aligned} EFF_2 &= \frac{1}{4}\left[\frac{O_n/Z_n}{(O_n + B_{nO}^* O_n)/(Z_n - B_{nZ}^* Z_n)} + \frac{O_n/X_n}{(O_n + B_{nO}^* O_n)/(X_n - B_{nX}^* X_n)}\right. \\ &\quad \left. + \frac{O_n/Y_n}{(O_n + B_{nO}^* O_n)/(Y_n - B_{nY}^* Y_n)} + \frac{O_n/T_n}{(O_n + B_{nO}^* O_n)/(T_n - B_{nT}^* T_n)}\right] \\ &= \frac{1}{4}\left[\frac{(1 - B_{nZ}^*) + (1 - B_{nX}^*) + (1 - B_{nY}^*) + (1 - B_{nT}^*)}{(1 + B_{nO}^*)}\right] \\ &= \frac{1 - (1/4)(B_{nZ}^* + B_{nX}^* + B_{nY}^* + B_{nT}^*)}{1 + B_{nO}^*}. \end{aligned} \tag{22}$$

The value range of $EFF_2$ is between 0 and 1, and the higher the $EFF_2$ value, the higher the level of energy efficiency. For capital input, the perpetual inventory means is employed to calculate each province's capital stock. Energy consumption is described as the product of each province's GDP and energy intensity because China does not make data related to energy sources such as coal and petroleum mandatory. For the sake of simplicity, the paper only takes gross regional product as the measure of desirable output. We construct a labor input index following the disclosure of the number of employees in each province at the end of the year. It is worth noting that, since industrial $SO_2$ emissions occupy an important position in pollutant emissions, the present article uses provincial $SO_2$ emissions to measure undesirable output.

Subsequently, Table 7 details the results of the robustness test after the substitution of the independent variable and the mediator. The empirical outcomes in Table 7 highlight that the key coefficients remain basically unchanged, indicating that the research results are robust.

In addition, two key sources of endogeny are the omission of variables and bidirectional causality. Provinces with high levels of sustainable economic development have sound financial systems or high levels of financial agglomeration, and such reverse causality may lead to deviation of the results. Therefore, IV-GMM regression, which can produce efficient estimates of coefficients as well as the consistent estimates of standard errors, is utilized to solve the potential endogeneity problem [53]. IV-GMM

Table 8: Endogeneity check.

| Variables | First stage FA | | Second stage RESD |
|---|---|---|---|
| $IV_1$ | 0.254*** (4.743) | | |
| FA | | | 0.261*** (5.093) |
| RD | 0.163*** (5.878) | | 0.140*** (4.124) |
| MD | 0.016 (0.461) | | 0.276*** (6.345) |
| GI | −0.042 (−0.629) | | 0.034 (0.504) |
| Individual | Yes | | Yes |
| Year | Yes | | Yes |
| Observations | 310 | | 310 |
| *F* statistic | | 52.89 | |
| Hansen J statistic | | 1.736 | |

Note: *, **, and *** indicate the significance level is 10%, 5%, and 1%, respectively.

estimation needs to find instrumental variables that are highly related to financial agglomeration but not correlated with RESD. Thus, we use the difference between the FA value of a province in the previous year and the average FA value of the local region (i.e., the eastern, central, or western region where the province is located) as an instrumental variable ($IV_1$).

The regression results of IV-GMM are reported in Table 8. There is a remarkable positive correlation between financial agglomeration and the instrumental variable, and financial agglomeration has a significant positive influence on RESD, which manifests that the main conclusion is robust. In addition, we offer statistical data, Hansen J statistics, which is employed to test overidentification of the tools used in the first stage. It is not statistically significant at any acceptable level, suggesting that the instrumental variable used is valid. Therefore, the paper better verifies the main hypothesis by adopting the IV-GMM method.

## 5. Conclusions

How to facilitate the sustainable development of Chinese cities under the background of increasingly intensified resource and environmental constraints and intensified macroeconomic volatility is a major issue that needs to be resolved urgently by authorities and academia. The sustainable development of economy is an important cornerstone of urban sustainability. Due to the economic, technological, and ecological effects of financial agglomeration, an attempt was developed to demonstrate that one important determinant of the sustainable development of a regional economy was financial agglomeration, using panel data of 29 provinces in China from 2009 to 2019. Meanwhile, by incorporating energy efficiency and economic policy uncertainty into the theoretical framework separately, the present article tried to shed light on the possible mechanism and economic policy scenarios that financial agglomeration affected the regional economy's sustainable development. Several major findings were obtained by adopting the individual-time bidirectional fixed-effect model and performing a robustness test.

First, financial agglomeration exhibited a positive effect on the sustainable development of the regional economy through economic effect, technological effect, and ecological effect, suggesting that the higher the degree of regional financial agglomeration, the higher the level of sustainable development of the Chinese regional economy. The result corroborated the intuition that financial agglomeration not only enabled companies to obtain economies of scale [6] but also ameliorated the corporate innovation environment and increased the proportion of green output by replacing outdated technology with new ones [5]. Second, financial agglomeration was conspicuous positive with energy efficiency, and energy efficiency had mediated the relationship between financial agglomeration and the sustainable development of a regional economy. This endorsed Qu et al.'s [10] narrative that financial agglomeration relied on innovation-driving effect, structural adjustment effect, and information spillover effect to promote energy efficiency. The results were also in line with the logic that energy efficiency not only was the prerequisite for economic growth and economic restructuring [36] but also was directly related to carbon emissions and environmental protection [54, 55]. Third, economic policy uncertainty acts as a remarkable moderating variable in the proceeding of evaluating the influence of financial agglomeration on energy efficiency, that is, when economic policy uncertainty escalates, financial agglomeration begins to exert a weak positive impact on energy efficiency. This may be because, as economic policy uncertainty increases, corporate agency conflicts have intensified and energy-saving technologies have been suppressed [15].

*5.1. Management Implications.* Based on the discussion of main conclusions, countermeasures in management for facilitating the sustainable development of China's regional economy were summarized as follows:

Firstly, authorities ought to recognize that raising the level of financial agglomeration remains a key option to balance economic growth and environmental quality. In practice, in order to encourage the accumulation of financial capital and financial talents and accelerate financial integration, policymakers must publish steadfast countermeasures, such as compensating policy shortcomings, introducing financial elements, and consolidating physical carriers. Governments should assist local organizations in efforts to establish financial agglomeration centers

commensurate with the development characteristics and geographic location of the city and thus build a national and gradient financial center network with the advantageous financial centers as the leading and multilevel financial centers as complementary. Secondly, enacting stringent measures to improve energy efficiency is regarded as another priority since it is not comprehensive to solely rely on the effect of financial agglomeration to impel sustainable economic development. The improvement of energy efficiency would yield a double dividend, bringing economic and environmental benefits at the same time to avoid the vicious circle. Thus, China should vigorously promote the reform of energy production and utilization mode, constantly revise the policy system, and strive to achieve the comprehensive, coordinated, and sustainable development of energy, economy, society, and ecology. Finally, Chinese authorities are supposed to maintain the stability and continuity of economic policies because there exists a suppression of economic policy uncertainty on the relation between financial agglomeration and regional energy efficiency. Appropriate measures related to financial agglomeration would be formulated based on the comprehensive identification and assessment of local economic policy uncertainties. In order to maintain the stability of city's economy, regulatory authorities should try to avoid issuing short-term economic policies when announcing economic policies. Especially in the context of intensified resource constraints and increasing downward pressure on the economy, the formulation of economic policies should keep the goals of economic growth and energy conservation and emission reduction unchanged.

*5.2. Limitations and Further Research.* As with other scientific studies, this paper is subject to certain conditions. First, a caveat of the study was that the research results cannot be simply extrapolated to other cases because this study only selected sample data from China and did not include samples from developed countries or other relatively backward regions for comparison. Hence, future research should endeavor to overcome the limitations of samples to obtain more precise and comparable conclusions. Secondly, according to the principle of data availability, the economic policy uncertainty index used in the present article belongs to the national level rather than the provincial level, which may cause deviation in regional data analysis. Then, it is plausible that subsequent research attempts to evaluate the economic policy uncertainty index of each province in China and further reinvestigates the interaction between EPU and financial agglomeration. Lastly, we call for more in-depth quantitative or qualitative research on institutional factors, economic opening, or bureaucratic factors to explore divergent antecedents of the sustainable development of China's regional economy.

## Data Availability

The data supporting the results of this study are available from the corresponding author upon request.

## Conflicts of Interest

The authors declare no conflicts of interest.

## Acknowledgments

The authors acknowledge the support of the Project of the Countermeasures of Innovation and Entrepreneurship Education for College Students in Shaanxi (2016ZD06).

## References

[1] C. Ye, C. Sun, and L. Chen, "New evidence for the impact of financial agglomeration on urbanization from a spatial econometrics analysis," *Journal of Cleaner Production*, vol. 200, pp. 65–73, 2018.

[2] J. L. Ruiz, "Financial development, institutional investors, and economic growth," *International Review of Economics & Finance*, vol. 54, pp. 218–224, 2017.

[3] A. M. Omer, "Energy, environment and sustainable development," *Renewable and Sustainable Energy Reviews*, vol. 12, no. 9, pp. 2265–2300, 2008.

[4] D. Durusu-Ciftci, M. S. Ispir, and H. Yetkiner, "Financial development and economic growth: some theory and more evidence," *Journal of Policy Modeling*, vol. 39, no. 2, pp. 290–306, 2017.

[5] H. Yuan, T. Zhang, Y. Feng, Y. Liu, and X. Ye, "Does financial agglomeration promote the green development in China? A spatial spillover perspective," *Journal of Cleaner Production*, vol. 237, Article ID 117808, 2019.

[6] H. Yuan, Y. Feng, J. Lee, H. Liu, and R. Li, "The spatial threshold effect and its regional boundary of financial agglomeration on green development: a case study in China," *Journal of Cleaner Production*, vol. 244, Article ID 118670, 2020.

[7] F. J. Buera, J. P. Kaboski, and Y. Shin, "Finance and development: a tale of two sectors," *American Economic Review*, vol. 101, no. 5, pp. 1964–2002, 2011.

[8] S. Tadesse, "Financial architecture and economic performance: international evidence," *Journal of Financial Intermediation*, vol. 11, no. 4, pp. 429–454, 2002.

[9] M. Peneder, "Industrial structure and aggregate growth," *Structural Change and Economic Dynamics*, vol. 14, no. 4, pp. 427–448, 2003.

[10] C. Qu, J. Shao, and Z. Shi, "Does financial agglomeration promote the increase of energy efficiency in China?" *Energy Policy*, vol. 146, Article ID 111810, 2020.

[11] F. Rubio, C. Llopis-Albert, F. Valero, and A. J. Besa, "Sustainability and optimization in the automotive sector for adaptation to government vehicle pollutant emission regulations," *Journal of Business Research*, vol. 112, pp. 561–566, 2020.

[12] W. Yang and L. Li, "Energy efficiency, ownership structure, and sustainable development: evidence from China," *Sustainability*, vol. 9, no. 6, p. 912, 2017.

[13] R. Ayres, H. Turton, and T. Casten, "Energy efficiency, sustainability and economic growth," *Energy*, vol. 32, no. 5, pp. 634–648, 2007.

[14] S. S. Mirza and T. Ahsan, "Corporates' strategic responses to economic policy uncertainty in China," *Business Strategy and the Environment*, vol. 29, no. 2, pp. 375–389, 2020.

[15] V. Ongsakul, S. Treepongkaruna, P. Jiraporn, and A. Uyar, "Do firms adjust corporate governance in response to

economic policy uncertainty? Evidence from board size," *Finance Research Letters*, vol. 39, Article ID 101613, 2021.

[16] K. Yung and A. Root, "Policy uncertainty and earnings management: international evidence," *Journal of Business Research*, vol. 100, pp. 255–267, 2019.

[17] Z. Xu, "Economic policy uncertainty, cost of capital, and corporate innovation," *Journal of Banking & Finance*, vol. 111, Article ID 105698, 2019.

[18] F. F. Adedoyin, S. Nathaniel, and N. Adeleye, "An investigation into the anthropogenic nexus among consumption of energy, tourism, and economic growth: do economic policy uncertainties matter?" *Environmental Science and Pollution Research*, vol. 28, no. 3, pp. 2835–2847, 2021.

[19] L. Cheng, S. Zhang, X. Lou, Y. Yang, and W. Jia, "The penetration of new generation information technology and sustainable development of regional economy in China-moderation effect of institutional environment," *Sustainability*, vol. 13, no. 3, p. 1163, 2021.

[20] R. Danish, R. Ulucak, and S. U. D. Khan, "Relationship between energy intensity and $CO_2$ emissions: does economic policy matter?" *Sustainable Development*, vol. 28, no. 5, pp. 1457–1464, 2020.

[21] J. Corpataux, O. Crevoisier, and T. Theurillat, "The expansion of the finance industry and its impact on the economy: a territorial approach based on Swiss pension funds," *Economic Geography*, vol. 85, no. 3, pp. 313–334, 2009.

[22] R. E. Baldwin, P. Martin, and G. I. P. Ottaviano, "Global income divergence, trade, and industrialization: the geography of growth take-offs," *Journal of Economic Growth*, vol. 6, no. 1, pp. 5–37, 2001.

[23] K. Karltorp, S. Guo, and B. A. Sandén, "Handling financial resource mobilisation in technological innovation systems-the case of Chinese wind power," *Journal of Cleaner Production*, vol. 142, no. 4, pp. 3872–3882, 2017.

[24] D. B. Audretsch and M. P. Feldman, "R&D spillovers and the geography of innovation and production," *American Economic Review*, vol. 86, no. 3, pp. 630–640, 1996.

[25] J. Fu and Y. Geng, "Public participation, regulatory compliance and green development in China based on provincial panel data," *Journal of Cleaner Production*, vol. 230, pp. 1344–1353, 2019.

[26] E. Kemp-Benedict, "Investing in a green transition," *Ecological Economics*, vol. 153, pp. 218–236, 2018.

[27] A. Nisar, M. Palacios, and M. Grijalvo, "Open organizational structures: a new framework for the energy industry," *Journal of Business Research*, vol. 69, no. 11, pp. 5175–5179, 2016.

[28] J. M. Simkoff, F. Lejarza, M. T. Kelley, C. Tsay, and M. Baldea, "Process control and energy efficiency," *Annual Review of Chemical and Biomolecular Engineering*, vol. 11, no. 1, pp. 423–445, 2020.

[29] Z. Cheng, J. Liu, L. Li, and X. Gu, "Research on meta-frontier total-factor energy efficiency and its spatial convergence in Chinese provinces," *Energy Economics*, vol. 86, Article ID 104702, 2020.

[30] B. Yu, "Industrial structure, technological innovation, and total-factor energy efficiency in China," *Environmental Science and Pollution Research*, vol. 27, no. 8, pp. 8371–8385, 2020.

[31] F. Pan and B. Yang, "Financial development and the geographies of startup cities: evidence from China," *Small Business Economics*, vol. 52, no. 3, pp. 743–758, 2019.

[32] P. Garrone, L. Grilli, and B. Mrkajic, "The role of institutional pressures in the introduction of energy-efficiency innovations," *Business Strategy and the Environment*, vol. 27, no. 8, pp. 1245–1257, 2018.

[33] N. Hanley, P. G. Mcgregor, J. K. Swales, and K. Turner, "Do increases in energy efficiency improve environmental quality and sustainability?" *Ecological Economics*, vol. 68, no. 3, pp. 692–709, 2009.

[34] F. C. Ozbugday and B. C. Erbas, "How effective are energy efficiency and renewable energy in curbing $CO_2$ emissions in the long run? A heterogeneous panel data analysis," *Energy*, vol. 82, pp. 734–745, 2015.

[35] I. Michele and T. D. Ketterer, "Energy efficiency gains from importing intermediate inputs: firm-level evidence from Indonesia," *Journal of Development Economics*, vol. 135, pp. 117–141, 2018.

[36] C. Bataille and N. Melton, "Energy efficiency and economic growth: a retrospective CGE analysis for Canada from 2002 to 2012," *Energy Economics*, vol. 64, pp. 118–130, 2017.

[37] Y. Zhou, M. Ma, F. Kong, K. Wang, and J. Bi, "Capturing the co-benefits of energy efficiency in China - a perspective from the water-energy nexus," *Resources, Conservation and Recycling*, vol. 132, pp. 93–101, 2018.

[38] I. Dincer and M. A. Rosen, "A worldwide perspective on energy, environment and sustainable development," *International Journal of Energy Research*, vol. 22, no. 15, pp. 1305–1321, 1998.

[39] L. Pástor and P. Veronesi, "Uncertainty about government policy and stock prices," *The Journal of Finance*, vol. 67, no. 4, pp. 1219–1264, 2012.

[40] H. N. Duong, J. H. Nguyen, M. Nguyen, and S. G. Rhee, "Navigating through economic policy uncertainty: the role of corporate cash holdings," *Journal of Corporate Finance*, vol. 62, Article ID 101607, 2020.

[41] S. A. Raza, N. Shah, and M. Shahbaz, "Does economic policy uncertainty influence gold prices? Evidence from a nonparametric causality-in-quantiles approach," *Resources Policy*, vol. 57, pp. 61–68, 2018.

[42] V. Nagar, J. Schoenfeld, and L. Wellman, "The effect of economic policy uncertainty on investor information asymmetry and management disclosures," *Journal of Accounting and Economics*, vol. 67, no. 1, pp. 36–57, 2019.

[43] E. Magnani and A. Tubb, "Green R&D, technology spillovers, and market uncertainty: an empirical investigation," *Land Economics*, vol. 88, no. 4, pp. 685–709, 2012.

[44] A. Markandya, S. Pedroso-Galinato, and D. Streimikiene, "Energy intensity in transition economies: is there convergence towards the EU average?" *Energy Economics*, vol. 28, no. 1, pp. 121–145, 2006.

[45] G. D. Jacobsen, "Do energy prices influence investment in energy efficiency? Evidence from energy star appliances," *Journal of Environmental Economics and Management*, vol. 74, pp. 94–106, 2015.

[46] B. Wilson, L. H. Trieu, and B. Bowen, "Energy efficiency trends in Australia," *Energy Policy*, vol. 22, no. 4, pp. 287–295, 1994.

[47] I. W. H. Parry, D. Evans, and W. E. Oates, "Are energy efficiency standards justified?" *Journal of Environmental Economics and Management*, vol. 67, no. 2, pp. 104–125, 2014.

[48] L. Cecchini, S. Venanzi, A. Pierri, and M. Chiorri, "Environmental efficiency analysis and estimation of $CO_2$ abatement costs in dairy cattle farms in Umbria (Italy): a SBM-DEA model with undesirable output," *Journal of Cleaner Production*, vol. 197, pp. 895–907, 2018.

[49] J. Du, L. Liang, and J. Zhu, "A slacks-based measure of super-efficiency in data envelopment analysis: a comment," *European Journal of Operational Research*, vol. 204, no. 3, pp. 694–697, 2010.

[50] Y. Zhang, W. Wang, L. Liang, D. Wang, X. Cui, and W. Wei, "Spatial-temporal pattern evolution and driving factors of China's energy efficiency under low-carbon economy," *The Science of the Total Environment*, vol. 739, Article ID 140197, 2020.

[51] S. R. Baker, N. Bloom, and S. J. Davis, "Measuring economic policy uncertainty," *Quarterly Journal of Economics*, vol. 131, no. 4, pp. 1593–1636, 2016.

[52] R. M. Baron and D. A. Kenny, "The moderator-mediator variable distinction in social psychological research: conceptual, strategic, and statistical considerations," *Journal of Personality and Social Psychology*, vol. 51, no. 6, pp. 1173–1182, 1986.

[53] S. Sheikh, "The impact of market competition on the relation between CEO power and firm innovation," *Journal of Multinational Financial Management*, vol. 44, pp. 36–50, 2018.

[54] S.-Y. Oh, S. Yun, and J.-K. Kim, "Process integration and design for maximizing energy efficiency of a coal-fired power plant integrated with amine-based CO2 capture process," *Applied Energy*, vol. 216, pp. 311–322, 2018.

[55] M. Vujanovic, Q. W. Wang, M. Mohsen, N. Duic, and J. Y. Yan, "Recent progress in sustainable energy-efficient technologies and environmental impacts on energy systems," *Applied Energy*, vol. 283, Article ID 116280, 2021.

Hindawi
Mathematical Problems in Engineering
Volume 2021, Article ID 9579325, 15 pages
https://doi.org/10.1155/2021/9579325

*Research Article*

# Understanding the Effects of Fare Discount Schemes to Metro Transit Ridership Based on Structural Change Analysis

**Zhe Li, Weifeng Li, and Qing Yu**

*Key Laboratory of Road and Traffic Engineering of the Ministry of Education, Tongji University, Tongji 201804, China*

Correspondence should be addressed to Weifeng Li; liweifeng@tongji.edu.cn

Received 5 July 2021; Accepted 18 September 2021; Published 7 October 2021

Academic Editor: Thomas Hanne



Since fare discounts have been regarded as an effective economical measure to increase passenger flow, it is helpful for local governments and transit operators to understand its impact on ridership. Taking Xiamen, China, as an example, this study uses transaction data to analyze the changes of weekday daily metro ridership after the opening of Xiamen Metro Line 1. At the initial stage of operation of Xiamen Metro Line 1, there are three preferential schemes: discount per trip, money reduced per trip, and discount after reaching the accumulated fare. Therefore, the algorithm of the iterated cumulative sums of squares is introduced to identify structural change points of the time series of daily ridership, which varies according to the type of ticket. The effects of different fare discounts on total ridership and ridership varied by ticket types are analyzed by the regression discontinuity method. The results show that the dates of structural change points are well-matched with the start and end dates of preferential schemes. Each preferential scheme has its own benefited groups. During the fare discount period, the number of passengers gradually increased. But after the cancellation of the favorable preferential scheme, the number of passengers decreased sharply. By understanding the impact of fare discounts on ridership in Xiamen, China, several metro ticketing policy recommendations are put forward, including raising the focus on E-Tickets, formulating more attractive preferential measures to promote the mode conversion of private cars and vehicles to metro, paying attention to high-frequency passengers, and seeking common subsidies from the financial industry to achieve a win-win situation. In addition, the analytical framework proposed in this study can be used to evaluate the effectiveness of other transportation policies in the future.

## 1. Introduction

In recent years, metro systems have developed rapidly in China. According to the data from the China Association of Metros, 19 cities have opened their first metro lines in the past 5 years. There have been 244 operating lines with a mileage of 7,970 km in China [1]. As a kind of large-capacity public transport, the metro system is considered the main skeleton of the public transport system. The opening of the first metro line may lead to a modal shift from the bus and private cars to the metro [2, 3]. Therefore, the government and metro operators are very concerned about the changes in ridership after the opening of the first metro line.

Due to the social benefit of public transport, passengers are more sensitive to prices and expect lower costs. During the opening period of the first metro line, several fare discount schemes are launched to attract stable passenger flow. Generally speaking, as a type of economic measure, fare discount schemes can have a positive impact on metro passenger flow [4]. However, if local government and transit operators lack experience in these fields, inappropriate fare discount policies may lead to a sharp decline in transit ridership and cause negative public reactions due to social inequality. Yang held the view that it is difficult to balance revenue, profit, demand, user benefits, and social welfare when determining ticket prices [5]. Therefore, it is necessary to explore the impact of fare discount schemes on ridership.

With the development of data collection progress, the emerging spatiotemporal data can help explore travel behavior and improve urban transport [6, 7]. In addition, it is

possible to monitor dynamic ridership for a long time, which provides us with a database to explore the impact of fare discount schemes on ridership. At the same time, with the popularity of smartphones, ticket types have also been revolutionized. Passengers can get E-Tickets through their smartphones. They no longer need to buy tickets from Ticket Vending Machine or carry a smart card with them. E-Tickets are attractive to many young people who are familiar with smartphones. At the same time, it is difficult for older passengers who are not familiar with smartphones to use E-Tickets. In general, E-Tickets have become an important ticket type and pose a subversive challenge to traditional ticket types such as Smart Card Tickets and Single Tickets. Therefore, studying the impact of different fare discount schemes on ridership of different ticket types, especially emerging ticket types, will help the government and operators to evaluate the effect of fare discount schemes. Meanwhile, the study can lay a foundation for the introduction of targeted preferential policies of different ticket types.

Smart Card Tickets, E-Tickets, Single Tickets, and Other Tickets can be used in the Xiamen Metro system. Fare discount schemes are issued by the government, metro companies, and Banking Alliance in China (UnionPay). We observed the results of fare discount schemes implemented in Xiamen City over the past 18 months, including discount per trip, money reduced per trip, and discount after reaching the accumulated fare. This case provides a reference for studying the impact of discount types on ridership. To reveal the different trends of ridership caused by the fare discount schemes of different ticket types, the iterated cumulative sums of squares (ICSS) algorithm is adopted in this study [8].

The main purposes of this paper are to (1) propose an analysis method to extract the variation of ridership and (2) discuss the impact of fare discount schemes on ridership after the opening of the first metro line. The remainder of this paper is organized as follows. In Section 2, relevant research studies are reviewed. In Section 3, the background of Xiamen city, the metro system of Xiamen, and its transaction data are introduced. The ICSS and RD algorithm are presented in Section 4. Policy recommendations are put forward based on analyzing the association between the structural change of ridership and the fare discount schemes in Section 5. Finally, Section 6 summarizes the main findings of this study.

## 2. Related Works

*2.1. Early Studies of Transit Fare.* In the early literature, Vickrey formulated transit fares based on the traditional marginal cost pricing theory [9]. Subsequently, Mohring developed a microeconomic foundation for public transportation services with fixed demand [10]. After completing an important empirical study, Small introduced the concept of generalized costs and calibrated the disutility function [11]. Attitude theory, social learning theory, and theories of social dilemmas were also developed when researching fare policies [12].

Fare elasticity is the most widely used method to evaluate the impact of fares on ridership. Price sensitivity is measured by elasticities, which refers to the percentage change in consumption caused by a one-percent change in price, all else held constant. A frequently used rule-of-thumb, known as the Simpson–Curtin rule, is that each 3% fare increase reduces ridership by 1%. Like most rules-of-thumb, this can be useful for rough analysis but it is too simplistic and outdated for detailed planning and modeling. Victoria Transport Policy Institute has reviewed the researches on fare elasticity. Some factors that affect transit elasticities are summarized as follows: user type, trip type, transit type, period, geography, type and direction of price change, etc. [13]. After a detailed review of international studies, Goodwin obtained the average elasticity values by different modes in the short run and long run. For instance, the elasticities of bus demand concerning fare cost are −0.28 in the short run and −0.55 in the long run. He noted that price impacts tended to increase over time because consumers have more options (related to increases in real incomes, car ownership, and telecommunications replacing physical travel) [14]. Gillen summarized transit fare elasticities for different user groups and trips types, illustrating how various factors affected transit price sensitivities. For example, it indicated that car owners had a greater elasticity (−0.41) than people who relied on public transport (−0.10), and work trips were less elastic than shopping trips [15]. Several fare discounts schemes have been launched to stimulate transit ridership. Public transportation ridership increased by 2–3% when public transportation subsidies increased by 10% and price decreased by 5–7% from a study by Cervero on urban public transportation in 18 countries [16].

Early methods are still quite useful for long-term public transit service planning in a static sense.

*2.2. Measurement Models.* In recent research, there have been four main measurement models proposed to determine the impact of transit fare discounts.

*2.2.1. Optimization Models.* The optimization model refers to the establishment of the objective function. When the objective function is optimal, the value of fare will be observed. The optimization model is mostly used to compare fare policies under different scenarios. Borndörfer et al. proposed a nonlinear optimization approach to pursue objectives such as the maximization of demand, revenue, profit, or social welfare [17]. Guo and Sun established two objective functions to analyze the fare discounts in terms of travel behavior, crowding, and waiting time [18].

*2.2.2. Disaggregate Models.* Disaggregate models mainly use survey data, combined with the user's social and economic attributes, to analyze the impact of fare change on individual passengers. Sharaby and Shiftan constructed a multinomial logit (MNL) model by using fare-box data and onboard survey data to analyze the impact of fare integration on travel behavior and transit ridership. The results indicated an increase of 7.7% in passenger trips and 18.6% in boarding.

The number of boarding per trip increased from 1.38 to 1.52. The modal results demonstrated that fare reduction encouraged travelers to shift from private cars or taxis to buses, and created new trips [4]. Farber et al. assessed equity of transit fare based on distance using household travel survey data based on a joint ordinal/continuous model [19].

*2.2.3. Regression Models.* Regression models are regularly built with survey data from the macro-level to analyze the impact of fare changes on ridership and travel behavior. There are two main types of regression models, the first of which are temporal regression models. Miller and Savage analyzed the demand response after fare changes in 2004, 2006, 2009, and 2013 based on the pooled regression (POLS) and fixed effects models [20]. Gkritza et al. established seemingly unrelated regression equation (SURE) models for monthly data from January 1995 to December 2006 (a total of 144 observations) to estimate multimodal transit ridership with a varying fare structure [21]. Spatial regression models are the second type of regression model. Liu et al. evaluated the effects of public transport fare policy changes together with built and nonbuilt environment features on ridership by using a spatial lag regression model [22]. Verbich and El-Geneidy discovered the association between fare structure and social vulnerability using a negative binomial regression model with smart card data [23].

*2.2.4. Statistical Models.* It mainly refers to the fare elasticity analysis method. Nahmias-Biran et al. introduced the Lorenz curve and the Gini Index from the perspective of macroeconomics to summarize the equity aspects of transit fare change projects [24]. Using detailed travel-diary data, Brown investigated equity of low-income and higher-income transit riders under five evaluated fare structures: flat, adjusted by travel distance, varied by time of day, varied by mode, and discounted based on rider characteristics [25]. Nuworsoo et al. used onboard survey data to evaluate the impacts of the various fare proposals (hikes, base fare reductions, eliminations of free transfers, and discontinuation of periodic passes) on different subsets of riders and to evaluate the equity of each proposal. Proposals for flat fares per ride were found to be the least equitable of the fare policies, even when the base fare was lowered, because lower-income riders, youth, and minorities make more trips and transfer more frequently than their more affluent counterparts [26]. Wang et al. assessed the impact on ridership by using prior stated preference (SP) survey data (2015) and ex-post smart card data (2017), respectively. The results showed that the SP survey significantly exaggerated the passengers' responses to the price adjustment [27, 28].

Sensitivity analysis and price elasticities are common methods to analyze the impact of fare changes on ridership and travel behavior.

*2.3. Summary of Relevant Research.* Previous studies are long-term static research, using data sources from the travel-diary, onboard survey, SP survey, etc. With the development of data collection methods, it is possible to collect and summarize daily ridership from transaction data. After the opening of the first metro line, the government and metro operators look forward to receiving timely feedback from passengers on fare policy. Therefore, a short-term dynamic ridership monitoring method is more worthy of expectation. Yeh and Lee analyzed the structural change of monthly ridership time series from 2001 to 2014 [12]. It provides the possibility for researching on effects of fare policy on ridership according to structural change analysis.

## 3. Study Case and Data

*3.1. Xiamen City and Xiamen Metro Line 1.* Xiamen City is an important central coastal city on the southeastern coast of China, with a population of 4.01 million. As one of the more developed cities in China, Xiamen's foreign population from other cities accounts for about 42.38%. Xiamen City is a famous tourist city in China. In 2018, there were 89 million tourists, with total tourism revenue of 140 billion RMB (RMB is the Chinese monetary unit, and 1 RMB is equal to 0.1545 US dollars). The most popular tour dates in Xiamen are from June to October, especially during the summer vacation.

Xiamen Metro Line 1, the first metro in Xiamen, began operation on Dec 31$^{st}$, 2017. It has 24 stations and is 30.3 kilometers long. By the end of 2018, the public transportation system in Xiamen was composed of 1metro line, 6 bus rapid transit (BRT) lines, and 358 bus lines (see Figure 1).

*3.2. Metro Ticket Types and Fare Discount Schemes.* There are four ticket types in the Xiamen metro:

(i) Smart Card Tickets: passengers swipe their smart cards when entering and exiting the station

(ii) E-Tickets (APP Tickets): passengers can purchase an electronic ticket through the "Xiamen Metro" mobile phone application, and they swipe their own E-Ticket/QR code via Bluetooth when entering and exiting the station

(iii) Single Tickets: passengers can only use this ticket once after selecting the entry and exit station on the Ticket Vending Machine. Single Tickets can be circulated and reused within the metro system

(iv) Other Tickets: multiday tickets, etc.

Xiamen Metro Line 1 adopts distance-based pricing. The further passengers travel, the lower fare per kilometer passengers pay. The ticket price will be calculated according to a segmentation system focusing on mileage: 2 RMB within 4 kilometers, 3 RMB for 4–8 kilometers, 4 RMB for 8–12 kilometers, 5 RMB for 12–18 kilometers, 6 RMB for 18–28 kilometers, and 7 RMB above 28 kilometers.

The fare of Xiamen BRT also adopts distance-based pricing. The starting price of BRT is 1 RMB within 10 kilometers. For passengers traveling above 10 kilometers, they will pay 0.15 RMB for traveling every one kilometer, and the maximum fare is 4 RMB.

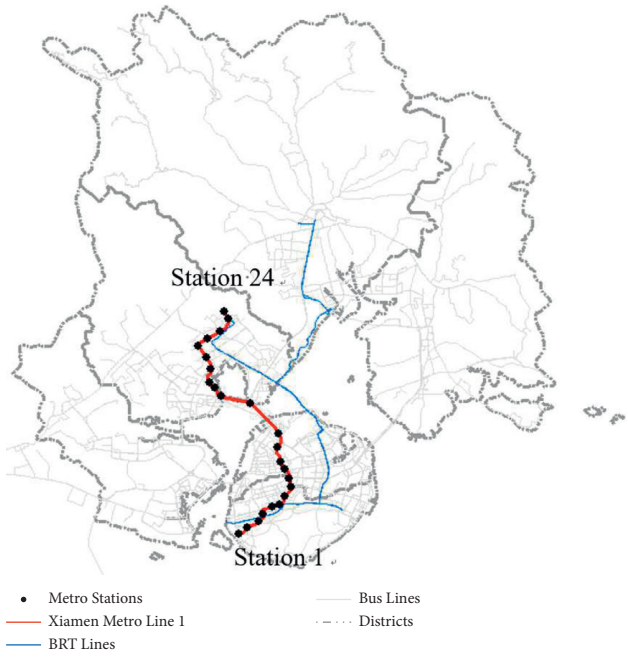


Figure 1: Xiamen city and Xiamen Metro Line 1.

The full fare of intra-district regular bus service is 1 RMB per trip, and 2 RMB for inter-district bus service.

Therefore, the original fare of the metro has no advantage over the fare of BRT and bus. To narrow the fare gap between different modes of transportation and enhance the attractiveness of Metro Line 1, the Xiamen government, Xiamen Metro Group, and Banking Alliance (UnionPay) have issued a series of preferential schemes. From Dec 31st, 2017 to Jun 30th, 2019, there were three fare discount schemes in Xiamen (see Table 1).

*3.3. Metro Transaction Data.* The metro transaction data used in this study were collected from Jan 1st, 2018 to Jun 30th, 2019 (a total of 18 months and 546 days) from the Xiamen Metro Group. Although there are separate records for each ticket type, there is a similar main field for each ticket type (see Table 2).

A total of 66.84 million metro transaction data records were collected in 18 months. Smart Card Tickets comprised the highest percentage of recorded tickets, accounting for 45.24% with 30.24 million records. The second-highest number of records was Single Tickets; there were 20.78 million records, accounting for 31.09%. Only 11.60 million E-Tickets were recorded, accounting for 17.36%. However, due to a series of preferential schemes, the share of E-Tickets increased from 12.93% (Jan 1st, 2018) to 23.93% (Jun 30th, 2019) (see Table 3).

Statistically, there are significant differences in ridership on weekdays, weekends, and holidays (see Table 4). Xiamen is a very famous tourist city. Many citizens and tourists from other cities also take the subway to tourist attractions. Due to the short operation time, there is less commute travel on weekdays than leisure travel on weekends. Therefore, there is more ridership on weekends than ridership on weekdays.

## 4. Methods

*4.1. Iterated Cumulative Sums of Squares (ICSS) Algorithm*

*4.1.1. Definition and Significance of Structural Change Points (SCPs).* The iterated cumulative sums of squares (ICSS) algorithm were first introduced into the financial field to detect multiple changes of variance in a sequence of independent observations [8]. The calculation flow chart of the ICSS algorithm is shown in Figure 2. For additional details about the ICSS algorithm, please refer to the literature [8].

There are series that do not follow the usual assumption of constant variance underlying most models for time series. This series exhibits a stationary behavior for some time, then the variability of the error term changes suddenly; it remains constant again at this new value for some time until another change occurs.

ICSS algorithm is mainly used to detect the structural change points (SCPs) and test the mutation of the time series. The structural change points from ICSS are defined as the moment of state change. Rules can be obtained after analyzing the association between the date of ridership structural change points and the start-end dates of the fare discount schemes.

*4.1.2. Constructing Fluctuation Rate Series and Stationary Test.* The original daily transit ridership $\{R_t\}$ can be regarded as a time series. The fluctuation rate series $\{Q_t\}$ of daily transit ridership series $\{R_t\}$ is defined as the first-order logarithmic difference of daily transit ridership $\{R_t\}$ in

$$Q_t = \ln R_{t+1} - \ln R_t, \quad t = 0, 1, 2, \ldots, N, \tag{1}$$

where $R_t$ is daily transit ridership at a certain line or station on date number $t$ and $N$ is the total number of dates. $\ln(x)$ is a synonym function of $x$.

Only when the time series is stable can its basic characteristics remain stable. These stable statistical characteristics can be used to obtain future forecasts. Before using the ICSS algorithm, it is necessary to check whether the fluctuation rate series $\{Q_t\}$ is a stationary time series.

If the time series meets the following criteria, it is a stationary time series:

(i) The average value $E(Q_t) = m$ is a constant $m$, independent of date number $t$.

(ii) The variance $\mathrm{Var}(Q_t) = s^2$ is a constant $s^2$, independent of date number $t$.

(iii) The covariance $\mathrm{Cov}(Q_t, Q_{t+k}) = gk$ is a constant $gk$. $k$ is the period interval of date number. $g$ is a constant coefficient. The covariance is independent of date number $t$.

The stationary of time series can be obtained by the logarithmic difference method, as shown in equation (2). The essence of the fluctuation rate series $\{Q_t\}$ is the growth rate of the original daily transit ridership $\{R_t\}$. Generally, the growth rate of the time series is stable.

Table 1: Fare discount schemes.

| Discount name | Ticket type | Details | Allowance providers | Start date-end date |
|---|---|---|---|---|
| 10% discount (discount per trip) | Smart Card/APP | Passengers can enjoy a 10% discount by using their smart card/"Xiamen Metro" APP. | Xiamen government and Xiamen metro group | 2017/12/31 till now |
| 2 RMB discount (money reduced per trip) | APP | Passengers can enjoy a 2 RMB discount per trip by using the "Xiamen Metro" APP and paying for the E-tickets with the "UnionPay" APP. Each passenger can only enjoy 2 preferential rides a day. | Banking alliance (UnionPay) | 2018/9/22–2018/12/31 |
| 50% discount (discount after reaching accumulated fare) | Smart Card/APP | According to the monthly statistics, when the total fare exceeds 40 RMB, there is a more than 50% discount for each ride. | Xiamen government and Xiamen metro group | 2018/12/1 till now |

Table 2: Main fields of metro transaction data.

| Name | Data type | Example | Note |
|---|---|---|---|
| ID | String | 04FBC094 (Single Tickets/Other Tickets); 8012013030903604 (Smart Card Tickets); 138xxxx4740 (E-tickets) | The IDs of Single Tickets and Other Tickets are the numbers on the card circled in the metro system and do not belong to the passenger. While the IDs of smart cards and E-Tickets are the passengers' individual information, the IDs of smart cards are the smart card numbers, and the IDs of E-Tickets are the encrypted registration telephone numbers |
| Transaction date | Date | 2019/1/1 | |
| Transaction time | Time | 6:24:09 | |
| Transaction type | Binary | 0/1 | 0 stands for entering the metro station; 1 stand for exiting the metro station |
| Price | Int | 200 | Unit: RMB cent |
| Gate number | String | 01010307 | The metro station's name and number can be obtained from the gate number |

$$Q_t = \ln R_{t+1} - \ln R_t = \frac{\ln R_{t+1} - \ln R_t}{(t+1)-(t)} = d(\ln R_t) = \frac{d(R_t)}{R_t}, \tag{2}$$

where $d(x)$ is the derivation of $x$.

*4.1.3. Constructing Uncorrelated Random Series.* To avoid the effects of mean and variance, a series of uncorrelated random variables are constructed. Thus, the following uncorrelated random series $\{a_t\}$ are obtained after standardization ($Z$-score normalization) in

$$a_t = \frac{Q_t - 1/t\sum_{i=0}^{t-1} Q_i}{\sqrt{(t+1/t)S_Q^2}}, \quad t = 0, 1, 2, \ldots, N, \tag{3}$$

where $S_Q^2$ represents the estimated variance of all observations for fluctuation rate $Q_t$.

*4.1.4. Constructing Centered Cumulative Sum of Squares.* A series of the cumulative sum of squares are constructed to influence the effect of negative values of uncorrelated random variables. And, it also enhances and highlights the mutation in uncorrelated random series. Let $C_t$ be the cumulative sum of squares of a series of uncorrelated random variables $\{a_t\}$ in

$$C_t = \sum_{i=0}^{t} a_i^2, \quad t = 0, 1, 2, \ldots, N. \tag{4}$$

Then, let $D_t$ be the centered (Zero-centered) cumulative sum of squares to avoid the effects of date number and detect whether the variances change significantly in

$$D_t = \sqrt{\frac{N}{2}}\left|\frac{C_t}{C_N} - \frac{t}{N}\right|, \quad t = 0, 1, 2, \ldots, N, \tag{5}$$

where $C_N$ represents the value of $C_t$ when $t$ is equal to $N$.

*4.1.5. Identification of SCPs.* Obviously, $D_t$ against $t$ will oscillate around 0 for series with homogeneous variance. If the uncorrelated random series $\{a_t\}$ maintains the same value at each time, $D_t$ will be equal to 0, which means that there are no SCPs in the fluctuation rate at time $t$.

Given a sudden change in the variance of $\{a_t\}$, when $D_t$ exceeds a predetermined threshold $D^*$(here, it is set to$D^*_{0.05} = 1.358$ at a confidence level of 95%.), the existence of an SCP is implied. The time $t^*$ is regarded as the time when this SCP occurs.

Table 3: Recorded numbers of metro transaction data for each ticket type.

| Ticket type | Record numbers for each ticket type | Percentage for each ticket type |
|---|---|---|
| Smart Card Tickets | 30238762 | 45.24 |
| E-Tickets | 11600640 | 17.36 |
| Single Tickets | 20780222 | 31.09 |
| Other Tickets | 4220397 | 6.31 |
| Total | 66840021 | 100 |

Table 4: Statistical characteristics of ridership on weekdays, weekends, and holidays.

| Day type | Weekdays | Weekends | Holidays |
|---|---|---|---|
| Numbers | 301 | 198 | 47 |
| Mean | 113918 | 130002 | 144902 |
| Median | 113936 | 130624.5 | 145001 |
| Standard deviation | 20636 | 20568 | 40792 |
| Maximum | 180077 | 176902 | 237830 |
| Minimum | 59218 | 85935 | 36295 |

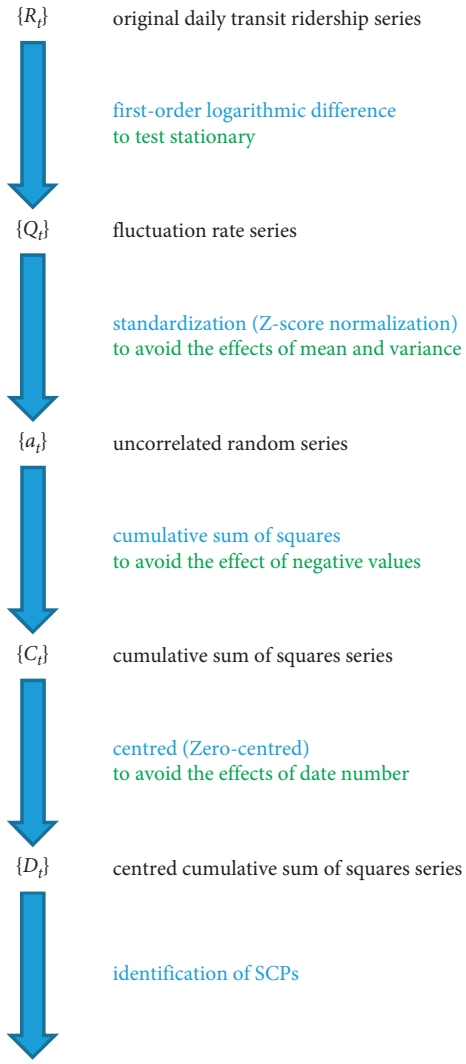


Figure 2: Calculation flow chart of ICSS algorithm.

*4.2. Regression Discontinuity (RD) Method.* Regression discontinuity (RD) analysis is a rigorous nonexperimental method that can be used to estimate program impacts in situations in which candidates are selected for treatment based on whether their value for a numeric rating exceeds a designated threshold or cut point [29].

The RD method was first introduced by Thistlethwaite and Campbell to study the impact of scholarships on students' career planning [30]. But it was not until the late 1990s that economists took it seriously. Hahn et al. provided the RD method as the theoretical basis of econometrics [31]. Then, economists revived the approach, formalized it, strengthened its estimation methods, and began to apply it to many different research questions. This renaissance culminated in a 2008 special issue on RD analysis in the *Journal of Econometrics*. At present, the applications of RD in educational economy, labour economy, health economy, political economy, and regional economy are still on the rise.

Sharp Regression Discontinuity means that at the breakpoint, the probability of the processed individual $P_i$ jumps from 0 to 1 when the independent variable $x_i$ is equal to the breakpoint $c$. Generally, we assume that the breakpoint is a constant $c$, and the classification rule is in

$$P_i = \begin{cases} 1, & x_i \geq c, \\ 0, & x_i < c. \end{cases} \tag{6}$$

Before the experiment, a linear relationship between the dependent variable $y_i$ and independent variable $x_i$ should be supposed, as shown in

$$y_i = \alpha + \beta x_i + \varepsilon_i \, (i = 1, \ldots, n). \tag{7}$$

Since there is no systematic difference in all aspects of the individual near $x = c$, the only reason for the jump in the conditional expectation function $E(y_i|x)$ here is only the processing effect $P_i$. To estimate this jump, equation (7) is rewritten as

$$y_i = \alpha + \beta (x_i - c) + \delta P_i + \gamma (x_i - c) P_i + \varepsilon_i \, (i = 1, \ldots, n), \tag{8}$$

where $(x_i - c)$ is the standardization of variable $x_i$, making $y_i = 0$ when $x_i$ is equal to $c$. Introducing an interactive item $\gamma (x_i - c) P_i$ allows different slopes on both sides of the breakpoints. Then, the local average effect $\delta$ can be estimated when $x_i$ is equal to $c$ by using the OLS (Ordinary Least Squares) regression.

The linear regression discontinuity method was applied between two adjacent SCPs. The growth trend of this stage can be obtained from the slope. It is also possible to test whether similar equations exist between different intervals.

## 5. Results and Discussion

*5.1. Construction of Time Series for Ridership.* The ridership series is a data sequence with an interval length of one day. There is no missing value during this period from Jan 1st, 2018 to Jun 30th, 2019 (see Figure 3). The time series of total daily ridership time series fluctuates greatly with the date due to the following reasons:

(i) Impact of the weekends (see Table 4)

(ii) Impact of the holidays (see Table 4)

(1) Xiamen is a tourist city. The metro ridership increases significantly during holidays, especially on Labour Day and National Day. In addition, Jan 1st, 2018 is the New Year's Holiday. As the new metro had just been opened, many citizens were eager to experience the new kind of transit. Therefore, ridership on Jan 1st, 2018 was much more than that on other days.

(2) Although there is more ridership on most holidays than that on weekdays and weekends, ridership during the Spring Festival is an exception. Spring Festival is the most important reunion festival in Chinese culture. The large foreign population from other cities led to a sharp decline in the number of passengers around the Spring Festival.

(3) In addition to holidays, ridership on weekdays near the holidays also has similar characteristics to that on holidays. This is because some passengers travel before or after the holidays to avoid congestion.

(iii) Impact of extreme weather. Xiamen is a coastal city, which often suffers from extreme weather, such as rainstorms and typhoons. Many passengers will choose cars and taxis to avoid delay and inconvenience.

Finally, 265 samples were selected to identify SCPs using the ICSS algorithm. Daily ridership time series can also be dynamically monitored.

*5.2. Result of SCPs Identification.* Stationary test results can be easily obtained from the adftest function in the Econometrics Toolbox of Matlab software. If the time series is stationary, the answer is 1, otherwise, the answer is 0. The initial daily transit ridership $\{R_t\}$ is not a stationary time series. However, the fluctuation rate series $\{Q_t\}$ is a stationary time series.

To better demonstrate the ICSS method, intermediate results are shown in Figure 4. The curve shapes of fluctuation rate series and uncorrelated random series are similar because uncorrelated random variables are the standardization of fluctuation rates. There are larger positive values and smaller negative values when SCPs are present (see Figure 4(b)). Values of the cumulative sum of squares are incremental and jump sharply when there are SCPs (see Figure 4(c)). The values of the centered cumulative sum of squares are around 0 if there are no SCPs. SCPs will be identified if values of the centered cumulative sum of squares exceed the predetermined threshold (see Figure 4(d)).

With 95% confidence, three SCPs were identified, and the time series was divided into four segments. The regression discontinuity method was utilized to explore the correlation between the total ridership ($Y$-axis) and the date ($X$-axis) (see Figure 5).

The second interval, from early July to the end of August, coincides with the summer vacation dates of Chinese students and the best tourist dates in Xiamen. The slope of the third linear regression equation is much higher than that of the other three equations, which indicates that the total ridership increased rapidly at this stage due to the influence of the preferential schemes. However, due to the end of a certain preferential scheme reducing attractiveness to passengers, the slope of the fourth linear regression equation is lower than that of the third equation. The $R^2$ values of the first and second linear regression equations are smaller, while the $R^2$ values of the third and fourth linear regression equations are closer to 1. This phenomenon indicates that the variability of ridership was larger in the early stages after the metro operation and that the ridership increased steadily after a period of operation.

*5.3. Discussion of Effects of Fare Discounts on Different Ticket Types.* The SCPs of ridership varied by ticket types were identified to explore the impact of fare discount schemes on ticket types (see Figure 6).

*5.3.1. Effects of Fare Discounts on Single Tickets and Other Tickets.* Similar to the total ridership, there are two SCPs of the ridership time series of Single Tickets. The interval between the two SCPs is from the beginning of July to the end of August, which coincides with the best tourist dates in Xiamen. Tourists were likely not to buy a smart card or download the "Xiamen Metro" APP specifically for this tour. In addition, some passengers, especially the elderly and child tourists, were not familiar with the APP and cannot obtain E-Tickets from the APP. Thus, Single Tickets are one of the most popular choices for tourists. Therefore, it is understandable that ridership for Single Tickets increases during the summer vacation.

With 95% confidence, there is no SCP of the ridership of Other Tickets, because fewer passengers use Other Tickets, which are all specific special ticket types.

*5.3.2. Effects of Fare Discounts on E-Tickets.* Interestingly, the dates of the SCPs coincide precisely with the start and end dates of the "2 RMB Discount" preferential scheme. During the dates of the two SCPs, the ridership of E-Tickets exhibits a linear and rapid growth.

Another interesting phenomenon is that after the launch of the "2 RMB Discount" preferential scheme, ridership did not increase suddenly, but gradually at a greater growth rate. This phenomenon may be due to the gradual understanding and adaptation of residents. The

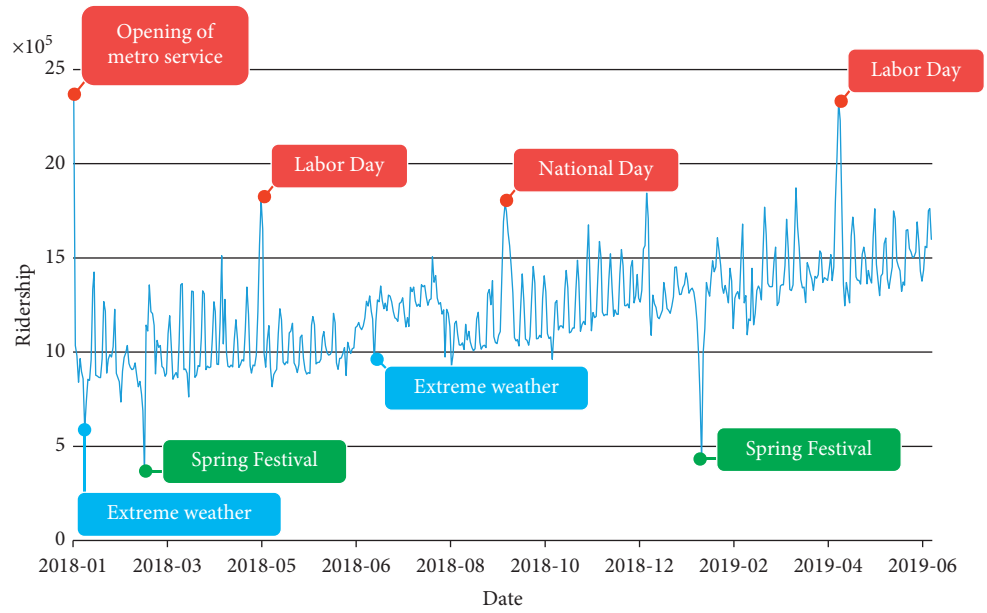


Figure 3: Raw data of daily total ridership time series with all dates.

allowance provider of the "2 RMB Discount" preferential scheme was the Banking Alliance, not the Xiamen government or Xiamen Metro Group. The dissemination of preferential information also takes time, and this process is more likely to be word-of-mouth.

Unfortunately, the goal of the "2 RMB Discount" preferential scheme was to increase the influence of the Banking Alliance and promote their paid APP (UnionPay) by taking advantage of the opening of the new metro. Citizens found that the discount was weakened after the end of the "2 RMB Discount" preferential scheme. So, the ridership of the E-Tickets plummeted significantly. The ridership on Jan 2$^{nd}$, 2019 decreased by 26.89% compared with that on Dec 27$^{th}$, 2018.

*5.3.3. Effects of Fare Discounts on Smart Card Tickets.* With 95% confidence, there was no SCP in the ridership of Smart Card Tickets. The ridership of Smart Card Tickets still fluctuated and there were even upward and downward trends. However, this process was gradual, not abrupt. Thus, the ICSS method based on variance mutation did not identify SCPs of the ridership of Smart Card Tickets.

The "50% Discount" preferential scheme ensured the slow growth of ridership, although this incentive scheme was not as attractive as the "2 RMB Discount" preferential scheme. In a sense, most users of the Smart Card Tickets and E-Tickets are Xiamen residents. Therefore, there was an opposite growth trend in the ridership of the Smart Card Tickets and E-Tickets. During the period of the "2 RMB Discount" preferential scheme, there was a downward trend in the ridership of Smart Card Tickets, while the ridership of E-Tickets increased.

However, after the end of the "2 RMB Discount" preferential scheme, there was an upward trend in the ridership of Smart Card Tickets, which exhibited a similar growth rate to that of E-Tickets. This win-win situation of Smart Card Tickets and E-Tickets may be caused by the internal driving effect of the metro.

*5.4. Maintained, Induced, and Disappeared Ridership.* Figure 6 clearly shows the trend from 2018/9/22 to 2019/1/2 when the share of Smart Card Tickets decreased and the share of E-Tickets increased at the same time. Unfortunately, passengers using Smart Card Tickets are marked with smart card numbers, while passengers using E-Tickets are marked with mobile phone numbers. There are no relationships between card numbers and mobile phone numbers. Therefore, there is a lack of direct evidence to accumulate the number of passengers shifting from Smart Card Tickets to E-Tickets.

We gave an example to illustrate this problem from the side. We chose passengers using Smart Card Tickets or E-Tickets that appeared in August 2018 or December 2018 or June 2019 as a whole. These three months were chosen because they were the last month of a certain stage. In these months, ridership was the most stable and travel characteristics were the most responsive. In Figure 7, grey boxes represent the proportion of passengers that appear in a certain month, while white boxes stand for the proportion of passengers that did not appear in a certain month.

Among all passengers using E-Tickets, 54.84 percent of passengers were induced from other modes of transport or Smart Card Tickets after the start of "2 RMB Discount." Subsequently, 34.98 percent of passengers were maintained while 19.86 percent of passengers disappeared after the end of "2 RMB Discount." 26.83 percent of passengers travelled in August 2018. After the incentives of "2 RMB Discount," 54.84 percent of passengers travelled in December 2018. Although the most affordable scheme of "2 RMB Discount" ended on 2018/12/31, the new discount scheme of "50% Discount"

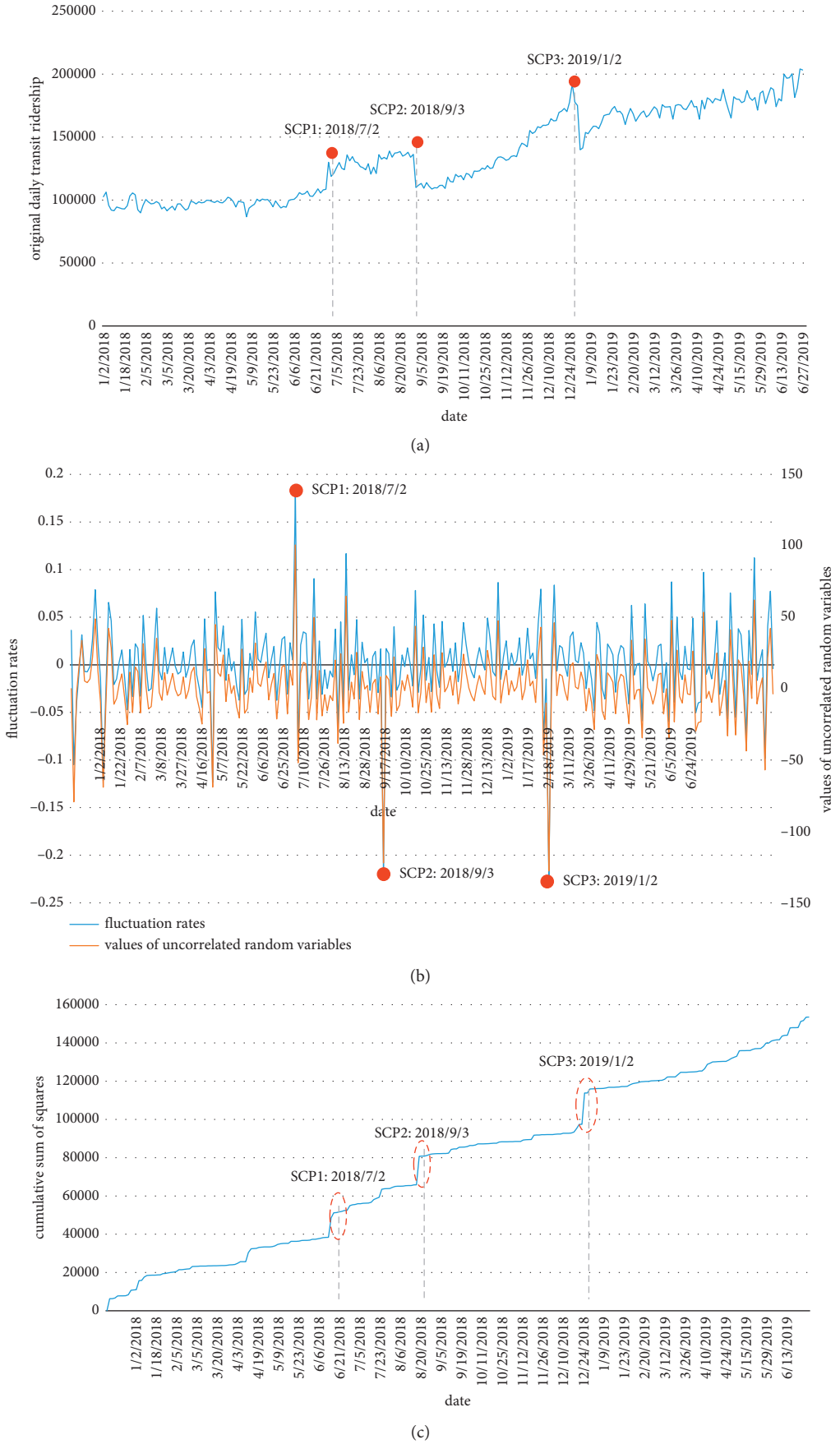


Figure 4: Continued.

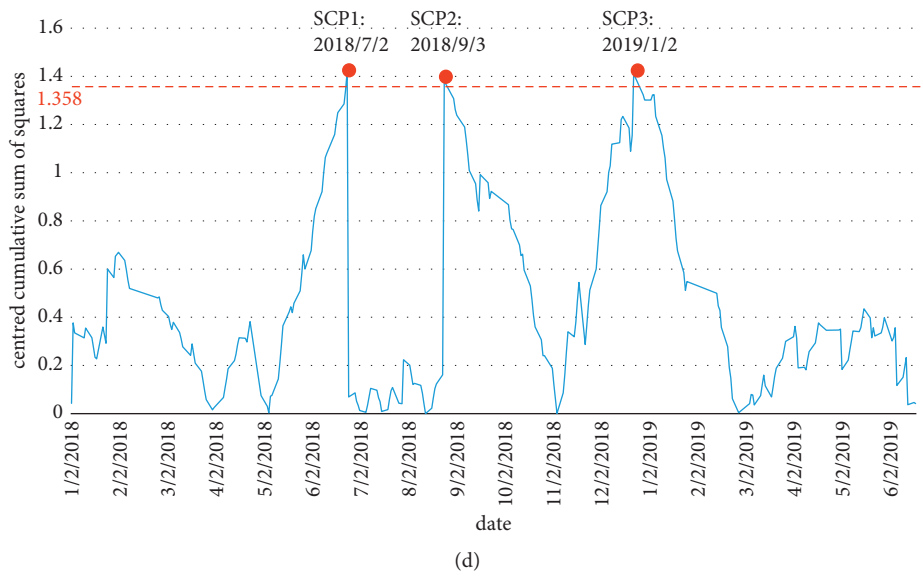


Figure 4: Intermediate results of ICSS method. (a) Original daily transit ridership. (b) Fluctuation rate series and uncorrelated random series. (c) Cumulative sum of squares. (d) Centered cumulative sum of squares.

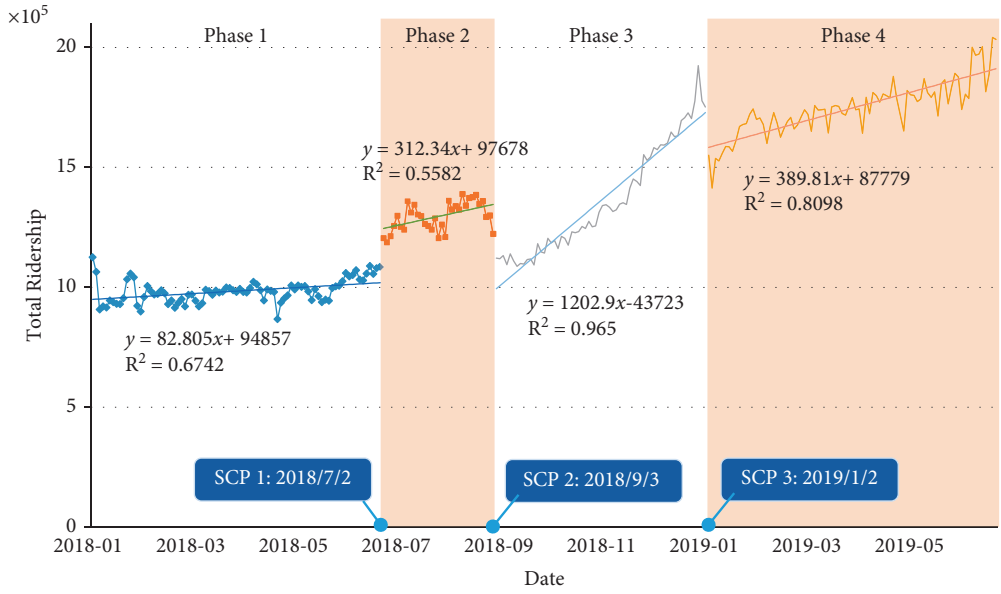


Figure 5: Regression discontinuity result of the total ridership time series with the chosen dates.

replaced "2 RMB Discount." 53.31 percent of passengers travelled in June 2019. There was no significant decrease compared with passengers in December 2018 (see Figure 7(b)).

Among all passengers using Smart Card Tickets, 28.49 percent of passengers disappeared after the start of the "2 RMB Discount." Owing to the more favorable discount scheme, they may shift from Smart Card Tickets to E-Tickets (see Figure 7(a)).

*5.5. Analysis of Passengers with Discount.* Compared with the "10% Discount" preferential scheme, the "2 RMB Discount" preferential scheme is more favorable; compared with the "50% Discount" preferential scheme, the "2 RMB Discount" preferential scheme is more direct without an accumulated fare. Short-distance passengers can even take the metro for free, while long-distance passengers can reduce their travel costs: two preferential rides per passenger per day, which is also very attractive to commuters. As a result, once the concessionary scheme is launched, the ridership surges steadily. "50% Discount" is a cumulative discount for high-frequency passengers. If the cumulative cost is less than 40 RMB, passengers will not be able to enjoy the "50% Discount." Therefore, this discount scheme is not available to all passengers, and it tends to subsidize high-frequency passengers.

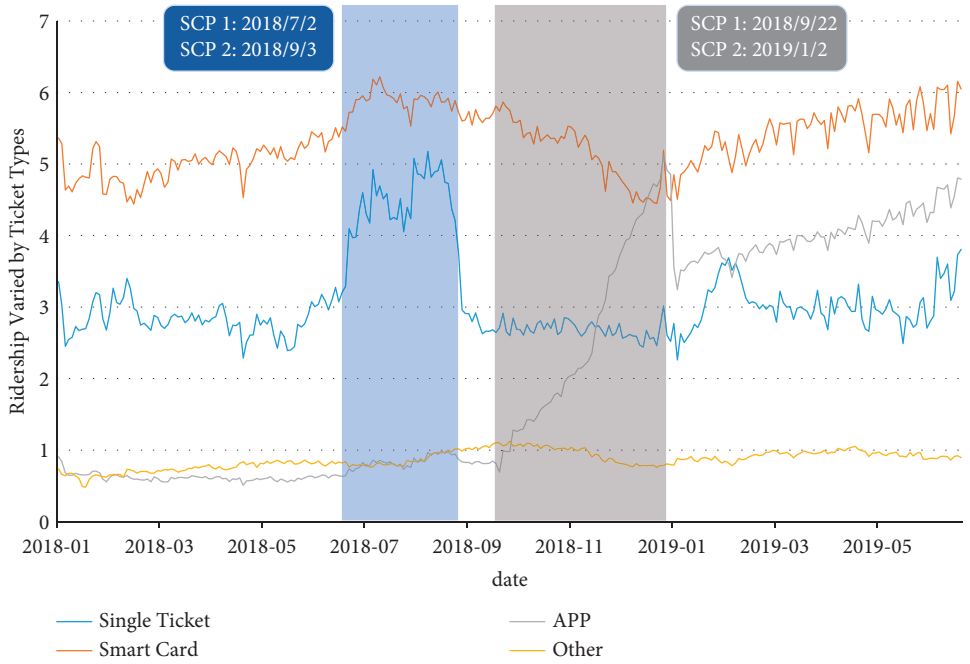


Figure 6: ICSS result of ridership time series varied by ticket types with the chosen dates.

*5.5.1. Passengers Using the Same Ticket with Different Discounts.* From 2018/12/01 to 2018/12/31, passengers using E-Tickets can enjoy both "2 RMB Discount" and "50% Discount." Each passenger can enjoy the "2 RMB Discount" twice per day, and only high-frequency passengers whose total cost is more than 40 RMB enjoy the "50% Discount."

The group enjoying both "2 RMB Discount" and "50% Discount" accounts for 23.80 percent of the total number of passengers, with the ratio of 69.08 percent of travels all day and 79.05 percent of travels in the peak hours. While the group with "2 RMB Discount" only accounts for 76.20 percent of the total number of passengers, with the ratio of 30.92 percent of travels all day and 20.95 percent of travels in the peak hours. Average trips per month of the group with both "2 RMB Discount" and "50% Discount" are 31.34, which is much higher than that of the group with "2 RMB Discount" only (4.38). Similarly, the average travel days per month of the group with both "2 RMB Discount" and "50% Discount" are 17.52, which is much higher than that of the group with "2 RMB Discount" (only 3.13). Average trips per day of the group with both "2 RMB Discount" and "50% Discount" are 1.78, which is higher than that of the group with "2 RMB Discount" only (1.39). There are no significant differences between the two groups when talking about stations per travel. Assuming that these two discount schemes do not exist, the group with both "2 RMB Discount" and "50% Discount" will spend 87.88 RMB/month. But now they just spend 24.53 RMB/month. Groups with "2 RMB Discount" only spend 7.48 RMB/month now and 16.82 RMB/month without these two discount schemes. Thanks to these two discount schemes, the cost per trip of the group with both "2 RMB Discount" and "50% Discount" (0.99) is much lower than that of the group with "2 RMB Discount" only (1.92). In general, there are more travels of the group with both "2 RMB Discount" and "50% Discount" than groups with "2 RMB Discount" only, because "50% Discount" is more beneficial to high-frequency passengers, possibly commuters (see Table 5).

*5.5.2. Passengers Using Different Tickets with the Same Discount.* Passengers who use Smart Card Tickets and E-Ticket both enjoy a "50% Discount" from 2019/01/01 to 2019/06/30. We defined a group with discounts as the passengers who enjoy the "50% Discount."

The group with a discount while using E-Tickets account for 19.79 percent of the total number of passengers with the ratio of 65.41 percent of travels all day and 55.07 percent of travels in the peak hours. While the group with a discount using Smart Card Tickets account for 7.57 percent of the total number of passengers with the ratio of 32.43 percent of travels all day and 45.97 percent of travels in the peak hours. Average trips per month for E-Ticket users are 31.28, much higher than that for Smart Card Tickets users (15.99). Similarly, the average travel days per month for E-Ticket users are 17.14, much higher than that for Smart Card Tickets users (9.83). Average trips per month and average travel days per month for the group with a discount are in sharp contrast to the group without a discount. Average trips per day of E-Tickets group with discount are 1.79, just a little higher than that of the other three groups. There are no significant differences between the four groups when talking about stations per travel. Assuming that the "50% Discount" does not exist, E-Ticket users with a discount will spend 119.41 RMB/month, but now they just spend 80.30 RMB/month on the metro fare. Smart Card Tickets group with discount spend 40.26 RMB/month, and other two groups spend lower fares. Due to the "50% Discount," the cost per

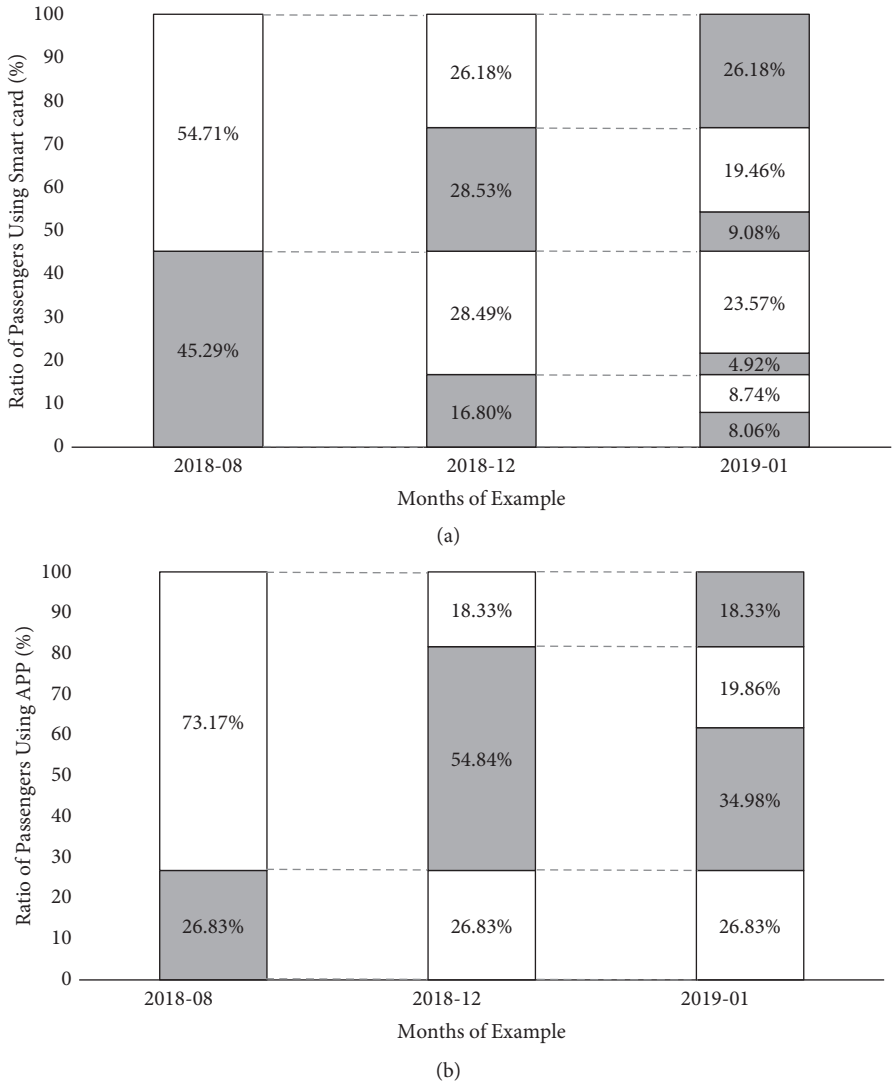


Figure 7: Maintained, induced, and disappeared ridership (grey: appear; white: disappear). (a) Smart Card Tickets. (b) E-Tickets.

trip of the group with a discount is lower than that of the group without a discount. Overall, there are more travels of the group with the discount than the group without a discount. Travel characteristics of E-Ticket users are more than that of Smart Card Tickets users, possibly because commuters are more likely to use E-Tickets (see Table 6).

Comparing Tables 5 and 6, travel characteristics, such as average trips per month, average travel days per month, average trips per day, etc., are similar to E-Ticket passengers both with discounts in Tables 5 and 6. Thanks to the "2 RMB Discount," travel costs have been greatly reduced. Passengers spent only 0.99 RMB per trip to take the metro if they enjoy both "2 RMB Discount" and "50% Discount." Low fees have greatly stimulated the growth of ridership.

*5.6. Policy Recommendations.* There is no doubt that fare discounts have a significant impact on ridership. E-Tickets are popular with users, especially high-frequency commuters because E-Tickets are more convenient to carry than Reality Cards, which should attract the attention of the governments and metro operators. Similar to the law of two to eight, fewer passengers produce more travel. Regardless of accumulated standards, the reduced cost of each trip will attract low-frequency passengers. Therefore, after the opening of the first metro line, money reduced per trip is the perfect discount scheme to attract bus passengers and car drivers to transfer to the metro system. When passengers spent less using one ticket type, they will give up using the previous ticket type to obtain the discount. When the discount schemes end, passengers will give up taking the metro or choose other ticket types. However, the number of passengers that increased due to the discount schemes is much more than that before the start of preferential policies. In the peak tourist season, Single Tickets are more popular with tourists.

This is an excellent cooperation mode of "tripartite win-win." First of all, these preferential measures not only help to reduce the operating pressure of the government and the metro operators but also help to promote the optimization of

Table 5: Travel characteristics of passengers using the same tickets with a different discount (2018/12/01–2018/12/31).

| Index | The group with both "2 RMB discount" and "50% discount" | The group with "2 RMB discount" only |
|---|---|---|
| Ratio of passengers | 23.80% | 76.20% |
| Ratio of travels | 69.08% | 30.92% |
| Ratio of travels in the peak-hours | 79.05% | 20.95% |
| Average trips per month (average travel days per month) | 31.34 (17.52) | 4.38 (3.13) |
| Average trips per day | 1.78 | 1.39 |
| Stations per travel | 7.93 | 7.73 |
| Cost per month (original cost without 50% discount per month), unit: RMB/month | 24.53 (87.88) | 7.48 (16.82) |
| Cost per trip, unit: RMB/trip | 0.99 | 1.92 |

Table 6: Travel characteristics of passengers using different tickets with the same discount (2019/01/01–2019/06/30).

| Index | Smart card tickets | | E-Tickets | |
|---|---|---|---|---|
| | Group with discount | Group without discount | Group with discount | Group without discount |
| Ratio of passengers | 7.57% | 92.43% | 19.79% | 80.21% |
| Ratio of travels | 32.43% | 67.57% | 65.41% | 34.59% |
| Ratio of travels in the peak-hours | 45.97% | 30.14% | 55.07% | 32.12% |
| Average trips per month (average travel days per month) | 15.99 (9.83) | 2.71 (2.03) | 31.28 (17.14) | 4.02 (2.92) |
| Average trips per day | 1.57 | 1.33 | 1.79 | 1.37 |
| Stations per travel | 7.25 | 7.54 | 7.54 | 7.89 |
| Cost per month (original cost without 50% discount per month), unit: RMB/month | 40.26 (59.66) | 9.08 (10.10) | 80.30 (119.41) | 13.83 (15.37) |
| Cost per trip, unit: RMB/trip | 2.51 | 3.34 | 2.57 | 3.44 |

the ridership structure. Secondly, metro passengers can enjoy real benefits. Third, the market share and influence of these financial companies have also increased. Therefore, paying attention to the preferential measures launched by financial companies will help to provide a reference for the government and metro operators to seek follow-up cooperation.

Therefore, the policy recommendations are mainly about the following:

(1) Raising the focus on E-Tickets

(2) Selecting more friendly preferential measures for low-frequency passengers to transfer passengers from buses and cars

(3) Paying attention to high-frequency passengers because they contribute more travel

(4) Seeking common subsidies from the financial industry to achieve win-win results

## 6. Conclusions

To test the impact of preferential schemes on ridership varied by different card types, the iterated cumulative sums of squares (ICSS) algorithm and regression discontinuity (RD) method were introduced. 18-month transaction data after the opening of the new metro was obtained, and ultimately 265-weekday samples were selected, excluding special circumstances. Long-term data provide an excellent opportunity for the dynamic observation of the effects of preferential schemes. The dates of structural change points (SCPs) were well matched with the start and end dates of preferential schemes.

The following conclusions can be drawn:

(1) There are significant differences in ridership on weekdays, weekends, and holidays. Apart from extreme weather, preferential schemes are also important factors affecting metro ridership.

(2) There are three preferential schemes in Xiamen after the opening of the new metro line: discount per trip, money reduced per trip, and discount after reaching the accumulated fare. There are different effects on ridership varied by ticket type for different preferential schemes. The most popular preferential scheme (money reduced per trip) is the most preferential and direct scheme without other conditions, such as accumulated fare.

(3) Each preferential scheme has its own benefited groups. Low-frequency passengers can benefit from the scheme of money reduced per trip. Governments and transit operators can formulate appropriate preferential schemes to guide car/taxi passengers to shift to public transport. While high-frequency passengers can obtain more benefits from the scheme of discount after reaching accumulated fare,

E-Tickets are more popular with high-frequency passengers, especially commuters. Governments and transit operators also need to pay attention to these passengers, because they contribute more travel.

(4) Interestingly, the residents' understanding and adaptation to the preferential schemes are gradual. Nevertheless, if the favorable preferential scheme is canceled, the number of passengers will drop sharply. Passengers will shift from a ticket type to another owing to the more favorable discount scheme. On the whole, the number of passengers increased due to the discount schemes is much higher than that before the preferential policy began.

However, we would prefer to analyze the transfer behavior from other modes of transport or between different ticket types with more data. The ICSS algorithm and RD method can also be used to evaluate the effectiveness of other transportation policies in the future.

## Data Availability

The data used to support the findings of this study are available from the corresponding author upon request.

## Conflicts of Interest

The authors declare that there are no conflicts of interest regarding the publication of this paper.

## Acknowledgments

This work was supported by the National Natural Science Foundation of China (Grant no. 71734004), the Technology Project of Fujian Province, China (Grant no. 2017Y062), and the Fundamental Research Funds for the Central Universities (Grant no. 300102210126).

## References

[1] China Association of Metros, "Urban rail transit statistics and analysis report (2015-2020)". https://www.camet.org.cn/.

[2] Y. Wang, L. Li, Z. Wang, T. Lv, and L. Wang, "Mode shift behavior impacts from the introduction of metro service: case study of Xi'an, China," *Journal of Urban Planning and Development*, vol. 139, no. 3, pp. 216–225, 2013.

[3] J. C. Golias, "Analysis of traffic corridor impacts from the introduction of the new Athens Metro system," *Journal of Transport Geography*, vol. 10, no. 2, pp. 91–97, 2002.

[4] N. Sharaby and Y. Shiftan, "The impact of fare integration on travel behavior and transit ridership," *Transport Policy*, vol. 21, pp. 63–70, 2012.

[5] Y. Yang, "Review on urban public transport subsidy," *Productivity Research*, vol. 8, pp. 206–209, 2011.

[6] Q. Yu, H. Zhang, W. Li et al., "Mobile phone data in urban bicycle-sharing: market-oriented sub-area division and spatial analysis on emission reduction potentials," *Journal of Cleaner Production*, vol. 254, Article ID 119974, 2020.

[7] Q. Yu, H. Zhang, W. Li, X. Song, D. Yang, and R. Shibasaki, "Mobile phone GPS data in urban customized bus: dynamic line design and emission reduction potentials analysis," *Journal of Cleaner Production*, vol. 272, Article ID 122471, 2020.

[8] C. Inclan and G. C. Tiao, "Use of cumulative sums of squares for retrospective detection of changes of varience," *Journal of the American Statistical Association*, vol. 89, no. 427, pp. 913–923, 1994.

[9] W. Vickrey, "Some implications of marginal cost pricing for public utilities," *The American Economic Review*, vol. 45, no. 2, pp. 605–620, 1955.

[10] H. Mohring, "Optimization and scale economies in urban bus transportation," *The American Economic Review*, vol. 62, no. 4, pp. 591–604, 1972.

[11] K. A. Small, "The scheduling of consumer activities: work trips," *The American Economic Review*, vol. 72, no. 3, pp. 467–479, 1982.

[12] C.-F. Yeh and M.-T. Lee, "Effects of taichung bus policy on ridership according to structural change analysis," *Transportation*, vol. 46, no. 1, pp. 1–16, 2019.

[13] Victoria Transport Policy Institute, *Transit Price Elasticities and Cross Elasticities*, Victoria Transport Policy Institute, Victoria, Canada, 2020.

[14] P. Goodwin, "Review of new demand elasticities with special reference to short and long run effects of price changes," *Journal of Transport Economics*, vol. 26, no. 2, pp. 155–171, 1992.

[15] D. Gillen, *Peak Pricing Strategies in Transportation, Utilities, and Telecommunications: Lessons for Road Pricing*, Transportation Research Board, Washingtong DC, USA, 1994.

[16] R. Cervero, *Land-use Mixing and Suburban Mobility*, Transportation, Berkeley, CA, USA, 1989.

[17] R. Borndörfer, M. Karbstein, and M. E. Pfetsch, "Models for fare planning in public transport," *Discrete Applied Mathematics*, vol. 160, no. 18, pp. 2591–2605, 2012.

[18] X. Guo and H. Sun, "Analysis of time of day fare discounts on urban mass transit travel behaviour, crowding, and waiting time," *Mathematical Problems in Engineering*, vol. 2014, Article ID 686705, 6 pages, 2014.

[19] S. Farber, K. Bartholomew, X. Li, A. Páez, and K. M. Nurul Habib, "Assessing social equity in distance based transit fares using a model of travel behaviour," *Transportation Research Part A: Policy and Practice*, vol. 67, pp. 291–303, 2014.

[20] C. Miller and I. Savage, "Does the demand response to transit fare increases vary by Income?" *Transport Policy*, vol. 55, pp. 79–86, 2017.

[21] K. Gkritza, M. G. Karlaftis, and F. L. Mannering, "Estimating multimodal transit ridership with a varying fare structure," *Transportation Research Part A: Policy and Practice*, vol. 45, no. 2, pp. 148–160, 2011.

[22] Y. Liu, S. Wang, and B. Xie, "Evaluating the effects of public transport fare policy change together with built and non-built environment features on ridership: the case in South East Queensland, Australia," *Transport Policy*, vol. 76, pp. 78–89, 2019.

[23] D. Verbich and A. El-Geneidy, "Public transit fare structure and social vulnerability in Montreal, Canada," *Transportation Research Part A: Policy and Practice*, vol. 96, pp. 43–53, 2017.

[24] B.-h. Nahmias-Biran, N. Sharaby, and Y. Shiftan, "Equity aspects in transportation projects: case study of transit fare change in Haifa," *International Journal of Sustainable Transportation*, vol. 8, no. 1, pp. 69–83, 2013.

[25] A. E. Brown, "Fair fares? How flat and variable fares affect transit equity in Los Angeles," *Case Studies on Transport Policy*, vol. 6, no. 4, pp. 765–773, 2018.

[26] C. Nuworsoo, A. Golub, and E. Deakin, "Analyzing equity impacts of transit fare changes: case study of alameda-contra costa transit, California," *Evaluation and Program Planning*, vol. 32, no. 4, pp. 360–368, 2009.

[27] Z.-j. Wang, X.-h. Li, and F. Chen, "Impact evaluation of a mass transit fare change on demand and revenue utilizing smart card data," *Transportation Research Part A: Policy and Practice*, vol. 77, pp. 213–224, 2015.

[28] Z.-j. Wang, F. Chen, B. Wang, and J.-l. Huang, "Passengers' response to transit fare change: an ex post appraisal using smart card data," *Transportation*, vol. 45, no. 5, pp. 1559–1578, 2017.

[29] J. Robin and Z. Pei, *A Practical Guide to Regression Discontinuity*, MDRC, New York, NY, USA, 2012.

[30] D. L. Thistlethwaite and D. T. Campbell, "Regression-discontinuity analysis: an alternative to the ex post facto experiment," *Journal of Educational Psychology*, vol. 51, no. 6, pp. 309–317, 1960.

[31] J. Hahn, P. Todd, and W. Klaauw, "Identification and estimation of treatment effects with a regression-discontinuity design," *Econometrica*, vol. 69, no. 1, pp. 201–209, 2001.

Hindawi
Mathematical Problems in Engineering
Volume 2021, Article ID 3055337, 9 pages
https://doi.org/10.1155/2021/3055337

*Research Article*

# Modeling the Impacts of Driver Income Distributions on Online Ride-Hailing Services

**Yuru Wu**,[1] **Weifeng Li**,[1] **Qing Yu**,[1] **and Jinyu Chen**[2]

[1]*Key Laboratory of Road and Traffic Engineering of the Ministry of Education, Tongji University, Shanghai 201804, China*
[2]*Center for Spatial Information Science, The University of Tokyo, 5-1-5 Kashiwanoha, Kashiwa, Chiba 277-8563, Japan*

Correspondence should be addressed to Weifeng Li; liweifeng@tongji.edu.cn

Received 6 July 2021; Accepted 2 September 2021; Published 20 September 2021

Academic Editor: A. M. Bastos Pereira



The online ride-hailing taxi brings new vitality into the traditional taxi market, as well as new issues and challenges. The pricing and profit distribution of online ride-hailing services is one of the major concerns. This study focuses on the pricing and income distribution in the online ride-hailing system. Queuing system model and birth and death process theory are introduced to describe the driver's flow process in the network. The social welfare maximization model and the platform profit maximization model are constructed based on the dynamic pricing mechanism, from the government's and platform's standpoint, respectively. Through numerical experiments, this paper analyzes the income distribution of drivers under different settings and the influence of different factors (average travel time, psychologically expected price of drivers and passengers, and probability of driver leaving the system) on the proportion of income distribution. The results show that the drivers' income distribution proportion is higher in the pursuit of social welfare maximization than that in the pursuit of platform profit maximization, and in different benefit pursuit models, various factors have a certain influence on the driver's income distribution proportion. The proposed method and conclusion in this study can be considered as references for online ride-hailing market supervision and policy-making.

## 1. Introduction

Ride-hailing, referring to the activity of calling a vehicle or driver to go to a destination, rises in many metropolitan areas and takes a considerable part of mobility services [1]. The online ride-hailing platform is a subversion of the traditional travel industry in the context of the Internet; it transmits the traditional service mode from the driver side to the passenger side by the combination of online information and offline experience [2, 3]. Customers are matched efficiently by an online platform with affiliated drivers nearby by requesting rides via a mobile application [4]. Such on-demand services greatly reduce search frictions in the ride-hailing market, bring passengers and drivers together at very low transaction costs, and meanwhile effectively reduce the vacancy rates of operating vehicles by matching demand and supply [5–7].

However, compared with the traditional taxi industry, the pricing and the income distribution of online ride-hailing lack transparency and consistency. The unreasonable and opaque income distribution harms the interests of drivers. On October 31, 2018, online taxi drivers in Chicago, the United States, delivered a rally and petition on the budget meeting held by the city government. They asked for more driver's share of the platform revenue. According to the survey conducted in August 2019 in the United States, the fare receipt information and more than 14756 real online taxi order service data showed that Uber averagely retains about 35% of the revenue per ride, while Lyft takes about 38%. However, in the regulatory documents submitted to the government, Uber reported that its platform share of fares was only close to 20%, while Lyft did not disclose its proportion publicly. What causes these situations is that the platforms can set the pricing and distribution mechanism by themselves, and under the goal of maximizing benefits, they can dynamically adjust the service price (some platforms even use dynamic pricing models for the same route, which may vary according to the demand and supply for rides) and

the drivers' distribution proportion, which will harm the interests of drivers and passengers.

In the new traffic model, the system layout design is very important, which will affect the operational efficiency of the whole system and public acceptance [8]. Therefore, it is necessary to study the price mechanism of online ride-hailing and the way of labor (drivers) drawing. However, most of the existing related research studies focus on the maximization of platform interests and seldom on the interests of drivers and study the pricing and distribution mechanisms. Therefore, from the perspective of government management, this paper constructs a social welfare maximization model to explore the relationship between social welfare and the way of interest distribution, to provide decision support for the regulation of the online ride-hailing market.

In this paper, the income distribution of drivers in the online ride-hailing market is discussed based on the dynamic pricing mechanism from the perspectives of social interest maximization and platform profit maximization. The contributions of this paper are as follows: (1) Queuing system model and birth and death process theory are introduced to describe the driver's flow process in the network. (2) The social welfare maximization model and the platform benefit maximization model are constructed, from the government's and platform's standpoint, respectively, based on the psychological expected price curve of passengers and drivers. (3) Numerical experiments are performed to analyze the driver's income distribution under the conditions of different settings. Suggestions on the government's regulation and guidance are put forward based on the experiment results.

The remainder of this paper is organized as follows. Section 2 presents a review of the related literature. Section 3 mainly focuses on the problem description and modeling. In Section 4, two numerical experiments are performed to analyze the driver's income distribution. Results and associated discussion are then carried out. Finally, conclusions and future directions are given in the last section.

## 2. Literature Review

The current discussion and studies on online ride-hailing are extensive. In terms of the price mechanism of online ride-hailing, Zha et al. [9] focused on the impact of dynamic pricing on online ride-hailing industry by structurally combining driver's work schedule selection. The numerical results show that the platform enjoyed higher revenue on the basis of dynamic pricing, while customers may be exploited in the peak period of taxi service. Fellows [10] uses cost advantage analysis technology to prove that reasonable platform pricing can bring about net income for society. However, Chang [11] thinks that the pricing structure of the platform will affect the output efficiency and social welfare and points out that it disturbs the market price rule. Xia et al. [12] believe that the dynamic pricing strategy can alleviate the pressure of the platform in the period of tight transport capacity by increasing the transport capacity of part-time drivers and reducing the number of price-sensitive user orders, so as to improve user satisfaction. Banergee et al. [13] use queuing theory model to simulate the flow of drivers and passengers in online ride-hailing market for the first time and study the volume and revenue of online ride-hailing platform by static pricing and dynamic pricing. In addition, a series of literature studies [14–16] show the pricing strategy of online ride-hailing platform to explore how pricing can balance the relationship between passengers, drivers, and the platform, to maximize the benefits.

In terms of the profit distribution and drivers' income, Xu et al. [17] investigated the C2C business model of online ride-hailing platform and concluded that, based on the technical characteristics of the online ride-hailing industry, the platforms are in an absolutely dominant position in income distribution and they can take advantage of the lower labor price of part-time drivers to force the contract drivers to reduce the labor price, thus causing a certain degree of labor market failure. Liu and Cai [18] analyzed the income distribution mode of platforms, employed drivers in China's online ride-hailing industry by using political economy theory, and demonstrated that the improvement of the exploitation rate with drivers and passengers comes from the monopoly of the platform and the profit-making nature of capital. Xie [19] made an in-depth analysis of the demand and behavior characteristics of drivers and passengers, focusing on the dynamic investigation of the income distribution proportion of drivers. The research shows that the optimal mileage price of online ride-hailing increases with the increase of tour taxi fare and decreases with the increase of "rebate." Through the analysis of the taxi platform, driver, and passenger involved in the process of online ride-hailing, Danlei [20] determined the distance, customer preference, and other influencing factors and analyzed how to maximize the interests of the three parties.

In terms of government regulation, previous studies mainly focused on the interpretation of the government's new policy on online ride-hailing and the research on the access regulation of drivers and platform based on the protection of passengers' interests. Xiang [21] believes that online ride-hailing is the product of market self-regulation, and its generation has objective market value and development prospects. Fang's study [22], based on the Bertrand model and Cournot model, constructs a repeated game with uncertain ending time and analyzes the competitive strategy of two stages of online ride-hailing market development, so as to get the path of promoting the development of online ride-hailing market. Recently, more and more attention has been paid to the supervision of pricing and distribution mechanisms. Lai [23] proposed that transparent pricing rules for online ride-hailing should be the basic consensus of the industry. Xia and Lin [24, 25] believe that government should strengthen the supervision of the pricing and distribution of online ride-hailing platforms. Li [26] proposes two problems in the government's regulation of online ride-hailing market: first, the government's regulatory concept lacks active guidance and cannot actively discover new problems and carry out advance management; second, the local government mechanically implements the central level regulatory measures for the online ride-hailing market, falling into the path dependence of regulatory means.

Previous studies explained and evaluated the proportion charged by platforms and paid less attention to the relationship between labor supply and the income distribution proportion. In addition, in terms of the income distribution, most of the studies paid attention to the interests of the platform and less attention to the rights and interests of drivers. Therefore, this paper clearly puts forward the proportion of income distribution of drivers and focuses on the rights and interests of drivers from the perspective of the government. And more importantly, this paper takes social welfare into consideration and forms a contrast with platform interests to put forward suggestions for better development of online ride-hailing.

## 3. Problem Description and Modeling

*3.1. Basic Assumptions and Queuing Model.* In this paper, it is assumed that the online ride-hailing market is composed of three parts: platform, driver, and passenger. The online ride-hailing system is abstracted as the queuing system shown in Figure 1. Unlike the general queuing system, since the demand of online ride-hailing market exceeds the supply, passengers in the online ride-hailing system are regarded as the service desks and drivers are regarded as the arriving customers [27]. Assuming that the new driver joins the queue of available drivers at a rate $\Lambda_e$, when the driver matches his own passengers, the average travel time of the passengers is $t$. After arriving at the destination, the passengers will leave the system, and the driver will either leave the system or return to the original queuing system. The probability of the driver leaving the system is set to be $q_{\text{leave}} > 0$.

Assuming that the price of each ride is $p$ (yuan/km) and the driver's income distribution proportion is $A$, the driver's income of each ride is $Ap$, and the income of the platform is supposed to be $(1 - A)\ p$.

Considering the platform, passengers are usually sensitive to the price of the ride, if the price is too high, price-sensitive customers will give up the ride. And the drivers are sensitive to the average amount of money earned over a longer period of time (a few hours or a day). If the profit is too low, the driver will give up. Therefore, this paper introduces the change curve of the expected price of passengers and drivers. For passengers, assuming that the adjusted price of passengers is independent of the distribution $F_V$ and $V$ is the expected price of each passenger, the distribution function of $V$ is denoted as $F_V(V)$. If $p \le V$, passengers are willing to ride; otherwise, they will give up. Similarly, suppose that the driver's adjusted price is independent of the distribution $F_C$ and $C$ is the expected revenue of each driver. The distribution function of $C$ is denoted as $F_C(C)$. If the actual average hourly income $Ap/t \ge C$, the driver will choose to accept the order; otherwise, he will give up.

Therefore, if the initial passenger arrival rate is $\mu_0$, then the actual passenger arrival rate $\mu$ is

$$\mu = \mu_0 \overline{F_V}(p) = (1 - F_V(p))\mu_0. \tag{1}$$

For drivers, when the order ends, the driver will leave the system with probability $q_{\text{leave}}$; meanwhile, the psychological price of drivers is independent of the distribution $F_C$, which affects the choice of drivers to receive orders (enter the system). Therefore, when the queue of drivers in Figure 1 is stable, the following equation relationship can be established for the probability of new drivers arriving at the system ($\Lambda_e$):

$$\Lambda_e = \lambda q_{\text{leave}} = \lambda_0 F_C\left(\frac{\eta}{f + t}\right). \tag{2}$$

In equation (2), $f$ is the expected free time per ride, $\eta$ is the expected revenue per ride, and $\lambda_0$ is the initial driver arrival rate.

In addition, the platform adopts a single threshold pricing method; that is, the price is set according to the number of drivers ($N$) available in the system. The pricing strategy has three parameters: low price $p_L$, high price $p_H$, and threshold $\theta$. When $N \ge \theta$ (here let $\theta = 2$), the platform pricing $P(N) = p_L$; when $N < \theta$, $P(N) = p_H$ [27]. As shown in Figure 2.

From the perspective of the platform, the strategy of income distribution should ensure the maximization of platform profit. The platform profit here refers to the platform's net income, which can be calculated by deducting the drivers' share and the platform costs (operating costs, etc.) from the platform's total income. Then, the platform profit is

$$T = [(1 - A)p - T_C]\lambda(A, p). \tag{3}$$

In equation (3), $\lambda(A, p)$ refers to the effective driver arrival rate under the equilibrium state when the extraction coefficient is A and the price is $p$. $T_C$ refers to the cost of platform.

From the perspective of the government, the operation of online ride-hailing system should ensure the maximization of social welfare. In this paper, social welfare $W_1$ is defined as the sum of passenger surplus ($S$), driver surplus ($D$), and platform profit ($T$), as expressed by the following equation:

$$W_1 = S + D + T. \tag{4}$$

The passenger surplus per ride is the average surplus of passengers who are willing to enter the queuing system. The passenger surplus can be obtained by deducting the price actually paid by passengers from the price that passengers are willing to pay. The transaction volume is the ratio of successful matching in the steady state, which is given by the effective driver arrival rate $\lambda(A, p)$. Then, the overall surplus of passengers can be calculated as follows:

$$S = \lambda(A, p)\frac{1}{\overline{F_V}(p)}\int_P^{\infty}(V - p)f_V(V)\mathrm{d}V. \tag{5}$$

Unlike the concept of surplus in traditional economics, the definition of driver surplus is similar to the passenger surplus. The driver surplus per ride can be calculated by deducting the driver's psychological expectation income and the driver's cost (fuel consumption, vehicle damage, etc.)

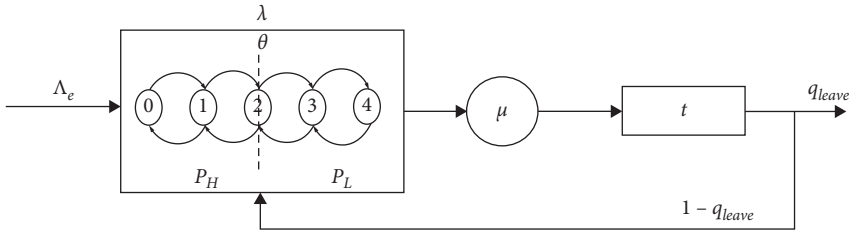


Figure 1: Flow process of driver in the system.

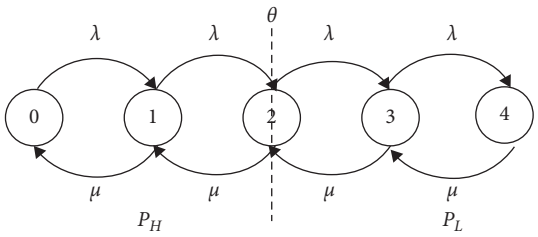


Figure 2: Birth and death process of the drivers in the platform.

from the driver's actual income. Then, the overall driver's surplus can be calculated as follows:

$$D = \lambda(A,p)\left[\frac{t}{F_C(Ap/t)}\int_0^{(Ap/t)}\left(\frac{Ap}{t}-C\right)f_C\mathrm{d}C - D_C\right]. \tag{6}$$

*3.2. The Dynamic Pricing Model.* Dynamic pricing strategies are common in revenue management. In the online ride-hailing industry, the service price is usually set by the software. The platform automatically generates a surge multiplier according to time, geographical location, demand, and other factors, to form a dynamic price.

Following the example of Banerjee et al. [13], a threshold-based dynamic pricing method is applied to model the peak time price. In the queuing model constructed above, only the number of vehicles available in the queue is considered to adjust the price, which means that the price is set according to the number of drivers ($N$) available in the system. The pricing strategy can be expressed as follows:

$$P(N) = \begin{cases} p_L, & N \geq \theta, \\ p_H, & N < \theta. \end{cases} \tag{7}$$

Among them, $p_L$, $p_H$, and $\theta$ represent the low price, high price, and the threshold, respectively. Set $\alpha_H = 1/\overline{F_V}(p_H)$ and $\alpha_L = 1/\overline{F_V}(p_L)$, and when the number of drivers is $n$, the platform pricing is $p$, and the driver's income distribution proportion is $A$, the equilibrium driver arrival rate in the online ride-hailing system is defined as $\lambda(A,p,n)$. In order to simplify the influence of the number ($n$) on the results, we use the equilibrium driver arrival rate under the large market limit $(\lambda(A,p) = \lim_{n\longrightarrow\infty}(\lambda(A,p,n)/n))$ to study the maximization of social welfare. The arrival rate of drivers meets the following requirements:

$$\lambda(A,p) = \begin{cases} \mu_0\overline{F_V}(p_L), & p_L > p_{\mathrm{BAL}}, \\ \dfrac{\lambda_0}{q_{\mathrm{leave}}}F_C\left(\dfrac{Ap_H}{t}\right), & p_H < p_{\mathrm{BAL}}, \\ \dfrac{\lambda_0}{q_{\mathrm{leave}}}F_C\left(\dfrac{AP}{t}\right), & p_L \leq p_{\mathrm{BAL}} \leq p_H, \end{cases} \tag{8}$$

where $p_{\mathrm{BAL}}$ is the equilibrium price when the drivers' supply is equal to the passengers' demand.

$$\mu_0\overline{F_V}(p_{\mathrm{BAL}}) = \frac{\lambda_0}{q_{\mathrm{leave}}}F_C\left(\frac{Ap_{\mathrm{BAL}}}{t}\right),$$

$$P = \frac{p_L[\alpha_H - \mu_0/\lambda(A,p)] + p_H[\mu_0/\lambda(A,p) - \alpha_L]}{\alpha_H - \alpha_L}. \tag{9}$$

From the above model, we can understand the leverage effect of fare adjustment in the supply-demand relationship of online ride-hailing market. The driver's income distribution proportion not only is affected by the driver supply, passenger demand, and platform but also affects the platform supply and demand in turn, to guide the rational allocation of resources according to the rules of supply and demand in economics.

On the basis of dynamic pricing, the social welfare maximization model can be expressed as follows:

$$\max W_1 = \begin{cases} \mu_0\overline{F_V}(p_L)f(p_L), & p_L > p_{\mathrm{BAL}}, \\ \dfrac{\lambda_0}{q_{\mathrm{leave}}}F_C\left(\dfrac{Ap_H}{t}\right)f(p_H), & p_H < p_{\mathrm{BAL}}, \\ \dfrac{\lambda_0}{q_{\mathrm{leave}}}F_C\left(\dfrac{AP}{t}\right)f(P), & p_L \leq p_{\mathrm{BAL}} \leq p_H. \end{cases} \tag{10}$$

The profit maximization model of online ride-hailing platform based on dynamic pricing can be expressed as follows:

$$\max W_2 = \begin{cases} \mu_0\overline{F_V}(p_L)[(1-A)p_L - T_c], & p_L > p_{\mathrm{BAL}}, \\ \dfrac{\lambda_0}{q_{\mathrm{leave}}}f_C\left(\dfrac{Ap_H}{t}\right)[(1-A)p_H - T_c], & p_H < p_{\mathrm{BAL}}, \\ \dfrac{\lambda_0}{q_{\mathrm{leave}}}f_C\left(\dfrac{AP}{t}\right)[(1-A)p - T], & p_L \leq p_{\mathrm{BAL}} \leq p_H. \end{cases} \tag{11}$$

The main parameters and meanings involved in this paper are shown in Table 1.

## 4. Numerical Experiments

*4.1. The Influence of City Scale on Driver's Distribution.* By comparing the situation of different levels of cities, this section investigates the comprehensive influence of different parameters on the pricing strategy and the distribution strategy of the platform.

*4.1.1. Case Setup.* We divided the following four scenes to represent different levels of cities, whose basic parameters are as shown in Table 2.

City $A$: megacity like Shanghai, Beijing. The population of city $A$ is more than 10 million. It has the highest population density and the most developed transportation system. Correspondingly, it has the largest supply and demand. People's consumption level is higher, and the psychological expected price acceptable to passengers and drivers is the highest.

City $B$: big city like Suzhou, Chongqing. The permanent population is between 5 million and 10 million, and the population density is around 1400 people per square kilometer.

City $C$: medium-sized city like Nanchang. Its permanent population ranges from 1 million to 5 million. The population density is around 700 people per square kilometer. The supply and demand of online ride-hailing are lower than those of cities $A$ and $B$, people's consumption level is not so high, and the service price acceptable to passengers is lower.

City $D$: small city. The supply and demand of online ride-hailing are relatively low; people's consumption level and the service price acceptable to passengers are the lowest. The permanent population of such cities is often less than 1 million, with a low population density.

*4.1.2. Result Analysis.* Models proposed in this paper are applied to calculate and obtain Table 3.

The following conclusions can be drawn from Table 3: (1) In cities $A$ and $B$, which have higher population density and higher levels of supply and demand, whether the pricing is high or low, the price in pursuit of platform benefits maximization is higher than that in pursuit of social welfare maximization. (2) In the outputs of the social welfare maximization model of different cities, the driver's income distribution proportion is between 0.5 and 0.7, while it is between 0.4 and 0.6 in the outputs of the platform benefit maximization model. In the social welfare maximization model, the driver's interests are more protected. (3) Compared with the social welfare maximization model, the platform profit maximization model not only obtains higher platform pricing but also lowers the driver's income distribution proportion. According to the above models, this is mainly because the platform profit is determined based on the drivers' income and platform pricing. The less the drivers' income distribution is, the higher the platform profit will be. In the contrast, social welfare maximization model considers the balance among online ride-hailing platforms, drivers, and passengers. (4) In addition, it is worth noting that, under the same city parameter conditions, although the quantitative value of social welfare includes platform benefits, the ultimate value obtained from the social welfare maximization model is lower than the platform benefit maximization (expect for city $A$).

Therefore, given the actual situation, from the government's point of view, if regulations are not issued to provide guidance for the income distribution proportion of drivers on the online ride-hailing platform, it is very likely that the monopoly price of online ride-hailing platform will be equal to the traditional taxi price, and the interests of drivers will be exploited.

*4.2. Relationships between Basic Parameters and Driver's Income Distribution Proportion.* In this section, numerical examples with different settings of model parameters are used to analyze the relationship between the driver's income distribution proportion and basic parameters in the two models. The conclusions can provide a reference for the government's decision and policy-making.

*4.2.1. Example Setup.* Set the initial arrival rate of drivers $\lambda_0 = 2500$ vehicles/h, the initial arrival rate of passengers $\mu_0 = 5000$ Passengers/h, the average travel time $t = 0.5$ hours, and the probability of drivers leaving the system $q_{\text{leave}} = 0.8$. Assuming the psychological expected price of drivers and passengers $f_c$, $f_V \sim N(3, 1)$. The driver cost is 1.11 yuan/km, and the platform cost is $0.14p$. By changing the value basic parameters, including the average travel time, the psychological expected price distribution of passengers and drivers, and the probability of driver leaving the system, the influence of basic parameters on driver's income distribution proportion is analyzed and compared in social welfare maximization model and platform profit maximization model, respectively.

*4.2.2. Relationship between Proportion and Average Travel Time.* As shown in Figure 3, as the value of average travel time increases in the model, the driver's income distribution proportion of the two models increases. From the perspective of economics, this is due to the decrease of supply caused by the increase of ride time. In the case of unchanged demand, the platform price will rise, and accordingly, the driver's bonus should also increase. Additionally, comparing the two broken lines, the income distribution proportion of drivers obtained in the platform profit maximization model is lower than that of the social welfare maximization model, which is consistent with the profit purpose of the platform.

Furthermore, in the platform profit maximization model, the average ride time of passengers significantly affects the driver's income distribution proportion. However, in the welfare maximization model, the driver's income

Table 1: Summary of parameters.

| Parameter | Description |
|---|---|
| $\Lambda_e$ | Probability of new drivers arriving at the system |
| $t$ | Average travel time |
| $q_{\text{leave}}$ | Probability of driver leaving the system |
| $\lambda_0$ | Initial driver arrival rate |
| $\mu_0$ | Initial passenger arrival rate |
| $\lambda$ | Effective driver arrival rate |
| $\mu$ | Effective passenger arrival rate |
| $A$ | Driver's income distribution proportion |
| $p$ | Price of each ride |
| $p_L$ | Low platform pricing |
| $p_H$ | High platform pricing |
| $\theta$ | Threshold |
| $N$ | Number of available drivers |
| $F_V$ | Psychological price distribution of passengers |
| $F_C$ | Psychological price distribution of drivers |
| $f_V$ | Probability density distribution of passenger psychological price |
| $f_c$ | Probability density distribution of driver's psychological price |
| $V$ | The expected price of each passenger |
| $C$ | The expected price of each driver |
| $f$ | Expected free time |
| $h$ | Expected ride income |
| $S$ | Passenger surplus |
| $D$ | Driver surplus |
| $T$ | Platform profit |
| $W_1$ | Social welfare |
| $W_2$ | Platform profit |
| $D_C$ | Driver cost |
| $T_C$ | Platform cost |
| $p_{\text{BAL}}$ | Balanced price |
| $d$ | Population density |

Table 2: Basic parameter settings of four cities of different levels.

| Parameter | City $A$ | City $B$ | City $C$ | City $D$ |
|---|---|---|---|---|
| $D$ | 3.40 | 1.40 | 0.70 | 0.15 |
| $\lambda_0$ | 1500 | 1100 | 1000 | 300 |
| $\mu_0$ | 3000 | 2200 | 2000 | 600 |
| $q_{\text{leave}}$ | 0.8 | 0.8 | 0.8 | 0.8 |
| $t$ | 0.75 | 0.5 | 0.5 | 0.33 |
| $f_V$ | $N(4,1)$ | $N(3,1)$ | $N(3,1)$ | $N(2,1)$ |
| $f_C$ | $N(4,1)$ | $N(4,1)$ | $N(2.5,1)$ | $N(3.5,1)$ |
| $D_C$ | 0.11 | 0.11 | 0.11 | 0.11 |
| $T_C$ | 0.14p | 0.14p | 0.14p | 0.14p |

distribution proportion is less significantly influenced by the average travel time.

It is inspired that, in reality, as the price of online ride-hailing services is generally determined by online ride-hailing platforms, they prefer longer service time [28], which is contrary to the traffic development of today's intensive cities and green transportation cities. However, in the welfare maximization model, the change of average travel time has no obvious effect on the driver's income distribution proportion.

*4.2.3. Relationship between Proportion and Psychological Expected Price of Drivers and Passengers.* The distribution of the psychological expected price of passengers and drivers, especially the psychological expected price of drivers, determines the supply of labor force in online ride-hailing market.

In Zha et al. [7] research on the labor supply of online ride-hailing platform, they focused on driver's behavioral decision-making and pointed out that the driver's supply decision-making is affected by the driver's psychological expected price and the average hourly income, which is closely related to driver's income distribution in work. Figure 4 shows the relationship between the income distribution proportion and the psychological expected price of drivers and passengers. It can be seen that, with the increase of the psychological expected price of passengers and drivers, the proportion of drivers' income distribution in the two models shows an increasing trend. This is due to the increase of driver supply caused by the increase of the psychological expected price of drivers and passengers, which leads to the increase of driver supply. Therefore, to achieve better social welfare and increase the income distribution proportion of drivers, it is necessary to raise the psychological expected price of passengers and drivers. For drivers, it is realistic to increase the psychologically expected price. For passengers, it can be realized by some methods: improving the quality of service, such as improve the convenience, safety, and comfort of service, which can increase the consumption intention of passengers and improve the price level acceptable to passengers. In addition, the

Table 3: Model outputs of the four cities.

| | City $A$ | | City $B$ | | City $C$ | | City $D$ | |
|---|---|---|---|---|---|---|---|---|
| | Welfare maximization | Profit maximization | Welfare maximization | Profit maximization | Welfare maximization | Profit maximization | Welfare maximization | Profit maximization |
| $A$ | 0.64 | 0.57 | 0.57 | 0.44 | 0.47 | 0.36 | 0.47 | 0.43 |
| $p_L$ | 4.39 | 4.76 | 2.00 | 3.36 | 1.55 | 1.18 | 2.54 | 1.18 |
| $p_H$ | 4.56 | 4.80 | 3.30 | 3.45 | 2.55 | 2.58 | 3.11 | 2.57 |
| $\lambda(A, p)$ | 635 | 488 | 1129 | 981 | 580 | 561 | 185 | 170 |
| $W_1/W_2$ | 686 | 672 | 1135 | 1409 | 517 | 721 | 145 | 186 |

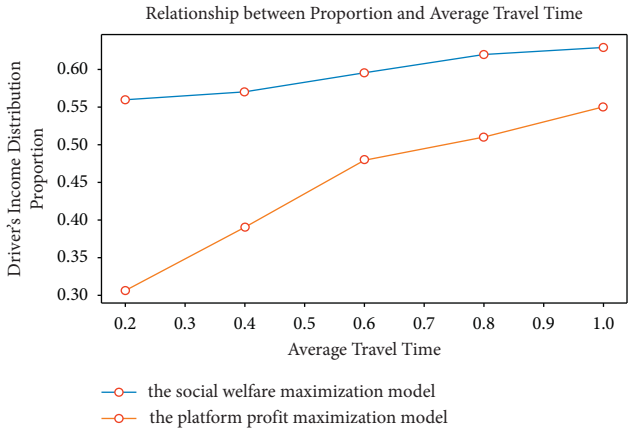


Figure 3: Relationship between proportion and average travel time.

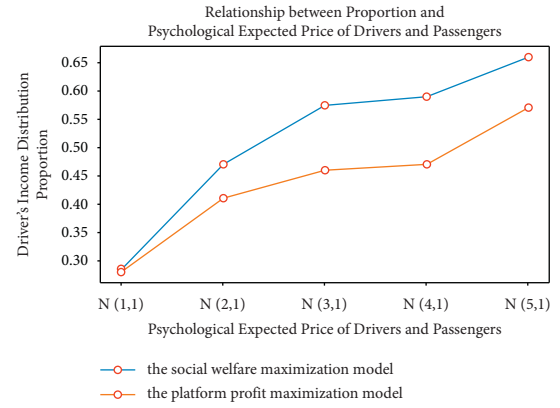


Figure 4: Relationship between proportion and psychological expected price of drivers and passengers.

increase of the psychological expected price is related to the economic development level of the whole society. When the overall economic level of the society is improved, the acceptable cost of passengers' transportation will be increased, and so will the psychological expected price of drivers and passengers.

*4.2.4. Relationship between Proportion and Probability of Driver Leaving the System.* The pricing strategy of online ride-hailing platforms and the income distribution proportion of drivers are closely related to the participation of drivers. The probability of drivers leaving the system determines the quantity of supply in the online ride-hailing system. Figure 5 examines the relationship between the income distribution proportion of drivers and the probability of drivers leaving the system. In the social welfare maximization model, with the increasing probability of drivers leaving the system, the driver's income distribution proportion gently increases. This is because, in the dynamic pricing model, the probability of drivers leaving the system hurts the supply of drivers. When the supply of drivers in the system decreases, it will inevitably lead to the increase of platform pricing and income distribution proportion, which is in line with the concept of economics. In the platform profit maximization model, the driver's income distribution proportion also shows an upward trend with the increase of the probability of drivers leaving the system, and the distribution proportion is smaller than that in the social welfare maximization model.

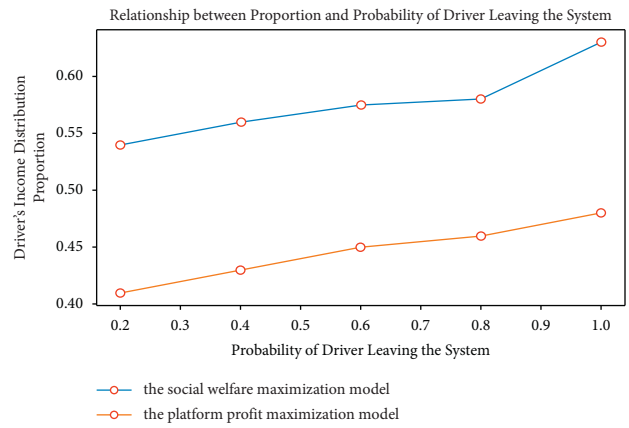


Figure 5: Relationship between proportion and probability of driver leaving the system.

*4.3. Summary.* In this chapter, through the analysis of two examples, we deeply discuss the proportion of the drivers on the online ride-hailing platform.

The first example is based on the basic parameters of supply and demand of four cities of different levels and calculates the extraction coefficient and maximum benefit in the social welfare maximization model and platform benefit maximization model, respectively. It compares the cities to understand the influence of basic parameters of different scales on the extraction coefficient. Finally, we find the following.

In the former model, the proportion of online ride-hailing platform drivers is significantly higher than the latter. This is in line with the reality of the platform's pursuit of interests and also reflects the need for the government to regulate the proportion of drivers.

In the second example, by controlling the variables, we change the average ride time of consumers, the psychological expected price of drivers and passengers, the probability of drivers leaving the system, and other parameters to explore their influence on the driver sharing coefficient in the two models. The example shows the following:

(1) With the increase of any parameter, the sharing coefficient of the two models will rise, but the rising rate is not the same; especially, the psychological expected price of the driver/passenger has a greater impact on the driver's proportion.

(2) At the same time, in the process of each parameter change, the sharing coefficient of the social welfare maximization model is significantly higher than that of the platform benefit maximization model.

## 5. Conclusions and Suggestions

Online ride-hailing platforms have operated in cities worldwide. In response to the lack of transparency and consistency in the pricing and income distribution of online ride-hailing platforms, this study investigated the mechanism of pricing and income distribution.

The contributions of this paper are as follows: (1) Queuing system model and birth and death process theory are introduced to describe the driver's flow process in the network. (2) The social welfare maximization model and the platform benefit maximization model are constructed, from the government's and platform's standpoint, respectively, based on the psychological expected price curve of passengers and drivers. (3) Numerical experiments are performed to analyze the driver's income distribution under the conditions of different settings. The results indicated that the income distribution proportion of drivers is higher in the context of social welfare maximization than that in the context of platform profit maximization. This is consistent with the reality of the platform's pursuit of interests. Moreover, the average riding time of consumers has little influence on the proportion of withdrawal in the context of social welfare maximization, while the psychological expected price of drivers and passengers has a significant impact on it.

Therefore, to maximize the social welfare and protect the driver's rights and interests, the government is suggested to flexibly regulate the pricing and the income distribution of online ride-hailing platforms on the premise of legal compliance. Government can limit the commission charged by the platform and set the lower limit of driver's proportion. First, the monopolized online ride-hailing platform charges a fee for the upper limit of each transaction at most. The setting of the upper limit maximizes the total transaction or the realized demand which is proportional to the consumer surplus. As long as the price is surging, the surge will be transferred to the driver's income to the maximum extent. Additionally, a lower limit should be set to the income distribution proportion of drivers. The setting of a lower limit guarantees the basic income of drivers in the monopolistic and opaque market. Moreover, in the long run, according to the impact of different parameters on the driver's income distribution proportion, the government can encourage long-distance online ride-hailing, develop bike-sharing and tram sharing in short-distance travel, improve residents' income and consumption level, maximize social welfare in urban development, and continuously improve the psychological expected price of consumers and drivers.

This study also has some limitations: for example, this paper only considers the impact of a single factor on the driver's income distribution ratio and does not consider the comprehensive impact of multiple factors. In addition, there is no existing data available online for ride-hailing trips which can be used to test the models. Therefore, these can be considered in future analysis, and other factors, such as spatial differences, traffic congestion, and driving costs, can also participate in discussions.

## Data Availability

The data used to support the findings of this study are included in the article.

## Conflicts of Interest

The authors declare that they have no conflicts of interest.

## Acknowledgments

This work was supported by the National Natural Science Foundation of China (Grant no. 71734004).

## References

[1] Y. Wang, J. Chen, N. Xu, W. Li, Q. Yu, and X. Song, "GPS data in urban online car-hailing: simulation on optimization and prediction in reducing void cruising distance," *Mathematical Problems in Engineering*, vol. 2020, Article ID 6890601, 2020.

[2] T. Wu, M. Zhang, X. Tian, S. Wang, and G. Hua, "Spatial differentiation and network externality in pricing mechanism of online car hailing platform," *International Journal of Production Economics*, vol. 219, pp. 275–283, 2020.

[3] Q. Yu, H. Zhang, W. Li et al., "Mobile phone data in urban bicycle-sharing: market-oriented sub-area division and spatial analysis on emission reduction potentials," *Journal of Cleaner Production*, vol. 254, Article ID 119974, 2020.

[4] S. Xu, X. Yang, and K. Peng, "Research on the proportion of online car-hailing and cruising taxi taking—based on the perspective of the company enterprise distribution mode of online taxi hailing," *Price theory and practice*, vol. 2019, no. 10, pp. 137–140, 2019, in Chinese.

[5] W. Jiang, H. Zhang, L. Yin et al., "GPS data in urban online ride-hailing: the technical potential analysis of demand prediction model," *Journal of Cleaner Production*, vol. 279, 2021.

[6] D. N. Anderson, ""Not just a taxi?" For-profit ridesharing, driver strategies, and VMT," *Transportation*, vol. 41, no. 5, pp. 1099–1117, 2014.

[7] L. Zha, Y. Yin, and H. Yang, "Economic analysis of ride-sourcing markets," *Transportation Research Part C: Emerging Technologies*, vol. 71, pp. 249–266, 2016.

[8] Q. Yu, W. Li, D. Yang, and H. Zhang, "Mobile phone data in urban commuting: a network community detection-based framework to unveil the spatial structure of commuting demand," *Journal of Advanced Transportation*, vol. 2020, Article ID 8835981, 15 pages, 2020.

[9] L. Zha, Y. Yin, and Y. Du, "Surge pricing and labor supply in the ride-sourcing market," *Transportation Research Part B: Methodological*, vol. 117, pp. 708–722, 2018.

[10] N. T. Fellows and D. E. Pitfield, "An economic and operational evaluation of urban car-sharing," *Transportation Research Part D: Transport and Environment*, vol. 5, no. 1, pp. 1–10, 2000.

[11] Y. Chang, "Economic thinking on the price war of mobile software," *Price theory and Practice*, vol. 2014, no. 4, pp. 116–118, 2014, in Chinese.

[12] Y. Xia, J. Zhu, and Y. Jiang, "Research on peak pressure relief mechanism of online car Hailing based on dynamic price," *Computer and digital engineering*, vol. 48, no. 12, pp. 2912–2918, 2020, in Chinese.

[13] S. Banerjee, C. Riquelme, and R. Johari, "Pricing in ride-share platforms: a queueing-theoretic approach," *SSRN Electronic Journal*, vol. 2015, Article ID 2568258, 2015.

[14] T. Rangel, J. N. Gonzalez, J. Gomez, F. Romero, and J. M. Vassallo, "Exploring ride-hailing fares: an empirical analysis of the case of Madrid," *Transportation*, vol. 2021, 2021.

[15] L. U. Ke, J. Zhou, and H. E. Xin, "Research on pricing strategy of ride-hailing platform considering user's preference of service quality," *Soft Science*, vol. 32, 2018.

[16] Y. Lu, Y. Qi, S. Qi, Y. Li, H. Song, and Y. Liu, "Say No to price discrimination: decentralized and automated incentives for price auditing in ride-hailing services," *IEEE Transactions on Mobile Computing*, vol. 2020, no. 99, p. 1, 2020.

[17] Z. Xu, Y. Yin, and J. Ye, "On the supply curve of ride-hailing systems," *Transportation Research Part B: Methodological*, vol. 132, pp. 29–43, 2020.

[18] Z. Liu and Z. Cai, "Political economy analysis of income distribution mode in sharing economy—taking China's internet private car industry as an example," *Political economy review*, vol. 10, no. 02, pp. 162–177, 2019, in Chinese.

[19] Y. Xie, "*Research on bounded rational game behavior of stakeholders in online ride-hailing*," Master's thesis, Xiangtan University, Xiangtan, China, in Chinese, 2018..

[20] F. Danlei, "Profit analysis of taxi software platform based on sharing economy," *China business theory*, vol. 2021, no. 9, pp. 9–11, 2021, in Chinese.

[21] C. Xiang, "Legal regulation of online ride-hailing: logic and thinking -- also on the interim measures for the management of online booking taxi service," *Journal of Southwest University of political science and law*, vol. 19, no. 6, pp. 53–62, 2017, in Chinese.

[22] L. Fang and X. Zhong, "Research on the development path of online car Hailing Market -- Based on the dual perspective of internal competition and government supervision [J/OL]," *Financial and economic treatise*, vol. 2021, in Chinese, 2021.

[23] X. Lai, "Transparent pricing rules for online car Hailing should be the basic consensus of the industry," *Consumer daily*, vol. 2021, in Chinese, 2021.

[24] J. Xia, "A willful online car Hailing platform needs reasonable transparency," *China economic times*, vol. 2021, in Chinese, 2021.

[25] M. Lin, "Promoting standardized management of online car Hailing," *Anhui Daily*, vol. 2021, in Chinese, 2021.

[26] Q. Li, "Research on regulatory policy of online ride-hailing in China from the perspective of government regulation," *Shandong University*, vol. 2017, in Chinese, 2017.

[27] T. Hu and Y. Zhang, "Dynamic pricing strategy of online ride-hailing platform," *Shandong Science*, vol. 33, no. 2, pp. 79–90, 2020, in Chinese.

[28] Y. Li and S. H. Chung, "Ride-sharing under travel time uncertainty: robust optimization and clustering approaches," *Computers & Industrial Engineering*, vol. 149, Article ID 106601, 2020.

Hindawi
Mathematical Problems in Engineering
Volume 2021, Article ID 2429714, 17 pages
https://doi.org/10.1155/2021/2429714

*Research Article*

# Effect of the Fund Policy in a Remanufacturing System considering Ecodesign and Responsibility Transfer

**Shan Wang, Xiang-Yun Chang, and Xin Huang**

*Department of Management Science and Engineering, East China University of Science and Technology, Shanghai 200237, China*

Correspondence should be addressed to Xiang-Yun Chang; xychang@ecust.edu.cn

Received 3 May 2021; Revised 17 August 2021; Accepted 18 August 2021; Published 8 September 2021

Academic Editor: Jinyu Chen



This paper aims to evaluate the effectiveness of the fund policy on ecodesign and manufacturing/remanufacturing activities and the effectiveness of the manufacturer's ecodesign responsibility transfer strategy. It considers a manufacturing and remanufacturing system composed of a single manufacturer and a single remanufacturer performing under relevant fund policy. The fund policy is innovatively designed by considering three dimensions: tax, reduction, and subsidy. Based on mathematical models and comparative analysis, the principal results show the following: (1) the impact scope of either the tax or the reduction dimension of the fund policy is larger than that of subsidy. The subsidy for encouraging remanufacturing is effective only when the remanufacturer uses some of the collected returns for remanufacturing. (2) The impact direction of tax, reduction, or subsidy is complicated, changing when the remanufacturer uses some of the collected returns for remanufacturing. (3) The responsibility transfer behavior of the manufacturer does not change the impact scope of the fund policy, but changes its impact strength and impact path. The impact of the responsibility transfer strategy on enterprises' decision-making varies with different remanufacturing scenarios.

## 1. Introduction

A range of Extended Producer Responsibility (EPR) programs around the world have been developed for managing waste. EPR is an environmental protection strategy to enforce take-back, recycling, and final disposal efforts by manufacturers [1].

Fund policy is one typical form of EPR regulation implementation, which is prevalent in Mainland China and Taiwan [2–4]. For example, Taiwan initialized the Recycling Fund Management Board of the Environmental Protection Administration (EPA) in 1998, and the Ministry of Finance in Mainland China created the E-waste Processing Fund Collection and the Subsidy Management Approach in 2012.

The fund policy can be considered a synthesis of environmental taxes and subsidies. A waste tax is levied on manufacturers per unit product sold to consumers. Proceeds are then channeled into a recycling management fund and used to promote recycling incentives. At the recycling and reuse stage, the disassembling enterprises or recyclers are subsidized according to the actual amount of waste they process [3, 5].

Fund policy and other forms of EPR regulation across the world are similar in purpose, which is twofold. One task is to promote product ecodesign at the product development stage. The other task is to promote the recycling rate or recycling quantities at the recycling stage [6, 7]. The former focuses on resource consumption reduction and waste prevention, while the latter focuses on resource reuse and recycling.

Ecodesign is defined as "the integration of environmental aspects into product design and development with the aim of reducing adverse environmental impacts throughout the whole product's life cycle" [8]. In fact, product ecodesign has an important impact on recycling and environmental protection. If producers adopt recycle and reuse-oriented ecodesign at the product development stage, the recycle frequency of waste products can be increased and pollution levels throughout the life cycle can be reduced. Many enterprises, such as Xerox and Kodak, take

remanufacturing into consideration when they design their products [9].

Regardless of the fact that adoption of ecodesign strategies in product development can offer several advantages in industry, ecodesign is actually an environmental responsibility; however, performing ecodesign often raises a manufacturer's operating costs. At the same time, dealers or retailers often benefit from the manufacturer's ecodesign. It is unfair for a manufacturer to solely bear the ecodesign responsibilities. That is why manufacturers are not as supportive of ecodesign as expected [5] and often adopt responsibility transfer strategies to share their environmental responsibilities with other actors in the supply chain [10]. As such, how relative responsibilities are shared among supply chain members becomes an intriguing issue [10, 11].

Remanufacturing is generally perceived as an environmentally friendly end-of-use management option for many companies [12]. Companies can reduce production costs by extracting core components from used products instead of using new raw materials [13]. For example, Caterpillar, HP, and Xerox have saved 30–70% production costs from their recycling and remanufacturing activities of end-of-life products. In 2015, Apple signed an agreement with Foxconn in which the latter acquired proprietary rights to remanufacture the end-of-life iPhone mobile phones and remarket them in China [14]. In general, remanufactured products have similar valuations to new products, and they are competitive substitutes for each other in the market.

Then, for a manufacturing-remanufacturing competition system considering ecodesign and its responsibility transfer strategy under the constraints of fund policy, the following questions are worth studying:

(1) How will the fund policy affect the ecodesign and production decisions of a manufacturer, and how will it affect the remanufacturing decisions of a remanufacturer?

(2) When a manufacturer adopts an ecodesign responsibility transfer strategy to transfer his own ecodesign responsibilities to other members in a supply chain, how will the impact of fund policy change? And how will the decisions of the manufacturer and remanufacturer change?

This paper will try to answer these questions by using game theory. The paper considers a manufacturing-remanufacturing competition system under the constraints of fund policy. A regulator designs the fund policy, which mainly consists of three dimensions—*tax*, *reduction*, and *subsidy*—that influence ecodesign efforts and manufacturing/remanufacturing decisions. A manufacturer produces a key component and a new product in the market. The key component cannot be remanufactured and can only be sold by the manufacturer at a buyer-specific wholesale price or through a responsibility transfer strategy. A remanufacturer recycles old parts and purchases key components from the manufacturer for remanufacturing. The new product and remanufactured product are competitive substitutes in the market.

The aim of this paper is to investigate the effect of fund policy on ecodesign and manufacturing/remanufacturing activities and to investigate the effect of the manufacturer's ecodesign responsibility transfer strategy. The main contributions of this research are as follows.

(1) A new fund reduction policy is proposed as an alternative scheme, and the fund policy is refined to consider three dimensions: *tax*, *reduction,* and *subsidy*. The reduction dimension is used to provide better incentives for manufacturers to carry out ecodesign, which was seldom considered in the previous research, but which has extended the existing research that mainly considers tax and subsidy.

(2) Ecodesign (waste prevention measure) and remanufacturing (waste end-treatment measure) will be considered at the same time. This means that waste prevention and waste end-treatment are both considered in one system, which is innovative.

(3) The paper considers a key component that cannot be remanufactured in the manufacturing-remanufacturing competition system, as well as ecodesign responsibility transfer strategy, which makes this research more sophisticated.

The remainder of this paper is organized as follows. Section 2 reviews the relevant literature. Section 3 presents the basic model (B-model) and analyzes the obtained perfect equilibria. Section 4 considers ecodesign responsibility transfer and presents the T-model. Section 5 comparatively analyzes the system equilibrium of the two models. Section 6 concludes the paper.

## 2. Literature Review

This research is closely related to four research directions: EPR regulation, fund policy, ecodesign, and responsibility transfer. In this section, the relevant studies are reviewed to provide an overview of previous studies and bring forward an innovative perception of the paper.

*2.1. EPR Regulation.* Mainly aimed at the disposal responsibility of waste products, EPR requires producers to undertake the responsibility of recycling or disposing of products after use. This means that the producer bears the actual responsibility for product recovery and disposal, or the responsibility for product recovery and disposal costs; that is, the producer can transfer his responsibility under the EPR to a third party using a paid transfer strategy.

The implementation of EPR is flexible and diverse all around the world. Generally speaking, EPR legislation is implemented in two typical ways: M-operated systems and G-operated systems. M-operated systems (manufacturer-operated) indicate that manufacturers operate their own recycling network (self-operated or outsourced) to manage and recycle their products' waste. The government assigns recycling tasks (minimum recovery and recycling) to the

manufacturer. For example, the WEEE Directive of the European Union adopts M-operated systems. As for G-operated systems (government-operated), the government is responsible for recycling waste products, and the manufacturer pays the government a certain fee for the process. For example, G-operated systems are adopted in the Chinese mainland and Taiwan region for the management of waste household appliances and electronic products. However, the fund system still needs to be further standardized. There are some problems, such as incomplete extension of responsibility, insufficient correlation between economic responsibility and ecodesign for producers, and lack of an incentive system for multiagent responsibility. Kautto and Melanen [15] pointed out that since the EU WEEE Directive did not have any contribution to waste prevention, the scope of policy should be drastically shifted from waste management to society's overall cycles of materials and products. Wang et al. [16] systematically analyzed the physical and financial operating mechanisms of EPR systems in Japan, Germany, Switzerland, and China and pointed out that although the operation mechanism of EPR systems varied greatly in different countries, there were some common problems. Li et al. [17] used the newsvendor model and numerical simulation method and concluded that the EPR coefficient policy was an appropriate and effective approach to promote the EPR practice of the Chinese government.

*2.2. Fund Policy.* Taking these considerations into effect, scholars have carried out varied research on fund policy. Pazoki et al. [18] discussed how to set the values of subsidies and penalties in several environmental regulations to minimize the environmental impact of production or to maximize product recovery. Cao et al. [19] analyzed the effect of environmental regulations and financial measures stipulated by the government. Guo et al. [20] used the system dynamic method to analyze how China's "WEEE processing fund" policy influences the economic and environmental conditions of participants in the WEEE management system. Chang et al. [21] found that the joint tax-subsidy mechanism can motivate the manufacturer to pursue ecoinnovation and to incorporate recycling considerations into its production and ecoinnovation decisions. Chen et al. [22] investigated the behavior of supply-chain members in green supply chain management under the reward-penalty mechanism and found that the return rate and green effort can be improved by the reward-penalty mechanism. Hong and Guo [23] found that the policy balanced the interests of manufacturers, importers, sellers, and recyclers by choosing an optimal selling quantity in the market and optimal reward money for customers bringing end-of-life products to recyclers. Pazoki and Samarghandi [24] found that a regulated manufacturer practiced remanufacturing for a costly ecodesign. Wang et al. [25] presented a tripartite evolutionary game model consisting of the government, the recycler, and the consumer, determined the payoff matrices of the system, and calculated the replicator dynamic equation of each participant. The results showed that the government should play a leading role in the development of the e-waste recycling industry. Zhang et al. [26] found that government tax and subsidy policies could not always improve enterprises' remanufacturing behavior. Zhang et al. [27] researched optimal pricing and remanufacturing modes in a closed-loop supply chain of WEEE under government fund policy. Liu et al. [28] introduced a dual regulation regime characterized by the deposit-refund policy and a minimal collection rate of used products. They found that regulating the minimal collection rate was beneficial to the environment and helped to reduce the deposit-refund policy deficit under certain conditions.

It can be seen that scholars mainly pay attention to the recycling fund policy in terms of fund collection, subsidies, and fund management. However, the current research on policy design seldom considers the ecodesign behavior of the manufacturer and waste prevention at the source.

*2.3. Ecodesign.* In fact, product ecodesign has an important impact on recycling and environmental protection. If producers adopt recyclable and reuse-oriented ecodesign in the product design stage, the recycling frequency of waste products can be improved and life cycle pollution can be reduced. Örsdemir et al. [12] believed that about two-thirds of the remanufacturability of recycled products depended on the remanufacturing design at the initial stage of product design. Calcotta and Walls [29] examined the impacts of policies to encourage efficient product design and recycling and found that optimal outcomes could be attained by combining a "deposit-refund" policy. Zhu and He [30] indicated that supply chain price competition at the retailer level might positively influence equilibrium greenness, while product greenness competition reduces equilibrium greenness. Zand et al. [31] found that the green level of the products positively contributed to the amount of collected used products and increased the retailer's profit. Zheng et al. [32] put forward a theoretical model to discuss the influence of competitive strategy on Design for Environment (DFE). DFE can help reduce the impact of products on the environment, but high levels of DFE may harm the environment by substantially increasing total sales.

Therefore, most of the current quantitative modeling research on ecodesign simply takes ecodesign as a decision variable, which is far from detailed and in-depth.

*2.4. Responsibility Transfer.* Ecodesign responsibility is actually an environmental responsibility. Performing environmental responsibility often brings relevant operating costs to enterprises. Therefore, manufacturers often adopt different ecological design strategies according to cost, income, market competition, and other factors. Subramanian et al. [33] found that the competition between manufacturing and remanufacturing products would change the ecodesign strategy. Hong and Guo [23] studied several cooperation contracts within a green product supply chain and investigated their environmental performance. Mathiyazhagan et al. [34] found that OEMs could complete green supply chain management requirements by merging

and splitting responsibilities. Cheng et al. [10] found that when the OEM and retailer worked together, the responsibility transfer factor did not affect their dual performance. Governments and retailers should consider ecological and environmental protection targets and profits in the OEM strategy.

To sum up, the existing literature has provided an important theoretical basis for fund policy. However, many of these studies pay more attention to recycling and end-treatment of waste, but less attention to ecodesign of the production stage in a closed-loop supply chain. It is necessary to explore new incentive methods and new fund policy operation modes considering both ecodesign (waste prevention measure) and remanufacturing (waste end-treatment measure), as well as ecodesign responsibility transfer strategies.

## 3. Basic Model and Analysis

*3.1. Model and Solution.* This paper considers a manufacturing-remanufacturing competition system under fund policy. To promote ecodesign and recycling, the government designs the fund policy considering three dimensions, namely, *tax*, *reduction*, and *subsidy*, which are assumed to be exogenous. The manufacturer produces products, sells them to consumers in the market, and produces a key component that cannot be remanufactured. The remanufacturer recycles waste products and purchases the key component from the manufacturer for remanufacturing. The new product and the remanufactured product are competitive substitutes in the market. The structure of the system is depicted in Figure 1, and a summary of notations can be found in Table 1.

Next, we will describe the assumptions and basic model in detail. We assume the manufacturer sets a buyer-specific wholesale price of the key component tailored to the remanufacturer in the basic model (B-model).

*3.1.1. The Regulator.* The regulator designs the fund policy, which mainly includes three dimensions: *tax*, *reduction,* and *subsidy*. The regulator levies the waste tax $T_0$ on the manufacturer per product sold to consumers (*tax mechanism*) and issues quota subsidies $s$ to qualified remanufacturers for waste recycling and dismantling (*subsidy mechanism*). At the same time, in order to encourage the manufacturer to conduct ecodesign, tax reduction is carried out based on ecodesign effort. The unit tax reduction is $\sigma e$ (*reduction mechanism*).

*3.1.2. The Manufacturer.* The manufacturer ($m$) strategically decides on product ecodesign effort $e$ and fulfills its ecodesign responsibility under the constraints of fund policy. Meanwhile, the manufacturer needs to decide on the production quantity of the new product $q_n$. It costs the manufacturer $(1/2)de^2$ to exert ecodesign effort $e$; this formula $(1/2)de^2$ is widely used in other literatures, such as Zhu and He [30] and Chen and Ulya [35]. New products and remanufactured products are competitive substitutes in the market. Given the quantities of new and remanufactured products $q_n, q_r$, the market-clearing prices for new and remanufactured products are $p_n = 1 - q_n - \delta q_r$ and $p_r = \delta(1 - q_n - q_r)$, respectively. These functions are widely used in the literature for closed-loop supply chain management; see Zheng et al. [32]; Wu and Zhou [36]; and Jacobs and Subramanian [11]. The manufacturer has the technology to produce a key component that cannot be remanufactured. Referring to Chen et al. [22], it is assumed that the manufacturer incurs two costs when producing a new product: the unit cost of the key component $m$ and the unit production cost of the new product $c_n$.

*3.1.3. The Remanufacturer.* The remanufacturer ($r$) determines remanufacturing quantity $q_r$ under the constraint of fund policy. Assume that $q_r \le \tau q_n$ and all remanufactured products can be sold. The unit remanufacturing cost is $c_r$. The ecodesign effort of the manufacturer (such as modular design to make disassembly easier) benefits the remanufacturer, and the reduction of unit remanufacturing cost is $\alpha e$. The remanufacturer needs to purchase the key component from the manufacturer at a buyer-specific wholesale price $w_0$ during the process of remanufacturing.

The manufacturer and remanufacturer pursue profit maximization, and the decision model is

$$\begin{cases} \underset{(e,q_n)}{\text{Max}}\ \pi_m = \underbrace{(p_n - c_n - m)q_n}_{\text{Sales revenue of new product}} - \underbrace{\frac{d}{2}e^2}_{\text{Eco-design cost}} + \underbrace{(w_0 - m)q_r}_{\text{Sales revenue of key compoment}} - \underbrace{(T_0 - \sigma e)q_n}_{\text{Waste tax}}, \\ \underset{(q_r)}{\text{Max}}\ \pi_r = \underbrace{[p_r - (c_r - \alpha e) - w_0]q_r}_{\text{Sales revenue of remanufacturing product}} + \underbrace{sq_r}_{\text{Government subsidy}}, \\ 0 \le q_r \le \tau q_n. \end{cases} \tag{1}$$

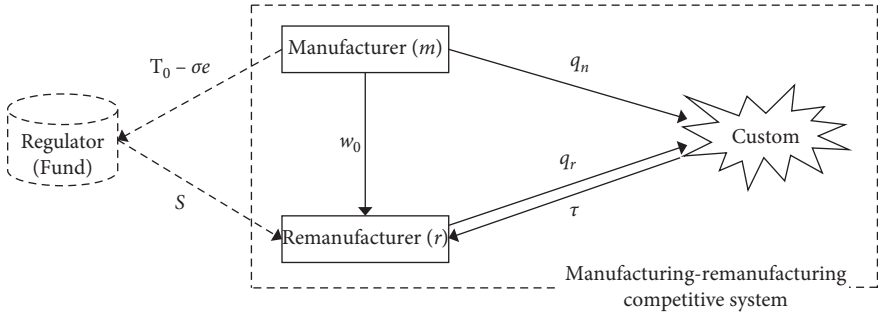


Figure 1: A manufacturing-remanufacturing competitive system with the fund policy.

Table 1: Notations.

| | | Descriptions |
|---|---|---|
| Parameters | $T_0$ | Waste tax per unit product sold to consumers imposed by the regulator on the manufacturer |
| | $\sigma$ | Tax reduction coefficient per unit product given by the government for encouraging the manufacture's ecodesign activity,$\sigma \in (0,1)$ |
| | $s$ | Unit subsidy per unit remanufactured product received from the regulator |
| | $d$ | The sensitivity of production cost to the ecodesign |
| | $\delta$ | Consumer's willingness to pay for the remanufactured product $\delta \in (0,1)$ |
| | $c_n$ | Unit production cost of a new product |
| | $c_r$ | Unit production cost of a remanufactured product |
| | $m$ | Unit cost of a key component |
| | $\Delta$ | The unit cost savings of production through remanufacturing, $\Delta = c_n - c_r$ |
| | $\alpha$ | Unit remanufacturing cost reduction coefficient that the manufacturer's ecodesign brings to the remanufacturer |
| | $w_0$ | A buyer-specific wholesale price of the key component to the remanufacturer |
| | $p_n$ | Unit sale price of a new product |
| | $p_r$ | Unit sale price of a remanufactured product |
| | $\tau$ | Recycling rate of used products $(0 < \tau \leq 1)$ |
| Decision variables | $q_n$ | Sales quantity of new products |
| | $q_r$ | Sales quantity of remanufactured products |
| | $e$ | The manufacturer's ecodesign effort |

Manufacturer and remanufacturer's decision goal is to maximize profit. The order of game is as follows: in the first stage, the manufacturer decides product ecodesign effort $e$. In the second stage, the remanufacturer decides on the remanufactured product quantity $q_r$ according to the ecodesign effort of the manufacturer. At the same time, the manufacturer also decides on new product quantity $q_n$. This game order has been used in the literatures, such as Zheng et al. [32] and Reimann et al. [37], in order to make all decisions within a period of stability and not disperse the time-cycle effect when studying the interactions within the manufacturing-remanufacturing supply chain. Assuming that the manufacturer and the remanufacturer make the same decision at each stage in the steady-state equilibrium, the production quantity decision made by the manufacturer and the remanufacturer in the second stage can be regarded as simultaneous.

We solve the two-stage game described above by backward induction. First, $q_n, q_r$ are obtained and substituted back to $\pi_m, \pi_n$, and then $e$ can be got. Proposition 1 presents the optimal equilibrium strategies of the manufacturer and remanufacturer.

Next, for convenience in writing, the *BA* scenario represents the case when the remanufacturer uses all the collected returns for remanufacturing in the B-model, and the *BS* scenario represents the case when the remanufacturer uses some of the collected returns for remanufacturing in the B-model.

**Proposition 1.** *In the manufacturing-remanufacturing competition system under the constraints of fund policy, the optimal equilibrium strategies of the manufacturer and remanufacturer can be seen in Table 2, where* $K = 1 - c_n - m$; $d(2+\delta\tau)^2 - 2\sigma^2 > 0$; *and* $d(4-\delta)^2 - 2(\alpha - 2\sigma)^2 > 0$.

*Proof.* All proofs are relegated to Appendix. □

*3.2. Analysis.* As described in Section 3.1, the fund policy we researched in this paper includes three dimensions: *tax*, *reduction,* and *subsidy*, which are, respectively, represented by the parameters $T_0, \sigma, s$ in the B-model. The impacts of the three parameters on ecodesign decision and manufacturing/remanufacturing activities will be analyzed next.

*3.2.1. Impact Scope of the Fund Policy.* By observing the relationship between the optimal solution $e^{i^*}, q_n^{i^*}, q_r^{i^*}$ $(i = BA, BS)$ and the fund policy factors $T_0$, $\sigma$, $s$ in Table 2, Conclusion 1 can be obtained.

Table 2: Optimal equilibrium strategies of the B-model.

| | The remanufacturer uses all the collected returns for remanufacturing (*BA* scenario) | The remanufacturer uses some of the collected returns for remanufacturing (*BS* scenario) |
|---|---|---|
| $e^*$ | $([2(K-T_0)+\tau(w_0-m)(2+\delta\tau)]\sigma/(d(2+\delta\tau)^2-2\sigma^2))$ | $(2\delta(2\sigma-\alpha)(1+K-\Delta-\delta-s-2T_0)+(8\alpha-4\alpha\delta+\sigma\delta^2)(w_0-m)/\delta[d(4-\delta)^2-2(\alpha-2\sigma)^2])$ |
| $q_n^*$ | $(d(2+\delta\tau)(K-T_0)+(w_0-m)\tau\sigma^2/(d(2+\delta\tau)^2-2\sigma^2))$ | $(d\delta(4-\delta)(1+K-\Delta-\delta-s-2T_0)+[d\delta(4-\delta)-(\alpha-2\sigma)(2\alpha-\delta\sigma)](w_0-m)/\delta[d(4-\delta)^2-2(\alpha-2\sigma)^2])$ |
| $q_r^*$ | $(\tau[d(2+\delta\tau)(K-T_0)+(w_0-m)\tau\sigma^2]/(d(2+\delta\tau)^2-2\sigma^2))$ | $(\{d\delta(4-\delta)[\delta(1+c_n+m+T_0)-2c_r-2(m-s+w_0)]+2\alpha\sigma\delta(1+K-\Delta-2m+s-2T_0-3w_0)+\delta\sigma^2[4c_r-4(\delta-m+s)+(4+\delta)w_0]-2\alpha^2[\delta(K-T_0)-2w_0]\}/\delta^2[d(4-\delta)^2-2(\alpha-2\sigma)^2])$ |

*Conclusion 1.* The tax factor $T_0$ and the reduction factor $\sigma$ affect all decisions $e^{i^*}, q_n^{i^*}, q_r^{i^*}$ $(i = BA, BS)$ both in the *BA* scenario and in the *BS* scenario, while the subsidy factor $s$ only affects the decisions $e_n^{BS^*}, q_n^{BS^*}, q_r^{BS^*}$ in *BS* scenario.

Therefore, the impact scope of fund policy is larger in the *BS* scenario than in the *BA* scenario.

(a) In the *BA* scenario, the market environment is extremely favorable for remanufacturing, and the subsidy policy for encouraging recycling and remanufacturing is ineffective. Therefore, once the remanufacturer decides on using all the collected returns for remanufacturing based on market conditions, the government should focus on the policy factors for the manufacturer rather than the remanufacturer, so as to bolster the manufacturer's focus on ecodesign and waste prevention measures at the production stage.

(b) In the *BS* scenario, the factors of *tax*, *reduction,* and *subsidy* affect both the manufacturer's and remanufacturer's decisions. So, the government should not only consider the impact of one single policy factor, but should consider the impact of three factors—*tax*, *reduction,* and *subsidy*—as a whole when designing the fund policy in the *BS* scenario.

*3.2.2. Impacts of Fund Policy Factors on Decision-Making.* The relationships between the optimal solution in Table 2 and the first-order partial derivatives $T_0, \sigma, s$ are shown in Proposition 2.

**Proposition 2.** *For the manufacturing-remanufacturing competition system under the constraints of fund policy, the relationship between optimal equilibrium strategies and the first-order partial derivatives, $T_0, \sigma, s$, in the BA and BS scenarios is shown in line 1 and line 2 of Table 3, respectively.*

From Table 3, we observe the following: (a) In the *BA* scenario, $e^{BA^*}, q_n^{BA^*}, q_r^{BA^*}$ all decrease with respect to $T_0$. The effect of the reduction factor $\sigma$ is opposite to that of the tax factor $T_0$, and the subsidy factor, $s$, does not affect the decisions of the manufacturer and remanufacturer. (b) In the *BS* scenario, $T_0, \sigma, s$ have a complex impact on decisions of the manufacturer and remanufacturer. Take $T_0$ for example. It can promote ecodesign efforts in some cases, while it will weaken ecodesign efforts in other cases. The key is the relationship between $\alpha$ and $\sigma$; the turning point of policy impact is $\sigma = (\alpha/2)$.

In order to observe the complex impact of $T_0, \sigma, s$ on the optimal decisions $e^{BS^*}, q_n^{BS^*}, q_r^{BS^*}$ in *BS* scenario, we plot Figure 2 where $\alpha = 0.6, \sigma = 0.3$. Given the impact of $T_0, s$ that has been shown in Table 3, the focus here is on the complex impact of $\sigma$ on the manufacturer's and remanufacturer's decisions.

From Figure 2, we can observe the following:

(i) When subsidy $s$ is constant and tax $T_0$ is low, as $\sigma$ increases, the ecodesign effort $e^{BS^*}$ is higher (Figure 2(a)), $q_n^{BS^*}$ increases (Figure 2(b)), and $q_r^{BS^*}$ first decreases and then increases (Figure 2(c)). However, the effect of $\sigma$ is changed when $s$ is constant and $T_0$ is high (Figures 2(a)–2(c)).

(ii) When $T_0$ is constant and subsidy $s$ is low, as $\sigma$ increases, the ecodesign effort $e$ first decreases and then increases (Figure 2(d)), $q_n^{BS^*}$ increases (Figure 2(e)), $q_r^{BS^*}$ first decreases and then increases (Figure 2(f)).

From the perspective of fund policy design by the government, we can put forward managerial implications as follows:

(a) In the *BA* scenario, the focus of fund policy design by the government should be the *tax* dimension and the *reduction* dimension. By reducing the tax and increasing tax reduction, the manufacturer can be encouraged to improve ecodesign efforts and strengthen the prevention of waste management at the production stage.

(b) In the *BS* scenario, the impact mechanism of the *tax, reduction*, and *subsidy* dimensions of fund policy is complex and changeable, so the government should integrate design of the three dimensions——*tax, reduction*, and *subsidy*——to create a balanced guidance of fund policy on ecodesign and remanufacturing behavior. In particular, the reduction dimension of fund policy must be set carefully in the *BS* scenario; otherwise, it will not only weaken ecodesign and remanufacturing at the supply chain level, but will also lead to negative impacts from the tax and subsidy dimensions of fund policy on ecodesign and remanufacturing at the policy level.

## 4. Impact of Ecodesign Responsibility Transfer

Based on the B-model in Section 3, we will introduce the manufacturer's ecodesign responsibility transfer strategy to explore the impact of ecodesign responsibility transfer strategy in this chapter.

*4.1. Modeling and Solution.* Referring to the research of Cheng et al. [10], the manufacturer's ecodesign responsibility transfer is reflected in the wholesale price of the key component, which is set as $(w_0 + h_e e)$ instead of the buyer-specific wholesale price in the B-model in Section 3, where $h_e \in [0, 1]$ is the transfer coefficient; the greater the value is, the more the ecodesign responsibility is transferred.

The decision model of the ecodesign responsibility transfer strategy (T-model) is

Table 3: The relationship between optimal equilibrium strategies and $T_0$, $\sigma$, and $s$.

| | $(\partial e^*/\partial T_0)$ | $(\partial q_n^*/\partial T_0)$ | $(\partial q_r^*/\partial T_0)$ | $(\partial e^*/\partial \sigma)$ | $(\partial q_n^*/\partial \sigma)$ | $(\partial q_r^*/\partial \sigma)$ | $(\partial e^*/\partial s)$ | $(\partial q_n^*/\partial s)$ | $(\partial q_r^*/\partial s)$ |
|---|---|---|---|---|---|---|---|---|---|
| *BA* scenario | − | − | − | + | + | + | × | × | × |
| *BS* scenario $(\sigma < \alpha/2 \mid \sigma > \alpha/2)$ | +/− | − | +/∼ | ∼ | ∼ | ∼ | +/− | − | +/∼ |

*Note.* +, −, ∼ and × indicate monotone increase, monotone decrease, and monotone uncertainty, respectively.

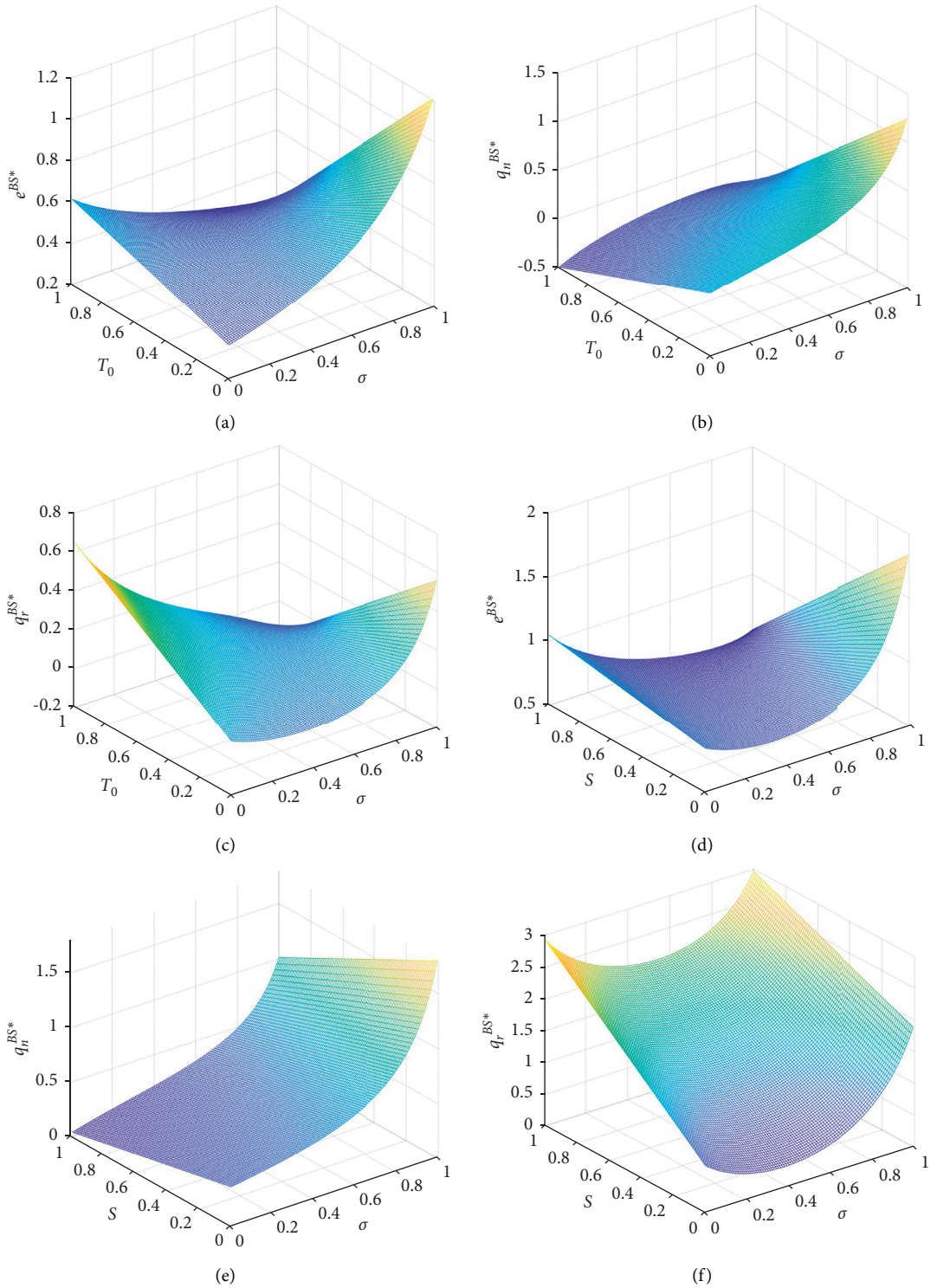


Figure 2: Effects of $T_0$, $\sigma$, and $s$ on $e^{BS^*}$, $q_n^{BS^*}$, and $q_r^{BS^*}$. (a) Effects of $T_0$ and $\sigma$ on $e^{BS^*}$. (b) Effects of $T_0$ and $\sigma$ on $q_n^{BS^*}$. (c) Effects of $T_0$ and $\sigma$ on $q_r^{BS^*}$. (d) Effects of $s$ and $\sigma$ on $e^{BS^*}$. (e) Effects of $s$ and $\sigma$ on $q_n^{BS^*}$. (f) Effects of $s$ and $\sigma$ on $q_r^{BS^*}$.

$$\begin{cases} \underset{(e,q_n)}{\text{Max}}\ \pi_m = \underbrace{(p_n - c_n - m)q_n}_{\text{Sales revenue of new product}} - \underbrace{\frac{d}{2}e^2}_{\text{Eco-design cost}} + \underbrace{(w_0 + h_e e - m)q_r}_{\text{Sales revenue of key compoment}} - \underbrace{(T_0 - \sigma e)q_n}_{\text{Waste tax}}, \\ \underset{(q_r)}{\text{Max}}\ \pi_r = \underbrace{[p_r - c_r - (w_0 + h_e e) + \alpha e]q_r}_{\text{Sales revenue of remanufacturing product}} + \underbrace{sq_r}_{\text{Government subsidy}}, \\ 0 \le q_r \le \tau q_n. \end{cases} \tag{2}$$

Next, the *TA* scenario represents the case where the remanufacturer uses all the collected returns for remanufacturing in the T-model, and the *TS* scenario represents the case where the remanufacturer uses some of the collected returns for remanufacturing in the T-model.

The manufacturer and remanufacturer pursue profit maximization, and the solution process is similar to Section 3.1. The detailed proof is omitted. The optimal solution is as follows:

(a) *TA* scenario: when the remanufacturer uses all the collected returns for remanufacturing:

$$e^{TA^*} = \frac{[2(K - T_0) + \tau(w_0 - m)(2 + \delta\tau)]\sigma + h_e\tau(2 + \delta\tau)K}{d(2 + \delta\tau)^2 - 2\sigma^2 - 2\sigma h_e\tau(2 + \delta\tau)}, \tag{3}$$

$$q_n^{TA^*} = \frac{d(2 + \delta\tau)(K - T_0) + (w_0 - m)\tau\sigma^2 - \tau\sigma h_e(K - T_0)}{d(2 + \delta\tau)^2 - 2\sigma^2 - 2\sigma h_e\tau(2 + \delta\tau)}, \tag{4}$$

$$q_r^{TA^*} = \frac{\tau\{d(2 + \delta\tau)(K - T_0) + (w_0 - m)\tau\sigma^2 - \tau\sigma h_e(K - T_0)\}}{d(2 + \delta\tau)^2 - 2\sigma^2 - 2\sigma h_e\tau(2 + \delta\tau)}, \tag{5}$$

where $d(2 + \delta\tau)^2 - 2\sigma^2 - 2\sigma h_e\tau(2 + \delta\tau) > 0$.

(b) *TS* scenario: when the remanufacturer uses some of the collected returns for remanufacturing:

$$e^{TS^*} = \frac{\begin{array}{l} 2\delta(2\sigma - \alpha)(1 + K - \Delta - \delta - s - 2T_0) + (8\alpha - 4\alpha\delta + \delta\sigma\delta)(w_0 - m) \\ -h_e\{4c_r(2 - \delta) + \delta[\delta(3 + c_n + m + T_0) + 2(m + 2s - 3w_0)] - 8(\delta + m + s - 2w_0)\} \end{array}}{\delta[d(4 - \delta)^2 - 2(\alpha - 2\sigma)^2] - 2(8 - 3\delta)h_e^2 - 2\delta^2 h_e\sigma + 8\alpha h_e(2 - \delta)}, \tag{6}$$

$$q_n^{TS^*} = \frac{\begin{array}{l} (\alpha - h_e)\{h_e[-2c_r + c_n(8 - \delta) + \delta(3 - m - T_0) - 2(4 - 3m - s - 4T_0)] - 2a(w_0 - m)\} \\ +d\delta(4 - \delta)(2 + w_0 - 2c_n + c_r - \delta - 2m - s - 2T_0) \\ -\{2c_r(2 - \delta)h_e + 2\delta^2 h_e + 4\alpha m + 4h_e(2w_0 - m - s) - \alpha\delta(w_0 - m) \\ +\delta h_e[2c_n + m + 2(-3 + s + T_0) - w_0] - 4\alpha w_0\}\sigma - 2\delta(w_0 - m)xgm^2 \end{array}}{\delta[d(4 - \delta)^2 - 2(\alpha - 2\sigma)^2] - 2(8 - 3\delta)h_e^2 - 2\delta^2 h_e\sigma + 8\alpha h_e(2 - \delta)}, \tag{7}$$

$$
\begin{aligned}
&8c_r\mathrm{d}\delta - 4\mathrm{d}\delta^2 - 4c_n\mathrm{d}\delta^2 - 2c_r\mathrm{d}\delta^2 + \mathrm{d}\delta^3 + c_n\mathrm{d}\delta^3 + 4c_r h_e^2 + 4c_n\delta h_e^2 - 4\ d\delta^2 m\\
&+\mathrm{d}\delta^3 m + 4h_e^2 m - 4\delta h_e^2 m - 8\mathrm{d}\delta s + 2\mathrm{d}\delta^2 s - 4h_e^2 s - 4\mathrm{d}\delta^2 T_0 + \mathrm{d}\delta^3 T_0 - 4\delta h_e^2 T_0\\
&+8\mathrm{d}\delta w_0 - 2\mathrm{d}\delta^2 w_0 - 2\alpha^2\left[2w_0 - 2m - \delta\left(1 - c_n - m - T_0\right)\right]\\
&-\delta h_e\left[c_n(4+\delta) - \delta\left(1 - m - T_0\right) + 4\left(T_0 + w_0 - 1\right)\right]\sigma\\
&-\delta\sigma^2\left[4c_r - 4s + 4w_0 + \delta\left(w_0 - m - 4\right)\right]\\
&-2\alpha h_e\left[2c_r + 4m + \delta\left(1 - 3c_n - 3m - 3T_0\right) - 2\left(s + w_0\right)\right]\\
q_r^{TS^*} = &\frac{+2\alpha\sigma\delta\left(2 - 2c_n - c_r + \delta + s - 2T_0 - 3w_0\right)}{\delta\left[d(4-\delta)^2 - 2(\alpha - 2\sigma)^2\right] - 2(8-3\delta)h_e^2 - 2\delta^2 h_e\sigma + 8\alpha h_e(2-\delta)],}
\end{aligned}
\tag{8}
$$

where $\delta[d(4-\delta)^2 - 2(\alpha - 2\sigma)^2] \quad -2(8-3\delta)h_e^2 -2\delta^2 h_e\sigma + 8\alpha h_e(2-\delta)] > 0$.

### 4.2. The Impact of Responsibility Transfer

*4.2.1. TA Scenario.* Based on formulas (3)–(5), the partial derivative results can be obtained as follows

:

$$
\begin{aligned}
\frac{\partial e^{TA^*}}{\partial h_e} &= \frac{\tau(2+\delta\tau)\left\{d(2+\delta\tau)^2\left(K - T_0\right) + 2\sigma^2\left[K - T_0 + \tau(2+\delta\tau)\left(w_0 - m\right)\right]\right\}}{\left\{d(2+\delta\tau)^2 - 2\sigma\left[h_e\tau(2+\delta\tau) + \sigma\right]\right\}^2} > 0,\\
\frac{\partial q_n^{TA^*}}{\partial h_e} &= \frac{\tau\left\{d\sigma\ (2+\delta\tau)^2\left(K - T_0\right) + 2\sigma^3\left[K - T_0 + \tau(2+\delta\tau)\left(w_0 - m\right)\right]\right\}}{\left\{d(2+\delta\tau)^2 - 2\sigma\left[h_e\tau(2+\delta\tau) + \sigma\right]\right\}^2} > 0,\\
\frac{\partial q_r^{TA^*}}{\partial h_e} &= \frac{\tau^2\left\{d\sigma\ (2+\delta\tau)^2\left(K - T_0\right) + 2\sigma^3\left[K - T_0 + \tau(2+\delta\tau)\left(w_0 - m\right)\right]\right\}}{\left\{d(2+\delta\tau)^2 - 2\sigma\left[h_e\tau(2+\delta\tau) + \sigma\right]\right\}^2} > 0.
\end{aligned}
\tag{9}
$$

It can be seen that in the *TA* scenario, $e^{TA^*}, q_n^{TA^*}, q_r^{TA^*}$ are increasing with respect to the transfer coefficient $h_e$. So, the larger the transfer coefficient $h_e$ is, the more beneficial it is to the ecodesign and manufacturing/remanufacturing activities at the supply chain level.

*4.2.2. TS Scenario.* The effects of $h_e$ on the optimal solutions $e^{TS^*}, q_n^{TS^*}, q_r^{TS^*}$ in the *TS* scenario can be plotted as shown in Figure 3.

From Figure 3, we can observe the following:

(a) In the production stage, both the manufacturer's ecodesign effort and the production quantity of new products first increase and then decrease with respect to $h_e$ (Figures 3(a) and 3(b))

(b) In the remanufacturing stage, both the quantity of remanufactured products and the remanufacturing rate first decrease and then increase with respect to $h_e$ (Figures 3(c) and 3(d))

(c) There is a threshold of $h_e$ (Figure 3(e)), above which an increase in $h_e$ has a negative impact on the total quantity of new and remanufactured products

In conclusion, the manufacturer should comprehensively consider the impact of $h_e$ on itself, the remanufacturer, and the overall production activities, and carefully set the ecodesign responsibility transfer coefficient, which should stay beneath a certain threshold in the *TS* scenario.

## 5. Comparative Analysis

*5.1. The Overall Impact of the Fund Policy.* By comparing the optimal decision expressions (3)–(8) in Section 4 with the optimal decisions in Table 2 of Section 3, it is evident that when the responsibility transfer strategy is adopted by the manufacturer, the impact scope of $T_0, \sigma, s$ on the decision-making $e^*, q_n^*, q_r^*$ remains unchanged. However, when the partial derivatives of the optimal solution with respect to $T_0, \sigma, s$ are changed, the parameters involved are also changed. Take the partial derivative of $e^{BA^*}$ and $e^{TA^*}$ with respect to $T_0$ as an example.

$$
\frac{\partial e^{BA^*}}{\partial T_0} = \frac{-2\sigma}{d(2+\delta\tau)^2 - 2\sigma^2} > \frac{\partial e^{TA^*}}{\partial T_0} = \frac{-2\sigma}{d(2+\delta\tau)^2 - 2\sigma^2 - 2\sigma h_e\tau(2+\delta\tau)}.
\tag{10}
$$

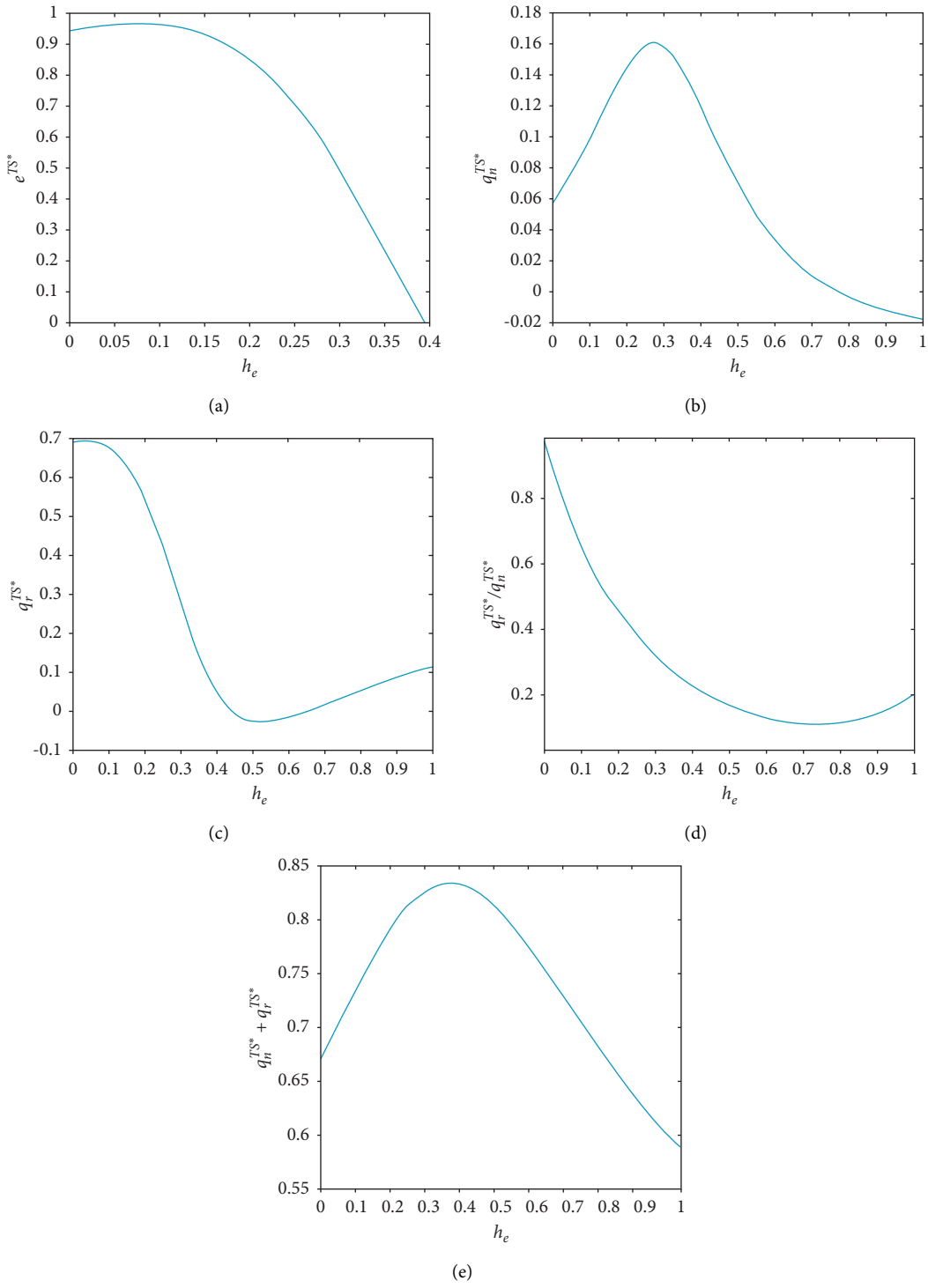


Figure 3: Effect of $h_e$ in the *TS* scenario. (a) Effect of $h_e$ on $e^{TS^*}$. (b) Effect of $h_e$ on $q_n^{TS^*}$. (c) Effect of $h_e$ on $q_r^{TS^*}$. (d) Effect of $h_e$ on $q_r^{TS^*}/q_n^{TS^*}$. (e) Effect of $h_e$ on $q_n^{TS^*} + q_r^{TS^*}$.

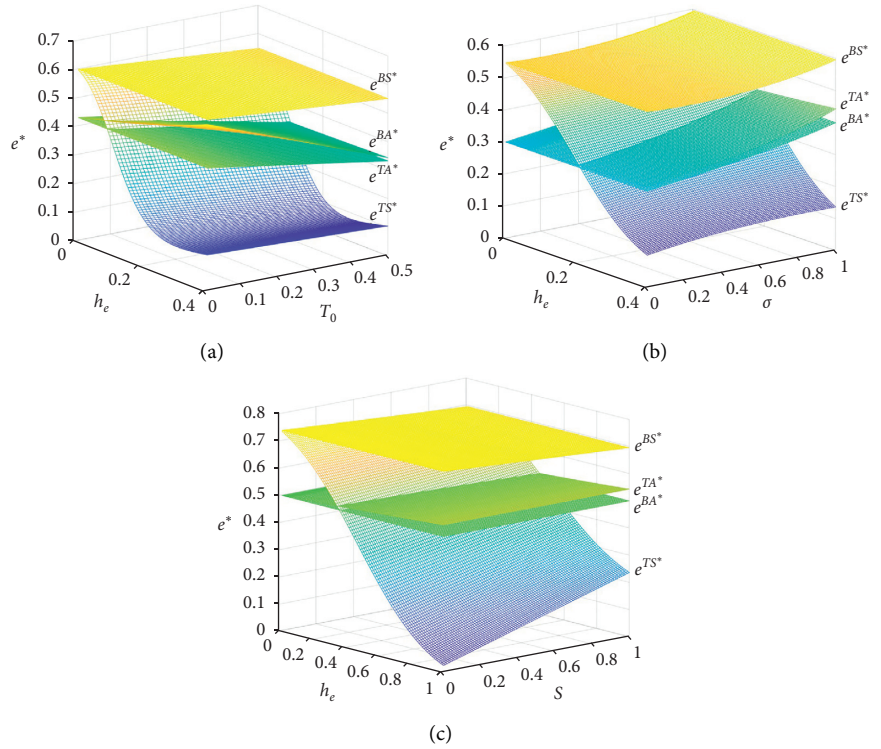


Figure 4: Effects of parameters $T_0$, $\sigma$, $s$, and $h_e$ on $e^*$. (a) Effects of $T_0$ and $h_e$ on $e^*$. (b) Effects of $\sigma$ and $h_e$ on $e^*$. (c) Effects of $s$ and $h_e$ on $e^*$.

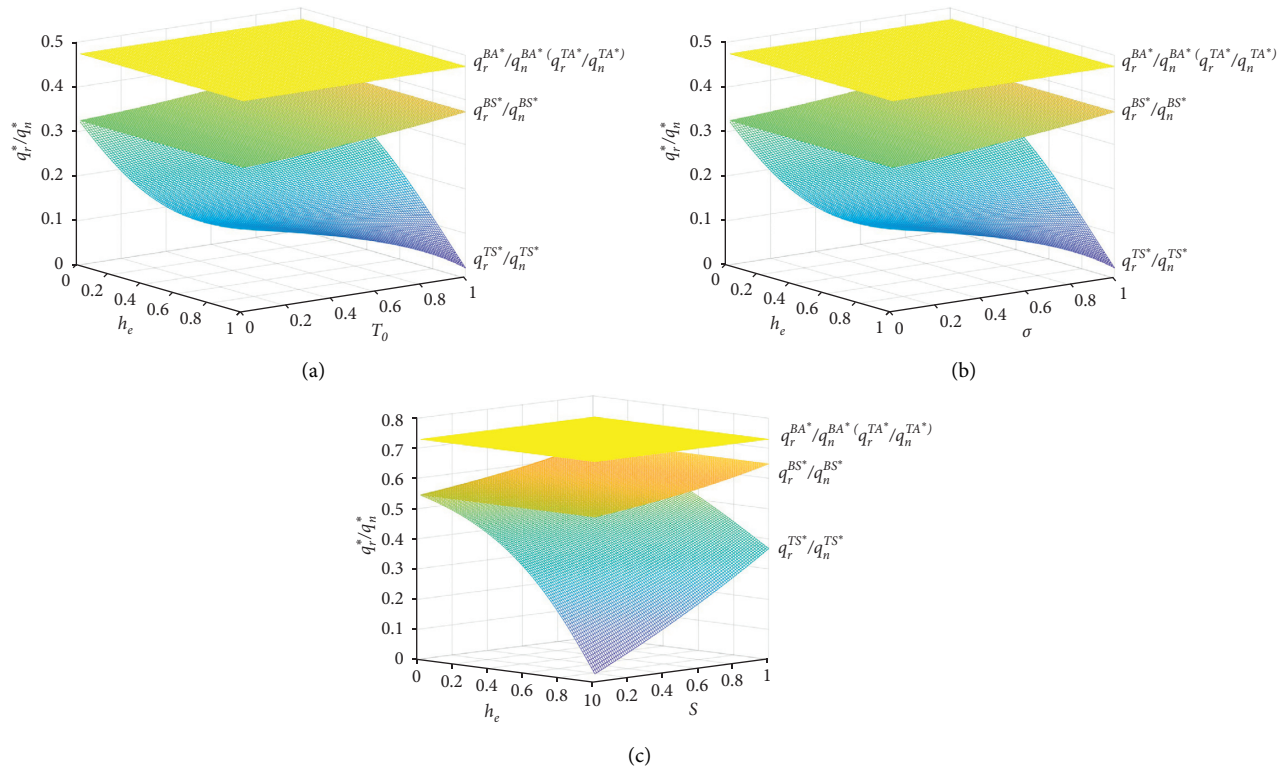


Figure 5: Effects of $T_0$, $\sigma$, and $h_e$ on $q_r^*/q_n^*$. (a) Effects of $T_0$ and $h_e$ on $q_r^*/q_n^*$. (b) Effects of $\sigma$ and $h_e$ on $q_r^*/q_n^*$. (c) Effects of $s$ and $h_e$ on $q_r^*/q_n^*$.

It is evident that the manufacturer's production decision behavior is more sensitive to the *tax* $T_0$ and parameters in the partial derivative also change when the responsibility transfer strategy is adopted by the manufacturer. Therefore, Conclusion 2 can be drawn.

*Conclusion 2.* When the manufacturer adopts an ecodesign responsibility transfer strategy, the impact scope of fund policy does not change. However, both the impact strength and the impact path of fund policy change when the manufacturer adopts the responsibility transfer strategy in a manufacturing-remanufacturing competition system.

*5.2. Ecodesign Behavior.* The impacts of the three dimensions of the fund policy $T_0, \sigma, s$, and transfer coefficient $h_e$, on the ecodesign effort of the manufacturer are plotted in Figure 4.

From Figure 4, we can observe the following:

(a) In the *TS* scenario, the transfer coefficient $h_e$ has a significant influence on the manufacturer's ecodesign behavior, and the manufacturer's ecodesign effort generally declines with the increase of the transfer coefficient $h_e$

(b) $e^{BS^*} > e^{TS^*} > e^{TA^*} > e^{BA^*}$ when the transfer coefficient $h_e$ is beneath a certain threshold; otherwise, $e^{BS^*} > e^{TA^*} > e^{BA^*} > e^{TS^*}$

Therefore, the manufacturer's ecodesign effort is the highest in the *BS* scenario under the constraints of fund policy, while ecodesign effort is relatively low in the *BA* scenario. The ecodesign transfer coefficient $h_e$ of the manufacturer should be beneath a certain threshold in the *TS* scenario to avoid having the responsibility transfer strategy negatively affect ecodesign.

*5.3. Remanufacturing Rate.* The impacts of the three dimensions of the fund policy $T_0, \sigma, s$, and transfer coefficient $h_e$ on the remanufacturing rate are plotted in Figure 5.

From Figure 5, we can observe that the remanufacturing rate has a complex and sensitive response to parameters $T_0, \sigma, s$ and transfer coefficient $h_e$. We can also observe that the remanufacturing rate decreases with the increase of the transfer coefficient $h_e$ in the *TP* scenario.

Therefore, the ecodesign transfer coefficient $h_e$ of the manufacturer should be beneath a certain threshold in the *TS* scenario to avoid having the responsibility transfer strategy negatively affect the remanufacturing rate.

## 6. Conclusion

The paper considers a manufacturing-remanufacturing competition system composed of a single manufacturer and a single remanufacturer under the constraints of fund policy. The government designs the fund policy, which mainly includes three dimensions, namely, *tax*, *reduction*, and *subsidy*. The manufacturer produces a key component and a new product in the market. The key component cannot be remanufactured and can only be sold by the manufacturer at a buyer-specific wholesale price or through a responsibility transfer strategy. The remanufacturer recycles old parts and purchases key components from the manufacturer for remanufacturing activities. The new product and remanufactured product are competitive substitutes in the market.

Based on game models and the obtained perfect equilibria, the main conclusions of this paper are as follows: (1) The impact scope of tax or reduction is larger than that of subsidy. The factors of tax, reduction, and subsidy affect all the decisions in both the *BS* and *BA* scenarios. However, the subsidy for encouraging remanufacturing is ineffective in the *BA* scenario. (2) In the *BA* scenario, the tax and the reduction have opposite effects on supply chain decisions, where the increase of tax will lead to the decline of ecodesign effort and the reduction of manufacturing and remanufacturing quantity. (3) In the *BS* scenario, the impact mechanism on decisions of the tax, reduction, and subsidy dimensions of fund policy changes complexly. In particular, the reduction dimension of fund policy may not only weaken ecodesign and remanufacturing at the supply chain level, but also lead to negative impacts from the tax and subsidy dimensions of fund policy at the policy level. (4) The responsibility transfer behavior of the manufacturer does not change the impact scope of the fund policy, but changes its impact strength and impact path. (5) The impact of the transfer coefficient on enterprises' decision-making varies with different remanufacturing scenarios. The higher the transfer coefficient, the higher the ecodesign effort will be, and the more the manufacturing and remanufacturing quantities will be in the *TA* scenario. However, the effect of the transfer coefficient on enterprises' decision-making is generally negative in the *TS* scenario.

Based on the above conclusions, the following guidelines are proposed to regulators and manufacturers in this paper: (1) The regulator needs flexibility in allocation of the tax, reduction, and subsidy factors of fund policy according to market conditions, considering the impact scope, strength, and path of fund subsidy, and the different remanufacturing strategies and manufacturer's ecodesign responsibility transfer behavior. (2) When the market environment is extremely favorable for remanufacturing and the remanufacturer decides to use all the collected returns for remanufacturing, the subsidy policy for encouraging recycling and remanufacturing is ineffective. The focus of fund policy design by the government should be the tax dimension and the reduction dimension. By reducing the tax or increasing tax reduction, the manufacturer can be encouraged to improve ecodesign efforts and strengthen the prevention of waste management at the production stage. (3) When the manufacturer uses some of the collected returns for remanufacturing, the impact mechanism of fund policy factors changes complexly. Thus, the government should integrate the design of the three dimensions, tax, reduction, and subsidy, of the fund policy to ensure a balanced guidance of fund policy on ecodesign behavior and remanufacturing behavior. In particular, the reduction dimension of fund policy must be set carefully; otherwise, it will not only weaken ecodesign and remanufacturing at the supply chain level, but will also lead to negative impacts from the tax and

subsidy factors of fund policy on ecodesign and remanufacturing at the policy level. (4) In order to achieve better ecodesign and manufacturing/remanufacturing activities at the supply chain level, the manufacturer should adopt different ecodesign responsibility transfer strategies according to the remanufacturer's remanufacturing strategy. When the remanufacturer uses all collected returns for remanufacturing, the manufacturer can adopt the responsibility transfer strategy to achieve higher ecodesign and remanufacturing performance. On the contrary, when the remanufacturer uses some of the collected returns for remanufacturing, the manufacturer should keep the ecodesign transfer coefficient beneath a certain threshold and even forgo adopting a responsibility transfer strategy.

Finally, there are still some limitations in the research process of this paper. This paper only considers a single monopoly manufacturer in the manufacturing-remanufacturing system. It would be worthwhile to extend our study to the setting with competing manufacturers and examine how competition among manufacturers impacts the design of fund subsidies. In addition, there are various forms of responsibility transfer. Future studies can explore the effect of various responsibility transfer strategies in the manufacturing-remanufacturing system, including ecodesign responsibility transfer strategies, recycling, and remanufacturing responsibility transfer strategies.

## Appendix

*Proof.* of Proposition 1. We solve the two-stage game by backward induction. First, $q_n, q_r$ are obtained and substituted back to $\pi_m, \pi_r$, and then $e$ can be obtained. □

### Second Stage

$$\frac{\partial^2 \pi_m}{\partial q_n^2} = -2 < 0,$$
$$\frac{\partial^2 \pi_r}{\partial q_r^2} = -2\delta < 0. \tag{A.1}$$

Therefore, the manufacturer's profit function $\pi_m$ is a concave function of new product quantity $q_n$. The remanufacturer's profit function $\pi_r$ is a concave function of remanufactured product quantity $q_r$.

Construct Lagrangian functions: $L_r = \pi_r - \lambda_1 (q_r - \tau q_n) - \lambda_2 (-q_r)$, $(\partial L_r / \partial q_r) = 0$.

$$\lambda_1 (q_r - \tau q_n) = \lambda_2 q_r = 0, \quad 0 \le q_r \le \tau q_n. \tag{A.2}$$

(a) *BA* scenario: the remanufacturer uses all the collected returns for remanufacturing.

Let $\lambda_1 > 0, \lambda_2 = 0$, get $q_r = \tau q_n$, combine $(\partial L_r / \partial q_r) = 0, \lambda_2 = 0, (\partial \pi_m / \partial q_n) = 0$.

Then, $q_n^{BA} = ((1 - T_0 - c_n - m + \sigma e)/(2 + \delta\tau))$, $q_r^{BA} = ((1 - T_0 - c_n - m + \sigma e)\tau/(2 + \delta\tau))$:

$$\lambda_1 = \frac{2(\alpha e + s - w_0) + \delta[1 + c_n + m + 2m\tau + 2c_n\tau + T_0 + \tau(\delta + \alpha e + s + m + 2T_0 - w_0 - 2) - e\sigma(1 + 2\tau)] - c_r(2 + \delta\tau)}{2 + \delta\tau}. \tag{A.3}$$

(b) *BS* scenario: the remanufacturer uses some of the collected returns for remanufacturing.

Let $\lambda_1 = 0, \lambda_2 = 0$, get $0 < q_r < \tau q_n$, and combine $(\partial L_r / \partial q_r) = 0$, $(\partial \pi_m / \partial q_n) = 0$; then,

$$q_n^{BS} = \frac{2 - 2c_n + c_r - \delta - \alpha e - m - s - 2T_0 + w_0 + 2\sigma e}{4 - \delta},$$
$$q_r^{BS} = \frac{2(\alpha e + s - w_0) - 2c_r + \delta(1 + c_n + m + T_0 - \sigma e)}{(4 - \delta)\delta}. \tag{A.4}$$

(c) *BN* scenario: no remanufacturing.

Let $\lambda_1 = 0, \lambda_2 > 0$, get $q_r = 0$, and combine $(\partial L_r / \partial q_r) = 0, \lambda_1 = 0, (\partial \pi_m / \partial q_n) = 0$; then, $q_n^{BN} = ((1 - cn - m - T_0 + \delta e)/2)$, $q_r^{BN} = 0$, $\lambda_2 = c_r - \alpha e - s + w_0 - (\delta(1 + c_n + m + T_0 - \sigma e)/2)$.

Since there is no remanufacturing behavior in the *BN* scenario, which is not consistent with the main focus of this paper, it will not be discussed below.

### First Stage

(a) *BA* scenario: the remanufacturer uses all the collected returns for remanufacturing.

$$\frac{\partial^2 \pi_m}{\partial^2 e} = -d + \frac{2\sigma^2}{(2 + \delta\tau)^2} = \frac{2\sigma^2 - d(2 + \delta\tau)^2}{(2 + \delta\tau)^2}. \tag{A.5}$$

Let $d(2 + \delta\tau)^2 - 2\sigma^2 < 0$; make $(\partial \pi_m / \partial e) = 0$

$$e^{BA^*} = \frac{\{2 - 2c_n - m[2 + \tau(2 + \delta\tau)] - 2T_0 + w_0\tau(2 + \delta\tau)\}\sigma}{d(2 + \delta\tau)^2 - 2\sigma^2},$$

$$q_n^{BA^*} = \frac{d(2 + \delta\tau)(1 - c_n - m - T_0) + (w_0 - m)\tau\sigma^2}{d(2 + \delta\tau)^2 - 2\sigma^2},$$

$$q_r^{BA^*} = \frac{\left[d(2 + \delta\tau)(1 - c_n - m - T_0) + (w_0 - m)\tau\sigma^2\right]\tau}{d(2 + \delta\tau)^2 - 2\sigma^2}. \tag{A.6}$$

(b) *BS* scenario: the remanufacturer uses some of the collected returns for remanufacturing.

$$\frac{\partial^2\pi_m}{\partial^2 e} = \frac{2(\alpha - 2\sigma)^2 - d(4 - \delta)^2}{(4 - \delta)^2}. \tag{A.7}$$

Let $d(4 - \delta)^2 - 2(\alpha - 2\sigma)^2 > 0$; make $(\partial\pi_m/\partial e) = 0$:

$$e^{BS^*} = \frac{2\delta(2\sigma - \alpha)(2 - c_n - m - \Delta - \delta - s - 2T_0) + \left(8\alpha - 4\alpha\delta + \sigma\delta^2\right)(w_0 - m)}{\delta\left[d(4 - \delta)^2 - 2(\alpha - 2\sigma)^2\right]},$$

$$q_n^{BS^*} = \frac{d\delta(4 - \delta)(2 - c_n - m - \Delta - \delta - s - 2T_0) + [d\delta(4 - \delta) - (\alpha - 2\sigma)(2\alpha - \delta\sigma)](w_0 - m)}{\delta\left[d(4 - \delta)^2 - 2(\alpha - 2\sigma)^2\right]},$$

$$q_r^{BS^*} = \frac{\left\{\begin{array}{c} d\delta(4 - \delta)[\delta(1 + c_n + m + T_0) - 2c_r - 2(m - s + w_0)] \\ +2\alpha\sigma\delta(2 - c_n - m - \Delta - 2m + s - 2T_0 - 3m) \\ +\delta\sigma^2[4c_r - 4(\delta - m + s) + (4 + \delta)w_0] - 2\alpha^2[\delta(1 - c_n - m - T_0) - 2w_0] \end{array}\right\}}{\delta^2\left[d(4 - \delta)^2 - 2(\alpha - 2\sigma)^2\right]}. \tag{A.8}$$

*Proof.* of Proposition 2

(a) *BA* scenario: the remanufacturer uses all the collected returns for remanufacturing.

$$\frac{\partial e^{BA^*}}{\partial T_0} = \frac{-2\sigma}{d(2 + \delta\tau)^2 - 2\sigma^2} < 0,$$

$$\frac{\partial q_n^{BA^*}}{\partial T_0} = \frac{-d(2 + \delta\tau)}{d(2 + \delta\tau)^2 - 2\sigma^2} < 0,$$

$$\frac{\partial q_r^{BA^*}}{\partial T_0} = \frac{-d\tau(2 + \delta\tau)}{d(2 + \delta\tau)^2 - 2\sigma^2} < 0,$$

$$\frac{\partial e^{BA^*}}{\partial \sigma} = \frac{\left[2(K - T_0) + \tau(2 + \delta\tau)(w_0 - m)\right]\left[d(2 + \delta\tau)^2 + 2\sigma^2\right]}{\left[d(2 + \delta\tau)^2 - 2\sigma^2\right]^2} > 0,$$

$$\frac{\partial q_n^{BA^*}}{\partial \sigma} = \frac{2\,d(2 + \delta\tau)\left[2(K - T_0) + \tau(2 + \delta\tau)(w_0 - m)\right]\sigma}{\left[d(2 + \delta\tau)^2 - 2\sigma^2\right]^2} > 0,$$

$$\frac{\partial q_r^{BA^*}}{\partial \sigma} = \frac{2\,d\tau(2 + \delta\tau)\left[2(K - T_0) + \tau(2 + \delta\tau)(w_0 - m)\right]\sigma}{\left[d(2 + \delta\tau)^2 - 2\sigma^2\right]^2} > 0. \tag{A.9}$$

$e^{BA^*}, q_r^{BA^*}, q_n^{BA^*}$ expressions have no $s$, so they are not affected by $s$.

(b) *BS* scenario: the remanufacturer uses some of the collected returns for remanufacturing $(\partial e^{BS^*}/\partial T_0)$

$= (4(\alpha - 2\sigma)/(d(4-\delta)^2 - 2(\alpha - 2\sigma)^2))$,
$(\partial e^{BS^*}/\partial T_0) > 0$ when $\alpha - 2\sigma > 0$, and vice versa.

$(\partial q_r^{BS^*}/\partial T_0) = (2\alpha(\alpha - 2\sigma) + d\delta(4-\delta)/\delta[d(4-\delta)^2 - 2(\alpha - 2\sigma)^2]) > 0$ $(\partial q_r^{BS^*}/\partial T_0) > 0$ when $\alpha - 2\sigma > 0$, otherwise uncertain.

$$\frac{\partial q_n^{BS^*}}{\partial T_0} = \frac{-2\,d(4-\delta)}{d(4-\delta)^2 - 2(\alpha - 2\sigma)^2} < 0, \tag{A.10}$$

$$\begin{aligned}
&2\alpha^2\left\{4\delta\left[2(K-T_0) + c_r - 3m - s + 4w_0\right] - 32(w_0 - m) - \delta^2(4 + w_0 - m)\right\}\\
&-32\alpha\sigma\left\{\delta\left[2(K-T_0) + c_r - \delta - m - s + 2w_0\right] - 4(w_0 - m)\right\}\\
\frac{\partial e^{BS^*}}{\partial \sigma} &= \frac{-\delta\left[4s + 4\delta - 4m - 4c_r - (w_0 - m)\delta - 8(K - T_0)\right]\left[d(4-\delta)^2 + 8\sigma^2\right]}{\delta\left[d(4-\delta)^2 - 2(\alpha - 2\sigma)^2\right]^2},\\
\frac{\partial q_n^{BS^*}}{\partial \sigma} &= \frac{(4-\delta)\left\{\begin{array}{c} 2\alpha^3(w_0 - m) + \alpha\, d\{16(w_0 - m) + \delta[16(K - T_0) + 8(w_0 - m) + 8c_r - 8s - 8\delta - \delta w_0]\}\\ +4\, d\delta\, \sigma[8c_n + 4c_r + 4(2 - m - s - 2T_0) + \delta(4 + w_0 - m)] - 8\alpha^2(w_0 - m)\sigma + 8\alpha(w_0 - m)\sigma^2 \end{array}\right\}}{\delta\left[d(4-\delta)^2 - 2(\alpha - 2\sigma)^2\right]^2},\\
\frac{\partial q_r^{BS^*}}{\partial \sigma} &= \frac{2\left\{\begin{array}{c} 2\alpha^3\{\delta[2(K-T_0) + c_r - \delta - 2m - s + 3w_0] - 8(w_0 - m)\}\\ +d\delta^2\sigma(4-\delta)[8c_n - 4c_r + 4(-2 + m + s + 2T_0) + \delta(4 + m - w_0)]\\ +2\alpha^2\{16(w_0 - m) + \delta[-4c_r + 4\delta + \delta m + 4s - 8(K - T_0)\\ -(4+\delta)w_0]\}\sigma + \alpha\delta\{-d(-4+\delta)[2c_n(4+\delta) - c_r(4+\delta)\\ +\delta(2 + \delta + 4m + s + 2T_0 - 3w_0) + 4(-2 + s + 2T_0 + w_0)]\\ +4\sigma^2[4c_n - 2c_r + \delta(2 + m - w_0) + 2(-2 + s + 2T_0 + w_0)]\} \end{array}\right\}}{\delta^2\left[d(4-\delta)^2 - 2(\alpha - 2\sigma)^2\right]^2},
\end{aligned} \tag{A.11}$$

$(\partial e^{BS^*}/\partial s) = (2(\alpha - 2\sigma)/[d(4-\delta)^2 - 2(\alpha - 2\sigma)^2])$,
$(\partial e^{BS^*}/\partial s) > 0$ when $\alpha - 2\sigma > 0$, otherwise $(\partial e^{BS^*}/\partial s) \le 0$

$$\frac{\partial q_n^{BS^*}}{\partial s} = \frac{-d(4-\delta)}{d(4-\delta)^2 - 2(\alpha - 2\sigma)^2} < 0, \tag{A.12}$$

$(\partial q_r^{BS^*}/\partial s) = (2 + 2\sigma\delta(\alpha - 2\sigma)/\delta^2[d(4-\delta)^2 - 2(\alpha - 2\sigma)^2]) > 0$, $(\partial q_r^{BS^*}/\partial T_0) > 0$ when $\alpha - 2\sigma > 0$, otherwise uncertain.

## Data Availability

The model of this paper is the authors' innovative construction on the basis of referring to the relevant literature. The data used are computer simulation data, and the relevant data have been indicated in the paper. According to the appendix, this paper has two propositions and two stages. Each stage has different calculation methods and formulas.

## Conflicts of Interest

The authors declare that they have no conflicts of interest.

## Acknowledgments

This study was supported by the National Natural Science Foundation of China (72074078, 71473085, and 71871117), the Shanghai Natural Science Foundation (20ZR1413300), and the Fundamental Research Funds for Central Universities of China.

## References

[1] OECD, *Extended Producer Responsibility A Guidance Manual For Governments*, OECD, Paris, France, 2001.

[2] I.-H. Hong and J.-S. Ke, "Determining advanced recycling fees and subsidies in "E-scrap" reverse supply chains," *Journal of Environmental Management*, vol. 92, no. 6, pp. 1495–1502, 2011.

[3] H.-S. Shih, "Policy analysis on recycling fund management for E-waste in Taiwan under uncertainty," *Journal of Cleaner Production*, vol. 143, no. 2, pp. 345–355, 2017.

[4] J. Cao, B. Lu, Y. Chen et al., "Extended producer responsibility system in China improves e-waste recycling: government

policies, enterprise, and public awareness," *Renewable and Sustainable Energy Reviews*, vol. 62, no. 4, pp. 882–894, 2016.

[5] G. Liu, Y. Xu, T. T. Tian, T. Wang, and Y. Liu, "The impacts of China's fund policy on waste electrical and electronic equipment utilization," *Journal of Cleaner Production*, vol. 251, no. 4, pp. 582–587, 2020.

[6] E. Plambeck and Q. Wang, "Effects of e-waste regulation on new product introduction," *Management Science*, vol. 55, no. 3, pp. 333–347, 2009.

[7] A. Atasu, L. N. Van Wassenhove, and M. Sarvary, "Efficient take-back legislation," *Production and Operations Management*, vol. 18, no. 3, pp. 243–258, 2009.

[8] ISO, *14006:2020. Environmental Management Systems-Guidelines for Incorporating Eco-Design*, ISO, Geneva, Switzerland, 2011.

[9] A. Atasu and G. C. Souza, "How does product recovery affect quality choice?" *Production and Operations Management* vol. 22, no. 4, pp. 242–261, 2013.

[10] J. Cheng, B. Li, B. Gong, M. Cheng, and L. Xu, "The optimal power structure of environmental protection responsibilities transfer in remanufacturing supply chain," *Journal of Cleaner Production*, vol. 153, no. 2, pp. 558–569, 2017.

[11] B. W. Jacobs and R. Subramanian, "Sharing responsibility for product recovery across the supply chain," *Production and Operations Management*, vol. 21, no. 1, pp. 85–100, 2012.

[12] A. Örsdemir, E. Kemahlıoğlu-Ziya, and A. K. Parlaktürk, "Competitive quality choice and remanufacturing," *Production and Operations Management*, vol. 23, no. 1, pp. 48–64, 2014.

[13] P. He, Y. He, and H. Xu, "Product variety and recovery strategies for a manufacturer in a personalised and sustainable consumption era," *International Journal of Production Research*, vol. 28, 2021.

[14] P. He, Y. He, and H. Xu, "Channel structure and pricing in a dual-channel closed-loop supply chain with government subsidy," *International Journal of Production Economics*, vol. 213, pp. 108–123, 2019.

[15] P. Kautto and M. Melanen, "How does industry respond to waste policy instruments-Finnish experiences," *Journal of Cleaner Production*, vol. 12, no. 1, pp. 1–11, 2004.

[16] H. Wang, Y. Gu, L. Li, T. Liu, Y. Wu, and T. Zuo, "Operating models and development trends in the extended producer responsibility system for waste electrical and electronic equipment," *Resources, Conservation and Recycling*, vol. 127, no. 9, pp. 159–167, 2017.

[17] Y. J. Li, S. Y. Niu, X. K. Zhao, and W. Wang, "Effect of EPR coefficient policy on the production decision in precious metal accessory recycling," *International Journal of Production Research*, vol. 74, no. 3, pp. 1129–1146, 2017.

[18] M. Pazoki, G. Zaccour, and Georges, "A mechanism to promote product recovery and environmental performance," *European Journal of Operational Research*, vol. 274, no. 2, pp. 601–614, 2019.

[19] G. Cao, Z. Dong, and Z. Zhang, "Research on threshold effect of environmental regulation and green total factor productivity," *EDP Sciences*, vol. 118, p. 3002, 2018.

[20] Q. Guo, E. Wang, Y. Nie, and J. Shen, "Profit or environment? a system dynamic model analysis of waste electrical and electronic equipment management system in China," *Journal of Cleaner Production*, vol. 194, no. 5, pp. 34–42, 2018.

[21] X. Chang, J. Wu, T. Li, and T.-J. Fan, "The joint tax-subsidy mechanism incorporating extended producer responsibility in a manufacturing-recycling system," *Journal of Cleaner Production*, vol. 210, no. 10, pp. 821–836, 2019.

[22] X. Chen, X. Wang, and Y. Xia, "Production coopetition strategies for competing manufacturers that produce partially substitutable products," *Production and Operations Management*, vol. 28, no. 6, pp. 1446–1464, 2019.

[23] Z. Hong and X. Guo, "Green product supply chain contracts considering environmental responsibilities," *Omega*, vol. 83, no. 3, pp. 155–166, 2019.

[24] M. Pazoki and H. Samarghandi, "Take-back regulation: remanufacturing or eco-design?" *International Journal of Production Economics* vol. 227, no. 1, Article ID 107674, 2020.

[25] Z. Wang, Q. Wang, B. Chen, and Y. Wang, "Evolutionary game analysis on behavioral strategies of multiple stakeholders in E-waste recycling industry," *Resources, Conservation and Recycling*, vol. 155, Article ID 104618, 2020.

[26] X. M. Zhang, J. Cao, X. H. Chen, YC. Gao, XP. Zhang, and S. Kumar, "Overview of remanufacturing industry in China: government policies, enterprise, and public awareness," *Journal of Cleaner Production*, vol. 242, no. 1, pp. 10–16, 2020.

[27] X. M. Zhang, Q. W. Li, Z. Liu, and C. T. Chang, "Optimal pricing and remanufacturing mode in a closed-loop supply chain of WEEE under government fund policy," *Journal of Computers & Industrial Engineering*, vol. 151, pp. 1–17, Article ID 106951, 2021.

[28] Z. Liu, K. W. Li, J. Tang, B. Gong, and J. Huang, "Optimal operations of a closed-loop supply chain under a dual regulation," *International Journal of Production Economics*, vol. 233, Article ID 107991, 2021.

[29] P. Calcott and M. Walls, "Waste, recycling, and "Design for Environment": roles for markets and policy instruments," *Resource and Energy Economics*, vol. 27, no. 4, pp. 287–305, 2005.

[30] W. Zhu and Y. He, "Green product design in supply chains under competition," *European Journal of Operational Research*, vol. 258, no. 1, pp. 165–180, 2017.

[31] F. Zand, S. Yaghoubi, and S. J. Sadjadi, "Impacts of government direct limitation on pricing, greening activities and recycling management in an online to offline closed loop supply chain," *Journal of Cleaner Production*, vol. 215, no. 1, pp. 1327–1340, 2019.

[32] X. Zheng, K. Govindan, and Q. Deng, "Effects of design for the environment on firms' production and remanufacturing strategies," *International Journal of Production Economics*, vol. 213, pp. 217–228, 2019.

[33] R. Subramanian, M. E. Ferguson, and L. B. Toktay, "Remanufacturing and the component commonality decision," *Production and Operations Management*, vol. 22, no. 1, pp. 36–53, 2013.

[34] K. Mathiyazhagan, A. Diabat, A. Al-Refaie, and L. Xu, "Application of analytical hierarchy process to evaluate pressures to implement green supply chain management," *Journal of Cleaner Production*, vol. 117, pp. 229–236, 2015.

[35] C. K. Chen and M. A. Ulya, "Analyses of the reward-penalty mechanism in green closed-loop supply chains with product remanufacturing," *International Journal of Production Economics*, vol. 210, pp. 211–223, 2019.

[36] X. L. Wu and Y. Zhou, "Buyer-specific versus uniform pricing in a closed-loop supply chain with third-party remanufacturing," *European Journal of Operational Research*, vol. 273, no. 2, pp. 548–560, 2018.

[37] M. Reimann, Y. Xiong, and Y. Zhou, "Managing a closed-loop supply chain with process innovation for remanufacturing," *European Journal of Operational Research*, vol. 276, no. 2, pp. 510–518, 2019.

Hindawi
Mathematical Problems in Engineering
Volume 2021, Article ID 5977460, 10 pages
https://doi.org/10.1155/2021/5977460

*Research Article*

# Natural Gas Hydrate Prediction and Prevention Methods of City Gate Stations

**Lili Zuo**,[1] **Sirui Zhao**,[1] **Yaxin Ma**,[1] **Fangmei Jiang**,[2] **and Yue Zu**[2]

[1]*National Engineering Laboratory for Pipeline Safety, MOE Key Laboratory of Petroleum Engineering, Beijing Key Laboratory of Urban Oil and Gas Distribution Technology, China University of Petroleum-Beijing, Beijing 102249, China*
[2]*Pipe China Beijing Pipeline Co., Ltd., Beijing, China*

Correspondence should be addressed to Lili Zuo; zuolili@cup.edu.cn

Received 11 May 2021; Accepted 8 July 2021; Published 14 July 2021

Academic Editor: Jinyu Chen



During the process of distributing natural gas to urban users through city gate stations, hydrate is easy to form due to the existence of throttling effect which causes safety risks. To handle this problem, a program to quickly calculate hydrate prediction and prevention methods for city gate stations is developed. The hydrate formation temperature is calculated through the Chen–Guo model, and the Peng–Robinson equation of state combined with the balance criterion is used to analyze the water condensation in the throttling process. The Wilson activity coefficient model is used to calculate the mass fraction in the liquid phase of thermodynamic inhibitors for preventing hydrates. Considering the volatility of inhibitors, the principle of isothermal flash has been utilized to calculate the total injection volume of the inhibitor. Moreover, the effects of commonly used methanol and ethylene glycol inhibitors are discussed. In terms of safety and sustainability, the ethanol inhibitor, which is considered for the first time, exhibited better prevention and control effects under conditions with relatively high temperature and low pressure after throttling. Combined with the actual working conditions of a gate station, methanol has the best inhibitory effect, followed by ethylene glycol. From an economic point of view, the benefits of the gas phase of the inhibitor during the delivery of natural gas are obvious; therefore, the method of methanol injection is recommended for hydrate prevention. If the gas phase benefits of the inhibitor are not considered, the ethylene glycol injection method becomes more economical.

## 1. Introduction

Due to the uneven distribution of resources, natural gas is mainly transported through long-distance pipelines and distributed to urban users through city gate stations. Considering the existence of throttling effect, the pressure regulation on the city gate station will produce a certain temperature drop. If the water dew point of gas is high, the water is likely to condensate during the pressure regulation, leading to the formation of hydrates and triggering a series of safety accidents to both stations and urban users [1, 2], such as hydrate blockage in the pressure regulating valve, resulting in a drop in the gas supply pressure to urban users. Therefore, in order to ensure safe gas supply to urban users, it is necessary to study the prediction and prevention methods of hydrate formation and to obtain a safe, environment-friendly, and economical thermodynamic inhibitor for city gate stations.

The formation of hydrates usually needs to meet three conditions: ① the water condition that indicates enough liquid water in the system; ② reaching the temperature and pressure conditions for hydrate formation; and, ③ the gas flow is unstable, and there are hydrate seeds. The first condition is mainly based on the phase equilibrium theory [3]. The Soave–Redlich–Kwong (SRK) or Peng–Robinson (PR) equation of state (EOS) can be used to calculate and analyze the water content and water condensation in the natural gas transportation process [4, 5]. Temperature and pressure conditions are mainly studied by the thermodynamic model. Under certain temperature

and pressure conditions, when the pore occupancy rate reaches a certain level, hydrate crystals can exist stably. According to the different structures, hydrate crystals can be divided into three forms: type I, type II, and type *H*, of which type I hydrate and type II hydrate unit cells are composed of two different sizes of cage cavities, and the *H* type hydrate unit cell is composed of three different sizes of cage cavities [6]. At present, the thermodynamic models of hydrate formation can be divided into two main categories: the first is the van der Waals–Platteeuw [7] model based on the isotherm adsorption theory; the second is the Chen–Guo model [8] based on the mechanism of hydrate formation. In addition to the strict thermodynamic model and in order to facilitate the calculation efficiency, many researchers have proposed the correlation equations of hydrate formation temperature, pressure, and relative density [9–11], but the calculation accuracy is limited.

The prevention and control of hydrates can be started by destroying the formation conditions of hydrates. The main methods include heating, depressurization, injecting inhibitors, and dehydration. Injecting thermodynamic inhibitors to pipelines is currently the main method of gas hydrate inhibition in the oil and gas industry [12]. The hydrate formation model under the inhibitor system can be established by modifying the parameters of the Chen–Guo model [4]. At present, the more commonly used thermodynamic inhibitors are methanol and ethylene glycol. Methanol is cheap but has certain toxicity, and ethylene glycol is relatively less toxic but more expensive. For the natural gas system with methanol injected, some scholars [13] established a phase equilibrium model based on the PR EOS and stochastic-nonstochastic theory, combined with its improved Holder–John hydrate model to predict the formation conditions of the hydrate containing the methanol inhibitor system. In addition, some scholars [14] used the Patel–Teja (PT) EOS combined with the Kurihara mixing rule to calculate the fugacity of each component in the gas phase and the water activity for prediction. Some scholars chose the Stryjek and Vera modification of Peng–Robinson (PRSV2) EOS combined with the non-density-dependent (NDD) mixing rules to calculate the fugacity of water in the gas phase and the liquid phase, so as to predict the formation conditions of the hydrate containing the alcohol inhibitor system [15].

At present, the software that can be used for hydrate formation prediction and inhibitor injection volume calculation mainly includes process simulation software such as HYSYS and PVTsim software [16–18]. Although the calculation methods and theories of these commercial software are quite mature, there are still many limitations in actual use. In these commercial software, the calculation of hydrate formation prediction and inhibitor injection volume only exists as a module, and additional environmental configuration is required for calculation, which increases the complexity of software operations. Therefore, it is necessary to design a software to achieve the purpose of quick calculation for on-site personnel.

This article mainly focuses on the actual pressure regulation on site, carries on the prediction of hydrate formation and the discussion of prevention and control measures to form a program to quickly calculate hydrate formation conditions and prevention measures for city gate stations, provides reference for on-site operation and management, and realizes the goal of safe gas transmission. Based on safety and economic considerations, this article also proposes and calculates the possibility of using ethanol for inhibition.

## 2. Hydrate Formation Prediction

It can be seen from Section 1 that the formation of hydrates needs to meet the conditions of water, pressure and temperature, and disturbance at the same time. This article mainly studies the prediction of hydrate formation in the pressure regulation of the city gate station, which obviously meets the third condition. Hence, this section mainly analyzes the first two conditions.

*2.1. Water Condition.* The analysis of water content and water dew point of natural gas plays an important role in the safe operation of pipelines. After knowing the corresponding water dew point of natural gas under certain pressure, when the temperature is reduced to the water dew point during pressure regulation, it is the critical state of liquid water condensation. When the temperature is lower than the water dew point, the water vapor in the natural gas will condense into liquid water. At this time, the amount of water can be indicated by the change in the water content before and after the water condensation. Establishing the relationship between water dew point and water content can facilitate the analysis of water condensation by field personnel.

Calculating the water content of natural gas based on the known dry gas mole fraction, water dew point, and pressure of natural gas can be done through the calculation of gas-liquid two-phase equilibrium. When the water reaches equilibrium in the gas phase and the liquid phase, it is the critical state of condensate water. At this time, the fugacity of water in the gas phase is equal to its fugacity in the liquid phase, namely,

$$f_{vw} = f_{lw}, \tag{1}$$

where $f_{vw}$ refers to the fugacity of water in the gas phase (natural gas) and $f_{lw}$ refers to the fugacity of water in the liquid phase.

Fugacity is a function of pressure and temperature and needs to be calculated using the gas EOS [19]. The cubic EOS has a wide range of applications in engineering due to its simplicity and accuracy of calculation, such as the PR EOS and the SRK EOS. In this paper, the PR EOS is used in combination with the classic mixing rules for calculation.

The expression of the fugacity coefficient of water vapor in natural gas, which is derived from the PR EOS combined with the mixing rule, can be expressed as follows [20]:

$$\ln \varphi_{vw} = \frac{B_i}{B}(Z-1) - \ln(Z-B) - \frac{A}{2\sqrt{2}B}\left(\frac{B_i}{B} - \frac{2}{a}\sum_{i=1}^{n} x_i a_{wi}\right) \cdot \ln\left[\frac{Z+(1+\sqrt{2})B}{Z+(1-\sqrt{2})B}\right]. \quad (2)$$

The fugacity coefficient of liquid water is expressed as [20]

$$\ln \varphi_{lw} = Z - 1 - \ln(Z-B) - \frac{A}{2\sqrt{2}B}\ln\left[\frac{Z+(1+\sqrt{2})B}{Z+(1-\sqrt{2})B}\right], \quad (3)$$

where $A$, $B$, $a$, and $a_{wi}$ are parameters in the PR EOS.

The steps to calculate the water content from the water dew point are shown in Figure 1. The steps for calculating the water dew point from the water content are similar to those shown in Figure 1, where the input condition is changed from water dew point to water content, and the iteration variable is changed from water content to water dew point.

*2.2. Pressure and Temperature Conditions.* The Chen–Guo model proposed by Guo Tianmin and Chen Guangjin is a thermodynamic model of hydrate formation based on statistical mechanics. Mainly, there are two kinetic processes simultaneously in the nucleation process of hydrate [21]: ① the gas molecule complexes with water to form a stoichiometric basic hydrate that can be represented by a chemical formula and ② the existence of the void cavity in the basic hydrate formed by gas and water that adsorbs some smaller gas molecules into it, resulting in the nonstoichiometry of the entire hydrate.

Therefore, assuming that the mixed basic hydrate is an ideal solution, Guo et al. established a basic equilibrium relationship in the natural gas hydrate system [21], namely,

$$f_i = x_i f_i^0 \left(1 - \sum_j \theta_j\right)^{\alpha}, \quad (4)$$

where $f_i$ is the fugacity of component $i$ in the gas phase, which can be solved by the PR EOS, $x_i$ is the mole fraction of the basic hydrate formed by component $i$ in the mixed basic hydrate, and $\alpha$ is related to the hydrate structure type; when the hydrate structure is type I, it is 1/3; when the hydrate structure is type II, it is 2.

$\theta_j$ is the occupancy rate of the small gas molecule $j$ in the cavity of the basic hydrate, which can be calculated according to the following formula [21]:

$$\theta_i = \frac{C_i f_i}{1 + \sum_j C_j f_j}, \quad (5)$$

where $C_i$ is the Langmuir constant of the small gas component $i$, which can be expressed in the form of the following formula [21]:

$$C_i = X_i \exp\left(\frac{Y_i}{T - Z_i}\right). \quad (6)$$

$f_i^0$ is the fugacity of the basic hydrate formed by component $i$, which can be calculated according to the following formula [21]:

$$f_i^0 = \exp\left(\frac{-\sum_j A_{ij}\theta_j}{T}\right)\left[a_i \exp\left(\frac{b_i}{T - c_i}\right)\right]\exp\left(\frac{\beta P}{T}\right)a_w^{1/\lambda_2}, \quad (7)$$

where $A_{ij}$ is the binary interaction coefficient of the type II hydrate system, the binary interaction coefficient of type I hydrate is very small and can be ignored, $a_i$, $b_i$, and $c_i$ are parameters in the model, and the values of $\beta$ and $\lambda_2$ are related to the type of the hydrate structure. When the hydrate structure is type I, $\beta$ is 4.242 K/MPa and $\lambda_2$ is 3/23. When the hydrate structure is type II, $\beta$ is 10.224 K/MPa and $\lambda_2$ is 1/17; $a_w$ is the activity of water. When the water does not contain inhibitors or electrolytes, it can be regarded as pure water, and its value is approximately 1. When the water contains inhibitors or electrolytes, it needs to be calculated by the activity coefficient model.

After calculating the above parameters and substituting them into formula (7), the hydrate formation conditions can be predicted under the condition that the sum of the mole fractions of the components is 1 [21].

Based on the above analysis, under a given pressure, the iterative method can be used to predict the formation temperature of hydrate. If the error is within the allowable range, the iteration can be ended; otherwise, the secant method can be used to adjust the temperature value for the next iteration. When the temperature is known, the process of predicting the pressure of natural gas hydrate formation is similar to this process, except that the known condition becomes temperature and the iteration variable becomes pressure.

*2.3. Judgment of Hydrate Formation for a Certain City Gate Station.* In a certain city gate station, which has always made a reduction in gas supply by hydrate formation in the past, the gas flow is $30 \times 10^4\ \mathrm{Nm^3/h}$ at the peak of gas consumption; the average inlet pressure is 3.83 MPa, the average inlet temperature is −8°C, the average outlet pressure is 2.05 MPa, and the outlet temperature is −19°C; the average water content measured when the gas enters the gate station is 79.15 mg/Nm$^3$. Based on the previous analysis, the average operating condition of the gate station, the water dew point curve (water content of 79.15 mg/Nm$^3$), and the hydrate formation curve are plotted in Figure 2.

It can be seen from Figure 2 that the average operating condition after pressure regulation at the gate station is in the hydrate formation zone; the operation point is located on the left side of the water dew point curve, indicating that there is liquid water condensation in the throttling process. At the temperature and pressure point of the curve, if the actual water content of the gas is higher than 79.15 mg/Nm$^3$, there is also a risk of water condensation. The gas has the temperature, pressure, and water conditions for hydrate formation, and it is in a strong turbulent state during the throttling process. Therefore, the gate station has the risk of

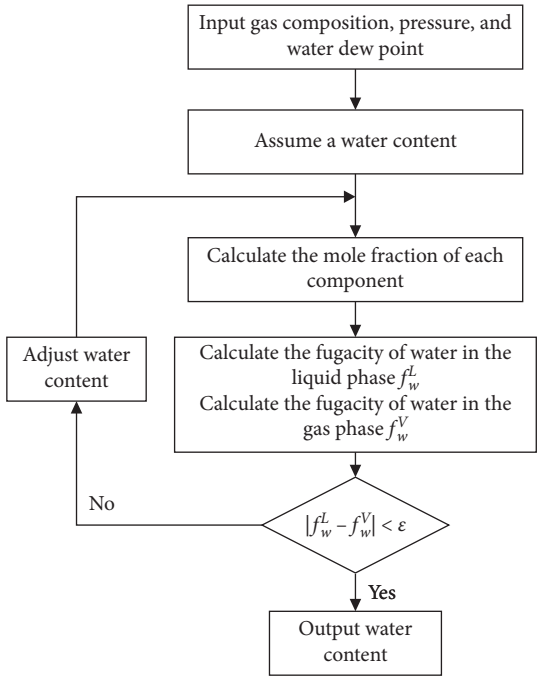


Figure 1: Steps to calculate water content based on the water dew point.

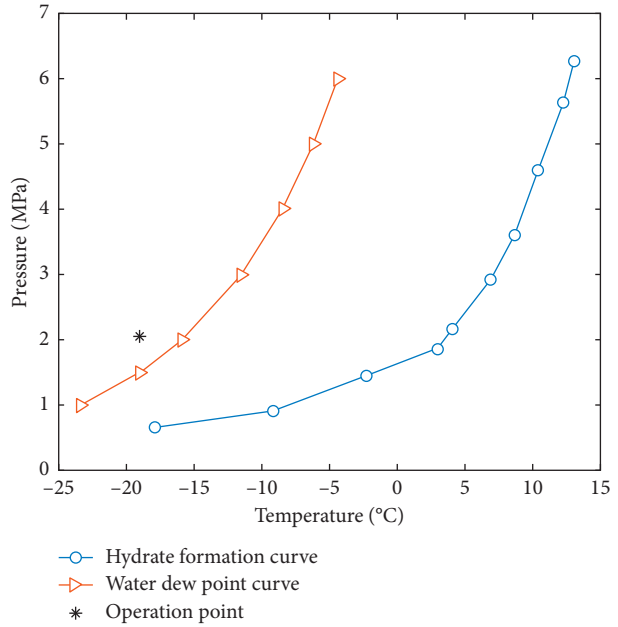


Figure 2: Analysis of hydrate formation in the throttling process of the gate station.

hydrate formation, and hydrate prevention measures are required.

## 3. Hydrate Prevention and Control Measures

The method of injecting thermodynamic inhibitors such as methanol/ethylene glycol is often used in the field to prevent and control hydrates. Based on safety considerations, the possibility of ethanol is discussed in this section. The injection volume of the thermodynamic inhibitor should include three parts, some dissolved in the liquid phase, some volatilized in the gas phase, and the other dissolved in the liquid hydrocarbon phase. The inhibitory part is the part dissolved in the liquid phase. Considering the low content of heavy hydrocarbon components in the gas entering the gate station, only a small amount of liquid hydrocarbon precipitates in the throttling process, and the loss of inhibitors in the liquid hydrocarbon phase is ignored.

*3.1. Calculation of the Mass Fraction of Inhibitor in Liquid Phase.* By reducing the activity of water in the aqueous solution, the stable temperature of hydrate phase equilibrium can be reduced, which is the main principle of the inhibitory effect of thermodynamic inhibitors [22]. In Section 2, the activity of water in the Chen–Guo model was discussed, as shown in formula (7). Therefore, the Chen–Guo model can still be used to analyze the prediction of hydrate formation with inhibitors, so as to calculate the liquid required amount of the three inhibitors.

The mole fraction of each component in the ideal solution is the concentration of the component. Considering the deviation between the actual solution and the ideal solution, the concept of activity is introduced. It characterizes the effective concentration of the component in the mixture, which can be expressed by molar fraction and activity coefficient as follows:

$$a_i = x_i \gamma_i, \tag{8}$$

where $a_i$ is the activity for component $i$, $x_i$ is the mole fraction of component $i$ in the solution, and $\gamma_i$ is the activity coefficient for component $i$.

The activity coefficient can be calculated using the Wilson activity coefficient model [23]. The formula is as follows:

$$\ln \gamma_k = 1 - \ln\left(\sum_{i=1}^{m} x_i \Lambda_{ik}\right) - \sum_{i=1}^{m} \frac{x_i \Lambda_{ik}}{\sum_{j=1}^{m} x_j \Lambda_{ij}}, \tag{9}$$

where $\Lambda_{ij}$ is the Wilson parameter value, which can be calculated by the following formula:

$$\Lambda_{ij} = \frac{v_j}{v_i} \exp\left(-\frac{\lambda_{ij} - \lambda_{ii}}{\mathrm{RT}}\right), \tag{10}$$

where $v_i$ and $v_j$ is the molar volume of the component $i$ and $j$, $m^3$/mol, and $\lambda_{ij} - \lambda_{ii}$ is the energy parameter of the binary interaction between the components.

The activity of water in the liquid phase can be obtained using formulas (8)–(10), which is substituted into formula (7) of the Chen–Guo model to iteratively solve the mass fraction of the inhibitor liquid phase. The result obtained should satisfy the requirement that the temperature at the most dangerous operating point (when the pressure and temperature are the smallest after pressure regulation) is greater than or equal to the hydrate formation temperature corresponding to the pressure at that point. Due to the high viscosity of ethylene glycol, 80% concentration is considered in calculation.

*3.2. Calculation of Total Injection Volume.* Since methanol and ethanol have strong volatility, their loss in the gas phase needs to be considered. The process of total injection volume calculation is essentially considered as a gas-liquid isothermal flash calculation.

The steps for calculating the total injection volume are shown in Figure 3.

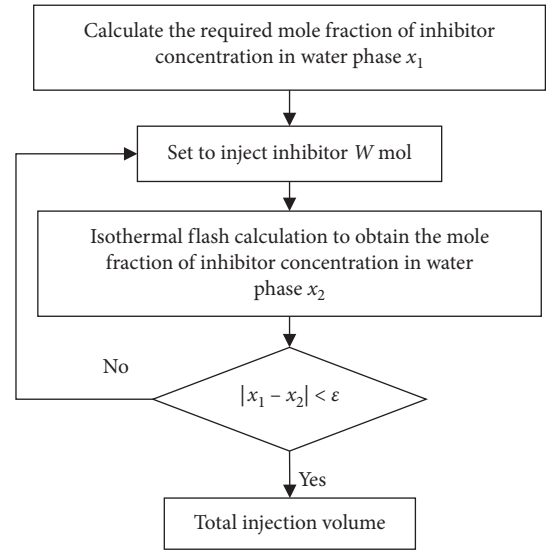


Figure 3: Block diagram of calculation steps for total injection volume.

The initial step is to calculate the required inhibitor concentration in the liquid phase by combining the Wilson activity coefficient model with the Chen–Guo model. Then, set the initial value of the molar amount of the inhibitor injected to 1 mol natural gas, and perform gas-liquid two-phase isothermal flash calculation at the temperature and pressure after throttling to obtain the initial value of the mole fraction of each substance in the water and inhibitor-containing gas system. Next, judge whether the difference between the concentration of the inhibitor in the liquid phase and the required concentration meets the accuracy requirements; if it meets the requirements, stop the calculation; otherwise, change the mole amount of the inhibitor injected until the accuracy meets the requirements. Because within a certain concentration range, when the mole amount of the inhibitor injected to 1 mol natural gas increases, the concentration of the inhibitor in the liquid phase also increases; the two are positively correlated, so the dichotomy method is used for iterative calculation.

Finally, the mole amount of the inhibitor needed to be injected in 1 mol natural gas can be obtained as the output and converted into the volume of the inhibitor needed to be injected in each $10^4$ $Nm^3$ natural gas by unit conversion.

## 4. Results and Discussion

*4.1. Program Interface.* Based on the above analysis, the hydrate prediction and prevention simulator program can be developed. There are two calculation interfaces in the program; the first interface is shown in Figure 4, and the second one is shown in Figure 5.

In Figure 4, the calculation interface of throttling process parameters can realize the mutual conversion of water dew point and water content, calculate throttling temperature drop, and judge whether there is water condensation in the throttling process. The actual water content of natural gas

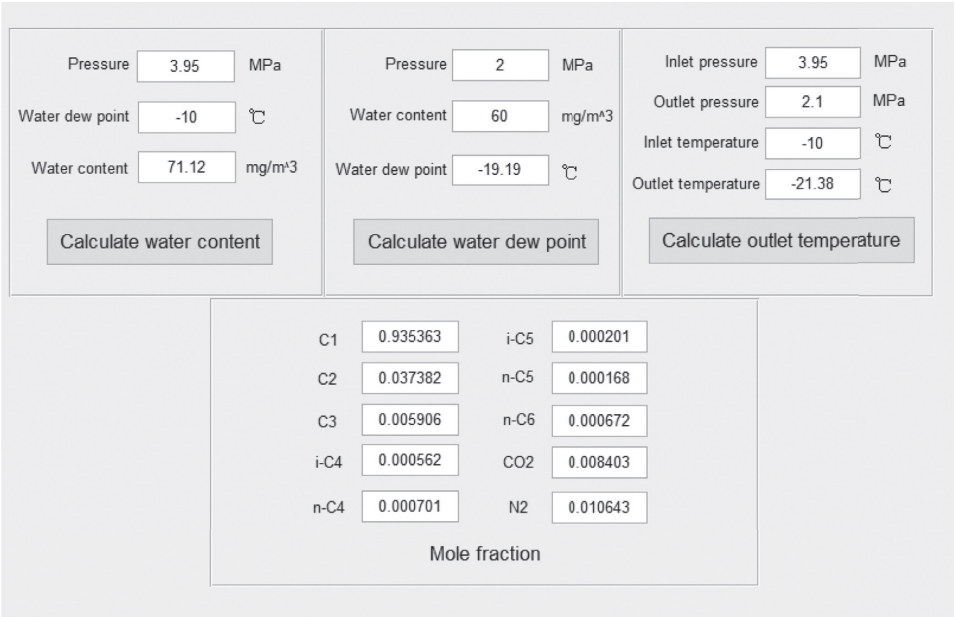


Figure 4: Calculation interface of throttling process parameters.

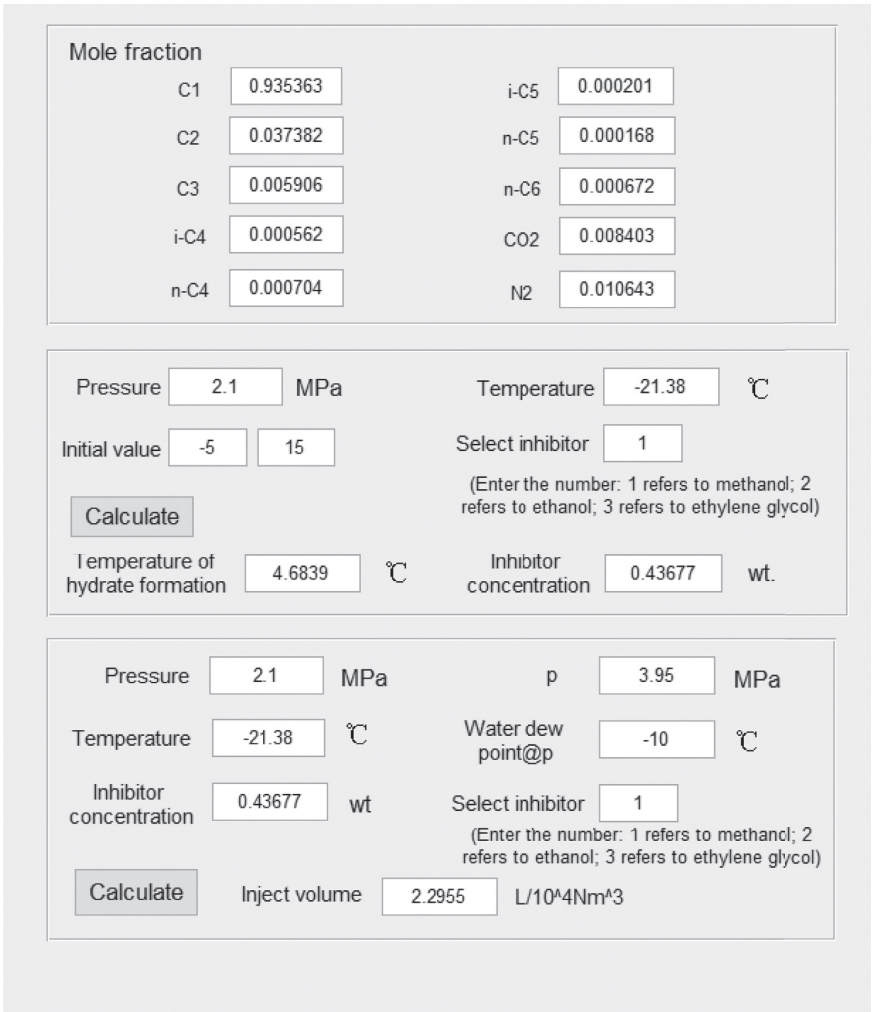


Figure 5: Calculation interface of hydrate prediction and prevention.

can be calculated according to the pressure and water dew point before throttling. The maximum water content of the gas can be calculated according to the pressure and temperature after throttling. If the actual water content is greater than the maximum water content, there will be water condensation. At the same time, it can also be calculated to determine the water dew point index of noncondensable water before throttling, which is to calculate the maximum water content according to the temperature and pressure after the throttling, and converge the result obtained to the water dew point under the pressure before throttling, which should be higher than the known water dew point value before throttling to prevent water condensation.

In Figure 5, the hydrate formation temperature can be calculated according to the Chen–Guo model, and the required inhibitor concentration in the liquid phase can be calculated according to the Wilson activity coefficient and the Chen–Guo model, and then, the volume of inhibitor injected to prevent hydrate formation can be calculated by isothermal flash. For the operating condition with water condensation, it needs to input the water dew point, the corresponding pressure and dry gas components, the mole fraction of the inhibitor required for the liquid-phase, and finally temperature and pressure after throttling. Thus, the inhibitor's total injection volume can be calculated.

*4.2. Result Verification.* Taking the typical pressure regulation condition (3.95~2.10 MPa) as an example, the injection volume of the inhibitor required under different temperature before throttling and water dew point was calculated by using the simulator program and compared with the HYSYS calculation results, as shown in Table 1. Select Ng–Robinson as the hydrate thermodynamic model in HYSYS.

Table 1 shows that when the pressure before and after throttling is known and the temperature before throttling is given, the inhibitor injection volume calculated by the program is close to the calculation results of HYSYS, and the absolute value of the error is between 0~0.09 $L/10^4Nm^3$. The calculation accuracy meets engineering requirements.

Also, among the three inhibitors, the injection volume of the ethylene glycol inhibitor is the lowest and the injection volume of ethanol is the highest among the three inhibitors. The main reason is that, under the same conditions, the mass fraction of ethanol required in the liquid phase is much greater than that of methanol and ethylene glycol. It means that, under these conditions, the inhibitory effect of ethanol on hydrates is poor.

*4.3. Discussion on the Effect and Economy of Inhibitors.* Considering that the inhibitor in the liquid phase is the main part of the inhibitor's inhibitory effect, in order to analyze and compare the inhibitory effects of the three inhibitors more vividly, the program is used to calculate the liquid mass fractions of the three inhibitors in the liquid phase under different temperature (−8°C~3°C) and different pressures (2.1 MPa and 4 MPa) after throttling, as shown in Figure 6, where the gas composition used in different working conditions remains the same.

Figure 6 shows that, under the same condition, the mass fraction of thermodynamic inhibitors required in the liquid phase increases with the decrease of the temperature after throttling. When the pressure is 2.1 MPa, it can be seen from the figure that there is an intersection between 2°C and 3°C, where the temperature value is about 2.4°C. When the temperature after throttling is lower than the intersection temperature, the mass fraction of the required methanol-water solution is the least, and when the temperature after throttling is higher than this temperature, the mass fraction of the required ethanol-water solution is the least. When the pressure is 4 MPa, the mass fraction of the methanol aqueous solution is the least at any temperature. Thus, only methanol has the best inhibitory effect among the three inhibitors, followed by ethylene glycol. Moreover, it can be seen from the figure that, as the pressure decreases, the amount of inhibitor decreases, and the amount of ethanol decreases the most. Ethanol inhibitors have better inhibitory effect mainly under the conditions of high temperature and low pressure after throttling.

From the perspective of inhibitory effect, the mass fraction of methanol required is the least under the same condition. However, due to the strong volatility of methanol, its loss in the gas phase is large so that the total injection amount of methanol in Table 1 is greater than that of ethylene glycol.

In addition to considering the inhibitory effect, the final inhibitor selection must also be economical. For the gate station studied in this article, considering that the operating conditions after throttling are mostly concentrated in the pressure range of 2.00 MPa~2.10 MPa and the temperature range of −16°C~−22°C, the inhibitory effect of ethanol is poor under this condition, and ethanol is the most expensive; hence, only the economics of methanol and ethylene glycol will be discussed below. The price of methanol is 3,000 yuan/ton, and the price of ethylene glycol is 4,800 yuan/ton. The calculation of the total investment cost within 3 years is considered (the winter supply period is 4 months, 30 days per month, and the calculated flow rate is $30 \times 10^4\ m^3/h$), without considering the use of a glycol inhibitor recovery device to reuse it. The price of natural gas fuel is 2.5 yuan/$m^3$. The temperature, pressure, and water dew point parameters of the three working conditions are shown in Table 2.

Since methanol will volatilize into the gas phase and mix with natural gas, when natural gas handover settlement occurs, this part of the gas may be considered as natural gas to be sold to the docking downstream users, which will generate certain benefits to the station. Therefore, when calculating the total cost of methanol, there are two situations. Situation 1 is to consider benefits of the gas phase of the inhibitor, and situation 2 is not to consider.

Finally, the total investment costs of the two inhibitors in the three-year operation period are shown in Table 3.

It can be seen from Table 3 that when not considering benefits of the gas phase of the inhibitor, it is more economical to choose the method of ethylene glycol injection

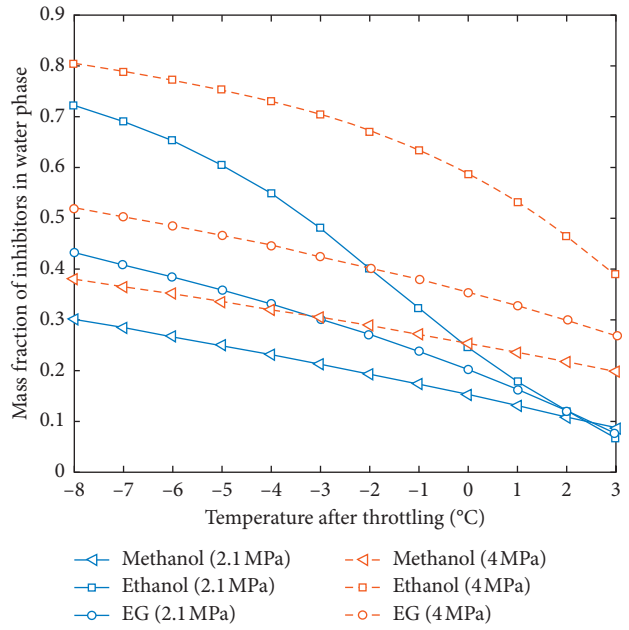


Figure 6: Comparison of inhibitory effect of different inhibitors.

Table 1: Comparison of inhibitor injection volume calculation.

| Temperature before throttling (°C) | Water dew point (°C) | Injection volume of methanol $L$ ($10^4$ Nm$^3$) | | | Injection volume of ethanol $L$ ($10^4$ Nm$^3$) | | | Injection volume of ethylene glycol $L$ ($10^4$ Nm$^3$) | | |
|---|---|---|---|---|---|---|---|---|---|---|
| | | HYSYS | Program | Abs. e | HYSYS | Program | Abs. e | HYSYS | Program | Abs. e |
| −5 | −5 | 3.02 | 3.01 | 0.01 | 3.24 | 3.26 | 0.02 | 0.89 | 0.87 | 0.02 |
| | −6 | 2.95 | 2.94 | 0.01 | 3.19 | 3.19 | 0 | 0.77 | 0.76 | 0.01 |
| | −7 | 2.88 | 2.88 | 0 | 3.12 | 3.13 | 0.01 | 0.68 | 0.66 | 0.02 |
| | −8 | 2.82 | 2.82 | 0 | 3.06 | 3.07 | 0.01 | 0.58 | 0.56 | 0.02 |
| | −9 | 2.76 | 2.77 | 0.01 | 3.00 | 3.02 | 0.02 | 0.47 | 0.47 | 0 |
| −10 | −10 | 2.76 | 2.67 | 0.09 | 2.86 | 2.92 | 0.06 | 0.95 | 0.91 | 0.04 |
| | −11 | 2.69 | 2.61 | 0.08 | 2.81 | 2.86 | 0.05 | 0.84 | 0.80 | 0.04 |
| | −12 | 2.63 | 2.56 | 0.07 | 2.75 | 2.81 | 0.06 | 0.75 | 0.70 | 0.05 |
| | −13 | 2.57 | 2.51 | 0.06 | 2.70 | 2.76 | 0.06 | 0.64 | 0.61 | 0.03 |
| | −14 | 2.52 | 2.45 | 0.07 | 2.65 | 2.7 | 0.05 | 0.56 | 0.52 | 0.04 |

Table 2: Parameters of the three working conditions.

| | Temperature before throttling (°C) | Pressure before throttling (MPa) | Water dew point (°C) | Pressure after throttling (MPa) |
|---|---|---|---|---|
| Condition 1 | 0 | 3.95 | 0 | 2.10 |
| Condition 2 | −5 | 3.95 | −5 | 2.10 |
| Condition 3 | −10 | 3.95 | −10 | 2.10 |

Table 3: Total investment costs of the two inhibitors.

| | Methanol (per 10,000 yuan) | | Ethylene glycol (per 10,000 yuan) |
|---|---|---|---|
| | Situation 1 | Situation 2 | |
| Condition 1 | 80.3 | 165 | 89.6 |
| Condition 2 | 81.7 | 167 | 104.4 |
| Condition 3 | 74.3 | 152 | 108.2 |

for hydrate prevention and control, and when considering benefits of the gas-phase of the inhibitor, the method of methanol injection is economical.

## 5. Conclusion

In this paper, a quick and convenient program to predict and prevent hydrate formation for city gate stations is developed. After inputting the gas composition, pressure and temperature before throttling, and water dew point and pressure after throttling, hydrate formation temperature can be calculated. The required mass fraction of the inhibitor in the liquid phase and the injection volume of a thermodynamic inhibitor to prevent hydrate formation for city gate stations can be obtained. Based on the research, some remarkable conclusions can be drawn as follows:

(1) Using the developed program, the result of the inhibitor injection volume is close to HYSYS, and the absolute value of the error is between 0~0.09 L/$10^4$Nm$^3$, which has a certain engineering guiding significance.

(2) In addition to the calculation of commonly used methanol and ethylene glycol inhibitors, this article considers the use of ethanol for inhibition for the first time from a safety perspective. The calculation results show that ethanol is mainly suitable for the operating conditions with higher temperature and lower pressure after throttling.

(3) Applying the program to the actual working conditions of a certain gate station, from the point of view of the suppression effect, methanol has the best suppression effect among the three inhibitors, followed by ethylene glycol. Due to the large loss of methanol in the gas phase, the total injection volume of the inhibitor is the least of ethylene glycol. From an economic point of view, this article highlighted the benefits brought by the volatilization of inhibitors to the gas phase when natural gas is delivered. Finally, it is recommended to use methanol injection for hydrate prevention and control. Moreover, if the gas phase benefits of the inhibitor are not considered, the method of ethylene glycol injection is more economical.

## Data Availability

The data used to support the findings of this study are included within the article.

## Conflicts of Interest

The authors declare that they have no conflicts of interest.

## References

[1] D. Q. Li, M. Y. Ai, Y. B. Wang et al., "Hydrate accident and prevention in sebei-xining-lanzhou gas pipeline," *Oil & Gas Storage and Transportation*, vol. 31, no. 4, pp. 267–269, 2012.

[2] C. Y. Sun, Q. Huang, and G. J. Chen, "Progress of thermodynamics and kinetics of gas hydrate formation," *Journal of Chemical Industry and Engineering (China)*, no. 5, pp. 1031–1039, 2006.

[3] B. Y. Liu, M. Hao, and B. D. Chen, "Prediction of maximal allowable water content in long distance pipelines," *Journal of Petrochemical Universities*, no. 2, pp. 75–78, 2004.

[4] B. H. Shi, K. Quan, G. C. Qiao et al., "Prevention measures for hydrate ice blockage in Yu-Ji gas pipeline," *Oil & Gas Storage and Transportation*, vol. 33, no. 3, pp. 274–278, 2014.

[5] B. H. Shi, Y. L. Qian, H. Q. Wang et al., "Calculation method of water content/water dew point of natural gas," *Oil & Gas Storage and Transportation*, vol. 31, no. 3, pp. 188–192, 2012.

[6] M. Mesbah, S. Habibnia, S. Ahmadi et al., "Developing a robust Correlation for prediction of sweet and sour gas hydrate formation temperature," *Petroleum*, 2020.

[7] J. H. Waals and J. C. Platteeuw, "Clathrate solutions," *Advances in Chemical Physics*, vol. 2, pp. 1–57, 1958.

[8] G. Chen and T. Guo, "Thermodynamic modeling of hydrate formation based on new concepts," *Fluid Phase Equilibria*, vol. 122, no. 1, pp. 43–65, 1996.

[9] M. Motiee, "Estimate possibility of hydrates," *Hydrocarbon Processing*, vol. 70, no. 7, pp. 98-99, 1991.

[10] K. K. Ostergaard, B. Tohidi, and A. Danesh, "A general correlation for predicting the hydrate-free zone of reservoir fluids," *SPE Production & Facilities*, vol. 15, no. 4, pp. 228–233, 2000.

[11] B. F. Towler and S. Mokhatab, "Quickly estimate hydrate formation conditions in natural gases," *Hydrocarbon Processing*, vol. 84, no. 4, pp. 61-62, 2005.

[12] W. C. Wang, Y. X. Li, S. S. Fan, D. Liang et al., "Hydrate inhibiting policy based on risk management for oil and gas pipelines," *Natural Gas Industry*, vol. 30, no. 10, pp. 69–72, 2010.

[13] Y. H. Du and T. M. Guo, "The prediction of hydrate formation conditions of natural gas II;. inhibitor containing systems," *Acta Petrolei Sinica (Petroleum Processing Section)*, no. 4, pp. 67–76, 1988.

[14] Q. L. Ma, G. J. Chen, and T. M. Guo, "Modelling the gas hydrate formation of inhibitor containing systems," *Fluid Phase Equilibria*, vol. 205, no. 2, pp. 291–302, 2003.

[15] E. Khosravani, G. Moradi, and S. Sajjadifar, "An accurate thermodynamic model to predict phase behavior of clathrate hydrates in the absence and presence of methanol based on the genetic algorithm," *Journal of Chemical Thermodynamics*, vol. 57, pp. 286–294, 2013.

[16] M. Ayijiamal, Y. X. Li, Y. Q. Che et al., "Hydrate control scheme of hutubi gas storage and its optimization," *Oil & Gas Storage and Transportation*, vol. 36, no. 9, pp. 1024–1029, 2017.

[17] Z. Guo, X. Jing, and Y. S. Cao, "Calculate the injection volume of natural gas hydrate inhibitor by HYSYS," *Oil and Gas Treating and Processing*, vol. 31, no. 6, pp. 49–51, 2013.

[18] R. Davarnejad and J. Azizi, "Prediction of gas hydrate formation using HYSYS software," *International Journal of Engineering-Transactions C: Aspects*, vol. 27, no. 9, pp. 1325–1330, 2014.

[19] S. G. Li, Y. J. Li, L. B. Yang et al., "Prediction of phase equilibrium of gas hydrates based on different equations of state," *Journal of Chemical Industry and Engineering (China)*, vol. 69, no. S1, pp. 8–14, 2018.

[20] D. Y. Peng and D. B. Robinson, "A new two-constant equation of state," *Industrial & Engineering Chemistry Fundamentals*, vol. 15, no. 1, pp. 59–64, 1976.

[21] G. J. Chen, Q. L. Ma, and T. M. Guo, "A new mechanism for hydrate formation and development of thermodynamic model," *Journal of Chemical Industry and Engineering (China)*, no. 5, pp. 52–57, 2000.

[22] X. Zhao, Z. S. Qiu, W. A. Huang et al., "Inhibition mechanism and optimized design of thermodynamic gas hydrate inhibitors," *Acta Petrolei Sinica*, no. 6, pp. 124–130, 2015.

[23] Y. F. Yu, B. H. Shi, J. Q. Wang et al., "A calculation method for the critical minimum dosage of hydrate thermodynamic inhibitor," *Oil & Gas Storage and Transportation*, vol. 38, no. 5, pp. 547–553, 2019.